frontiers
RESEARCH TOPICS

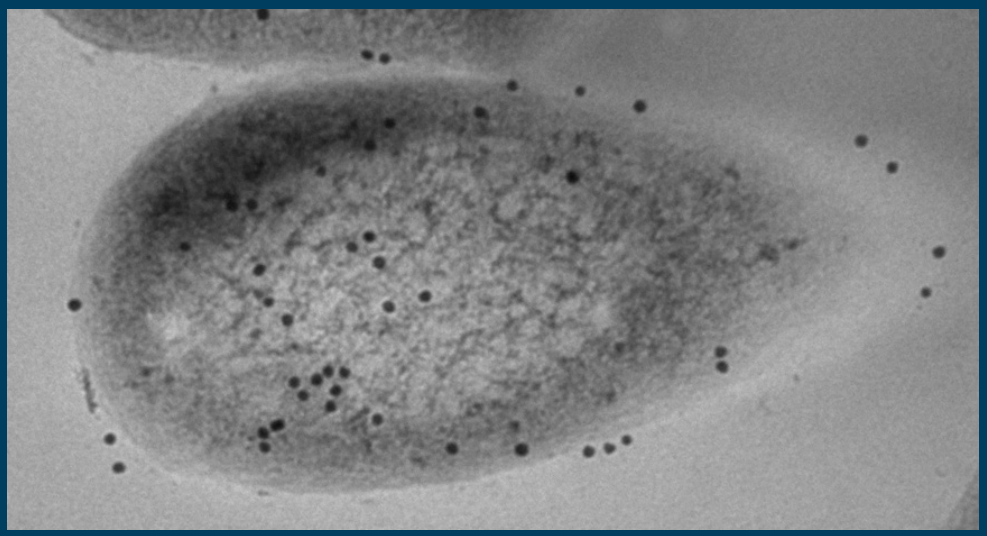

VACCINATION AGAINST MYCOBACTERIAL DISEASES IN ANIMALS

Topic Editors
John P. Bannantine and Adel M. Talaat

frontiers in
CELLULAR AND INFECTION MICROBIOLOGY

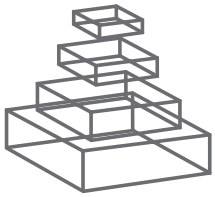

frontiers

ISSN 1664-8714
ISBN 978-2-88919-476-6
DOI 10.3389/978-2-88919-476-6

ABOUT FRONTIERS

Frontiers is more than just an open-access publisher of scholarly articles: it is a pioneering approach to the world of academia, radically improving the way scholarly research is managed. The grand vision of Frontiers is a world where all people have an equal opportunity to seek, share and generate knowledge. Frontiers provides immediate and permanent online open access to all its publications, but this alone is not enough to realize our grand goals.

FRONTIERS JOURNAL SERIES

The Frontiers Journal Series is a multi-tier and interdisciplinary set of open-access, online journals, promising a paradigm shift from the current review, selection and dissemination processes in academic publishing.
All Frontiers journals are driven by researchers for researchers; therefore, they constitute a service to the scholarly community. At the same time, the Frontiers Journal Series operates on a revolutionary invention, the tiered publishing system, initially addressing specific communities of scholars, and gradually climbing up to broader public understanding, thus serving the interests of the lay society, too.

DEDICATION TO QUALITY

Each Frontiers article is a landmark of the highest quality, thanks to genuinely collaborative interactions between authors and review editors, who include some of the world's best academicians. Research must be certified by peers before entering a stream of knowledge that may eventually reach the public - and shape society; therefore, Frontiers only applies the most rigorous and unbiased reviews.
Frontiers revolutionizes research publishing by freely delivering the most outstanding research, evaluated with no bias from both the academic and social point of view.
By applying the most advanced information technologies, Frontiers is catapulting scholarly publishing into a new generation.

WHAT ARE FRONTIERS RESEARCH TOPICS?

Frontiers Research Topics are very popular trademarks of the Frontiers Journals Series: they are collections of at least ten articles, all centered on a particular subject. With their unique mix of varied contributions from Original Research to Review Articles, Frontiers Research Topics unify the most influential researchers, the latest key findings and historical advances in a hot research area!
Find out more on how to host your own Frontiers Research Topic or contribute to one as an author by contacting the Frontiers Editorial Office: researchtopics@frontiersin.org

VACCINATION AGAINST MYCOBACTERIAL DISEASES IN ANIMALS

Topic Editors:
John P. Bannantine, National Animal Disease Center, U.S.A.
Adel M. Talaat, University of Wisconsin, U.S.A.

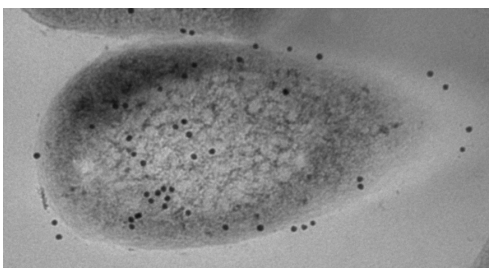

Transmission electron microscopy of *Mycobacterium avium* subspecies *paratuberculosis* bacilli taken at 73,100x magnification. Bacilli are labeled with 10 nm colloidal gold particles that show the location of rabbit anti-MAP antibody binding

The two most prominent mycobacterial diseases in animals include bovine tuberculosis, caused by *Mycobacterium bovis* and Johne's disease, caused by *Mycobacterium avium* subspecies *paratuberculosis*. Erradication of both diseases has been hampered by a variety of factors. In many countries, the persistence of tuberculosis in cattle has been attributed to reservoirs of *M. bovis* in wildlife species. Brushtail possums, deer and badgers are notable examples of wildlife reservoirs for *M. bovis*. The difficulties in eliminating the wildlife reservoir for *M. bovis* further suggest the need for vaccination of farmed livestock. Vaccination of wildlife species has also been attempted with mixed results. Delivery of the vaccine to wildlife species appears to be a chief obstacle. Vaccination itself leads to complications for diagnostics. For example, when cattle are vaccinated with both BCG and a commercial Johne's vaccine there is a biased toward the avian tuberculin skin test reaction. Despite these issues, BCG seems to be the clear standard for vaccination against *M. bovis*, yet many laboratories are investigating ways to improve on BCG.

For Johne's disease, the available commercial vaccines consist of whole-cell preparations in one form or another. But with the ability to generate directed knockouts of specific genes, a number of defined mutants have been constructed in a few laboratories. These should be tested and directly compared with each other and alongside commercial vaccine formulations to determine not only which vaccine is most protective, but which animal model is best for predicting protection in the target host. To this end, there has been a nation-wide, multi-institutional effort to test the best live, attenuated vaccine against Johne's disease in

cattle, sheep and goats. This vaccine trial has spanned six years and was conducted in three phases. The first phase examined attenuation in bovine macrophages, the second phase was colonization of spleen and liver in mice and the third phase was protection from bacterial challenge in goats. Many new ideas and retrospective approaches have emerged from this unprecedented effort. These aspects will be captured in this Research Topic.

In this Research Topic, we will seek articles on these above topics, but other issues surrounding vaccination of animals against mycobacteria will also be explored. These include immune parameters, correlates of protection, adjuvants and other vaccine formulations, etc.

Table of Contents

frontiers in
CELLULAR AND INFECTION MICROBIOLOGY

EDITORIAL
published: 21 January 2015
doi: 10.3389/fcimb.2015.00002

Controlling Johne's disease: vaccination is the way forward

John P. Bannantine[1]* and Adel M. Talaat[2]

[1] *Infectious Bacterial Diseases, National Animal Disease Center, United States Department of Agriculture - Agricultural Research Service, Ames, IA, USA*
[2] *Department of Pathobiological Sciences, University of Wisconsin, Madison, WI, USA*
**Correspondence: john.bannantine@ars.usda.gov*

Edited and reviewed by:
Yousef Abu Kwaik, University of Louisville School of Medicine, USA

Keywords: Johne's disease, vaccines, Mycobacterium, paratuberculosis, veterinary medicine

M. avium subspecies *paratuberculosis*, hereafter referred to as *MAP*, is a significant veterinary pathogen that causes Johne's disease in ruminants, including cattle, sheep, and goats. This chronic intestinal disease is distributed worldwide and exacts a heavy economic toll on animal producers. For example, the dairy industry incurs substantial economic losses due to reduced milk production, premature culling, and reduced slaughter value (Raizman et al., 2009). It takes years for clinical signs to appear in animals after initial infection. The bacterium is shed in high numbers in the feces during this clinical phase of disease. Transmission is by ingestion of the bacterium while grazing on pastures contaminated by this shedding process. Milk, passed from the infected dam to the daughter, has also been shown as a transmission route (Stabel, 2008). To best combat this chronic infection, vaccination has the promise to reduce economic losses and control Johne's disease. In the conception of this eBook for Frontiers in Cellular and Infection Microbiology, we solicited communications describing technologies and approaches to immunize animals against Johne's disease.

Among the first large-scale vaccine trials for Johne's disease began in the early 1990s using killed whole cells in oil injected into cattle (Kormendy, 1994; Wentink et al., 1994). Those trials showed vaccination was useful to reduce shedding of the bacteria in the feces, thus potentially reducing cow-to-calf transmission, but was ineffective at preventing infection. Since that time, experiments have evaluated extracts of the bacteria and live cells in all hosts including sheep, goats, deer, and cattle. Furthermore, the strain of *MAP* used has varied greatly in those studies. Then in 2007, an effort was made to standardize the challenge models used to test new vaccines for combating Johne's disease (Hines et al., 2007). The parameters outlined for the goat model in that article were used to test the best available live attenuated candidates (Hines et al., 2014) as described in this eBook compilation.

The genome sequence and re-sequence of *MAP* (Li et al., 2005; Wynne et al., 2010) has greatly expanded our knowledge about proteins predicted to be located in the mycobacterial envelope through annotation and bioinformatic analyses. Even now, most of what is known can be obtained only from annotation predictions and computer modeling algorithms that suggest protein locations within a cell (Yu et al., 2010). A perfect example of the power of genomics was demonstrated a few years later when libraries of transposon mutants and transcriptomic studies were reported by several groups working with *MAP* (Shin et al., 2006; Wu et al., 2006, 2007; Janagama et al., 2010). Furthermore, genomics provided an important resource for targeted construction of live-attenuated vaccine (LAV) candidates, which is the focus of several articles in this eBook. It is noteworthy that despite a focus on LAV strategies, we do not discount efforts directed toward the development of other vaccine technologies such as subunit or vectored vaccines (Hoek et al., 2010; Faisal et al., 2013; Thakur et al., 2013). Although these technologies are still under development, they could provide effective vaccines in the future.

Live attenuated vaccine strains of *MAP* are thought to be the best approach for vaccination against Johne's disease. Although traditional inactivated and LAV candidates cannot satisfy the DIVA approach, they will completely stimulate both cell-mediated and humoral immune responses (Park et al., 2011; Faisal et al., 2013). Numerous studies have suggested the role of cell-mediated immunity to provide protective responses against *MAP* infection, as suggested before in both the murine (Ghosh et al., 2014; Settles et al., 2014) and bovine models (Stabel et al., 2011) of Johne's disease. A partial analysis of the generated immune responses following immunization with novel LAV candidates is reported in this eBook (Hines et al., 2014) as part of a large scale vaccine trial. Additional analyses on the T cell populations and specific antigens detected will be forthcoming (Bannantine et al., unpublished).

To summarize the contributions to this research topic, the opening article reviews efforts by the Johne's disease research community to test available LAV strains of *MAP* through a series of three gated trials (Bannantine et al., 2014b). This trial series has been a coordinated international, multi-institutional effort that spanned several years. Many new ideas and retrospective approaches have emerged from this unprecedented effort. These aspects have been captured in this research topic. Details surrounding the construction of the attenuated mutants are also included as well as a list of the lessons learned from this integrated study. The next two articles describe a knockout mutant of *relA* (Park et al., 2014) and a library of transposon mutants (Rathnaiah et al., 2014). Both approaches are useful for generating live attenuated strains. The next three articles (Bannantine et al., 2014a; Hines et al., 2014; Lamont et al., 2014) describe in detail the three phases of the vaccine project summarized in the opening article. The remaining articles highlight immunological evaluation of subunit vaccines (Gurung et al., 2014), production of subunit vaccines using heterologous hosts (Johnston et al., 2014) and finally, take a unique look at the importance of post-translational modifications for vaccine design, with a highlight on glycoproteins (Facciuolo and Mutharia, 2014).

REFERENCES

Bannantine, J. P., Everman, J. L., Rose, S. J., Babrak, L., Katani, R., Barletta, R. G., et al. (2014a). Evaluation of eight live attenuated vaccine candidates for protection against challenge with virulent *Mycobacterium avium* subspecies *paratuberculosis* in mice. *Front. Cell. Infect. Microbiol.* 4:88. doi: 10.3389/fcimb.2014.00088

Bannantine, J. P., Hines, M. E. II, Bermudez, L. E., Talaat, A. M., Sreevatsan, S., Stabel, J. R., et al. (2014b). A rational framework for evaluating the next generation of vaccines against *Mycobacterium avium* subspecies *paratuberculosis*. *Front. Cell. Infect. Microbiol.* 4:126. doi: 10.3389/fcimb.2014.00126

Facciuolo, A., and Mutharia, L. M. (2014). Mycobacterial glycoproteins: a novel subset of vaccine candidates. *Front. Cell. Infect. Microbiol.* 4:133. doi: 10.3389/fcimb.2014.00133

Faisal, S. M., Yan, F., Chen, T. T., Useh, N. M., Guo, S., Yan, W., et al. (2013). Evaluation of a Salmonella vectored vaccine expressing *Mycobacterium avium* subsp. *paratuberculosis* antigens against challenge in a goat model. *PLoS ONE* 8:e70171. doi: 10.1371/journal.pone.0070171

Ghosh, P., Steinberg, H., and Talaat, A. M. (2014). Virulence and immunity orchestrated by the global gene regulator sigL in *Mycobacterium avium* subsp. *paratuberculosis*. *Infect. Immun.* 82, 3066–3075. doi: 10.1128/IAI.00001-14

Gurung, R. B., Purdie, A. C., Whittington, R. J., and Begg, D. J. (2014). Cellular and humoral immune responses in sheep vaccinated with candidate antigens MAP2698c and MAP3567 from *Mycobacterium avium* subspecies *paratuberculosis*. *Front. Cell. Infect. Microbiol.* 4:93. doi: 10.3389/fcimb.2014.00093

Hines, M. E. II, Stabel, J. R., Sweeney, R. W., Griffin, F., Talaat, A. M., Bakker, D., et al. (2007). Experimental challenge models for Johne's disease: a review and proposed international guidelines. *Vet. Microbiol.* 122, 197–222. doi: 10.1016/j.vetmic.2007.03.009

Hines, M. E. II, Turnquist, S. E., Ilha, M. R. S., Rajeev, S., Jones, A. L., Whittington, L., et al. (2014). Evaluation of novel oral vaccine candidates and validation of a caprine model of Johne's disease. *Front. Cell. Infect. Microbiol.* 4:26. doi: 10.3389/fcimb.2014.00026

Hoek, A., Rutten, V. P., van der Zee, R., Davies, C. J., and Koets, A. P. (2010). Epitopes of *Mycobacterium avium* ssp. *paratuberculosis* 70kDa heat-shock protein activate bovine helper T cells in outbred cattle. *Vaccine* 28, 5910–5919. doi: 10.1016/j.vaccine.2010.06.042

Janagama, H. K., Lamont, E. A., George, S., Bannantine, J. P., Xu, W. W., Tu, Z. J., et al. (2010). Primary transcriptomes of *Mycobacterium avium* subsp. *paratuberculosis* reveal proprietary pathways in tissue and macrophages. *BMC Genomics* 11:561. doi: 10.1186/1471-2164-11-561

Johnston, C. D., Bannantine, J. P., Govender, R., Endersen, L., Pletzer, D., Weingart, H., et al. (2014). Enhanced expression of codon optimized *Mycobacterium avium* subsp. *paratuberculosis* antigens in *Lactobacillus salivarius*. *Front. Cell. Infect. Microbiol.* 4:120. doi: 10.3389/fcimb.2014.00120

Kormendy, B. (1994). The effect of vaccination on the prevalence of paratuberculosis in large dairy herds. *Vet. Microbiol.* 41, 117–125. doi: 10.1016/0378-1135(94)90141-4

Lamont, E. A., Talaat, A. M., Coussens, P. M., Bannantine, J. P., Grohn, Y. T., Katani, R., et al. (2014). Screening of *Mycobacterium avium* subsp. *paratuberculosis* mutants for attenuation in a bovine monocyte-derived macrophage model. *Front. Cell. Infect. Microbiol.* 4:87. doi: 10.3389/fcimb.2014.00087

Li, L., Bannantine, J. P., Zhang, Q., Amonsin, A., May, B. J., Alt, D., et al. (2005). The complete genome sequence of *Mycobacterium avium* subspecies *paratuberculosis*. *Proc. Natl. Acad. Sci. U.S.A.* 102, 12344–12349. doi: 10.1073/pnas.0505662102

Park, K. T., Allen, A. J., Bannantine, J. P., Seo, K. S., Hamilton, M. J., Abdellrazeq, G. S., et al. (2011). Evaluation of two mutants of *Mycobacterium avium* subsp. *paratuberculosis* as candidates for a live attenuated vaccine for Johne's disease. *Vaccine* 29, 4709–4719. doi: 10.1016/j.vaccine.2011.04.090

Park, K. T., Allen, A. J., Barrington, G. M., and Davis, W. C. (2014). Deletion of relA abrogates the capacity of *Mycobacterium avium paratuberculosis* to establish an infection in calves. *Front. Cell. Infect. Microbiol.* 4:64. doi: 10.3389/fcimb.2014.00064

Raizman, E. A., Fetrow, J. P., and Wells, S. J. (2009). Loss of income from cows shedding *Mycobacterium avium* subspecies *paratuberculosis* prior to calving compared with cows not shedding the organism on two Minnesota dairy farms. *J. Dairy Sci.* 92, 4929–4936. doi: 10.3168/jds.2009-2133

Rathnaiah, G., Lamont, E. A., Harris, N. B., Fenton, R. J., Zinniel, D. K., Liu, X., et al. (2014). Generation and screening of a comprehensive *Mycobacterium avium* subsp. *paratuberculosis* transposon mutant bank. *Front. Cell. Infect. Microbiol.* 4:144. doi: 10.3389/fcimb.2014.00144

Settles, E. W., Kink, J. A., and Talaat, A. (2014). Attenuated strains of *Mycobacterium avium* subspecies *paratuberculosis* as vaccine candidates against Johne's disease. *Vaccine* 32, 2062–2069. doi: 10.1016/j.vaccine.2014.02.010

Shin, S. J., Wu, C. W., Steinberg, H., and Talaat, A. M. (2006). Identification of novel virulence determinants in *Mycobacterium paratuberculosis* by screening a library of insertional mutants. *Infect. Immun.* 74, 3825–3833. doi: 10.1128/IAI.01742-05

Stabel, J. R. (2008). Pasteurization of colostrum reduces the incidence of paratuberculosis in neonatal dairy calves. *J. Dairy Sci.* 91, 3600–3606. doi: 10.3168/jds.2008-1107

Stabel, J. R., Waters, W. R., Bannantine, J. P., and Lyashchenko, K. (2011). Mediation of host immune responses after immunization of neonatal calves with a heat-killed *Mycobacterium avium* subsp. *paratuberculosis* vaccine. *Clin. Vaccine Immunol.* 18, 2079–2089. doi: 10.1128/CVI.05421-11

Thakur, A., Aagaard, C., Stockmarr, A., Andersen, P., and Jungersen, G. (2013). Cell-mediated and humoral immune responses after immunization of calves with a recombinant multiantigenic *Mycobacterium avium* subsp. *paratuberculosis* subunit vaccine at different ages. *Clin. Vaccine Immunol.* 20, 551–558. doi: 10.1128/CVI.05574-11

Wentink, G. H., Bongers, J. H., Zeeuwen, A. A., and Jaartsveld, F. H. (1994). Incidence of paratuberculosis after vaccination against M. paratuberculosis in two infected dairy herds. *Zentralbl. Veterinarmed. B* 41, 517–522.

Wu, C. W., Glasner, J., Collins, M., Naser, S., and Talaat, A. M. (2006). Whole-genome plasticity among *Mycobacterium avium* subspecies: insights from comparative genomic hybridizations. *J. Bacteriol.* 188, 711–723. doi: 10.1128/JB.188.2.711-723.2006

Wu, C. W., Schmoller, S. K., Shin, S. J., and Talaat, A. M. (2007). Defining the stressome of *Mycobacterium avium* subsp. *paratuberculosis in vitro* and in naturally infected cows. *J. Bacteriol.* 189, 7877–7886. doi: 10.1128/JB.00780-07

Wynne, J. W., Seemann, T., Bulach, D. M., Coutts, S. A., Talaat, A. M., and Michalski, W. P. (2010). Resequencing the *Mycobacterium avium* subsp. *paratuberculosis* K10 genome: improved annotation and revised genome sequence. *J. Bacteriol.* 192, 6319–6320. doi: 10.1128/JB.00972-10

Yu, N. Y., Wagner, J. R., Laird, M. R., Melli, G., Rey, S., Lo, R., et al. (2010). PSORTb 3.0: improved protein subcellular localization prediction with refined localization subcategories and predictive capabilities for all prokaryotes. *Bioinformatics* 26, 1608–1615. doi: 10.1093/bioinformatics/btq249

Conflict of Interest Statement: The authors declare that the research was conducted in the absence of any commercial or financial relationships that could be construed as a potential conflict of interest.

Received: 19 December 2014; accepted: 05 January 2015; published online: 21 January 2015.

Citation: Bannantine JP and Talaat AM (2015) Controlling Johne's disease: vaccination is the way forward. Front. Cell. Infect. Microbiol. ***5****:2. doi: 10.3389/fcimb.2015.00002*

This article was submitted to the journal Frontiers in Cellular and Infection Microbiology.

frontiers in
CELLULAR AND INFECTION MICROBIOLOGY

REVIEW ARTICLE
published: 09 September 2014
doi: 10.3389/fcimb.2014.00126

A rational framework for evaluating the next generation of vaccines against *Mycobacterium avium* subspecies *paratuberculosis*

John P. Bannantine[1]*, Murray E. Hines II[2], Luiz E. Bermudez[3], Adel M. Talaat[4,5], Srinand Sreevatsan[6], Judith R. Stabel[1], Yung-Fu Chang[7], Paul M. Coussens[8], Raúl G. Barletta[9], William C. Davis[10], Desmond M. Collins[11], Yrjö T. Gröhn[7] and Vivek Kapur[12]*

[1] *Infectious Bacterial Diseases USDA-ARS, National Animal Disease Center, Ames, IA, USA*
[2] *Tifton Veterinary Diagnostic and Investigational Lab, The University of Georgia, Tifton, GA, USA*
[3] *Departments of Microbiology and Biomedical Sciences, Oregon State University, Corvalis, OR, USA*
[4] *Department of Pathobiological Sciences, University of Wisconsin-Madison, Madison, WI, USA*
[5] *Department of Food Hygenie, Cairo University, Cairo, Egypt*
[6] *Veterinary Population Medicine Department, University of Minnesota, Minneapolis, MN, USA*
[7] *Department of Population Medicine and Diagnostic Sciences, College of Veterinary Medicine, Cornell University, Ithaca, NY, USA*
[8] *Department of Animal Science, Michigan State University, Lansing, MI, USA*
[9] *School of Veterinary Medicine and Biomedical Sciences, University of Nebraska, Lincoln, NE, USA*
[10] *Department of Veterinary Microbiology, Washington State University, Pullman, WA, USA*
[11] *AgResearch, Wallaceville, New Zealand*
[12] *Department of Veterinary and Biomedical Sciences, Pennsylvania State University, University Park, PA, USA*

Edited by:
Alfredo G. Torres, University of Texas Medical Branch, USA

Reviewed by:
John T. Belisle, Colorado State University, USA
Shen-An Hwang, University of Texas Medical School, USA

***Correspondence:**
John P. Bannantine, USDA-Agricultural Research Service, National Animal Disease Center, 1920 Dayton Ave., Ames, IA 50010, USA
e-mail: john.bannantine@ars.usda.gov;
Vivek Kapur, Pennsylvania State University, 205 Wartik Laboratory, University Park, PA 16802, USA
e-mail: vkapur@psu.edu

Since the early 1980s, several investigations have focused on developing a vaccine against *Mycobacterium avium* subspecies *paratuberculosis* (MAP), the causative agent of Johne's disease in cattle and sheep. These studies used whole-cell inactivated vaccines that have proven useful in limiting disease progression, but have not prevented infection. In contrast, modified live vaccines that invoke a Th1 type immune response, may improve protection against infection. Spurred by recent advances in the ability to create defined knockouts in MAP, several independent laboratories have developed modified live vaccine candidates by transpositional mutation of virulence and metabolic genes in MAP. In order to accelerate the process of identification and comparative evaluation of the most promising modified live MAP vaccine candidates, members of a multi-institutional USDA-funded research consortium, the Johne's disease integrated program (JDIP), met to establish a standardized testing platform using agreed upon protocols. A total of 22 candidates vaccine strains developed in five independent laboratories in the United States and New Zealand voluntarily entered into a double blind stage gated trial pipeline. In Phase I, the survival characteristics of each candidate were determined in bovine macrophages. Attenuated strains moved to Phase II, where tissue colonization of C57/BL6 mice were evaluated in a challenge model. In Phase III, five promising candidates from Phase I and II were evaluated for their ability to reduce fecal shedding, tissue colonization and pathology in a baby goat challenge model. Formation of a multi-institutional consortium for vaccine strain evaluation has revealed insights for the implementation of vaccine trials for Johne's disease and other animal pathogens. We conclude by suggesting the best way forward based on this 3-phase trial experience and challenge the rationale for use of a macrophage-to-mouse-to native host pipeline for MAP vaccine development.

Keywords: Johne's disease, *Mycobacterium*, vaccines, attenuated, transposons, animal models, genomics

INTRODUCTION

Johne's disease is caused by *Mycobacterium avium* subspecies *paratuberculosis* (hereafter referred to as MAP), an acid-fast bacillus that can be distinguished from other closely related mycobacteria by its unique requirement for the mycobactin J siderophore in artificial culture media (Merkal and Curran, 1974). This major veterinary pathogen can infect many species of animals (Whittington et al., 2011), but its impact is felt most profoundly on commercial ruminant livestock such as cattle, sheep, goats and deer. In the United States (US) alone, current economic loses to the dairy industry are unknown, but previously was estimated at between 200 million and 1.5 billion dollars annually (Stabel, 1998). Almost three decades ago, the prevalence of Johne's disease in US dairy cattle was estimated at between 3 and 18% based

on slaughterhouse surveys (Chiodini and Van Kruiningen, 1986; Merkal et al., 1987). A more recent national level serological survey conducted by the National Animal Health Monitoring System (NAHMS) in 2007 suggested MAP prevalence on US dairy farms had risen above 30%. Unfortunately, this percentage continues to climb with the passage of time and implementation of more sensitive diagnostic tests. The most recent US dairy herd prevalence estimates are as high as 90% (Lombard et al., 2013) and New Zealand farmed deer herd estimates are at 59% (Stringer et al., 2013a). Collectively, these data suggest that MAP infection has long been endemic in the US and most likely across the world wherever dairy cows, sheep, goats and deer are intensively raised.

Vaccination against MAP infection has long been thought to be the best intervention strategy for this chronic and debilitating disease that is difficult to diagnose and slow to manifest. Animals actively shed large quantities of MAP before being diagnosed or exhibiting clinical signs—resulting in a transmission cycle that is very difficult to interrupt using traditional management strategies alone. Sub clinically infected animals transmit disease while appearing healthy and remaining undetectable by culture or PCR based approaches since these animals often shed MAP in a sporadic or intermittent manner. In stark contrast to the subversive "trickle and stealth" shedding pattern of MAP frequently observed in subclinical animals, there exist symptomatic, high shedder animals that excrete prodigious levels of organisms (up to 10^8 CFU per gram) in their feces, which provide the source of significant on-farm contamination (Pradhan et al., 2011). Diagnostic tests for Johne's disease are improving, but accurate detection of all infected animals, especially those that are early in infection and transmitting the organism within a herd, is still not possible. This fact makes test and cull strategies ineffective, except when targeting only high-shedding animals (Lu et al., 2008; Bastida and Juste, 2011). Therefore, it is widely recognized that unless animals can be detected early during infection, vaccination remains the best hope for controlling and preventing Johne's disease.

The ideal vaccine would completely prevent infection and/or promote protective immunity thus blocking both horizontal and vertical transmission. The current vaccines for Johne's disease fall far short of this high standard. MAP vaccines have been shown to be effective at lowering fecal shedding levels (Kalis et al., 2001; Faisal et al., 2013a), tissue colonization (Sweeney et al., 2009) or clinical disease incidence (Stringer et al., 2013b), but do not completely eliminate all three. Subunit vaccines against MAP are likely to obviate some of the shortcomings of whole-cell vaccines, such as severe inflammation and granuloma formation at the injection site. However, subunit vaccines that have been tested thus far have yielded incomplete protection results in murine models of infection (Koets et al., 2006; Stabel et al., 2012) and even when combinations of proteins are used in calves and goats (Koets et al., 2006; Kathaperumal et al., 2008, 2009). For example, MAP was colonized in the lymph node and spleen at similar levels in control and vaccinate mice using a protein cocktail (Stabel et al., 2012). Similarly, there were no significant MAP burden differences in the liver and mesenteric lymph node at 8 weeks post-challenge when immunizing mice with a 74 kDa polyprotein, but there was a significant difference in the liver (Chen et al., 2008). However, additional studies using more animals, longer term to monitor protection (1–3 years) and field trials are needed. Unfortunately subunit vaccines are expensive to produce whereas the manufacture of attenuated mutants is low in cost and easy to produce. These considerations are even more important for food animal health. Thus, there are several considerations, but research in this area demonstrates the slow yet steady progress in vaccine development for Johne's disease.

Efforts to improve upon current vaccine formulations have long been hampered by the lack of standardized challenge models and the high costs associated with trials conducted in natural ovine, caprine, deer or bovine hosts. Progress is however being made, and standardized animal models (mouse, goat, cow) for Johne's disease have been developed by a group of international investigators under the auspices of the Johne's Disease Integrated Program (JDIP), a USDA-funded research consortium (Hines et al., 2007) to help facilitate comparisons between different vaccine trials. However, the costs and logistical challenges of MAP vaccine trials, particularly in the natural hosts, remain a major concern. And even with an efficacious vaccine, it is remotely possible that MAP could be maintained within a herd due to vertical transmission as noted in a recent vaccine modeling study (Lu et al., 2013). Finally, there are negative implications of JD vaccination on both Johne's disease and bovine TB diagnostics as will be discussed further below.

Consistent with what is known about other intracellular pathogens, a MAP vaccine that drives the immune response to a proinflammatory Th1 profile and prevents a shift to the humoral Th2 response, maybe more effective in delaying progression of the disease to a clinical state (Coussens, 2004; Stabel, 2010). However, it has recently been suggested that humoral immunity may also be important against *M. tuberculosis* infection (Achkar and Casadevall, 2013). Nonetheless, current dogma suggests a late humoral response is not a protective immune response against Johne's disease. The focus of the JDIP vaccine studies was on live attenuated mutants rather than subunit or DNA vaccines because they are more likely to generate the beneficial Th1 immune response, which is considered the most protective against mycobacterial infections (Stabel, 2000; Hostetter et al., 2002). The cause for the switch from Th1 to Th2 immune responses in Johne's disease is unknown, however mathematical modeling of the bovine immune response to MAP suggests it may be attributed to extracellular MAP that persists outside of macrophages (Magombedze et al., 2014). Although these inferences need to be carefully tested experimentally, it is possible a mutant strain deficient in this capability might be the critical factor to an efficacious vaccine for Johne's disease.

Despite significant recent advances in the ability to make defined mutants, there have been only a limited number of trials testing live attenuated vaccines against MAP. These have been largely limited to *in vitro* studies or trials in the mouse (Scandurra et al., 2009; Settles et al., 2014), and except in a few cases (Scandurra et al., 2010; Faisal et al., 2013b), reflect a striking absence of robust and cost effective strategies for evaluating vaccine candidates in the relevant natural ruminant host. To help address this unmet need, and establish a rational framework based for the evaluation of novel vaccine candidates against MAP,

we adopted an inclusive and collaborative approach that may also serve as a guide for future vaccine evaluation trials for MAP and other major animal pathogens. We here present the state-of-the-field summary for vaccination against Johne's disease, describe current candidate live attenuated mutants of MAP, and present an overview of the JDIP three-phase vaccine trial and lessons learned.

MAP VACCINES: WHAT IS AVAILABLE?

It is paradoxical that vaccination against MAP has not been widely used in the US given the high prevalence of Johne's disease in this country. Currently, there are at least three commercial Johne's disease vaccines worldwide, but only one (Mycopar®) approved vaccine for use in the US (Bastida and Juste, 2011). Silirum® is produced by Zoetis and was used as the control vaccine in the JDIP mouse and goat trials discussed below. Mycopar® is manufactured by Boehringer Ingelheim Vetmedica Inc. whereas Gudair® is produced by CZ Veterinaria in Spain and is being used in countries with large sheep populations (Bastida and Juste, 2011). Importantly, all three consist of an inactivated whole-cell preparation of either *M. avium* subspecies *avium* or subspecies *paratuberculosis*. As summarized by Bull et al. live attenuated strains were used in the 1960s and 1970s and then concerns about their use in the 1980s forced a shift to using killed vaccine formulations (Bull et al., 2013). Live vaccine strains can now be revisited with the technology used to create defined mutations.

What does the scientific literature report about the efficacy of these commercial MAP vaccines? In three dairy herd operations with Johne's disease, investigators showed that fewer Mycopar® vaccinated cattle had detectable fecal culture positive results compared with controls (Knust et al., 2013). This same vaccine also showed partial protection in a goat challenge model (Faisal et al., 2013a). However, the inactivated strain used in the Mycopar® formulation is not MAP, but an isolate called strain 18 that is nonetheless a member of the *M. avium* species. The manufacturer data sheet still lists Mycopar® as an "inactivated *M. paratuberculosis* bacterium suspended in oil." Interestingly, this parallelism occurs with the suboptimal response of BCG, derived from the related species *M. bovis*, as a vaccine against tuberculosis (Mangtani et al., 2014). Gudair consists of heat-killed MAP 316F and is designed for use in sheep and goats according to the manufacturer. Gudair® has been shown to be an effective vaccine in Merino sheep (Reddacliff et al., 2006). Vaccination not only delayed the onset of fecal shedding, but reduced mortality attributed to Johne's disease by 90% in the 200 vaccinated sheep. Silirum® is a killed strain of MAP, also related to 316F, that has been tested in Australian cattle. This vaccine has recently been shown to reduce prevalence of clinical disease, as measured by lymph node pathology and fecal culture at slaughter, in farmed deer in New Zealand (Stringer et al., 2013b). Currently, there are no subunit, live or DNA vaccines commercially available against Johne's disease.

CONSTRUCTION OF ATTENUATED MAP MUTANTS

Although attenuated MAP, generated by repeated subculture of the strain, had been used as a live vaccine long ago (Saxegaard and Fodstad, 1985), no defined mutants of MAP had been tested as a vaccine simply because no method was available for their construction. In 1995, the first concerted effort to develop the genetics of MAP was performed in Raúl Barletta's laboratory at the University of Nebraska (Foley-Thomas et al., 1995). Studies in his laboratory demonstrated for the first time that MAP could be transformed with foreign DNA as well as transfected with bacteriophage DNA. Furthermore, they found that MAP could be productively infected with the mycobacteriophage TM4 and later demonstrated the use of a thermosensitive derivative of TM4 to generate the first transposon mutant library (Harris et al., 1999). This methodological advance was adapted by other laboratories to create their own transposon mutant banks (Cavaignac et al., 2000; Shin et al., 2006). Phage-mediated techniques are now being applied to construct directed knockout mutations in MAP using allelic exchange. This technique worked well in *M. tuberculosis*, but the allelic exchange efficiency was low in MAP until investigators at Washington State University tweaked the protocol to increase efficiencies to generate Δ*relA,* Δ*lsr2*, and Δ*pknG* knockout strains (Park et al., 2008a). Now robust enough to be performed in other laboratories, this method enabled a more strategic approach to obtaining the precise knockout of a specific virulence gene rather than depend on random transposon mutagenesis and screening approaches to find a suitable knockout to try as a vaccine. The *ppiA* (Scandurra et al., 2010), *relA, lsr2, pknG* (Park et al., 2008a), *leuD, mpt64,* and *secA2* genes (Chen et al., 2012) have all been successfully knocked out using this method. Each of these mutants has also been evaluated as a vaccine candidate as discussed in the next section.

PREVIOUS MAP VACCINE STUDIES

MAP vaccination studies have been thoroughly summarized for cattle, sheep and goats by examining pathological, epidemiological and production effects of vaccination (Bastida and Juste, 2011). This meta-analysis revealed that while vaccination is useful in limiting microbial contamination and production losses, most of the vaccines are similar in content and preparation. These findings have recently been reinforced by the reduction of fecal contamination in three dairy herds using a killed vaccine (Knust et al., 2013). The possibility exists that new generations of vaccine formulations, including live attenuated, may further improve on the killed vaccine preparations currently being used. This section summarizes the pertinent literature on MAP vaccination as it relates to the JDIP trials.

Subunit vaccines have been delivered using heterologous hosts such as *Salmonella* (Chandra et al., 2012), or *Lactobacillus* (Johnston et al., 2014). Only two DNA vaccines against MAP have been tested in mice. One used expression library DNA immunization of Balb/cJ mice and challenged with a recently isolated bovine MAP strain 6112 (Huntley et al., 2005). Four pools of 108 clones each protected mice from colonization of spleen and mesenteric lymph nodes. The second study tested a cocktail of five genes encoding antigen 85A, B, and C along with superoxide dismutase and 35-kDa protein by intramuscular injection of C57/BL6 (Park et al., 2008b). There was a significant reduction in colonization of the liver and spleen of mice immunized with this

cocktail. The subunit vaccines from both studies induced a Th1 immune response as measured by interferon gamma; however, none of these DNA formulations were tested in cattle or other ruminant hosts.

Several *MAP* vaccine candidates have been analyzed in isolation making it difficult to directly compare candidates between studies. Some have been bench marked against a commercially available vaccine (Faisal et al., 2013a; Hines et al., 2014) while other studies lack even that as a reference. As mentioned, all commercial vaccine formulations consist of a killed whole-cell preparation of MAP in an oil emulsion, but there are many other types of vaccines. Still other vaccine formulations included live *M. avium* bacteria, but it is not clear if or how they were attenuated (Begg and Griffin, 2005). In the current JDIP vaccine trial, we took a different approach in identifying a viable, yet attenuated vaccine strain, reasoning that a live strain will maintain a proinflammatory Th1 response (Stabel, 2000; Coussens, 2004). Th1-associated cytokines including interferon gamma, interleukin-2 (IL-2), IL-12 and tumor necrosis factor alpha were measured after antigen stimulation of cultured peripheral blood monocytes in these studies.

While there are no published bovine vaccine trials in Johne's disease, there are a number of caprine and ovine vaccine trials. Furthermore, a number of MAP vaccine studies in mice have been reported, but they are too numerous to adequately be summarized here. Importantly, only a few studies that began using the mouse model were further evaluated in a ruminant host (Scandurra et al., 2010; Park et al., 2011) and none using the number of mutant strains in the JDIP trials. This was a key component in the design of the JDIP vaccine trial. Using the data described in this special topics issue, we can now assess the predictive value of the mouse trial in obtaining good candidates for the ruminant host.

ATTENUATED MUTANTS IN THE JDIP VACCINE STUDY

What was known about the mutants prior to enrollment in the JDIP vaccine study? Some of the mutants remain unpublished or have only recently been submitted for publication, however, others have been described prior to the JDIP trials. Information concerning all mutants included in the JDIP trials is summarized in **Table 1**. The first MAP mutants created by allelic exchange produced directed knockouts of *lsr2*, *relA,* and *pknG* mutants in 2008 (Park et al., 2008a) and all three were included in the JDIP trial (**Table 1**). These three genes were selected based on the virulence properties of their orthologs in *Mycobacterium tuberculosis* and *Mycobacterium bovis*. Lsr2 is a cytosolic protein implicated in cell wall lipid biosynthesis and antibiotic resistance in *M. smegmatis* (Chen et al., 2006; Colangeli et al., 2007). Protein kinase G, encoded by *pknG*, is secreted by *M. tuberculosis* and *M. bovis* within the phagosome of macrophages and is thought to inhibit phagolysosomal fusion (Walburger et al., 2004). RelA in *M. tuberculosis* is involved in the stringent response that is activated in nutrient limiting conditions. Specifically, RelA in *M. tuberculosis* synthesizes the hyperphosphorylated guanine nucleotides that accumulate in nutrient limiting conditions and inactivating this gene severely reduced long-term survival in mice (Dahl et al., 2003).

Two of these MAP mutants, Δ*pknG* and Δ*relA*, were later tested as vaccine candidates in cultured macrophages, calves and kid goats (Park et al., 2011). Although both were attenuated in bovine macrophages compared to the wild-type strain on day 6, it was shown that Δ*relA* was the better vaccine candidate since no MAP was found in the tissues of calves vaccinated with the *relA* mutant. Furthermore, vaccination with the *pknG* mutant did not inhibit challenge with MAP in the kid goats as the challenge bacteria were present in high numbers in all 9 tissues evaluated, whereas the *relA* mutant vaccinates were free of the challenge inoculum in 8 of the 9 tissues taken from kid goats (Park et al., 2011). However, both mutants induced effector memory T cells similar to the wild type strain. Although Δ*lsr2* was included in the study, further experiments were needed to assess the *in vivo* survival of Δ*lsr2* because of fungus problems in readout cultures (see Park et al., 2014, this issue). Of interest, a second mutant containing an *lsr2* transposon insertion was developed by another laboratory and included in the JDIP study and was coded 317 (**Table 1**). A report on this mutant has just been submitted publication, and it was evaluated in the mouse challenge model in phase II but not the phase III JDIP trial. Another interesting observation was that three independent investigators submitted mutants with insertions in the same gene, MAP1566, which encodes a hypothetical protein (Li et al., 2005). This is surprising because the MAP genome contains over 4300 targets for transposon insertion, yet of the 22 mutants enrolled in this study 3 are in the same target (MAP1566) and another two are in *lsr2*.

One of the three ΔMAP1566 mutants along with the *ppiA* mutant, coded as 322 and 323, respectively, in **Table 1**, were analyzed in macrophages, mice, and goats (Scandurra et al., 2010). All three model systems demonstrated that ΔMAP1566 was more attenuated than the *ppiA* mutant. However, macrophages produced less IL-10 when infected with the *ppiA* mutant and it persisted longer in mice. In the goat experiment, the challenge strain was not cultured from any of the tissues in goats vaccinated with ΔMAP1566, whereas 15% of the tissues taken from the Δ*ppiA* immunized goats were positive by Bactec 12B culture for the challenge strain (Scandurra et al., 2010). Collectively, these data suggest that the ΔMAP1566 strain is a better vaccine than Δ*ppiA*.

Other mutants that were shown to be attenuated in mice prior to testing in the JDIP vaccine trial include *kdpC*, *pstA*, *umaA1,* and *fabG2_2* (Shin et al., 2006). The *pstA* gene encodes a large (12 kb) non-ribosomal synthetase protein involved in glycopeptidolipid biosynthesis and was later shown to contribute to biofilm formation and invasion of the calf intestine (Wu et al., 2009). The *umaA1* gene codes for a mycolic acid synthase that was studied in *M. tuberculosis* (Yuan et al., 1995). The *kdpC* mutant showed significantly lower colonization levels in the liver and intestine of mice at all time points, compared to the wild-type and also displayed less granulomatous inflammation (Shin et al., 2006). The *pstA*, *umaA1,* and *fabG2_2* mutants showed reduced bacterial colonization of the mouse intestine at later time points. Finally, a manuscript is in preparation describing the mutants constructed at the University of Nebraska (**Table 1**). Among this group are transposon insertions between genes (intergenic) rather than within a gene.

Table 1 | Transposon mutant vaccine candidates of MAP enrolled in the JDIP vaccine trials.

Institution[a]	Blinded code[b]	Location of insertion[c]	MAP strain background[d]	Moved to		References
				Phase II?[e]	Phase III?[f]	
USDA-ARS-WRRC	311	MAP0482	Goat strain 43432-02	No	No	McGarvey, unpublished
Washington State University	312	MAP1047 (*relA*)	K-10	No	No	Park et al., 2008a
Washington State University	313	MAP3893c (*pknG*)	K-10	No	No	Park et al., 2008a
Washington State University	314	MAP0460 (*lsr2*)	K-10	No	No	Park et al., 2008a
University of Nebraska	315	MAP1566	K-10	Yes	Yes	Rathnaiah et al., in review
University of Nebraska	316	MAP3695 and *fadE5*	K-10	Yes	Yes	Rathnaiah et al., in review
University of Nebraska	317	MAP0460 (*lsr2*)	K-10	Yes	No	Rathnaiah et al., in review
University of Nebraska	318	MAP0282c and 0283c	K-10	Yes	Yes	Rathnaiah et al., in review
University of Nebraska	319	MAP1566	K-10	Yes	Yes	Rathnaiah et al., in review
University of Nebraska	320	MAP2296c and 2297c	K-10	Yes	No	Rathnaiah et al., in review
University of Nebraska	321	MAP1150c and 1151c	K-10	Yes	No	Rathnaiah et al., in review
AgResearch NZ	322	MAP1566	strain 989	No	No	Scandurra et al., 2010
AgResearch NZ	323	MAP0011 (*ppiA*)	K-10	No	No	Scandurra et al., 2010
University of Wisconsin	324	MAP0997c (*kdpC*)	ATCC19698	No	No	Shin et al., 2006
University of Wisconsin	325	MAP3006c (*lipN*)	K-10	No	No	
University of Wisconsin	326	MAP3963 (*umaA1*)	ATCC19698	No	No	Shin et al., 2006
University of Wisconsin	327	MAP4287c	K-10	No	No	
University of Wisconsin	328	MAP1242 (*pstA*)	ATCC19698	No	No	
University of Wisconsin	329	MAP2408c (*fabG2_2*)	ATCC19698	Yes	Yes	Shin et al., 2006
University of Wisconsin	330	MAP1719c	ATCC19698	No	No	
University of Wisconsin	331	MAP1872c (*mbtH_2*)	ATCC19698	No	No	Kabara and Coussens, 2012
University of Wisconsin	332	MAP4288 (*lpqP*)	ATCC19698	No	No	

[a] *The location of the laboratory where the mutant(s) was constructed.*

[b] *The stains were cultured and blinded at Penn State University prior to shipment to the testing labs.*

[c] *The MAP locus where the transposon inserted. If two genes are listed, the transposon is inserted in the intergenic region between the two. If the gene has been named, it is shown in parenthesis.*

[d] *The parental strain of MAP used to create the mutation.*

[e] *Indicates if the mutant strain was moved forward into the phase II (mouse) trial.*

[f] *Indicates if the mutant strain was moved forward into the phase III (goat) trial.*

A subset of the mutants in the JDIP study was examined for ability to regulate host cell apoptosis of macrophages (Scandurra et al., 2010; Kabara and Coussens, 2012). Apoptosis is an important tool in the fight against mycobacterial infections as apoptotic bodies are taken up by other antigen presenting cells. Mycobacteria contained in apoptotic bodies are destroyed and their antigens presented to immune cells. The *lsr2* knockout was most similar to the wild-type in terms of controlling apoptosis among the mutants tested, indicating that *lsr2* is not involved in this process. However, a Tn*5367* insertion in MAP1872c was not able to prevent apoptosis, indicating that this gene may be involved in regulating this host cell process. The gene encodes an iron acquisition protein (Zhu et al., 2008), which is an important process for MAP survival in the host. The other mutants tested were not significantly different from the uninfected control, which demonstrated the level of spontaneous apoptosis in culture. A second study examined apoptosis in bovine macrophages (Scandurra et al., 2010) and two of the mutants overlapped between that study and the Kabara and Coussens study. These mutants included the *ppiA* knockout (code 323 in **Table 1**) and MAP1566 (code 322). While neither of these mutants demonstrated control of apoptosis in the Kabara and Coussens study, ΔMAP1566 showed a significant reduction in apoptosis compared to the wild type strain in the Scandurra et al. study. The *ppiA* mutant was inconclusive since macrophages from the two cows examined gave divergent results (Scandurra et al., 2010). When tested independently all these mutants showed promise as a vaccine candidate for Johne's disease. So we developed a strategy to directly compare all of these mutants in the same vaccine trial through the JDIP research consortium.

INTERFERENCE WITH DIAGNOSTIC TESTING FOR TB OR JOHNE'S DISEASE

Although it has been suggested there might be an added benefit to vaccinate against MAP for cross protection with TB (Perez De Val et al., 2012), it is generally seen as a negative due to interference with diagnostic testing for TB, a highly regulated animal disease. In fact, a primary reason why whole cell vaccines against Johne's disease are not routinely used in the United States is due to the interference with diagnostic tests for both Johne's disease

and particularly bovine TB. This same reason is why vaccination was also reserved only for farms in the Netherlands with high incidence of Johne's disease (Muskens et al., 2002). Immunization with Mycopar® will interfere with Johne's diagnostic tests, particularly the IFN-γ test, but not with the comparative cervical skin test which was 100% specific within the first year of vaccination (Stabel et al., 2011). In addition, *M. bovis* serological tests, which included the ESAT-6, CFP-10, and MPB83 antigens, were also negative in MAP vaccinated calves. Likewise, an immediate strong and long-lasting MAP-specific IFN-γ response was observed in two herds vaccinated with a heat-killed vaccine (Muskens et al., 2002). Caution must be used if administering Gudair® to cattle since it appears to lower the sensitivity of the bovine TB skin test (Coad et al., 2013). Dairy herds vaccinated with Silirum® showed that the comparative intradermal test (CIT) had low cross reactivity; however the single bovine intradermal tubculin test would result in 5–6% false positive results for TB (Garrido et al., 2013). These results are similar with MAP vaccinated goats (Chartier et al., 2012). Thus, the CIT test can be considered useful if evaluating TB in a MAP vaccinated herd. This finding paves the way for live attenuated vaccines for MAP. Perhaps even more encouraging are the novel biomarkers identified from proteomics of both the host and pathogen that suggest peptides in circulation may overcome the issue of cross-reactivity (Seth et al., 2009). However, even if producers had to deal with a low level of false positive results for TB infection, we believe that if a strong live vaccine were developed that could prevent infection and enable effective disease control, the vaccine would be widely implemented.

CONCEPTION OF THE JDIP VACCINE TRIAL

It was against this background that the idea for establishing independent testing labs to evaluate all the available vaccine candidates was conceived. This multi-institutional study was based on the following principles. Through the formation of a research consortium on Johne's disease, which was funded by the USDA-NIFA from 2002 to 2011, this governing body was successful in setting up a world-wide search for the best performing vaccine candidates. The idea behind this project was to combine the resource and intellect of JDIP with the financial resource of USDA-APHIS-VS to identify the best possible attenuated vaccine available. On January 12, 2008 a meeting was held in Chicago, Illinois to devise a coordinated effort to test attenuated vaccine candidates submitted by Johne's disease researchers. Although a few vaccine trials have tested individual mutants in macrophages, mice and goats, no trial of this scope using 5 or more mutants tested in parallel has ever been performed.

TRIAL DESIGN

To begin, investigators around the world were asked to submit their best-attenuated mutants, along with any efficacy data generated in their labs, to the JDIP study. A multi-institutional universal material transfer agreement was drafted and finalized enabling all investigators to submit their vaccine candidate(s) to Penn State University (PSU) while at the same time, protecting intellectual property rights of the investigator. PSU cultured each strain to the specified optical density and coded each strain for blinding before sending onto specific labs to perform the efficacy trials.

Three gates were decided upon which the mutants had to pass through at each phase of the study. The first gate measured survival of mutants in primary bovine macrophages, where the most attenuated strains were considered the best candidates. The second gate was protection from colonization by challenge bacteria in the liver and spleen of mice and the third gate was protection from colonization using the goat challenge model (Hines et al., 2007). A triage process had to be implemented at each gate due to funding limitations, but we acknowledge it would have been ideal to test all the vaccine strains in all three trials.

Five investigators from the United States and New Zealand responded to the JDIP request and submitted their attenuated MAP mutants. It is noteworthy that directed or random knockouts in MAP are not trivial to obtain and hence, only a few investigators had possession of such mutants. A total of 22 transposon-marked mutants were submitted (**Table 1**). Interestingly, among the 22 mutants, a few had insertions in the same gene, but were submitted by different investigators. As mentioned above, MAP1566 insertions were present in 3 strains, 2 of them from the same lab contained insertions in different locations within the gene. Also 2 mutants submitted by independent labs were MAP0460 knockouts. Given the number of potential gene targets in this organism (>4300), this duplication was unexpected, but provided some interesting built-in comparisons.

VACCINE CANDIDATE SELECTION

The initial criteria for candidate vaccine selection were based on data obtained by the investigator who constructed the mutant. Each investigator determined independently the suitability of their mutant. In some cases these results were published, but regardless, the net was cast broad and wide to obtain as many MAP mutants as possible for testing. However, there were some minimal qualifications. To enter the first trial each mutant (1) must be viable *in vitro* (no sonicated extracts or heat-inactivated preps) and (2) growth rate in broth cultures must be similar to wild-type MAP. The mutant strains were sent to PSU under a unique pan-institutional material transfer agreement that allowed the submitting investigators to retain full intellectual property. Each mutant strain received was tested for culture, coded to blind testing labs and quality control tested prior to shipping to the testing labs. For example, the PSU lab confirmed a lack of contamination in the culture by PCR and plating on blood agar and/or BHI before shipping. Therefore, after receiving the strains, at least 60 days were needed to prepare each strain for shipment. Five submitted strains were not shipped to the phase I testing labs for the following reasons. One showed incredibly slow and anemic growth in both liquid and solid culture, regardless of several attempts. For two others, the reference colony forming units (CFU) was not obtainable by the end of phase I. And the remaining two arrived after the due date for submission. Although PSU started to grow them regardless, there was not enough time to include them in this initial trial. A general summary of each trial is listed below.

PHASE I: SURVIVAL IN PRIMARY BOVINE MACROPHAGES

The single goal of this experiment was to test survival in primary bovine macrophages because attenuation in this environment can infer potential vaccine candidates. Primary bovine macrophages were cultured and infected in two laboratories, one at the University of Minnesota (UMN) and the other at the University of Wisconsin (UW). In order for these labs to start their macrophage studies, a final CFU number was needed from PSU to infect at the correct multiplicity of infection. Once the cells reached $OD_{600} = 0.50$, the PSU lab determined the reference CFU and started to regrow the strains for shipment. The manuscript describing the results of this study was just published (Lamont et al., 2014).

Colony counts from cultures over time in macrophages were obtained to give the slope (growth over time). Basically, a negative slope demonstrated attenuation because it meant there were less viable bacteria recovered from bovine macrophages as time increased (Lamont et al., 2014). When examining the data by slope alone, it was evident which mutants had a negative slope and which did not, but when looking at the individual CFU data, it was clear that considering slope alone was misleading. Therefore, JDIP solicited the Michigan State University (MSU) lab to perform an apoptosis study of the mutants. Some mutants were not included in this study because of the staggered nature in which they were received or the lack of permission to include the mutant strain in a publication. Most of the strains were sent to the MSU lab for the apoptosis experiment (Kabara and Coussens, 2012). Some of the mutants arrived several months late, and at that point, JDIP needed the data from the study to help make a decision on which mutant strains to go forward in the mouse trial.

Results of the experiments from each trial were sent directly to Cornell University for data analysis. Slope of the growth in macrophages was used to compare mutants. The results showed subtle changes in survival of the mutant strains (manuscript in preparation). Once the analysis was complete and decisions made about which strains would advance to the next phase, the blind was decoded and recoded for the next experiment.

PHASE II: THE MOUSE TRIAL

This experiment was designed to test the remaining 8 attenuated vaccine strains in the mouse challenge model. The readout was colonization (CFU) of the liver and spleen from vaccinated and control mice (Bannantine et al., 2014). Silirum® was the commercial vaccine run in parallel for this trial. Each mouse received 10^5 CFU of the live attenuated vaccine strain in 0.5 ml PBS by intraperitoneal injection.

The persistence of the vaccine candidates was measured at 6, 12, and 18 weeks post-vaccination. Only strains 320, 321, and 329 colonized both the liver and spleens up until the 12-week time point. The remaining five mutants showed no survival in those tissues, indicating their complete attenuation in the mouse model. The vaccine strains demonstrated different levels of protection based on MAP colonization in liver and spleen tissues at 12 and 18 weeks post-vaccination. Based on total MAP burden in both tissues at both time points, strain 315 (MAP1566::Tn*5370*) was the most protective whereas strain 318 (intergenic Tn*5367* insertion between MAP0282c and MAP0283c) had the most colonization (Bannantine et al., 2014). Mice vaccinated with an undiluted commercial vaccine preparation displayed the strongest antibody responses as well as enlarged spleens.

The effect of persistence of the three vaccine strains in mice is unclear. However, it is clear from the goat trial described below that the vaccine strains did not persist indefinitely as only the challenge strain was identified by PCR analysis at the 2 month time point (Hines et al., 2014). It would have been interesting to see if the *pknG* mutant was persistent in the JDIP goat study, but that mutant was not included in phase III of the trial due to triage after the macrophage study (Lamont et al., 2014). Significantly the *relA* mutant, that also showed attenuation in macrophages, did not make it through to the last phases of the trial, even though a preliminary study in goats showed it was immune eliminated. The immune response elicited by the mutant limited infection with MAP under experimental challenge conditions (Park et al., 2011). A further study conducted in parallel with the JDIP attenuated vaccine studies, but using calves, has extended the findings in goats with similar results (Park et al., 2014).

PHASE III: THE GOAT TRIAL

Data from this final trial in a ruminant host were used to rank the remaining vaccine candidates to determine the best attenuated vaccine. Logistic issues interfered with testing and two strains that showed promising results in mice (strains 320 and 321) were not evaluated in goats (Bannantine et al., 2014). A second goal of this phase III vaccine trial was to validate the goat challenge model originally proposed in 2007 (Hines et al., 2007). Trial was performed at the University of Georgia-Tifton Veterinary Diagnostic and Investigational Laboratory.

Eighty 2-month-old goat kids were separated into 8 groups with 10 kids in each group. Three groups were dedicated to controls (wild-type MAP K-10, PBS and Silirum® vaccine). The remaining 5 groups consisted of the MAP vaccine candidates. The animals in each group were housed in identical treatment rooms in a manner to reduce "pen effect." Baseline blood and fecal samples were taken at the beginning of the study. As with the other trials, the investigators were blinded as to the identity of the experimental vaccines. The Silirum® vaccine was administered as a single dose and used according to manufacturer instructions. The study length was approximately 18 months with a full 12-month period post-challenge. Two doses of each mutant vaccine were administered as described (Hines et al., 2014). All vaccine and challenge doses were delivered orally by syringe in pasteurized commercial goat milk.

While none of the vaccines tested prevented MAP infection or eliminated fecal shedding in goats, the Δ*fabG2_2* vaccine strain (coded 329 in **Table 1**) did lower the incidence and severity of infection as measured by lesion score, tissue pathology, fecal culture and fecal PCR (Hines et al., 2014). The *fabG2_2* gene encodes a 3-ketoacyl reductase of MAP and the transposon is inserted in the C-terminal half of the gene (Settles et al., 2014). This mutant has recently been shown to have defects in intestinal and liver persistence (Settles et al., 2014). Additional preliminary studies suggest that this mutation may not be stable as it could not be confirmed by PCR analysis. The Δ*fabG2_2* vaccine strain did

not outperform the commercial vaccine control in the goat trial. This result may be explained by delivery route of the attenuated strains vs. the commercial vaccine. Attenuated strains were delivered orally and the commercial vaccine was delivered subcutaneously. Ideally, the route of vaccination should have been identical, but a second objective was to validate the goat challenge model proposed by the AMSC (Hines et al., 2007). In hindsight, the route of vaccination should have been the same for all vaccines.

CONCLUSIONS

Vaccination against Johne's disease has considerable potential as a key management tool to control disease and transmission in ruminant livestock. Specifically, the use of attenuated mutants provide several advantages that include stimulation of a broad cellular immune response, ease of delivery, built in adjuvant characteristics and comparative cost. Several lessons were learned from the three-phase JDIP vaccine project as discussed below, and provide a rational framework for testing future vaccines against Johne's disease.

First, the results suggest that single gene knockout strains may not represent optimal vaccine candidates for MAP given the need to satisfy the "Goldilocks rule"—where the level of attenuation has to be just right in order to survive or replicate in target cells and stimulate a protective immune response but without causing disease. Consistent with this, while MAP vaccine candidates evaluated in the current trials were single gene knockouts, recent studies showed that a double mutant constructed in *M. tuberculosis* (Δ*fbpA*Δ*sapM* was highly attenuated in human macrophages and, intriguingly, more immunogenic than the single knockout (Δ*fbpA*) (Saikolappan et al., 2012). These data also suggest the importance of careful targeting of genes/proteins for deletion based on prior knowledge of their role in pathogenesis, immunogenicity, or pathogen survival *in vivo*. For instance, the rationale for construction of the *M. tuberculosis* (Δ*fbpA*Δ*sapM* strain was that Δ*fbpA,* which lacks Ag85, had already demonstrated immunogenicity and protection in mice, but the additional deletion of the acid phosphatase gene (Δ*sapM*) enabled the host phagosome to mature (Saikolappan et al., 2012). A considered approach for MAP vaccine candidate development that target orthologs in *M. tuberculosis* that have shown promise in vaccine efficacy trials or are known to be highly immunogenic targets seems reasonable, but has its limitations. For instance, there is no corresponding ortholog to *sapM* in MAP (Li et al., 2005), and hence, construction of a double knockout involving that locus would not be possible.

We note that the MAP vaccines evaluated herein represented the most comprehensive screen of MAP attenuated mutants to date, and included vaccine candidates with prior evidence of attenuation with *in vitro* or *in vivo* model systems that were enrolled on a volunteer basis (i.e., investigators were broadly invited and those that volunteered to participate and submit candidate vaccines were enrolled). This appears a reasonable strategy to adopt since it provides a facile and transparent mechanism for benchmarking candidate vaccines to each other to help identify the most promising candidates. However, not all described or available candidate strains of MAP were enrolled in this trial. Notably, the recently described Δ*leuD*, which provides protection in a goat model of infection (Faisal et al., 2013a) was not submitted for evaluation in the current trials, and neither were a set of invasion mutants (Alonso-Hearn et al., 2008) which should be included in future investigations.

Our studies have highlighted several major lacuna in our understanding of *in vitro* correlates of vaccine immunity and strain attenuation in MAP. For instance, how long should a strain of MAP take to be killed by phagocytes to be considered attenuated? And what are the physiologic (e.g., doubling time) or immunological (e.g., cytokine profiles elicited) correlates of protective immunity for MAP that should be considered prior to advancing a vaccine candidate? These and other similar questions regarding *in vitro* correlates of protection remain and need to be the focus of future investigations.

Second, and perhaps more importantly, the rationale for the use of the macrophage-to-mouse-to-native host pipeline for MAP vaccine development needs to be reconsidered. The survival of MAP strains in cultured macrophages has been previously used as a criterion for the selection of candidate vaccines for further testing in animal models. For instance, transposon mutants of MAP that were attenuated in macrophages were also shown to be attenuated in mice (Scandurra et al., 2009). While this strategy has been applied for selection of vaccine candidates for numerous other pathogens, particularly those that impact humans, the lack of validated or well rationalized *in vitro* correlates of protection does not enable an accurate assessment of either attenuation or immunogenicity of a given candidate *in vivo*. This shortcoming is further exacerbated by the lack of context for the host immune system and the natural milieu, and the fact that only short-term attenuation can be measured in macrophages, even though these are long-lived cells *in vivo*, can remain viable for only 48-h or so in laboratory culture. And can only measure degrees of attenuation in a somewhat artificial system that does not predict protection (Lamont et al., 2014).

The results of our investigations raise important questions on whether mice are relevant or appropriate models for assessment of anti-MAP vaccines. It has been long recognized that the mouse is not a natural host for MAP, but rather employed as a model for cost and practical (e.g., availability of immunologic reagents) considerations that may not be of relevance to infection or immunity against MAP in the natural host. By not being a natural host, challenge and vaccine studies are made difficult since it is often not possible to consistently infect mice. Furthermore, culturing of MAP from intestinal tissues (the predominant site of infection in the natural ruminant host) is rarely achieved in mice, and successfully infected animals do not exhibit any of the typical clinical signs (e.g., diarrhea) that are associated with MAP infection in ruminants. In hindsight, this is not altogether surprising since MAP infection is primarily a chronic granulomatous infection of the intestinal tract, and given that recent studies suggest that the mouse is a poor model for inflammatory conditions in humans (Seok et al., 2013), mice are not very likely to represent good models for chromic inflammatory diseases such as JD in cattle either. This is also consistent with recent observations (Scandurra et al., 2010; Park et al., 2011) that suggest attenuation in macrophages and marginal protection in the mouse model may

not be a good predictor for the ruminant host. In addition, it was previously noted that a lack of survival in bovine macrophages does not predict survival in goats. For instance, the *pknG* mutant was attenuated in macrophages and yet showed persistence in goats and the immune response elicited by the mutant did not affect colonization by the MAP challenge (Park et al., 2011).

Thankfully, unlike the situation in humans, Johne's disease investigators have the luxury working with the natural (ruminant) host despite the apparent high costs. We suggest that the ability to quickly and relatively inexpensively use macrophage/mouse models, though tempting, may represent a situation of being "penny wise and pound foolish" and in the absence of clearly articulated and validated correlates of immune protection in these models, may result in perfectly good candidates being discarded during the triage process or, as was observed in the studies described herein, apparently promising targets move forward at considerable expense, only to fail to perform as expected when evaluated in the natural host.

In sum, the results of our studies strongly suggest that future investigations of MAP vaccine candidates are best conducted in the natural host, and considerable efficiencies can be realized by using a coordinated approach and standardized protocols for comparative benchmarking and evaluation of MAP vaccine candidates.

ACKNOWLEDGMENTS

This study was supported by the USDA-CAP program entitled the Johne's Disease Integrated Program and also by USDA-APHIS-Veterinary Services. We also thank the testing institutions against which some resources were leveraged. No endorsements of reagents or equipment are implied in these studies. Special thanks are given for the expert technical assistance of Robab Katani and Lingling Li who performed many behind the scenes experiments to keep these trials moving along.

REFERENCES

Achkar, J. M., and Casadevall, A. (2013). Antibody-mediated immunity against tuberculosis: implications for vaccine development. *Cell Host Microbe* 13, 250–262. doi: 10.1016/j.chom.2013.02.009

Alonso-Hearn, M., Patel, D., Danelishvili, L., Meunier-Goddik, L., and Bermudez, L. E. (2008). The *Mycobacterium avium* subsp. *paratuberculosis* MAP3464 gene encodes an oxidoreductase involved in invasion of bovine epithelial cells through the activation of host cell Cdc42. *Infect. Immun.* 76, 170–178. doi: 10.1128/IAI.01913-06

Bannantine, J. P., Everman, J. L., Rose, S. J., Babrak, L., Katani, R., Barletta, R. G., et al. (2014). Evaluation of eight live attenuated vaccine candidates for protection against challenge with virulent *Mycobacterium avium* subspecies *paratuberculosis* in mice. *Front. Cell. Infect. Microbiol.* 4:88. doi: 10.3389/fcimb.2014.00088

Bastida, F., and Juste, R. A. (2011). Paratuberculosis control: a review with a focus on vaccination. *J. Immune Based Ther. Vaccines* 9:8. doi: 10.1186/1476-8518-9-8

Begg, D. J., and Griffin, J. F. (2005). Vaccination of sheep against *M.* paratuberculosis: immune parameters and protective efficacy. *Vaccine* 23, 4999–5008. doi: 10.1016/j.vaccine.2005.05.031

Bull, T. J., Schock, A., Sharp, J. M., Greene, M., Mckendrick, I. J., Sales, J., et al. (2013). Genomic variations associated with attenuation in *Mycobacterium avium* subsp. *paratuberculosis* vaccine strains. *BMC Microbiol.* 13:11. doi: 10.1186/1471-2180-13-11

Cavaignac, S. M., White, S. J., De Lisle, G. W., and Collins, D. M. (2000). Construction and screening of *Mycobacterium paratuberculosis* insertional mutant libraries. *Arch. Microbiol.* 173, 229–231. doi: 10.1007/s002039900132

Chandra, S., Faisal, S. M., Chen, J. W., Chen, T. T., Mcdonough, S. P., Liu, S., et al. (2012). Immune response and protective efficacy of live attenuated Salmonella vaccine expressing antigens of *Mycobacterium avium* subsp. *paratuberculosis* against challenge in mice. *Vaccine* 31, 242–251. doi: 10.1016/j.vaccine.2012.09.024

Chartier, C., Mercier, P., Pellet, M. P., and Vialard, J. (2012). Effect of an inactivated paratuberculosis vaccine on the intradermal testing of goats for tuberculosis. *Vet. J.* 191, 360–363. doi: 10.1016/j.tvjl.2011.03.009

Chen, J. M., German, G. J., Alexander, D. C., Ren, H., Tan, T., and Liu, J. (2006). Roles of Lsr2 in colony morphology and biofilm formation of *Mycobacterium smegmatis*. *J. Bacteriol.* 188, 633–641. doi: 10.1128/JB.188.2.633-641.2006

Chen, J. W., Faisal, S. M., Chandra, S., Mcdonough, S. P., Moreira, M. A., Scaria, J., et al. (2012). Immunogenicity and protective efficacy of the *Mycobacterium avium* subsp. *paratuberculosis* attenuated mutants against challenge in a mouse model. *Vaccine* 30, 3015–3025. doi: 10.1016/j.vaccine.2011.11.029

Chen, L. H., Kathaperumal, K., Huang, C. J., Mcdonough, S. P., Stehman, S., Akey, B., et al. (2008). Immune responses in mice to *Mycobacterium avium* subsp. *paratuberculosis* following vaccination with a novel 74F recombinant polyprotein. *Vaccine* 26, 1253–1262. doi: 10.1016/j.vaccine.2007.12.014

Chiodini, R. J., and Van Kruiningen, H. J. (1986). The prevalence of paratuberculosis in culled New England cattle. *Cornell Vet.* 76, 91–104.

Coad, M., Clifford, D. J., Vordermeier, H. M., and Whelan, A. O. (2013). The consequences of vaccination with the Johne's disease vaccine, Gudair, on diagnosis of bovine tuberculosis. *Vet. Rec.* 172, 266. doi: 10.1136/vr.101201

Colangeli, R., Helb, D., Vilcheze, C., Hazbon, M. H., Lee, C. G., Safi, H., et al. (2007). Transcriptional regulation of multi-drug tolerance and antibiotic-induced responses by the histone-like protein Lsr2 in *M. tuberculosis*. *PLoS Pathog.* 3:e87. doi: 10.1371/journal.ppat.0030087

Coussens, P. M. (2004). Model for immune responses to *Mycobacterium avium* subspecies *paratuberculosis* in cattle. *Infect. Immun.* 72, 3089–3096. doi: 10.1128/IAI.72.6.3089-3096.2004

Dahl, J. L., Kraus, C. N., Boshoff, H. I., Doan, B., Foley, K., Avarbock, D., et al. (2003). The role of RelMtb-mediated adaptation to stationary phase in long-term persistence of *Mycobacterium tuberculosis* in mice. *Proc. Natl. Acad. Sci. U.S.A.* 100, 10026–10031. doi: 10.1073/pnas.1631248100

Faisal, S. M., Chen, J. W., Yan, F., Chen, T. T., Useh, N. M., Yan, W., et al. (2013a). Evaluation of a *Mycobacterium avium* subsp. *paratuberculosis leuD* mutant as a vaccine candidate against challenge in a caprine model. *Clin. Vaccine Immunol.* 20, 572–581. doi: 10.1128/CVI.00653-12

Faisal, S. M., Yan, F., Chen, T. T., Useh, N. M., Guo, S., Yan, W., et al. (2013b). Evaluation of a *Salmonella* vectored vaccine expressing *Mycobacterium avium* subsp. *paratuberculosis* antigens against challenge in a goat model. *PLoS ONE* 8:e70171. doi: 10.1371/journal.pone.0070171

Foley-Thomas, E. M., Whipple, D. L., Bermudez, L. E., and Barletta, R. G. (1995). Phage infection, transfection and transformation of *Mycobacterium avium* complex and *Mycobacterium paratuberculosis*. *Microbiology* 141(Pt 5), 1173–1181. doi: 10.1099/13500872-141-5-1173

Garrido, J. M., Vazquez, P., Molina, E., Plazaola, J. M., Sevilla, I. A., Geijo, M. V., et al. (2013). Paratuberculosis vaccination causes only limited cross-reactivity in the skin test for diagnosis of bovine tuberculosis. *PLoS ONE* 8:e80985. doi: 10.1371/journal.pone.0080985

Harris, N. B., Feng, Z., Liu, X., Cirillo, S. L., Cirillo, J. D., and Barletta, R. G. (1999). Development of a transposon mutagenesis system for *Mycobacterium avium* subsp. *paratuberculosis*. *FEMS Microbiol. Lett.* 175, 21–26.

Hines, M. E., 2nd, Stabel, J. R., Sweeney, R. W., Griffin, F., Talaat, A. M., Bakker, D., et al. (2007). Experimental challenge models for Johne's disease: a review and proposed international guidelines. *Vet. Microbiol.* 122, 197–222. doi: 10.1016/j.vetmic.2007.03.009

Hines, M. E., 2nd, Turnquist, S. E., Ilha, M. R. S., Rajeev, S., Jones, A. L., Whittington, L., et al. (2014). Evaluation of novel oral vaccine candidates and validation of a caprine model of Johne's disease. *Front. Cell. Infect. Microbiol.* 4:26. doi: 10.3389/fcimb.2014.00026

Hostetter, J. M., Steadham, E. M., Haynes, J. S., Bailey, T. B., and Cheville, N. F. (2002). Cytokine effects on maturation of the phagosomes containing *Mycobacteria avium* subspecies *paratuberculosis* in J774 cells. *FEMS Immunol. Med. Microbiol.* 34, 127–134. doi: 10.1111/j.1574-695X.2002.tb00613.x

Huntley, J. F., Stabel, J. R., Paustian, M. L., Reinhardt, T. A., and Bannantine, J. P. (2005). Expression library immunization confers protection against

Mycobacterium avium subsp. *paratuberculosis* infection. *Infect. Immun.* 73, 6877–6884. doi: 10.1128/IAI.73.10.6877-6884.2005

Johnston, C. D., Bannantine, J. P., Govender, R., Endersen, L., Pletzer, D., Weingart, H., et al. (2014). Enhanced expression of codon optimized *Mycobacterium avium* subsp. *paratuberculosis* antigens in *Lactobacillus* salivarius. *Front. Cell. Infect. Microbiol.* 4:120. doi: 10.3389/fcimb.2014.00120

Kabara, E., and Coussens, P. M. (2012). Infection of primary bovine macrophages with *Mycobacterium avium* subspecies *paratuberculosis* suppresses host cell apoptosis. *Front. Microbiol.* 3:215. doi: 10.3389/fmicb.2012.00215

Kalis, C. H., Hesselink, J. W., Barkema, H. W., and Collins, M. T. (2001). Use of long-term vaccination with a killed vaccine to prevent fecal shedding of *Mycobacterium avium* subsp *paratuberculosis* in dairy herds. *Am. J. Vet. Res.* 62, 270–274. doi: 10.2460/ajvr.2001.62.270

Kathaperumal, K., Kumanan, V., Mcdonough, S., Chen, L. H., Park, S. U., Moreira, M. A., et al. (2009). Evaluation of immune responses and protective efficacy in a goat model following immunization with a coctail of recombinant antigens and a polyprotein of *Mycobacterium avium* subsp. *paratuberculosis*. *Vaccine* 27, 123–135. doi: 10.1016/j.vaccine.2008.10.019

Kathaperumal, K., Park, S. U., Mcdonough, S., Stehman, S., Akey, B., Huntley, J., et al. (2008). Vaccination with recombinant *Mycobacterium avium* subsp. *paratuberculosis* proteins induces differential immune responses and protects calves against infection by oral challenge. *Vaccine* 26, 1652–1663. doi: 10.1016/j.vaccine.2008.01.015

Knust, B., Patton, E., Ribeiro-Lima, J., Bohn, J. J., and Wells, S. J. (2013). Evaluation of the effects of a killed whole-cell vaccine against *Mycobacterium avium* subsp. *paratuberculosis* in 3 herds of dairy cattle with natural exposure to the organism. *J. Am. Vet. Med. Assoc.* 242, 663–669. doi: 10.2460/javma.242.5.663

Koets, A., Hoek, A., Langelaar, M., Overdijk, M., Santema, W., Franken, P., et al. (2006). Mycobacterial 70 kD heat-shock protein is an effective subunit vaccine against bovine *paratuberculosis*. *Vaccine* 24, 2550–2559. doi: 10.1016/j.vaccine.2005.12.019

Lamont, E. A., Talaat, A. M., Coussens, P. M., Bannantine, J. P., Grohn, Y. T., Katani, R., et al. (2014). Screening of *Mycobacterium avium* subsp. *paratuberculosis* mutants for attenuation in a bovine monocyte-derived macrophage model. *Front. Cell. Infect. Microbiol.* 4:87. doi: 10.3389/fcimb.2014.00087

Li, L., Bannantine, J. P., Zhang, Q., Amonsin, A., May, B. J., Alt, D., et al. (2005). The complete genome sequence of *Mycobacterium avium* subspecies *paratuberculosis*. *Proc. Natl. Acad. Sci. U.S.A.* 102, 12344–12349. doi: 10.1073/pnas.0505662102

Lombard, J. E., Gardner, I. A., Jafarzadeh, S. R., Fossler, C. P., Harris, B., Capsel, R. T., et al. (2013). Herd-level prevalence of *Mycobacterium avium* subsp. *paratuberculosis* infection in United States dairy herds in 2007. *Prev. Vet. Med.* 108, 234–238. doi: 10.1016/j.prevetmed.2012.08.006

Lu, Z., Mitchell, R. M., Smith, R. L., Van Kessel, J. S., Chapagain, P. P., Schukken, Y. H., et al. (2008). The importance of culling in Johne's disease control. *J. Theor. Biol.* 254, 135–146. doi: 10.1016/j.jtbi.2008.05.008

Lu, Z., Schukken, Y. H., Smith, R. L., and Gröhn, Y. T. (2013). Using vaccination to prevent the invasion of *Mycobacterium avium* subsp. *paratuberculosis* in dairy herds: a stochastic simulation study. *Prev. Vet. Med*. 110, 335–345. doi: 10.1016/j.prevetmed.2013.01.006

Magombedze, G., Eda, S., and Ganusov, V. V. (2014). Competition for antigen between Th1 and Th2 responses determines the timing of the immune response switch during *Mycobaterium avium* subspecies *paratuberulosis* infection in ruminants. *PLoS Comput. Biol.* 10:e1003414. doi: 10.1371/journal.pcbi.1003414

Mangtani, P., Abubakar, I., Ariti, C., Beynon, R., Pimpin, L., Fine, P. E., et al. (2014). Protection by BCG vaccine against tuberculosis: a systematic review of randomized controlled trials. *Clin. Infect. Dis.* 58, 470–480. doi: 10.1093/cid/cit790

Merkal, R. S., and Curran, B. J. (1974). Growth and metabolic characteristics of Mycobacterium *paratuberculosis*. *Appl. Microbiol.* 28, 276–279.

Merkal, R. S., Whipple, D. L., Sacks, J. M., and Snyder, G. R. (1987). Prevalence of *Mycobacterium paratuberculosis* in ileocecal lymph nodes of cattle culled in the United States. *J. Am. Vet. Med. Assoc.* 190, 676–680.

Muskens, J., Van Zijderveld, F., Eger, A., and Bakker, D. (2002). Evaluation of the long-term immune response in cattle after vaccination against paratuberculosis in two Dutch dairy herds. *Vet. Microbiol.* 86, 269–278. doi: 10.1016/S0378-1135(02)00006-8

Park, K. T., Allen, A. J., Bannantine, J. P., Seo, K. S., Hamilton, M. J., Abdellrazeq, G. S., et al. (2011). Evaluation of two mutants of *Mycobacterium avium* subsp. *paratuberculosis* as candidates for a live attenuated vaccine for Johne's disease. *Vaccine* 29, 4709–4719. doi: 10.1016/j.vaccine.2011.04.090

Park, K. T., Allen, A. J., Barrington, G. M., and Davis, W. C. (2014). Deletion of *relA* abrogates the capacity of *Mycobacterium avium paratuberculosis* to establish an infection in calves. *Front. Cell. Infect. Microbiol.* 4:64. doi: 10.3389/fcimb.2014.00064

Park, K. T., Dahl, J. L., Bannantine, J. P., Barletta, R. G., Ahn, J., Allen, A. J., et al. (2008a). Demonstration of allelic exchange in the slow-growing bacterium *Mycobacterium avium* subsp. *paratuberculosis*, and generation of mutants with deletions at the *pknG*, *relA*, and *lsr2* loci. *Appl. Environ. Microbiol.* 74, 1687–1695. doi: 10.1128/AEM.01208-07

Park, S. U., Kathaperumal, K., Mcdonough, S., Akey, B., Huntley, J., Bannantine, J. P., et al. (2008b). Immunization with a DNA vaccine cocktail induces a Th1 response and protects mice against *Mycobacterium avium* subsp. *paratuberculosis* challenge. *Vaccine* 26, 4329–4337. doi: 10.1016/j.vaccine.2008.06.016

Perez De Val, B., Nofrarias, M., Lopez-Soria, S., Garrido, J. M., Vordermeier, H. M., Villarreal-Ramos, B., et al. (2012). Effects of vaccination against paratuberculosis on tuberculosis in goats: diagnostic interferences and cross-protection. *BMC Vet. Res.* 8:191. doi: 10.1186/1746-6148-8-191

Pradhan, A. K., Mitchell, R. M., Kramer, A. J., Zurakowski, M. J., Fyock, T. L., Whitlock, R. H., et al. (2011). Molecular epidemiology of *Mycobacterium avium* subsp. *paratuberculosis* in a longitudinal study of three dairy herds. *J. Clin. Microbiol.* 49, 893–901. doi: 10.1128/JCM.01107-10

Reddacliff, L., Eppleston, J., Windsor, P., Whittington, R., and Jones, S. (2006). Efficacy of a killed vaccine for the control of paratuberculosis in Australian sheep flocks. *Vet. Microbiol.* 115, 77–90. doi: 10.1016/j.vetmic.2005.12.021

Saikolappan, S., Estrella, J., Sasindran, S. J., Khan, A., Armitige, L. Y., Jagannath, C., et al. (2012). The *fbpA/sapM* double knock out strain of *Mycobacterium tuberculosis* is highly attenuated and immunogenic in macrophages. *PLoS ONE* 7:e36198. doi: 10.1371/journal.pone.0036198

Saxegaard, F., and Fodstad, F. H. (1985). Control of paratuberculosis (Johne's disease) in goats by vaccination. *Vet. Rec.* 116, 439–441. doi: 10.1136/vr.116.16.439

Scandurra, G. M., De Lisle, G. W., Cavaignac, S. M., Young, M., Kawakami, R. P., and Collins, D. M. (2010). Assessment of live candidate vaccines for paratuberculosis in animal models and macrophages. *Infect. Immun.* 78, 1383–1389. doi: 10.1128/IAI.01020-09

Scandurra, G. M., Young, M., De Lisle, G. W., and Collins, D. M. (2009). A bovine macrophage screening system for identifying attenuated transposon mutants of *Mycobacterium avium* subsp. paratuberculosis with vaccine potential. *J. Microbiol. Methods* 77, 58–62. doi: 10.1016/j.mimet.2009.01.005

Seok, J., Warren, H. S., Cuenca, A. G., Mindrinos, M. N., Baker, H. V., Xu, W., et al. (2013). Genomic responses in mouse models poorly mimic human inflammatory diseases. *Proc. Natl. Acad. Sci. U.S.A.* 110, 3507–3512. doi: 10.1073/pnas.1222878110

Seth, M., Lamont, E. A., Janagama, H. K., Widdel, A., Vulchanova, L., Stabel, J. R., et al. (2009). Biomarker discovery in subclinical mycobacterial infections of cattle. *PLoS ONE* 4:e5478. doi: 10.1371/journal.pone.0005478

Settles, E. W., Kink, J. A., and Talaat, A. (2014). Attenuated strains of *Mycobacterium avium* subspecies *paratuberculosis* as vaccine candidates against Johne's disease. *Vaccine* 32, 2062–2069. doi: 10.1016/j.vaccine.2014.02.010

Shin, S. J., Wu, C. W., Steinberg, H., and Talaat, A. M. (2006). Identification of novel virulence determinants in *Mycobacterium paratuberculosis* by screening a library of insertional mutants. *Infect. Immun.* 74, 3825–3833. doi: 10.1128/IAI.01742-05

Stabel, J. R. (1998). Johne's disease: a hidden threat. *J. Dairy Sci.* 81, 283–288. doi: 10.3168/jds.S0022-0302(98)75577-8

Stabel, J. R. (2000). Transitions in immune responses to *Mycobacterium paratuberculosis*. *Vet. Microbiol.* 77, 465–473. doi: 10.1016/S0378-1135(00)00331-X

Stabel, J. R. (2010). "Immunology of paratuberculosis infection and disease," in *Paratuberculosis: Organism, Disease, Control*, eds M. A. Behr and D. M. Collins (Cambridge: CAB International), 230–243.

Stabel, J. R., Barnhill, A., Bannantine, J. P., Chang, Y. F., and Osman, M. A. (2012). Evaluation of protection in a mouse model after vaccination with *Mycobacterium avium* subsp. *paratuberculois* protein cocktails. *Vaccine* 31, 127–134. doi: 10.1016/j.vaccine.2012.10.090

Stabel, J. R., Waters, W. R., Bannantine, J. P., and Lyashchenko, K. (2011). Mediation of host immune responses after immunization of neonatal calves

with a heat-killed *Mycobacterium avium* subsp. *paratuberculosis* vaccine. *Clin. Vaccine Immunol.* 18, 2079–2089. doi: 10.1128/CVI.05421-11

Stringer, L. A., Wilson, P. R., Heuer, C., Hunnam, J. C., Verdugo, C., and Mackintosh, C. G. (2013a). Prevalence of *Mycobacterium avium* subsp. *paratuberculosis* in farmed red deer (*Cervus elaphus*) with grossly normal mesenteric lymph nodes. *N. Z. Vet. J.* 61, 147–152. doi: 10.1080/00480169.2012.755888

Stringer, L. A., Wilson, P. R., Heuer, C., and Mackintosh, C. G. (2013b). A randomised controlled trial of Silirum vaccine for control of paratuberculosis in farmed red deer. *Vet. Rec.* 173:551. doi: 10.1136/vr.101799

Sweeney, R. W., Whitlock, R. H., Bowersock, T. L., Cleary, D. L., Meinert, T. R., Habecker, P. L., et al. (2009). Effect of subcutaneous administration of a killed *Mycobacterium avium* subsp. *paratuberculosis* vaccine on colonization of tissues following oral exposure to the organism in calves. *Am. J. Vet. Res.* 70, 493–497. doi: 10.2460/ajvr.70.4.493

Walburger, A., Koul, A., Ferrari, G., Nguyen, L., Prescianotto-Baschong, C., Huygen, K., et al. (2004). Protein kinase G from pathogenic mycobacteria promotes survival within macrophages. *Science* 304, 1800–1804. doi: 10.1126/science.1099384

Whittington, R. J., Marsh, I. B., Saunders, V., Grant, I. R., Juste, R., Sevilla, I. A., et al. (2011). Culture phenotypes of genomically and geographically diverse *Mycobacterium avium* subsp. *paratuberculosis* isolates from different hosts. *J. Clin. Microbiol.* 49, 1822–1830. doi: 10.1128/JCM.00210-11

Wu, C. W., Schmoller, S. K., Bannantine, J. P., Eckstein, T. M., Inamine, J. M., Livesey, M., et al. (2009). A novel cell wall lipopeptide is important for biofilm formation and pathogenicity of *Mycobacterium avium* subspecies *paratuberculosis*. *Microb. Pathog.* 46, 222–230. doi: 10.1016/j.micpath.2009.01.010

Yuan, Y., Lee, R. E., Besra, G. S., Belisle, J. T., and Barry, C. E. 3rd. (1995). Identification of a gene involved in the biosynthesis of cyclopropanated mycolic acids in *Mycobacterium tuberculosis*. *Proc. Natl. Acad. Sci. U.S.A.* 92, 6630–6634. doi: 10.1073/pnas.92.14.6630

Zhu, X., Tu, Z. J., Coussens, P. M., Kapur, V., Janagama, H., Naser, S., et al. (2008). Transcriptional analysis of diverse strains *Mycobacterium avium* subspecies *paratuberculosis* in primary bovine monocyte derived macrophages. *Microbes Infect.* 10, 1274–1282. doi: 10.1016/j.micinf.2008.07.025

Conflict of Interest Statement: The authors declare that the research was conducted in the absence of any commercial or financial relationships that could be construed as a potential conflict of interest.

Received: 20 June 2014; accepted: 20 August 2014; published online: 09 September 2014.

Citation: Bannantine JP, Hines ME II, Bermudez LE, Talaat AM, Sreevatsan S, Stabel JR, Chang Y-F, Coussens PM, Barletta RG, Davis WC, Collins DM, Gröhn YT and Kapur V (2014) A rational framework for evaluating the next generation of vaccines against Mycobacterium avium subspecies paratuberculosis. Front. Cell. Infect. Microbiol. ***4****:126. doi: 10.3389/fcimb.2014.00126*

This article was submitted to the journal Frontiers in Cellular and Infection Microbiology.

frontiers in
CELLULAR AND INFECTION MICROBIOLOGY

ORIGINAL RESEARCH ARTICLE
published: 15 May 2014
doi: 10.3389/fcimb.2014.00064

Deletion of *relA* abrogates the capacity of *Mycobacterium avium paratuberculosis* to establish an infection in calves

***Kun Taek Park*[1], *Andrew J. Allen*[2], *George M. Barrington*[2] *and William C. Davis*[1]*

[1] *Department of Microbiology and Pathology, College of Veterinary Medicine, Washington State University, Pullman, WA, USA*
[2] *Department of Veterinary Clinical Sciences, College of Veterinary Medicine, Washington State University, Pullman, WA, USA*

Edited by:
John Bannantine, National Animal Disease Center, USA

Reviewed by:
Eric Ghigo, National Centre for Scientific Research, France
John Bannantine, National Animal Disease Center, USA

****Correspondence:***
William C. Davis, Department of Microbiology and Pathology, College of Veterinary Medicine, Washington State University, Pullman, WA 99164-7040, USA
e-mail: davisw@vetmed.wsu.edu

Previous comparative studies in goats revealed deletion of *relA* but not *pknG* abrogates the capacity of *Mycobacterium avium* subsp. *paratuberculosis* (*Map*) to establish a persistent infection. The immune response elicited by the mutant cleared infection. The objective of the present study was to extend the studies in calves and compare the proliferative response elicited by the *relA* deletion mutant (Δ*relA*) and *Map* using flow cytometry and quantitative reverse transcription real-time PCR (qRT-PCR). Six 3-day-old calves were divided into two groups. Three were vaccinated with Δ*relA* and 3 inoculated with wild type *Map*. The calves were challenged with *Map* 1 month later and necropsied 3 months post challenge. Three untreated calves were used as uninfected controls. Examination of tissues revealed the Δ*relA* mutant was immune eliminated. Bacterial load of *Map* was significantly reduced in the calves vaccinated with Δ*relA* and challenged with *Map* in comparison with calves inoculated and challenged with *Map*. A vigorous CD4 memory T cell response was detected at necropsy in PBMC from both infected groups. CD8 positive NK cells proliferated in the presence and absence of antigen stimulation in both treated groups but not in the uninfected group. IFN-γ, IL17, and IL22 gene expression were up-regulated with an associated increase in their transcription factors, Tbet and RORC, in both treated groups. TGF-β, IL-10, and FoxP3 were not up-regulated, indicating no activation of regulatory T cells. The findings show that the immune response to Δ*relA* is clearly different than the response to *Map*. Understanding the immunological basis for this difference should facilitate development of a vaccine that elicits sterile immunity.

Keywords: *Mycobacterium avium* subsp. *paratuberculosis*, *relA*, immune response, IL-12R, IL-23R, regulatory T cells

INTRODUCTION

As part of an international effort to develop a vaccine that prevents or limits the capacity of *Mycobacterium avium* subsp. *paratuberculosis* (*Map*) to establish a persistent infection and cause disease, we focused on use of targeted allelic exchange mutagenesis to identify genes essential for establishment of a persistent infection. We selected 3 genes to initiate the studies and optimize use of allelic exchange mutagenesis with slow growing mycobacteria: *relA* (a global regulator), *pknG* (a gene encoding a kinase that interferes with phagosome lysosome fusion), and *lsr2* (a gene regulating lipid biosynthesis and antibiotic resistance) (Park et al., 2008). Our first studies revealed the efficiency of allelic exchange transduction, with a mycobacterial phage containing an allelic exchange substrate, could be enhanced by allowing aggregates of *Map* to sediment out of the culture to obtain a cell preparation comprised of single cells and by increasing the selective pressure with hygromycin (Park et al., 2008). Subsequent studies revealed deletion of these genes impaired survival in macrophages *ex vivo* in comparison with survival of *Map*, suggesting deletion of any of these genes might impair survival *in vivo*. Based on these findings, the mutants were submitted to the JDIP-APHIS Vaccine Testing Program for further evaluation along with other potential vaccine candidates. Studies were also conducted in parallel to test the capacity of the mutants to establish an infection. Preliminary studies in calves with the *relA* and *pknG* deletion mutants (Δ*relA* and Δ*pknG*) revealed immunization with Δ*relA* elicited an immune response that cleared infection, as assessed by screening tissues for the presence of Δ*relA*, whereas, immunization with *pknG* elicited an immune response that only impaired establishment of an infection with Δ*pknG* (Park et al., 2011). A subsequent challenge study in kid goats with all 3 mutants revealed Δ*relA* elicited an immune response that cleared the mutant and impaired establishment of an infection with *Map*. Deletion of *pknG* did not prevent establishment of an infection with Δ*pknG* or impair establishment of infection with *Map* (Park et al., 2011). Deletion of *lsr2* resulted in attenuation of *in vivo* survival, but immunization with the mutant did not elicit an immune response that limited infection with *Map* (unpublished observation). The present study was conducted to verify and extend observations made with Δ*relA* using a calf challenge model. The current study includes analyses of cytokine gene expression profiles and the proliferative response of NK cells, γδ and αβ T cells, and Foxp3 regulatory T cells following stimulation with live *Map* using quantitative reverse transcription real-time PCR (qRT-PCR) and flow cytometric (FC) analysis which were not done in the previous goat challenge study.

Group	Animal	JP	JM	JD	IP	IM	ID	ICV	ML	IL
K10	Steer 1	-[a]	-	TNTC[b,+]	TNTC[+]	TNTC[+]	2.0[c,+]	5.7[+]	29.3[+]	TNTC[+]
K10	Steer 2	1.7[+]	-	-[+]	2.7[+]	TNTC[+]	22.3[+]	TNTC[+]	197.7[+]	TNTC[+]
K10	Steer 6	-	-	5.3[+]	2.3[+]	24.7[+]	-	20.3[+]	TNTC[+]	TNTC[+]
RelA	Steer 3	-	-	-	-	-	-[+]	4.3[+]	12.3[+]	289.3[+]
RelA	Steer 4	-	-	55.3[+]	-	-	4.0[+]	-	1.3	174.3[+]
RelA	Steer 5	-	-	-	-[+]	-	56.3[+]	-	43.3[+]	135.3[+]

FIGURE 1 | *Map* culture results from nine tissue sites processed at necropsy. The data are expressed as the average CFU of triplicate agar cultures containing no hygromycin. No colonies were detected in the agar cultures containing hygromycin, which indicates Δ*relA* was cleared in the vaccinated animal. JP, JM, JD: jejunum proximal, middle, distal; IP, IM, ID: ileum proximal, middle, distal; ICV: ileocecal valve; ML, IL: mesenteric and ileocecal lymph nodes. a, Negative; b, too numerous to count; c, Values are expressed as the average CFU obtained from three agar cultures; +, positive by IS900 qPCR.

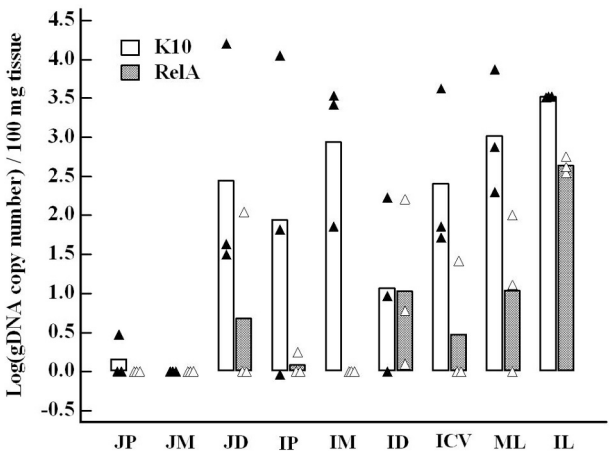

FIGURE 2 | Comparison of bacterial loads in each tissue site between K10 and RelA groups. *Map* gDNA copy number per 100 mg tissue of each sample measured by IS900 qPCR was transformed to a log scale. The results were compared for the same tissue site between the two groups. Data are presented as the average of three animals of each group (bar graph) with all individual data (K10 group, closed triangle, and RelA group, open triangle, respectively). JP, JM, JD: jejunum proximal, middle, distal; IP, IM, ID: ileum proximal, middle, distal; ICV: ileocecal valve; ML, IL: mesenteric and ileocecal lymph nodes. The bacterial loads in IM and IL were statistically significant between the two groups ($p < 0.05$).

MATERIALS AND METHODS

ANIMALS

Six bull calves were obtained from the Johne's disease-free Washington State University dairy herd and maintained according to the protocols and procedures approved by the Washington State University Institutional Animal Care and Use Committee. The calves were taken to a Biosafety Level 2 isolation unit within the first 24 h of life and separated into groups of three. They were fed 4 L of maternally derived colostrum within 6 h of birth and subsequently fed milk replacer, whey pellets, calf starter grain, and then free choice alfalfa hay during the study. Three additional calves (untreated control group) of the same age as the experimental calves, maintained at the dairy, were used as uninfected controls.

PREPARATION OF BACTERIA, INOCULATION, AND CHALLENGE

Cultures of *Map* and Δ*relA* were prepared as previously described (Park et al., 2011). Three calves were inoculated per os with 10^9 *Map* K10 strain (K10 group) and three with 10^9 Δ*relA* (RelA group) within 3 days of birth. At 1 month post inoculation they were challenged with 10^9 *Map* K10 per os and then necropsied at 3 months post challenge. All inoculation and challenge bacteria were prepared in 1 L of milk.

PERIPHERAL BLOOD MONONUCLEAR CELL ISOLATION AND STIMULATION

Blood was collected at the time of necropsy, and peripheral blood mononuclear cells (PBMC) were isolated and cultured in RPMI-1640 medium with and without live *Map* as previously described (Park et al., 2011). PBMC were processed for transcriptional analysis of cytokine genes at day 3 and for FC analysis at day 6 of culture as described below.

FLOW CYTOMETRY

Monoclonal antibodies (mAb) specific for NK (CD335, IgG1), TCR1 δ chain (GB21A, IgG2b), CD2 (MUC2A, IgG2a), CD4 (ILA11A, IgG2a), CD8 (7C2B, IgG2a), CD25 (LCTB2A, IgG3 and CACT116A, IgG1), and CD45R0 (ILA116A, IgG3) were used for FC analysis to study the response of PBMC *ex vivo* (Allen et al., 2009, 2011). A mAb specific for transcription factor FoxP3 (FOX5A, IgG1) was used to study the regulatory T cell (Tr) response (Seo et al., 2009). The intracellular labeling of FoxP3 was conducted using the Foxp3/Transcription Factor Staining Buffer Set following the manufacture's recommendation (eBioscience, CA).

GENE EXPRESSION

RNA extraction from PBMC, cDNA generation, and qRT-PCR were conducted as previously described (Park et al., 2011). The sequence information of all primers used in the current study were as previously described (Park et al., 2011). The following genes were examined for expression: IFN-γ, TGF-β, FoxP3, IL-10, IL-12p35, IL-17, IL-22, IL-23p19, and granulysin (a mycobactericidal peptide) (Dieli et al., 2001; Gansert et al., 2003).

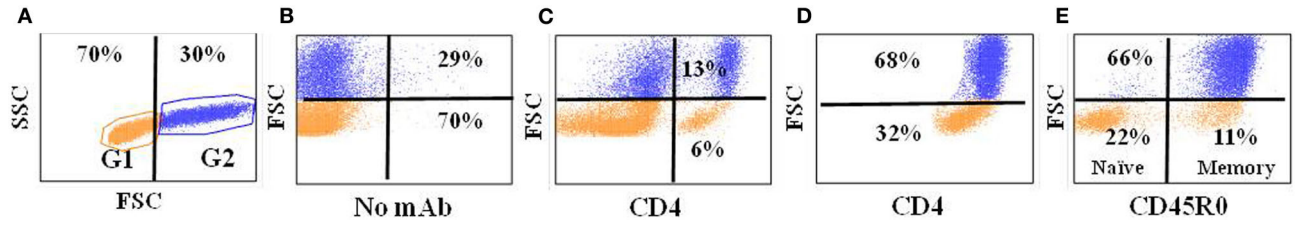

FIGURE 3 | Gating strategy used to analyze the proliferative response of peripheral blood mononuclear cells (PBMC) *ex vivo* following stimulation with live *Map*. Representative CD4 profiles obtained with PBMC from a calf inoculated/vaccinated with Δ*relA* and challenged with wild type *Map*. **(A)** Selective gates were placed on resting/unstimulated cells (G1) and stimulated proliferating cells (G2) and color coded to track activated cells. **(B)** Cells with no mAb. **(C)** Cells labeled with CD4 with no gate to show relative percent of resting and activated CD4 cells. **(D)** CD4 cells with a gate to select CD4 cells for analysis. **(E)** CD4 cells showing expression of CD45R0 only on memory cells. The activated cells (blue) also expressed CD25.

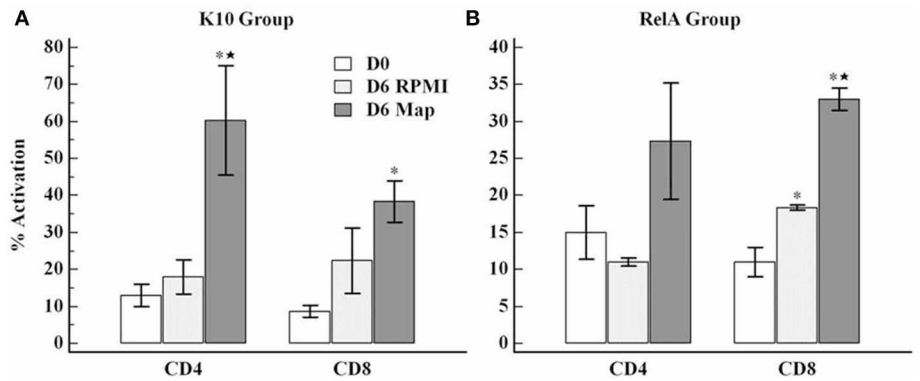

FIGURE 4 | Flow cytometric analysis of the proliferative response of PBMC cultured *ex vivo* in absence/presence of live *Map*. The figure shows the frequency of activated CD4 (CD4/CD25/CD45R0 positive) or CD8 (CD8/CD25/CD45R0 positive) cells obtained with PBMC from the K10 group **(A)** and the *relA* group **(B)**. The data represent the mean percent activation of CD4 and CD8 T cells with error bar (SE). D0, PBMC at day 0; D6 rpmI and D6 *Map*, PBMC cultured in medium alone and with live *Map* for 6 days, respectively; * and ★, significant difference compared to D0 and D6 rpmI, respectively ($p < 0.05$).

DETECTION AND QUANTIFICATION OF *Map* IN TISSUE AT NECROPSY

Triplicate samples of nine tissue sites were processed for *Map* culture and duplicates for quantitative real-time PCR (qPCR) detection of IS900 sequence to detect and quantify *Map* in tissues. Tissues were cultured with and without hygromycin to distinguish colonies of Δ*relA* from *Map*. An average colony forming unit (CFU) from each tissue site was obtained as previously described (Park et al., 2011). *Map* genomic DNA (gDNA) extraction from tissues was conducted as previously described (Park et al., 2014). The copy number of *Map* gDNA in the sample was quantified by IS900 qPCR (Irenge et al., 2009). *Map* gDNA copy number per 100 mg tissue of each tissue was transformed to a log scale, and compared between K10 and RelA groups for the same tissue sites. Note that the value of qPCR negative tissue (0 gDNA copy) was transformed to 0 of log value for a graph and comparison.

STATISTICS

MedCalc statistical software ver. 11. 2. 1 (Belgium) was used for all statistical analyses. The frequencies of *Map* tissue culture positive sites between K10 and RelA groups were compared using Fisher's exact test. The transformed log value of *Map* gDNA copy number was used to compare the bacterial loads in each tissue site between K10 and RelA groups using Kruskal–Wallis test or One-Way ANOVA. The results of FC analysis for CD4 and CD8 T cell activation and qRT-PCR for relative gene transcriptions were analyzed using Kruskal–Wallis test or One-Way ANOVA. In all tests, a *p*-value of less than 0.05 was considered to be significant.

RESULTS

No colonies of Δ*relA* were detected in any of the tissues from calves inoculated with Δ*relA* (**Figure 1**). The frequency of *Map* culture positive tissues was reduced in the RelA group (10 positive tissues out of 27 screened tissues, 37.0 %) in comparison with that in K10 group (20/27 positive tissues, 74.1 %) ($p < 0.05$, **Figure 1**). To compare the bacterial loads in the tissues, *Map* gDNA copy number per 100 mg tissue of each tissue sample was calculated using IS900 qPCR since the exact CFU information of many tissue sites of K10 group were not available due to the excess of countable ranges (too numerous to count, TNTC). We previously demonstrated an excellent correlation between the quantification of *Map* gDNA in tissues by qPCR and CFU obtained by *Map* culture from the samples (Park et al., 2014). The average gDNA copy numbers of the RelA group were higher than K10 group for all tissue sites processed, except the tissue samples of middle jejunum (all negative in both groups). For 5 tissue sites (distal jejunum, proximal ileum, middle ileum, ileocecal valve, and mesenteric lymph node) the differences of bacterial loads

between the two groups were more than 1.5 logs per 100 mg tissue (**Figure 2**).

A representative gating strategy used for FC analysis of fresh and cultured PBMC is shown in **Figure 3**. CD4 T cells proliferated in response to stimulation with live *Map* and expressed CD25 and CD45R0 (**Figures 3**, **4**). By using a negative electronic gate to exclude CD8 positive NK cells it was possible to show CD8 positive αβ T cells also proliferated in response to *Map* stimulation (**Figure 4**). FC analysis of NK cells revealed NK cells were activated and proliferated in culture medium alone and in the presence of *Map*. The majority of activated NK cells expressed CD2 and CD8 (**Figure 5**, data only shown for CD8). WC1 positive and WC1 negative γδ T cells were not activated in this study (data not shown).

FC analysis of FoxP 3 (**Figure 6**) showed the proportion of CD4 T cells expressing FoxP3 was low at initiation of culture in calves in the K10 group (2.4% ± 0.5 SE) and calves in the RelA group (4.7% ± 1.2 SE). The proportion of CD4 T cells expressing FoxP3 increased in cells cultured in medium alone (K10 group: 4.0% ± 0.3, and RelA group: 11.0% ± 2.6, respectively) while there was minimal change in cells cultured with live *Map* (K10 group: 2.0% ± 1.1, and *relA* group: 6.0 ± 0.9%, respectively). The overall proportion of Foxp3 expressing CD4 T cells was slightly higher in the RelA group than in the K10 group.

Analysis of expression of cytokines associated with the Th1 (IL-12p35, IFN-γ, and transcription factor Tbet) and Th17 (IL-23, IL-17, and IL-22, and transcription factor RORC) axes in cultured PBMC showed there was an increase in expression in both K10 and RelA groups in cells cultured in medium alone and in the presence of *Map* in comparison with the uninfected control group (**Figures 7**, **8**).

The regulatory cytokine gene responses in PBMC varied. In comparison with the uninfected control group, the transcription factor (FoxP3) and TGF-β were slightly up-regulated, but the expression of IL-10 was highly down-regulated in the infected groups (**Figure 9**).

The expression of granulysin, a mycobactericidal peptide, was slightly up-regulated against *Map* stimulation in the control group. However, the up-regulation was more significant in the challenged groups (**Figure 10**).

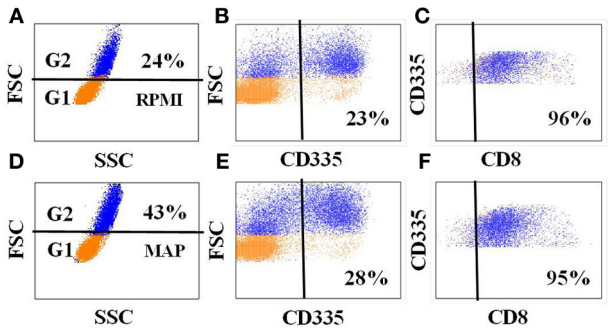

FIGURE 5 | Expression of CD8 on NK cells in PBMC from *Map* infected animals. Data show the expression of CD8 on NK cells in PBMC cultured in medium alone **(A–C)** and in the presence of *Map* **(D–F)**. An additional gate was placed on NK cells to show co-expression of CD8 **(C,F)**.

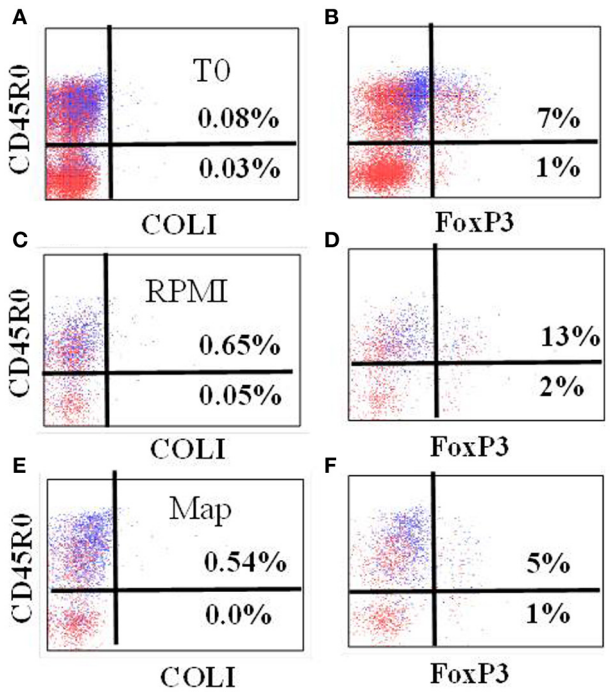

FIGURE 6 | Representative profiles showing expression of FoxP3 in gated CD4 T cells at T0 (A,B), and cultured in RPMI alone (C,D) and stimulated with live *Map* (E,F) from a calf of RelA group. As noted, use of anti-CD45R0 rather than anti-CD25 provides better resolution of cells expressing FoxP3. COLI = isotype control.

DISCUSSION

Methods for analysis of the effect of gene disruption on the immune response to *Map* remain a problem. The current strategy has been to examine the effect of mutation on survival in macrophages, then screen selected mutants for survival in mice and their ability to elicit an immune response that prevents or limits establishment of infection, and finally test promising mutants for efficacy in one of the natural hosts. Recent studies have emphasized the limitations of this approach and the potential of missing the best candidates for analysis (Scandurra et al., 2010; Park et al., 2011). A reduction in the capacity to survive in macrophages does not necessarily predict survival *in vivo* or the immune response to the mutant. Testing in an animal model, like the mouse, is more direct but it does not necessarily predict the immune response in the natural host (Scandurra et al., 2010). Clearly, the more reliable method would be to examine the immune response in the natural host. Even here, the ability to study the effect of gene deletion on the immune response is limited. Necropsy and examination of tissues is needed to determine if deletion of a gene abrogates the capacity of *Map* to subvert the immune response and evade immune elimination. Although arduous, this approach does provide a means for identifying candidate mutants for further evaluation.

Results from the first round of screening candidate mutants in macrophages for inclusion in the JDIP-APHIS Vaccine Testing Program, suggested none of the mutants we developed, including

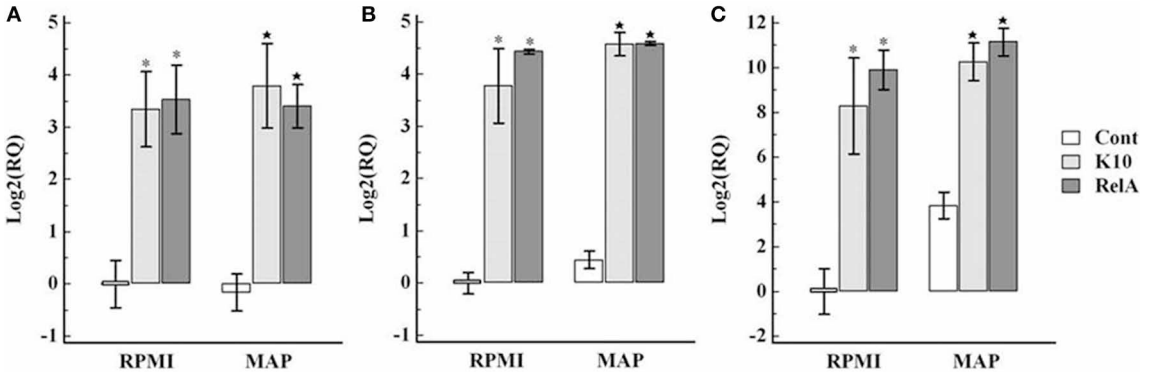

FIGURE 7 | Relative transcription of genes involved in Th1 type immune response in PBMC. PBMC were isolated from animals in each group and cultured with and without live *Map* for 3 days. The level of mRNA transcription of PBMC was measured by qRT-PCR. The relative quantification of each cytokine was calculated using the value of PBMC isolated from control animals (uninfected animals) and cultured in RPMI medium alone as the calibrator. The panels show the relative quantification of IL-12p35 **(A)**, Tbet **(B)**, IFN-γ **(C)**. RQ, relative quantification; RPMI and *MAP*, PBMC cultured in RPMI medium alone and with live *Map*, respectively; * and ★, significant difference compared to RPMI and MAP of the control group, respectively.

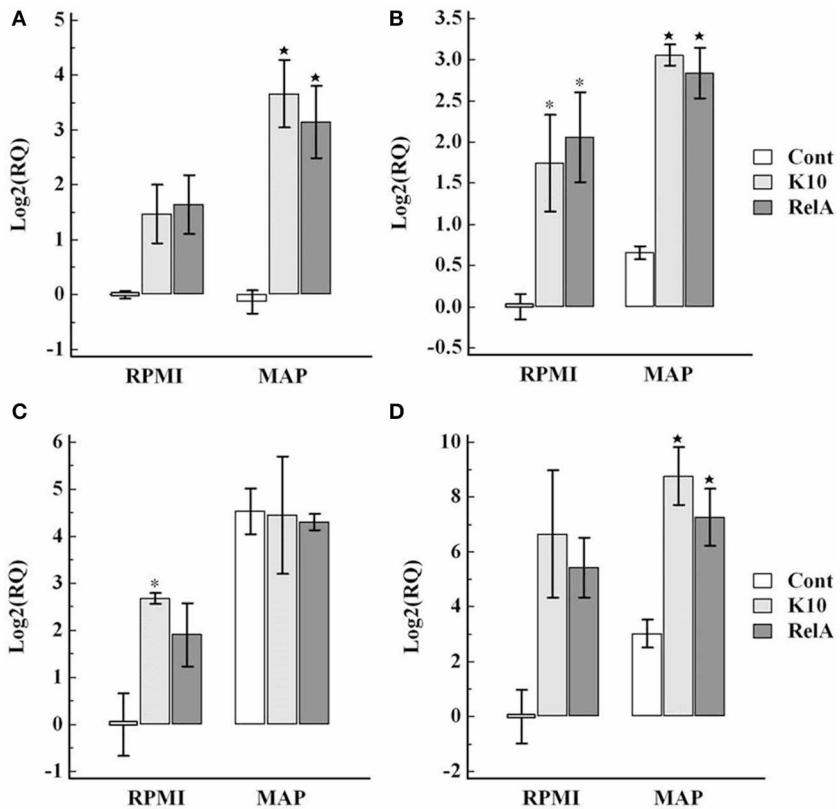

FIGURE 8 | Relative transcription of genes involved in Th17 type immune response in PBMC. The relative quantification of mRNA transcription was determined as described in the legend of **Figure 7**. The panels show the relative quantification of IL-23 **(A)**, RORC **(B)**, IL-17 **(C)**, IL22 **(D)**. RQ, relative quantification; RPMI and *MAP*, PBMC cultured in RPMI medium alone and with live *Map*, respectively; * and ★, significant difference compared to RPMI and MAP of the control group, respectively.

the Δ*relA* mutant, were candidates for inclusion and further evaluation. This emphasizes the difficulty of using an indirect method of screening mutants for their potential as a vaccine. Of the three mutants we submitted to the program, Δ*relA* is the only mutant shown to elicit an immune response that clears infection and limits colonization of *Map* under experimental challenge conditions. This response is clearly different than the immune response elicited by wild type *Map*. Exposure to Δ*relA*, per os at birth or through direct inoculation into the ileum through a cannula, elicits a response that clears infection of the mutant and

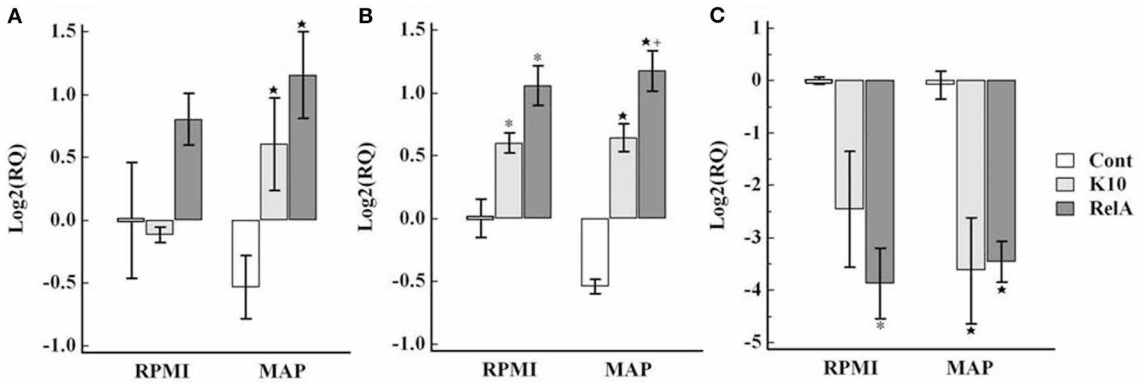

FIGURE 9 | Relative transcription of genes involved in regulating the immune response in PBMC. The relative quantification of mRNA transcription was determined as described in the legend of **Figure 7**. The panels show the relative quantification of FoxP3 **(A)**, TGF-β **(B)**, IL-10 **(C)**. RQ, relative quantification; RPMI and *MAP*, PBMC cultured in RPMI medium alone and with live *Map*, respectively; * and ★, significant difference compared to RPMI and MAP of the control group, respectively; $^{+}$, significant difference compared to MAP of K10 group.

limits the capacity of *Map* to colonize and establish an infection (Park et al., 2011). In contrast, exposure to *Map* by either route elicits a response that does not affect colonization.

How deletion of *relA* disrupts the pathway(s) involved in modulating the immune response remains to be elucidated. Comparison of the immune response to Δ*relA* and *Map* has thus far, not revealed any clear differences between the response to Δ*relA* and *Map*. The results have also revealed *ex vivo* analysis of the immune response in calves vaccinated with Δ*relA* is comparable to the response developed in calves inoculated with *Map*. The response is characterized by a CD4 and CD8 proliferative response to PPD, soluble antigens, and live *Map* (Koo et al., 2004). With the limited number of animals examined thus far, it is difficult to determine if there is a significant difference in the proliferative response to *Map* in calves inoculated with *Map* or Δ*relA*. In our previous study, live *Map* stimulation appeared to induce a more vigorous CD8 cell response than the CD4 cell response in PBMC from the wild type *Map* and Δ*relA* inoculated groups (Park et al., 2011). However, as shown here, the NK CD8 positive cell subset from animals exposed to *Map* proliferate nonspecifically. This population couldn't be distinguished from αβ CD8 cells in the previous study. This population most likely accounted for the increase noted in our earlier study. γδ T cells did not proliferate in this study.

Although the frequency was slightly higher in RelA group than in K10 group, the pattern of FoxP3 expression in CD4 T cells was similar in both challenged groups. The frequency was low in the circulating PBMC (at Time 0). The frequency was similar after stimulation with *Map*, but increased in cultures without *Map*. The interpretation should be done with the results of the CD4 T cell proliferation responses (**Figure 4**). CD4 T cells proliferated vigorously in both groups when cultured in the presence of *Map*, but not in medium alone. Foxp3 was expressed only in a subset of the memory T cell population (CD25+ and CD45R0+). Therefore, the apparent increase in the frequency of Foxp3 expressing cells in medium alone could be attributed to the change in proportion of naïve and activated proliferating CD4 T cells, not to proliferation of the Tr cells. Likewise, the frequency of Foxp3 cells in cultures

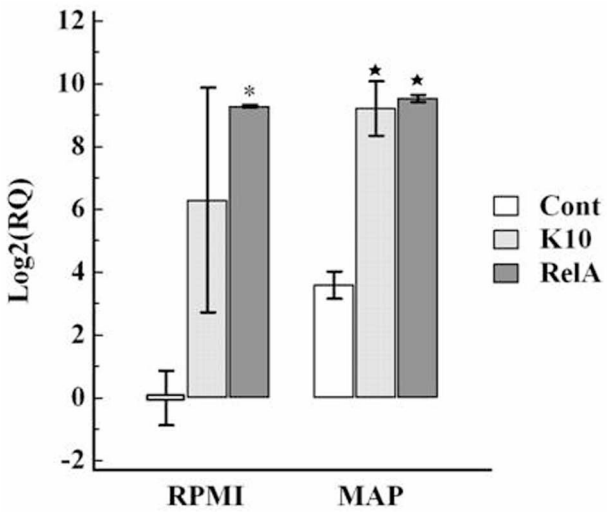

FIGURE 10 | Relative transcription of the granulysin gene in PBMC. The relative quantification of mRNA transcription was determined as described in the legend of **Figure 7**. RQ, relative quantification; RPMI and *MAP*, PBMC cultured in RPMI medium alone and with live *Map*, respectively; * and ★, significant difference compared to RPMI and *MAP* of the control group, respectively.

with *Map* may have appeared unchanged owing to the fact that proliferation of Tr cells and effector T cells was proportional following stimulation. This supposition is supported by the transcription analysis results which showed the expression of Foxp3 was slightly higher in cell cultured with *Map* compared to cells cultured in medium alone in both groups (**Figure 9**). The other regulatory cytokines (TGF-β and IL-10) were not up-regulated in both animal groups compared to the control group. These finding indicate there was no Tr mediated inhibitor effect detected in the present study. It would be expected that there would be very little activity during the initial response to *Map* when infection is under immune control. Later stages of infection need to

be examined to determine if Tr cells play a role in modulating the immune response to *Map*.

Interpretation of other cytokine gene expression profiles is difficult because of the non-specific proliferation of the CD8 positive NK cell subset and expression of cytokine genes in medium alone and in the presence of *Map*. The transcription of cytokines associated with Th1 response, IL-12p35 and IFN-γ, and the Th17 response, IL23, IL17, and IL-22, were up-regulated in both infected groups when cultured in medium alone in comparison with values obtained with cells from the control group. The expression levels were slightly elevated when stimulated with live *Map*. Inherent increase of IFN-γ and granulysin gene expression in unstimulated cells from *Map* infected cows and further increase in response to live *Map* stimulation has been observed in previous studies (Coussens et al., 2004; Park et al., 2011). The current study extends the observation to other cytokines associated with Th1 and Th17 type immune responses. Further studies are needed to explain these observations. These cytokines can also be produced by other types of immune cells, such as NK cells. NK cells proliferated in the presence and absence of *Map* stimulation, potentially explaining increased expression in medium alone. The increase of IL-17 mRNA transcription was also observed in PBMC from uninfected animals when stimulated with live *Map*. However, this stimulation did not induce an increase in IL-23 or IL-22.

In summary, the present study has provided further data showing deletion of *relA* abrogates the ability of *Map* to establish a persistent infection. Exposure/vaccination with Δ*relA* elicited an immune response that cleared the infection with Δ*relA*. This is in contrast to the other two mutants we selected for evaluation. Studies with *Mycobacterium bovis* (*Mbv*), *pknG* in *Mbv* BCG and in *M. smegmatis* (with the inserted gene) showed the enzyme was essential for survival in macrophages (Walburger et al., 2004). This strongly suggested that, if survival in macrophages was an important predictor of survival *in vivo*, deletion of *pknG* in *Map* should affect the survival of *Map in vivo*. The Δ*pknG* mutant of *Map* showed a similar result to that of the *pknG* deletion mutant in *Mbv* BCG in bovine monocyte-derived macrophages. The survival of Δ*pknG* was significantly reduced compared to wild type *Map* and Δ*relA*. However, the *in vivo* survival of Δ*pknG* was not attenuated in calves and kid goats (Park et al., 2011). Lsr2 was initially known to be associated with lipid biosynthesis in mycobaterial cell wall (Chen et al., 2006). More recent studies revealed that it is a global regulator which regulates expression of multiple genes, including genes associated with cell wall biosynthesis, antibiotic resistance, and mycobacterial pathogenesis (Chen et al., 2008; Gordon et al., 2010; Liu and Gordon, 2012). In comparison to Δ*pknG*, the *lsr2* deletion mutant of *Map* showed less attenuation in macrophages, but significant attenuation in kid goats. However, the Δ*lsr2* did not elicit an immune response that affected establishment of infection with *Map* under experimental challenge conditions (unpublished data). The results from *ex vivo* and *in vivo* studies with these mutants provide further evidence that survival in macrophages is not a good predictor of survival *in vivo* or the capacity of the mutants to elicit a response that clears infection. Studies in a mouse model showed deletion of *relA* in *Mtb* impaired the capacity of *Mtb* to survive *in vivo*. It was hypothesized that deletion of *relA* is critical for successful establishment of a persistent infection and that deletion of *relA* alters expression of antigenic and enzymatic factors essential for establishment of a latent infection (Dahl et al., 2003). The data obtained in our studies support this hypothesis. Further studies are needed now to identify the enzymatic pathways and their expressed products that are altered by deletion of *relA*.

AUTHOR CONTRIBUTIONS

All authors were involved in the design of the experiments. William C. Davis and Kun Taek Park were responsible for overseeing the conduct of the studies and analysis of the data.

ACKNOWLEDGMENTS

We would like to acknowledge the assistance of Eric Lautzenheiser in the care and maintenance of the animals during the course of the studies. The studies were supported in part by an intramural grant 10S-3924-1016 and the Washington State University Monoclonal Antibody Center.

REFERENCES

Allen, A. J., Park, K. T., Barrington, G. M., Lahmers, K. K., Abdellrazeq, G. S., Rihan, H. M., et al. (2011). Experimental infection of a bovine model with human isolates of *Mycobacterium avium* subsp. *paratuberculosis*. *Vet. Immunol. Immunopathol.* 141, 258–266. doi: 10.1016/j.vetimm.2011.03.014

Allen, A. J., Park, K. T., Barrington, G. M., Lahmers, K. K., Hamilton, M. J., and Davis, W. C. (2009). Development of a bovine ileal cannulation model to study the immune response and mechanisms of pathogenesis of paratuberculosis. *Clin. Vaccine Immunol.* 16, 453–463. doi: 10.1128/CVI.00347-08

Chen, J. M., German, G. J., Alexander, D. C., Ren, H., Tan, T., and Liu, J. (2006). Roles of Lsr2 in colony morphology and biofilm formation of *Mycobacterium smegmatis*. *J. Bacteriol.* 188, 633–641. doi: 10.1128/JB.188.2.633-641.2006

Chen, J. M., Ren, H., Shaw, J. E., Wang, Y. J., Li, M., Leung, A. S., et al. (2008). Lsr2 of *Mycobacterium tuberculosis* is a DNA-bridging protein. *Nucleic. Acids. Res.* 36, 2123–2135. doi: 10.1093/nar/gkm1162

Coussens, P. M., Verman, N., Coussens, M. A., Elftman, M. D., and McNulty, A. M. (2004). Cytokine gene expression in peripheral blood mononuclear cells and tissues of cattle infected with *Mycobacterium avium* subsp. *paratuberculosis*: evidence for an inherent proinflammatory gene expression pattern. *Infect. Immun.* 72, 1409–1422. doi: 10.1128/IAI.72.3.1409-1422.2004

Dahl, J. L., Kraus, C. N., Boshoff, H. I., Doan, B., Foley, K., Avarbock, D., et al. (2003). The role of RelMtb-mediated adaptation to stationary phase in long-term persistence of *Mycobacterium tuberculosis* in mice. *Proc. Natl. Acad. Sci. U.S.A.* 100, 10026–10031. doi: 10.1073/pnas.1631248100

Dieli, F., Troye-Blomberg, M., Ivanyi, J., Fournie, J. J., Krensky, A. M., Bonneville, M., et al. (2001). Granulysin-dependent killing of intracellular and extracellular *Mycobacterium tuberculosis* by Vgamma9/Vdelta2 T lymphocytes. *J. Infect. Dis.* 184, 1082–1085. doi: 10.1086/323600

Gansert, J. L., Kiessler, V., Engele, M., Wittke, F., Rollinghoff, M., Krensky, A. M., et al. (2003). Human NKT cells express granulysin and exhibit antimycobacterial activity. *J. Immunol.* 170, 3154–3161. doi: 10.4049/jimmunol.170.6.3154

Gordon, B. R., Li, Y., Wang, L., Sintsova, A., van Bakel, H., Tian, S., et al. (2010). Lsr2 is a nucleoid-associated protein that targets AT-rich sequences and virulence genes in *Mycobacterium tuberculosis*. *Proc. Natl. Acad. Sci. U.S.A.* 107, 5154–5159. doi: 10.1073/pnas.0913551107

Irenge, L. M., Walravens, K., Govaerts, M., Godfroid, J., Rosseels, V., Huygen, K et al. (2009). Development and validation of a triplex real-time PCR for rapid detection and specific identification of *M. avium subsp. paratuberculosis* in faecal samples. *Vet. Microbiol.* 136, 166–172. doi: 10.1016/j.vetmic.2008.09.087

Koo, H. C., Park, Y. H., Hamilton, M. J., Barrington, G. M., Davies, C. J., Kim, J. B., et al. (2004). Analysis of the immune response to *Mycobacterium avium* subsp. *paratuberculosis* in experimentally infected calves. *Infect. Immun.* 72, 6870–6883. doi: 10.1128/IAI.72.12.6870-6883.2004

Liu, J., and Gordon, B. R. (2012). Targeting the global regulator Lsr2 as a novel approach for anti-tuberculosis drug development. *Expert. Rev. Anti. Infect. Ther.* 10, 1049–1053. doi: 10.1586/eri.12.86

Park, K. T., Allen, A. J., Bannantine, J. P., Seo, K. S., Hamilton, M. J., Abdellrazeq, G. S., et al. (2011). Evaluation of two mutants of *Mycobacterium avium* subsp. *paratuberculosis* as candidates for a live attenuated vaccine for Johne's disease. *Vaccine* 29, 4709–4719. doi: 10.1016/j.vaccine.2011.04.090

Park, K. T., Allen, A. J., and Davis, W. C. (2014). Development of a novel DNA extraction method for identification and quantification of *Mycobacterium avium* subsp. *paratuberculosis* from tissue samples by real-time PCR. *J. Microbiol. Methods* 99C, 58–65. doi: 10.1016/j.mimet.2014.02.003

Park, K. T., Dahl, J. L., Bannantine, J. P., Barletta, R. G., Ahn, J., Allen, A. J., et al. (2008). Demonstration of allelic exchange in the slow-growing bacterium *Mycobacterium avium* subsp. *paratuberculosis*, and generation of mutants with deletions at the *pknG*, *relA*, and *lsr2* loci. *Appl. Environ. Microbiol.* 74, 1687–1695. doi: 10.1128/AEM.01208-07

Scandurra, G. M., de Lisle, G. W., Cavaignac, S. M., Young, M., Kawakami, R. P., and Collins, D. M. (2010). Assessment of live candidate vaccines for paratuberculosis in animal models and macrophages. *Infect. Immun.* 78, 1383–1389. doi: 10.1128/IAI.01020-09

Seo, K. S., Davis, W. C., Hamilton, M. J., Park, Y. H., and Bohach, G. A. (2009). Development of monoclonal antibodies to detect bovine FOXP3 in PBMCs exposed to a staphylococcal superantigen. *Vet. Immunol. Immunopathol.* 128, 30–36. doi: 10.1016/j.vetimm.2008.10.292

Walburger, A., Koul, A., Ferrari, G., Nguyen, L., Prescianotto-Baschong, C., Huygen, K., et al. (2004). Protein kinase G from pathogenic mycobacteria promotes survival within macrophages. *Science* 304, 1800–1804. doi: 10.1126/science.1099384

Conflict of Interest Statement: The authors declare that the research was conducted in the absence of any commercial or financial relationships that could be construed as a potential conflict of interest.

Received: 22 March 2014; accepted: 25 April 2014; published online: 15 May 2014.
Citation: Park KT, Allen AJ, Barrington GM and Davis WC (2014) Deletion of relA abrogates the capacity of Mycobacterium avium paratuberculosis to establish an infection in calves. Front. Cell. Infect. Microbiol. ***4****:64. doi: 10.3389/fcimb.2014.00064*
This article was submitted to the journal Frontiers in Cellular and Infection Microbiology.

frontiers in
CELLULAR AND INFECTION MICROBIOLOGY

ORIGINAL RESEARCH ARTICLE
published: 15 October 2014
doi: 10.3389/fcimb.2014.00144

Generation and screening of a comprehensive *Mycobacterium avium* subsp. *paratuberculosis* transposon mutant bank

Govardhan Rathnaiah[1], Elise A. Lamont[2], N. Beth Harris[1], Robert J. Fenton[1], Denise K. Zinniel[1], Xiaofei Liu[1], Josh Sotos[3], Zhengyu Feng[1], Ayala Livneh-Kol[4], Nahum Y. Shpigel[4], Charles J. Czuprynski[3], Srinand Sreevatsan[2] and Raúl G. Barletta[1]*

[1] School of Veterinary Medicine and Biomedical Sciences, University of Nebraska, Lincoln, NE, USA
[2] Department of Veterinary Population Medicine, University of Minnesota, St. Paul, MN, USA
[3] School of Veterinary Medicine, University of Wisconsin, Madison, WI, USA
[4] The Koret School of Veterinary Medicine, The Hebrew University of Jerusalem, Rehovot, Israel

Edited by:
Thomas A. Ficht, Texas A&M University, USA

Reviewed by:
Thomas C. Zahrt, Medical College of Wisconsin, USA
Jeffrey Cirillo, Texas A&M Health Science Center, USA

***Correspondence:**
Raúl G. Barletta, School of Veterinary Medicine and Biomedical Sciences, University of Nebraska, 211 VBS, Fair Street and East Campus Loop, Lincoln, NE 68583-0905, USA
e-mail: rbarletta@unl.edu

Mycobacterium avium subsp. *paratuberculosis* (MAP) is the etiologic agent of Johne's Disease in ruminants. This enteritis has significant economic impact and worldwide distribution. Vaccination is one of the most cost effective infectious disease control measures. Unfortunately, current vaccines reduce clinical disease and shedding, but are of limited efficacy and do not provide long-term protective immunity. Several strategies have been followed to mine the MAP genome for virulence determinants that could be applied to vaccine and diagnostic assay development. In this study, a comprehensive mutant bank of 13,536 MAP K-10 Tn*5367* mutants ($P > 95\%$) was constructed and screened *in vitro* for phenotypes related to virulence. This strategy was designated to maximize identification of genes important to MAP pathogenesis without relying on studies of other mycobacterial species that may not translate into similar effects in MAP. This bank was screened for mutants with colony morphology alterations, susceptibility to D-cycloserine, impairment in siderophore production or secretion, reduced cell association, and decreased biofilm and clump formation. Mutants with interesting phenotypes were analyzed by PCR, Southern blotting and DNA sequencing to determine transposon insertion sites. These insertion sites mapped upstream from the MAP1152-MAP1156 cluster, internal to either the Mod operon gene MAP1566 or within the coding sequence of *lsr2*, and several intergenic regions. Growth curves in broth cultures, invasion assays and kinetics of survival and replication in primary bovine macrophages were also determined. The ability of vectors carrying Tn*5370* to generate stable MAP mutants was also investigated.

Keywords: Johne's Disease, *Mycobacterium paratuberculosis*, transposon, mutant bank, bovine macrophages

INTRODUCTION

Mycobacterium avium subsp. *paratuberculosis* (MAP) is the etiologic agent of Johne's Disease (JD) in ruminants. This enteritis has significant economic impact and worldwide distribution (Sweeney, 1996). In the United States, annual losses to the dairy industry have been estimated from 250 million (Ott et al., 1999) to $1.5 billion (Stabel, 1998). Vaccination is one of the most cost effective disease control measures. Unfortunately, though there are JD vaccines that reduce clinical disease and shedding, their efficacies are limited and none afford long-term protective immunity. For example in the United States, Mycopar® (Boehringer Ingelheim Vetmedica, Inc.) is the only licensed vaccine against JD. However, this vaccine is derived from *M. avium* Strain 18 (Bastida and Juste, 2011), and therefore does not have an optimal antigenic repertoire. Another bacterin, Silirum® (Zoetis Animal Health) is being tested in Australia and approved for limited use. It is a heat-killed MAP vaccine strain with improved safety. This formulation may possess a better antigenic repertoire but heat-killing may reduce efficacy. Neoparasec® (Rhone-Merieux) contains the live-attenuated MAP strain 316F while Gudair® (Zoetis Animal Health) is heat-killed 316F and licensed for use in sheep and goats. However, current vaccines cannot distinguish vaccinated from infected animals, thus compromising JD diagnostic tests (Hines et al., 2014), and strain 316F was generated in the 1920's by random attenuation procedures (e.g., passages on ox bile) and their attenuating mutations are only now being investigated (Bull et al., 2013). In last analysis, a vaccine of high efficacy is needed for an effective control of JD (Lu et al., 2013).

Abbreviations: CAS, Chrome azurol S; CFU, Colony forming units; DCS, D-cycloserine; Hyg, Hygromycin; JD, Johne's Disease; Kan, Kanamycin; MAP, *Mycobacterium avium* subsp. *paratuberculosis*; MDM, Monocyte-derived macrophage; MOADC, Middlebrook 7H9 broth enriched with oleic acid albumin dextrose complex; Msmeg, *Mycobacterium smegmatis*; MTB, *Mycobacterium tuberculosis*; OD, Optical density; ORF, Open reading frame; PBS, Phosphate buffered saline; SEM, Standard error of the mean.

The MAP wild type strain K-10 genome has been sequenced, annotated and reannotated by optical mapping (Li et al., 2005; Wu et al., 2009). The updated K-10 genome is represented by a circular map of 4,829,781 bp encoding 4350 open reading frames (ORFs) with 69.3% GC content. In this genome, about 60% of the ORFs have known homologs in databases but only 30% have definitive function predictions (Bannantine et al., 2012). Several strategies have been followed to mine the MAP genome for virulence determinants or antigens of diagnostic importance (Bannantine and Paustian, 2006; Cho et al., 2007; Li et al., 2007). One approach relied on identifying MAP genes with known *M. tuberculosis* (MTB) homologs or orthologs (Sampson et al., 2004; Bach et al., 2006). For example, based on the attenuation of MTB *leuD* mutants (Sampson et al., 2004), the corresponding MAP *leuD* mutants were constructed by allelic exchange, characterized by carbon and nitrogen source utilization, showed to be attenuated in mice (Chen et al., 2012a,b), and provide protection against wild type challenge in goats (Faisal et al., 2013). Indeed, differences in gene organization may lead to context-dependent function: e.g., even homologous genes in MAP and *M. avium* subsp. *hominissuis* (MAH) may play different roles in pathogenesis (Wu et al., 2006). In addition, genomic differences may be associated with specific hosts (Bannantine et al., 2012). Thus, strategies based on gene homology are not comprehensive. We have previously demonstrated that transposon Tn*5367* inserts relatively random into the MAP genome (Harris et al., 1999). Another study generated a mutant bank of 5060 K-10 mutants ($P > 70\%$) (Shin et al., 2006). Based on bioinformatic analysis, 11 mutants were selected for mouse infection experiments (Shin et al., 2006), identifying potential virulence genes (*gcpE*, *pstA*, *kdpC*, *papA2*, *impA*, *umaA1*, and *fabG2_2*). In this study, we constructed an expanded and comprehensive bank of 13,536 K-10 mutants ($P > 95\%$) and performed phenotypic screens *in vitro*. We believe this strategy maximizes possible hits in genes important to MAP pathogenesis without relying on studies on other mycobacterial species that may not always translate into similar effects in MAP. We also tested the utility of vectors carrying Tn*5370* (McAdam et al., 2002) to generate stable MAP mutants.

MATERIALS AND METHODS

BACTERIAL STRAINS, GROWTH CONDITIONS AND RECOMBINANT DNA

A virulent clinical isolate of MAP (original stock of strain K-10) was used throughout the study (Foley-Thomas et al., 1995). MAP cultures were grown standing with occasional shaking at 37°C in complete Middlebrook 7H9 media (MOADC-Plus) as previously described (Harris et al., 1999); see also Section Transposon mutagenesis below. Depending on the experiment, the supplementation with mycobactin J (Allied Monitor, Fayette, MO) varied from 0.5 to 2.0 μg/ml. For further characterization of the selected mutants, we used this media without L-tryptophan and casamino acids containing vitamins (MOADC). *E. coli* DH5α cells, used as cloning hosts, were grown on Luria-Bertani agar or broth supplemented with 50 μg/ml kanamycin (Kan). The conditionally replicating (temperature sensitive) recombinant mycobacteriophage phAE94 (Bardarov et al., 1997) was used to deliver the transposon Tn*5367,* and signature-tag TM4 phage derivatives of the thermosensitive vector phAE87 were used to deliver Tn*5370* (Bardarov et al., 1997; Cox et al., 1999; McAdam et al., 2002). Phage vectors were propagated in *M. smegmatis* (Msmeg) mc^2155 at 30°C as described previously (Bardarov et al., 1997). The Kan-resistance (Kan^r) Tn*5367* and the hygromycin (Hyg)-resistant (Hyg^r) Tn*5370* transposons are derived from the insertion sequence IS*1096* from Msmeg (Cirillo et al., 1991).

TRANSPOSON MUTAGENESIS

MAP cultures were grown to ca. 1.5×10^8 colony forming units (CFU)/ml (OD_{600} 0.38 to 0.75). Cultures (50 ml) were concentrated by centrifugation and resuspended in 1 ml of MP buffer (50 mM Tris-HCl, pH 7.6; 150 mM NaCl; 2 mM $CaCl_2$). Bacteria and phage were incubated at the non-permissive temperature (37°C) and stop buffer was added as described previously (Bardarov et al., 1997; Harris et al., 1999). The addition of the stop buffer with sodium citrate helps to prevent further phage infections that may lead to multiple transposon insertions in a single strain. Under these conditions, the potential number of double insertions was shown to be at most 1 in 12 mutants (8.3%). Kan^r or Hyg^r colonies were selected on MOADC-Plus medium without Tween plus 15 g/l agar containing 50 μg/ml Kan or 75 μg/ml Hyg, supplemented with 0.4% Bacto Casamino Acids (Difco, Becton Dickinson, Franklin Lakes, NJ), and 40 μg/ml L-tryptophan. Transductants were isolated from these plates after 6–8 week incubation period at 37°C.

MUTANT SCREENING AND CHARACTERIZATION ASSAYS

Visual screen for colony morphology mutants

To identify colony morphology, MAP mutant strains were grown individually in 96-well microtiter plates in MOADC-Plus fully-supplemented media with 0.5 μg/ml mycobactin J, as described above. Plates were photographed and pictures visually inspected for colony morphology alterations in the bottom of the corresponding wells. Colony morphology alterations were confirmed by further observations on the corresponding agar plates.

Susceptibility to D-cycloserine

Screen was accomplished by first determining the highest concentration of D-cycloserine (DCS) that would allow wild type growth to occur on MOADC-Plus fully-supplemented solid media (without Tween) for both MAP wild type K-10 and most randomly selected transposon mutants. All mutant strains were then individually replicated onto solid media without and with DCS at the established concentration. After 8 week incubation at 37°C, DCS susceptibility phenotypes were evaluated and classified as hypersusceptible (failed to grow or grew poorly on DCS), wild type (grew normally, similarly to K-10 on DCS), and resistant (grew faster than K-10 on DCS, reaching a larger colony size).

Miscellaneous screening procedures

To screen for mutants deficient in siderophore production or secretion, individual mutant colonies were grown on MOADC-Plus media, as previously described (Harris et al., 1999). A portion of the bacterial colony was then aseptically transferred onto modified Chrome azurol S (CAS) plates. This media consisted of 72.9 mg/l of hexadecyltrimethylammonium bromide (Sigma, St Louis, MO), 60.5 mg/l of CAS (Sigma), 10 ml/l of iron solution

(1 mM $FeCl_3 \cdot 6H_2O$, 10 mM HCl), 4.7 g/l of Middlebrook 7H9 broth base (Difco, Becton Dickinson), 2 ml/l glycerol and 15 g/l agar adjusted to pH 5.9. The transferred cell patches were incubated at 37°C for 2 weeks and visually screened for the absence of a yellowish halo around the colonies, as previously described (Schwyn and Neilands, 1987). The presence of a halo indicates that siderophores produced and secreted by the colony bind ferric iron in the media.

Biofilm production, thought to be linked to bacterial virulence was also examined. Bacteria were grown in MOADC-Plus broth using plastic tubes and for several weeks. The presence of biofilm was established by visual observation at the sides of the tubes and at the liquid-air interphase. Additional miscellaneous screens are described in the Supplementary Material.

Mutant characterization in BoMac cells

BoMac (Stabel and Stabel, 1995) monolayers adherent to glass coverslips were infected with approximately the same inoculum (MOI 10:1) in RPMI standard tissue culture medium supplemented with 2% fetal bovine serum for 2–3 h (invasion incubation) at 39°C. Cells were washed, coverslips removed, fixed and acid-fast stained. For each experimental group, a minimum of at least 100 cells were examined at 1000X magnification under a microscope to determine the percentage of macrophages containing acid-fast bacilli and to enumerate the number of bacteria per macrophage. Bacterial growth at various times post-infection (e.g., Day 0 after invasion incubation and Day 4) was determined by colony counts and BACTEC radiometric assays. Monolayers were lysed with 0.05% sodium dodecyl sulfate for 30 min, and lysates were inoculated into BACTEC 12B vials containing ^{14}C-palmitate supplemented with 2.0 μg/ml of mycobactin J and 1 ml of egg yolk. The BACTEC 460 instrument (Becton Dickinson Diagnostic Instrument Systems, Sparks, MD) was utilized to determine the release of $^{14}CO_2$ from palmitate that was recorded by the instrument as a growth index (recorded every 24 h until the cumulative index reached 2000 in about 20 days). These indices were converted into viable cell numbers per well (CFUs) using a previously described formula (Lambrecht et al., 1988). The full validation of this method is given elsewhere (Zhao et al., 1997, 1999). As needed, results were confirmed by CFU determinations on MOADC-Plus agar with 2.0 μg/ml mycobactin J.

OLIGONUCLEOTIDE PRIMERS AND PCR

The oligonucleotide primers used in this study are listed in **Table 1**. The general conditions for the PCR reactions were: 0.03 ml reaction mixture volume containing 170 nM of each specific primer pair, in the presence of 1× NH4-based Reaction Buffer (Bioline USA, Inc., Taunton, MA), 1.7 mM $MgCl_2$, 8.3% (v/v) DMSO, 0.25 mM deoxynucleoside triphosphates and 1.5 units of Biolase™ DNA Polymerase (Bioline USA, Inc.). Thermo cycler settings of 95°C for 5 min, followed by 30 cycles of 95°C for 30 s, 61°C for 45 s, 72°C for 1 min and a final extension at 72°C for 7 min.

SOUTHERN BLOTTING

Chromosomal DNA was isolated from wild type and mutant stains. To determine the presence of a transposon insertion, for mutants derived from Tn*5367*, DNA samples were digested with *EcoRI*, which does not cut within this transposon. For Tn*5370* derivatives, DNA samples were digested with *NheI* and *NdeI*, which do not cut within this transposon. Digested DNA fragments from both wild type and mutant strains were electrophoresed on a standard agarose gel and transferred to a nylon membrane (Osmonics, Inc., GE Water and Process Technologies, Trevose, PA). Probes were prepared by PCR-amplification using specific primers (**Table 1**): IS*1096* probe was amplified from Msmeg genomic DNA with IS1096-F and IS1096-R and IS*900* probe was amplified from MAP genomic DNA using IS900-F and IS900-R. The Kan-resistant *aph* gene probe for Tn*5367* was amplified from pMV262 (Connell et al., 1993), or plasmids derived there from, with Kan-F and Kan-R. The Hyg-resistant *hyg* gene probe for Tn*5370* was amplified from pYUB854 (Bardarov et al., 2002), or plasmids derived there from, using Hygro-F and Hygro-R. Probes were labeled with α-[32P]-dCTP (3000 Ci/mmol) using the *Redi*prime DNA Labeling System (Amersham-Pharmacia Biotech, Inc., Molecular Dynamics Div., Piscataway, NJ) as described by the manufacturer. Hybridization and detection were done as described previously with minor modifications (Feng et al., 2002). Southern blot images were digitally captured and processed only to enhance brightness and contrast (Bio-Rad Imaging system, Hercules, CA).

Table 1 | List of primers used in this study.

Primer	Sequence (5′–3′)
2E11-IP-F	GCTGCAGCAACCAGCCGA
2E11-IP-R	CCACCGTCACCGCAGGTAGA
3H4-F	TCGCGGTCCTCGTATTCGCT
3H4-R	TGTCGGACGTGTCCGGTCAC
4H2-F	TCAAGTGGGTTGTGCCCCGT
4H2-R	GCTACCCAGGAGACGCGCCT
22F4-F	GTATCGACCGGTTGTTGATG
22F4-R	GCCGATGTAGTTGTGGTTGA
40A9-IP1-F	GGATGAATCCTCGGCCTTGG
40A9-IP1-R	CCGACGGCGTAGTCTGCAAT
AMT32	CTCTTGCTCTTCCGCTTCTTCTCC
AMT152	TTGCTCTTCCGCTTCTTCT
Hygro-F	ATAGACGTCGGTGAAGTCGACGAT
Hygro-R	GAATCCCTGTTACTTCTCGACCGT
IS900-F	GGATGGCCGAAGGAGATTGG
IS900-R	GCAGCTCGACTGCGATGTCA
IS1096-F	TCGCACTTGACGGTGTA
IS1096-R	GTCGGCTCATCGAACAT
Kan-F	TCGAGGCCGCGATTAAATTCCACC
Kan-R	ATTCATTCGTGATTGCGCCTGAGC
MAP1566-F	GCTCTAGAGCTGGCATCAGGGCACTCAAGAAA
MAP1566-R	CCCAAGCTTGGGTATTCGCTGCACAGCATGTCAGGT
RS6-4	GTAATACGACTCACTATAGGGCNNNNCATG
SP1	TGCAGCAACGCCAGGTCCACACT
SP2	CTCTTGCTCTTCCGCTTCTTCTCC
STM5370-1	TGCTAGGCGTCGGCCATTAGC
T7	TAATACGACTCACTATAGGG

SEQUENCING OF THE TRANSPOSON-INSERTION SITE

In order to locate the transposon insertion sites in the K-10 genome, DNA was amplified for sequencing analysis by a nested PCR as previously described (McAdam et al., 2002). A new primer designated STM5370-1, common to both transposons, was used in place of the original SP1 primer due to differences in the Tn*5367* and Tn*5370* transposon sequences. This primer was designed based on sequence information of Tn*5370* provided Dr. Jeffrey Cirillo (Texas A&M Health Science Center) that was further supplemented by our own sequencing studies. The first PCR used the following primers: RS6-4 (degenerate) and STM5370-1. The variable size PCR products (1 μl) from the first cycle were used in a second PCR cycle with primers T7 and SP2 that are internal to the first cycle PCR product. These final PCR products were purified by Wizard PCR Preps DNA Purification System (Promega, Madison, WI). The samples were run on 1.5% agarose gel electrophoresis to recover the most concentrated DNA bands and purified by the GeneClean® III Kit (Qbiogene, MP Biomedicals, LLC, Solon, OH). DNA samples were sent to The University of Nebraska Genomics Core Research Facility for sequencing, using AMT152 as primer (Shin et al., 2006). Sample runs were performed on a Beckman-Coulter CEQ8000 or CEQ2000XL 8-capillary DNA sequencer using dye-terminator chemistry to provide 500–650 bp of sequence.

GROWTH CURVES IN BROTH CULTURES

MAP strains were grown to late exponential phase (OD_{600} between 1.0 and 1.5) at 37°C from glycerol stocks in MOADC media (1.0 μg/ml mycobactin J), appropriately supplemented with antibiotics as needed. Applicable culture volumes were inoculated into 45 ml of MOADC media in T75 flasks with vented caps so that the initial OD_{600} was approximately 0.05. Each culture was incubated at 37°C standing with OD_{600} readings being taken on days 0, 3, 5, 7, 10, 12, 14, 17, 21, 24, and 28 around the same time each day. CFU counts were also determined on MOADC agar.

PRIMARY BOVINE MACROPHAGE ASSAY

Monocyte-derived macrophages (MDMs) from a JD negative dairy cow were elutriated and enriched as described (Lamont and Sreevatsan, 2010). Incubations were conducted in a 37°C humidified chamber containing 5% CO_2. Approximately 2.0×10^7 MDMs were seeded into separate T25 flasks and allowed to adhere for 2 h. MDMs were washed thrice to remove non-adherent cells and fresh RPMI 1640 supplemented with 2% autologous serum was added prior to MAP infection. Subcultured MAP (K-10 wild type or mutant strains) were grown to an OD_{600} of 0.5 (approximately 1.0×10^8 cells/ml) and pelleted at 8000 × g for 10 min. The pellet was washed thrice using 1X phosphate buffered saline (PBS), resuspended in RPMI 1640 containing 2% autologous serum (MOI 10:1), and vortexed for 5 min. MAP cells were repeatedly drawn through a 21-gage needle to break bacterial clumps. Cells were incubated at 37°C for 5 min to sediment any remaining clumps and only the upper 2/3rd volume was used for infection. MDMs were infected with MAP for 2 h (invasion incubation), washed thrice with 1X PBS to remove non-adherent bacteria, and recovered in RPMI 1640 supplemented with 2% autologous serum for the following post-infection time points: 0, 2, 6, 12, 24, and 48 h after the completion of the invasion incubation period. Upon completion of each post-infection time point, MDMs were washed thrice in 1X PBS and incubated with 0.01% Triton X-100 in PBS for 5 min at room temperature. The lysate was subjected to differential centrifugation at 388 ×g and 8000 × g for 5 min each to remove MDMs and pellet bacteria, respectively. MAP pellets were washed thrice in 1X PBS at 8000 ×g for 5 min to remove any remaining detergent, and resuspended in 1.0 ml of 1X PBS. All time points were assayed in triplicate. MAP inoculum and post-infection time points were separately stained using the Baclight Live/Dead kit (Invitrogen, Carlsbad, CA) and gated for live cells on a flow cytometer per manufacturer's instructions as described (Lamont and Sreevatsan, 2010).

CALCULATION OF GROWTH PARAMETERS AND STATISTICAL ANALYSIS

Statistical analyses to determine *P*-values presented in the text and figures were performed using the Statistical Analysis System (SAS) software version 9.1.3, 2004 (SAS Institute) using the Mixed Procedure Subroutine. *Post-hoc* comparisons were carried out using Tukey adjusted *P*-values. For calculations involving ODs and CFUs, logarithmic transformations were applied.

NUCLEOTIDE SEQUENCE ACCESSION NUMBERS

The DNA sequences of transposons Tn*5367* (Cirillo, J. D., McAdam, R. A., Weisbrod, T. R., Barletta, R. G. and Jacobs, W. R. Jr.) and Tn*5370* (Cirillo, J. D., Rathnaiah, G., McAdam, R. A., Weisbrod, T. R., Barletta, R. G. and Jacobs, W. R. Jr.) have been assigned GenBank accession numbers KM232614 and KM232615, respectively.

RESULTS

GENERATION AND SCREENING OF A TRANSPOSON MUTANT BANK

To investigate virulence factors of MAP, a transposon mutant bank of MAP wild type K-10 was constructed. The transposon Tn*5367* carrying a Kan resistance marker (Bardarov et al., 1997) randomly inserted into the bacterial chromosome by transposition from a thermosensitive phage delivery vector. Nine independent infections (8 with phage and 1 control with no phage) were carried out to ensure that sibling mutants were minimally represented. A total of 13,536 Kan-resistant mutants were collected and stored individually in an indexed collection of 141 96-well plates stored at −80°C. Each mutant is identified by the plate number and the coordinates of the well (a letter for the row and a number for the column): e.g., mutant 4H2 is stocked in plate 4 and the well that intersects row H and column 2 in a 96-well microtiter plate. In addition, to facilitate screening procedures, pools of 96 or 24 mutants were also stocked so they could be easily referred to individual mutants in the indexed collection. Assuming random transposition and 4500 target genes with single transposon insertions [$\ln(1-P) = N \times \ln(1\text{-}1/4500)$], this number of mutants yields a *P*-value of approximately 95% for insertions in non-essential genes. The full library or a subset of strains were subjected to various individual screens to find strains of interest for studying MAP physiology and pathogenesis, and

principally to search for attenuated strains that could be used as first-generation vaccine candidates in animal trials. A set of 123 strains, fairly well distributed through the various plates, were analyzed to show that the library was composed of strains with diverse phenotypes (Table S1).

Visual screen for colony morphology mutants

Colony morphology of microorganisms is well known to influence virulence, drug susceptibility and macrophage survival (Reddy et al., 1996). To identify colony morphology of MAP mutants, each of the 13,536 mutant strains was grown on MOADC-Plus media, visually observed and photographed with a camera. Using this procedure, eight mutants were found that exhibited colony morphologies different from the wild type strain (1F3, 4H2, 16B11, 22F4, 65E9, 69D12, 73D7, and 84D12). In particular, 4H2 displayed highly irregular colony borders and a rougher surface appearance as compared to K-10 (**Figure 1** and **Figure S1A**). In contrast, mutant 22F4 displayed a smooth colony morphotype (**Figure S1C**). These two mutant strains were further tested in BoMac cells (see Section Miscellaneous screening). It is noted that visual screens may depend on the media used and undoubtedly have a degree of subjectivity. Thus, less obvious but yet relevant differences in colony morphotype may not have been identified.

Susceptibility to DCS

DCS inhibits peptidoglycan biosynthesis in mycobacteria by the combined inhibition of D-alanine racemase (Alr) and D-alanine ligase (Chacon et al., 2002, 2009; Feng and Barletta, 2003; Halouska et al., 2014). Inactivation of the Msmeg *alr* gene results in a 500-fold reduction in the ability of Msmeg to survive within phagocytic cells and also determines a DCS hypersusceptible phenotype (Chacon et al., 2009). In addition, there are several potential alterations that can lead to DCS susceptibility or resistance including alterations of surface proteins that may also play a role in pathogenesis. To test this hypothesis in MAP, the entire mutant bank was screened for DCS susceptibility. First, it was determined that 20 μg/ml DCS was the maximum concentration that had no effect on the growth of K-10 and a subset of randomly picked transposon mutant strains. Using this approach, 98 mutant strains were found hypersusceptible to DCS. Sixty-three strains did not grow: e.g., colony morphotypes 1F3, 16B1, and 22F4 (**Figures S1C,D**); and normal colony morphotypes 12G8, 37D1, and 30H9. Thirty-five mutants grew poorly: e.g., normal colony morphotypes 3D4 and 23B5, but displayed normal growth without the drug. However, 15 DCS resistant mutants grew faster, as evidenced by expanded colony sizes: e.g., colony morphotypes 4H2 (**Figures S1A,B**), 65E9 and 69D12; and normal colony morphotype 40A9. The colony morphotypes 4H2 and 22F4 (see Section Visual screen for colony morphology mutants), as well as strains 30H9 and 40A9, were selected for further testing in BoMac cells (see Section Miscellaneous screening). In contrast, colony morphology mutants 73D7 and 84D12 displayed wild type susceptibility. In summary, this screen yielded 113 potentially attenuated strains, the greatest number among the assays performed.

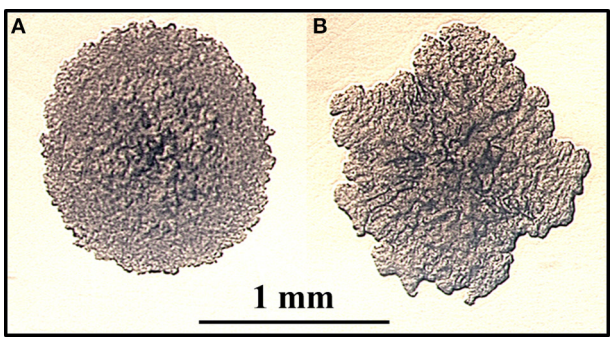

FIGURE 1 | (A,B) Identification of a MAP mutant with altered colony morphology. MAP strains were grown on fully supplemented MOADC-Plus medium until colonies were approximately 1 mm in diameter (see scale bar) and photographed at 100X magnification. Colony morphologies for the wild type strain K-10 **(A)** and the Tn*5367* transposon mutant 4H2 **(B)** are displayed.

Miscellaneous screening

Chromogenic screening of the entire mutant bank was performed to identify mutants unable to synthesize and/or secrete siderophores other than mycobactin. Since MAP is a known auxotroph for mycobactin, the goal of this experiment was to test the hypothesis that mycobacterial mutants unable to synthesize and/or secrete any other type of siderophore may be attenuated (Fiss et al., 1994). This method identified mutant 1F3 that grew significantly slower than K-10 in standard mycobactin J supplemented media did not produce a halo on the modified CAS medium plates (**Figure 2**). This phenotype suggests an impairment of the synthesis or transport of an alternative siderophore different from mycobactin. This mutant also displayed colony morphology alterations (see Section Visual screen for colony morphology mutants) and DCS hypersusceptibility (see Section Susceptibility to DCS). As stated in Section Generation and screening of a transposon mutant bank, the entire mutant bank, as well as 1F3, was stocked as a 96 well-plate culture. Replicate plating on MOADC-Plus for the CAS assay was conducted 6 months thereafter with all mutants, except 75, being viable. However, in a subsequent replication years later, mutant 1F3 grew poorly but in sufficient amounts to conduct a preliminary goat experiment when sent to collaborators in Israel (Livneh et al., 2005). Unfortunately, subcultures at both laboratories no longer grew.

Biofilm screening was also performed with a limited set of ca. 300 mutants to identify strains deficient in biofilm production (**Figure S2**). We identified mutants 2E11, 4E1, and 4E7 that were impaired in biofilm production. However, mutant 2E11 biofilm deficiency was due to poor growth in the assay. In contrast, mutant 4F3 produced more biofilm than the wild type strain. Additional screens identified mutants 3D4 and 3B11 with impaired cell association in BoMac cells (**Figure S3**), and strain 3D9 and 4E7 displayed impaired clump formation (**Figure S4**). All of these seven mutants did not display altered colony morphotypes. In addition, all of these mutants, except for 3D4, had normal DCS susceptibilities. Nonetheless, serendipitously, mutant 2E11 was selected for further studies as preliminary

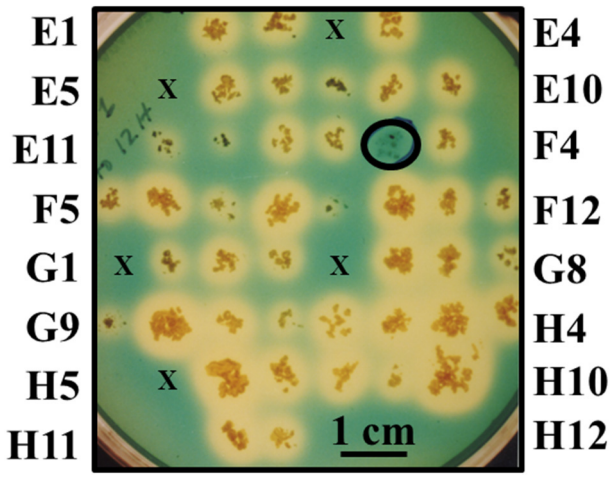

FIGURE 2 | Direct visual screen for MAP mutants unable to produce or secrete siderophores. Mutants were grown on MOADC-Plus media for about 8 weeks, transferring a portion of the colony to Chrome azurol S plates since this media does not allow for growth. Labels for the outermost colonies are shown for each row and column (according to 96-well plate nomenclature) to designate individual mutants. Mutants that failed to grow initially are represented by an "×" and mutants that produced a halo are controls. A scale bar is provided to estimate halo size (blue to yellow color change when a strong chelating agent removes iron from the dye) after 2 weeks of incubation at 37°C. The circled colony without a halo is mutant 1F3 impaired in siderophore production or secretion.

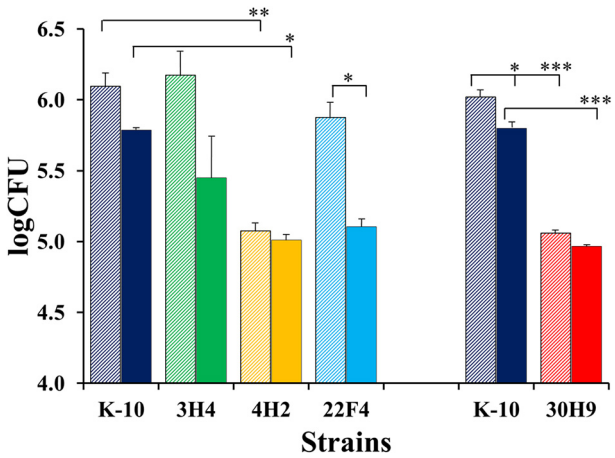

FIGURE 3 | Interaction of MAP wild type K-10 and mutant strains with the BoMac cell line. Macrophage monolayers were infected with bacteria at a multiplicity of 10:1, incubated and lysed. Counts were taken at Day 0 (after invasion; stripe bars) and Day 4 (post-infection; solid bars). Bacilli were enumerated using the BACTEC radiometric assay system by recording growth indices every 24 h until this cumulative index reached 2000 (usually 20 days). These indices were converted into viable cell numbers per well (CFUs) using a previously described formula that has been extensively validated for MAP (Lambrecht et al., 1988; Zhao et al., 1997, 1999). Results represent means ($n = 2$) ± standard error of the mean. Statistical significance for pairwise determinations displayed by a line with tick marks is denoted with asterisks: *P-value < 0.05, **P-value < 0.01 and ***P-value < 0.001.

assays with MDMs indicated significant attenuation (see Section Interaction of wild type and mutant strains with primary bovine macrophages).

MAP mutant characterization in BoMac cells

The invasion, survival and/or replication of selected MAP strains were first tested in the BoMac cell line, as these cells provide reproducibility over primary macrophages for the extended period of time that would be required to test a large number of mutants. Preliminary assessment of bacillary counts for representative strains was performed by microscopic examination of acid-fast stained monolayers on glass coverslips. Results were confirmed by CFU determination and BACTEC assays that were better suited for screening assays. Finally, the more promising mutants were screened in this fashion by BACTEC assays. Representative results are shown for two sets of independent experiments (**Figure 3**).

In the first set (**Figure 3**, left), K-10 was compared with 3H4 (with normal colony morphology, but unable to grow in DCS), 4H2 and 22F4. Results at Day 0 (after invasion incubation) showed that the invasiveness of 3H4 and 22F4 were similar to K-10 ($P > 0.1$), but 4H2 was significantly less invasive than the wild type strain K-10 ($P < 0.01$), and also less invasive than 3H4 ($P < 0.01$) and 22F4 ($P < 0.05$). Survivability for each strain was estimated by comparing the CFUs at Day 0 and Day 4: interaction of K-10 with BoMac cells resulted in decreased survival but the effect was not statistically significant ($P > 0.1$), reduced survivability was more pronounced and approached significance for 3H4 ($P = 0.055$), there was almost no change for 4H2 ($P > 0.1$), but reduction in CFUs was significant for 22F4 ($P < 0.05$). Comparison of the overall macrophage CFUs at Day 4 among all strains indicated that the 3H4 burden was not significantly different from K-10 ($P > 0.1$), while 22F4 showed a reduced burden but was not significantly different ($P = 0.075$), while 4H2 showed significantly less CFUs ($P = 0.039$).

Results for the second set (**Figure 3**, right), indicated that 30H9 was less invasive than K-10 ($P < 0.001$), but showed no significant difference ($P > 0.1$) in survivability from Day 0 to Day 4. In addition, 30H9 had a significantly lesser CFU burden than K-10 at Day 4 ($P < 0.001$). Notably, for this set, K-10 displayed a similar reduction in survivability from Day 0 to Day 4, but in this case, on account of more precise measurements and reduced number of means comparisons, the decrease was statistically significant ($P < 0.05$). In a separate assay, mutants 12G8 and 37D1 were also shown to be attenuated in BoMac cells. Mutant 23B5 displayed an attenuated phenotype when directly tested in MDMs infection assays (Table S1).

In summary, 4H2 and 30H9 were less invasive than the wild type K-10 strain, but had similar intracellular survival as K-10. In contrast, 22F4 was the only strain that was significantly less able to survive, by the end point, at Day 4 post-infection. The combined effects of invasion and survival, as indicated by the absolute CFU burdens as determined by the BACTEC assay, at Day 4, indicated that 4H2 and 30H9 were definitely attenuated in BoMac cells, predominantly by their reduced invasiveness. Thus, these two strains, once internalized at lower CFU burdens, persisted post-infection at approximately constant numbers. In contrast, 22F4 was attenuated because of its reduced survival, but the effect

was of lesser degree. The normal colony morphotype mutant 3H4 behaved similarly to the wild type strain K-10.

FURTHER CHARACTERIZATION OF TRANSPOSON MUTANTS OF INTEREST

To further characterize mutants of interest, Southern hybridization analyses, and identification of transposon insertion sites by nested PCR sequencing were performed. Tests to identify specific transposon mutants in mixed infections were developed. In addition, these mutants were characterized by determination of growth curves in broth cultures and their interactions with primary bovine macrophages.

Southern hybridization

To characterize the molecular events that gave rise to the mutant strains, Southern hybridizations were performed with various probes. Hybridization with a probe specific for the common transposon insertion sequence IS*1096* showed unique size bands for 33 mutant strains (not all positive strains shown in **Figure 4**; see Table S1), indicating the presence of a single copy of the corresponding transposon (**Figures 4A–B**). These results were confirmed by hybridization with a probe specific for either the Kan-resistant *aph* marker for Tn*5367* derivatives, or the Hyg-resistant *hyg* marker for Tn*5370* derivatives. Both probes yielded bands in the same gel positions as the IS*1096* probe (unpublished results). To verify that mutant strains were derived from K-10 and that no major molecular rearrangements have occurred, a probe specific for IS*900* was used. As expected, this analysis showed that all mutant strains analyzed had the same hybridization banding pattern as the wild type strain K-10 (**Figures 4C–D**). As mutants were directly analyzed from the original stocks (**Figure 4A**), we noted that 22F4 did not show a clear hybridization band with IS*1096*, and mutant 40A9 showed a very faint band. Upon replication to make large stocks for further analyses, mutant 22F4 clearly displayed the corresponding hybridization band, but 40A9 displayed no band, indicating the potential loss of the transposon insertion (**Figure 4B**). In addition, the original stock of mutant 5E5 did not display a hybridization band.

Transposon insertion site identification by sequencing of nested PCR amplicons

The genomic regions containing transposon insertions of interest were amplified by nested PCR and sequenced as described (see Section Sequencing of the transposon-insertion site). Transposon insertion sites were identified by performing BLASTN identity searches of the MAP DNA sequences adjacent to transposon insertion sites against the K-10 complete genome sequence. In mutants 22F4, 30H9 and STM68, the transposon inserted within genes of interest (**Figure 5A**). In mutant 22F4, the transposon insertion site was mapped internal to MAP0460 (*lsr2*) and located 110 bp from the ATG start codon. For mutant 30H9, transposon insertion sites were mapped as internal to MAP1566.

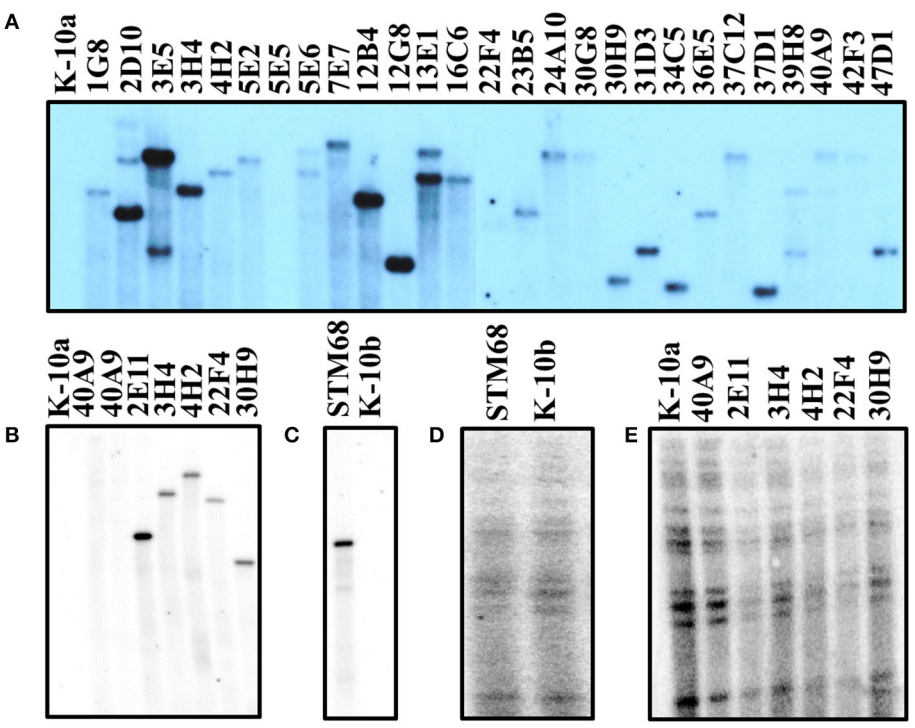

FIGURE 4 | (A–E) Southern blot analysis of MAP wild type K-10 and transposon insertion mutants. DNA samples from Tn*5367* mutants and the wild type strain (K-10a) were digested with *Eco*RI **(A,B,E)**. DNA samples from the Tn*5370* mutant STM68 and the wild type strain (K-10b) were digested with *Nhe*I and *Nde*I **(C,D)**. DNA samples were run on agarose gels, transferred to a nylon membrane and hybridized with the IS*1096* probe to verify the presence of the transposon **(A–C)** and the IS*900* probe to confirm that the mutants were derived from MAP **(C,D)**. **(B–E)** are hybridization images generated from the same Southern transfer, while **(A)** was from an independent transfer.

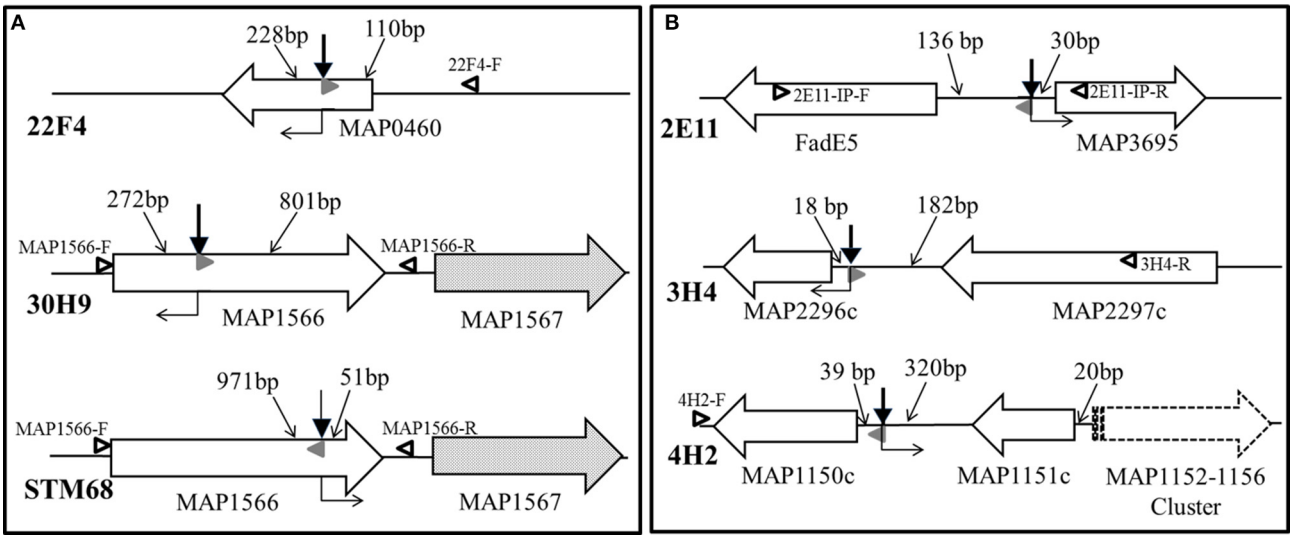

FIGURE 5 | (A,B) Transposon insertion sites of MAP mutants. Solid line wide arrows represent ORFs and indicate the direction of transcription. Dotted fill wide arrows exemplify ORFs subjected to a potential polar effect due to the transposon insertion. The dashed line wide arrow represents a gene cluster transcribed in the same direction. Bold thick vertical arrows stand for Tn*5367* while the bold thin arrow symbolizes Tn*5370* insertion points. Regular thin arrows point to the DNA segments indicating distances (bp) between the transposon insertion point and the start or end of the corresponding ORF. Open black and solid gray (AMT32) sideway triangles represent primers used in PCR mutant identifications for mixed infection experiments (see **Figure 6**). Right angle bent arrows indicate the direction of transcription of the drug selection markers (*aph* in Tn*5367* derivatives; *hyg* in Tn*5370* derivative STM68) in the transposon. Diagram representing relevant genomic regions for mutants are represented: **(A)** 22F4, 30H9, and STM68; and **(B)** 2E11, 3H4, and 4H2.

Serendipitously, another screen from a signature-tagged mutagenesis experiment (ca. 300 mutants) identified a Tn*5370* mutant (STM68) with an insertion in the same gene as in 30H9, but the insertion in STM68 was mapped toward the 3′-end coding sequence of MAP1566. STM68 is a stable mutant because Tn*5370* lacks the transposase within the transposed region avoiding the potential for further rearrangements in the mutant strain. In 30H9, Tn*5367* is located 272 bp from the ATG start codon, while mutant STM68 carries a Tn*5370* insertion 51 bp from the TAA termination codon. Thus, for STM68, the insertion may also exert a polar effect on MAP1567 located downstream within the operon. Likewise, though the insertion in 30H9 is well upstream within the MAP1566 coding sequence, a polar effect on MAP1567 cannot be ruled out.

In mutants 2E11, 3H4, and 4H2, the transposon Tn*5367* inserted in the intergenic regions (**Figure 5B**). For mutant 2E11, Tn*5367* inserted 130 bp upstream from FadE5 and 30 bp upstream from MAP3695. In 3H4, the insertion site was 18 bp upstream from MAP2296c and 182 bp downstream from MAP2297c. In 4H2, the transposon insertion was 39 bp upstream from MAP1150c and 320 bp downstream from MAP1151c. In all these cases, it is hypothesized that the transposon affects the expression of either or both genes adjacent to the insertion sites, or other genes in close proximity. Sequencing of the original isolate of 40A9 putatively identified a transposon insertion site in the intergenic region between MAP0282c and MAP0283c. However, as this insertion point could not be further verified and 7 consecutive nucleotides of primer STM5370-1 matched within MAP0282c sequence, the possibility of spurious priming could not be ruled out. Comparison of the full genomic sequence of 40A9 with K-10 may be necessary to identify any sequence change in this mutant strain. However, this analysis is beyond the scope of this work.

Polymerase chain reaction for mutant verification

To demonstrate the presence of specific transposon insertion mutants in mixed infections, such as protection challenge experiments, it was necessary to develop a specific PCR test for each mutant strain. The test is also confirmatory of the sequencing studies to rule out any spurious transposon insertion site identifications. To accomplish this goal, based on the sequencing results, amplicons were synthesized with primers specific for the sequences adjacent to the transposon insertion sites (**Table 1**), and analyzed on agarose gels (**Figure 6**). Amplification of wild type K-10 DNA with primers MAP1566-F (within MAP1566 but upstream from the insertion point) and MAP1566-R (within the intergenic region between MAP1566 and MAP1567) resulted in a DNA fragment of 1179 bp (Lanes 3 and 7); these primers yielded fragments of 3474 bp (Lane 4) and 4560 bp (Lane 8), respectively for mutants STM68 and 30H9. These sizes are as expected for the insertion of Tn*5370* (2295 bp) or Tn*5367* (3381 bp), respectively. Likewise, amplification of K-10 (Lane 5) and 2E11 (Lane 6) with primers 2E11-IP-F (within MAP3695) and 2E11-IP-R (within FadE5) resulted in a DNA fragment of 1845 bp and 5226 bp, respectively; thus confirming the predicted insertion of Tn*5367* in the FadE5 and MAP3695 intergenic region.

PCR of mutants 3H4, 4H2, and 22F4 with specific primers (3H4-F, 3H4-R, 4H2-F, 4H2-R, 22F4-F, and 22F4-R, respectively)

from regions adjacent to the insertion gave the same amplification product to that of K-10 (unpublished results). However, we were able to confirm the insertion point using a specific primer for the adjacent sequences and primer AMT32 specific for both Tn*5367* and Tn*5370* (McAdam et al., 2002; Shin et al., 2006). In this case, K-10 gave no amplification products (unpublished results). All of the mutant strains gave amplification products of the expected sizes: STM68 (1160 bp, Lane 10), 2E11 (1890 bp, Lane 11), 3H4 (1974 bp, Lane 12), 4H2 (1431 bp, Lane 13), 22F4 (561 bp, Lane 14), and 30H9 (941 bp, Lane 15). We obtained the same amplification product for K-10 and 40A9 using primers 40A9-IP1-F and 40A9-IP1-R adjacent to MAP0283c and MAP0282c (unpublished results). Thus, results confirmed the location of the transposon insertion sites obtained by DNA sequencing. Furthermore, the unique sizes of the PCR amplicons were successfully used to identify the presence of each mutant strain in animal experiments (Bannantine et al., 2014; Hines et al., 2014).

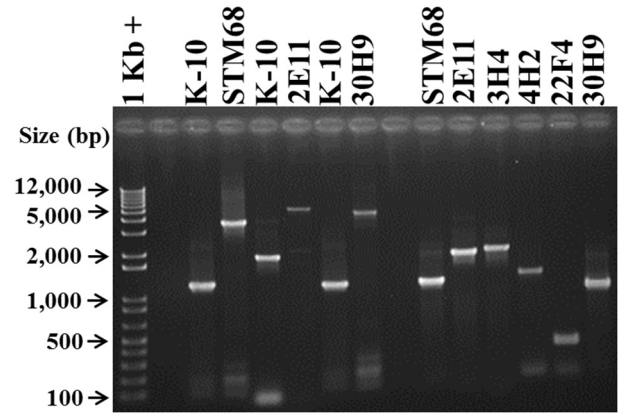

FIGURE 6 | Analysis of MAP Tn*5367* (3,381 bp) and Tn*5370* (2295 bp) insertion mutants by PCR. Lane 1, Invitrogen TrackIt™ 1 Kb Plus DNA Ladder; Lanes 2 and 9, empty. Amplicons for the DNA template-primer combinations and corresponding sizes are: Lanes 3 and 7, K-10 with MAP1566-F and MAP1566-R, 1179 bp; Lane 4, STM68 with MAP1566-F and MAP1566-R, 3474 bp; Lane 5, K-10 with 2E11-IP-F and 2E11-IP-R, 1845 bp; Lane 6, 2E11 with 2E11-IP-F and 2E11-IP-R, 5226 bp; Lane 8, 30H9 MAP1566-F and MAP1566-R, 4560 bp; Lane 10, STM68 with MAP1566-F and AMT32, 1160 bp; Lane 11, 2E11 with 2E11-IP-F and AMT32, 1890 bp; Lane 12, 3H4 with 3H4-R and AMT32, 1974 bp; Lane 13, 4H2 with 4H2-F and AMT32, 1431 bp; Lane 14, 22F4 with 22F4-F and AMT32, 561 bp; Lane 15, 30H9 with MAP1566-R and AMT32, 941 bp. Relevant band sizes (bp) for the DNA ladder are displayed to the left.

Determination of growth curves in broth cultures

As these MAP mutants were developed as first generation candidate vaccine strains, it was important to determine if their corresponding *in vitro* growth rates in broth cultures were similar to the wild type K-10 strain. Determination and statistical analysis of growth curves indicated that both wild type and mutant strains grew approximately at the same rate in MOADC, as assessed by OD (**Figure 7A**) or CFU (**Figure 7B**) determinations. In particular for OD values, growth rates of the mutant strains were not significantly different compared to K-10 ($P > 0.05$), except for 30H9 that grew slightly faster ($P = 0.047$). Likewise the more detailed CFU calculations showed a similar effect, but in this case 3H4 grew faster ($P = 0.021$), 22F4 had a slower rate ($P = 0.019$) and growth of 30H9 did not differ significantly ($P > 0.05$) from K-10. These results suggest that the mutations in these strains are related to properties that relate to virulence such as survival and replication in BoMac cells rather than standard physiological traits. This characteristic is desirable for candidate live-attenuated vaccine strains as the isolates can be readily propagated in broth cultures to prepare inoculums for vaccine delivery.

Interaction of wild type and mutant strains with primary bovine macrophages

As macrophages play a key role in MAP infections, to confirm the results obtained with BoMac cells and characterize additional mutants, we determined the interaction of wild type and mutant strains with primary macrophages. MDMs were infected with each strain at a MOI of 10:1, incubated to allow invasion, washed and lysed immediately or at various time points post-infection to determine colony counts (**Figures 8–10**). The results indicated that strains 2E11 ($P < 0.05$), 3H4 ($P < 0.01$) and 22F4 ($P < 0.001$) were significantly less invasive than K-10 (**Figure 8**). No major differences were observed for all four cases

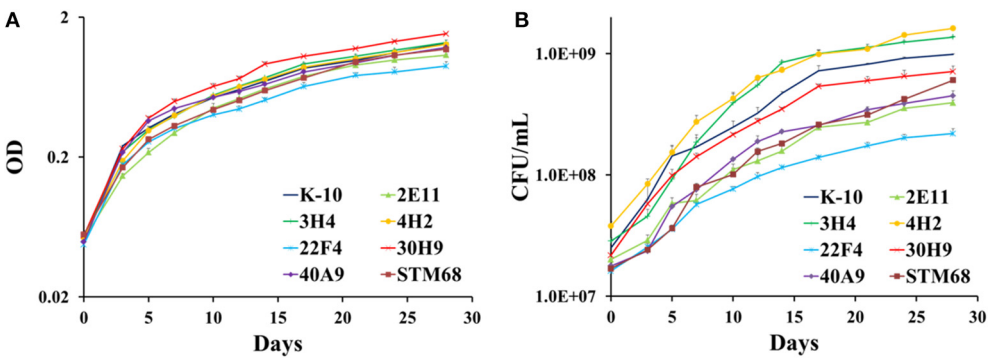

FIGURE 7 | (A,B) Growth curves of MAP wild type K-10 and mutant strains. Strains were inoculated into MOADC media at an initial optical density (OD_{600}) of approximately 0.05. Cultures were incubated at 37°C standing for 28 days. OD readings **(A)** and CFU after 5 weeks **(B)** were taken. Results represent means ($n = 3$) ± standard error of the mean. See text for relevant *P*-values.

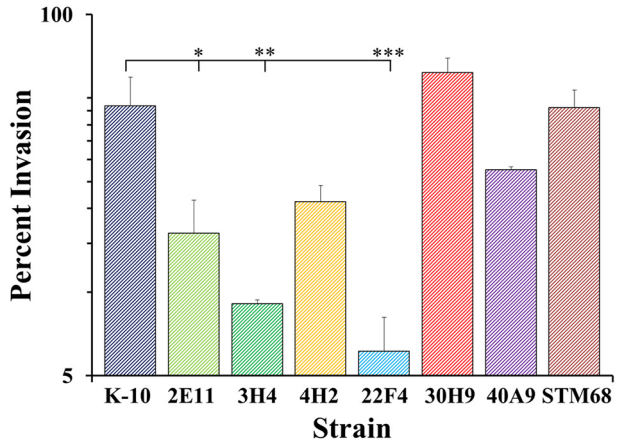

FIGURE 8 | Invasion of MAP wild type K-10 and mutant strains in bovine macrophages. Procedures followed are described in Lamont and Sreevatsan (2010). MAP uptake at the end of the invasion incubation period (percent invasion, 2 h after infection). Results represent means ($n = 3$) ± standard error of the mean. Statistical significance for pairwise determinations displayed by a line with tick marks is denoted with asterisks: * P-value < 0.05, ** P-value < 0.01 and *** P-value < 0.001.

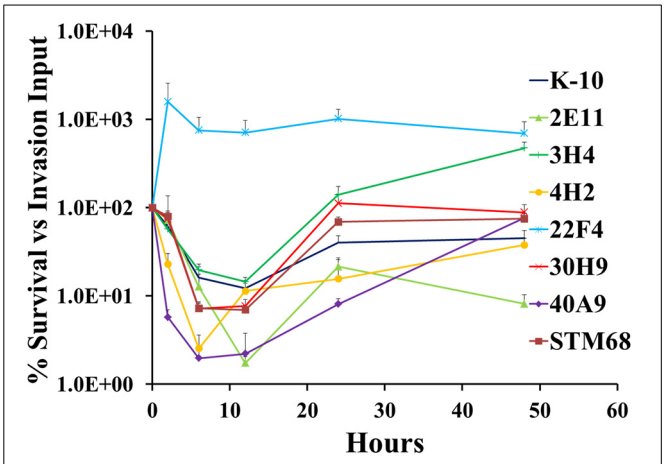

FIGURE 9 | Survival and replication of MAP wild type K-10 and mutant strains in bovine macrophages. Procedures followed are described in Lamont and Sreevatsan (2010). Kinetics of MAP intracellular survival and replication (after invasion) are based on the following formula: % Survival = $(CFU/ml_{time,t}/CFU/ml_{time,t=0}) \times 100\%$; time, t is any of the time points while time, $t = 0$ is the time point immediately after completion of invasion incubation. Results represent means ($n = 3$) ± standard error of the mean. See text for relevant P-values.

in comparison to K-10 $P > 0.1$. These results sharply contrast with strain invasiveness for BoMac cells (see Section Discussion).

The full short kinetics of the interaction of MAP strains with MDMs is shown in **Figure 9**. This analysis demonstrates that for most strains there is a pronounced killing phase immediately after invasion incubation up to 6–12 h, followed by a recovery phase and eventual stabilization of the CFU burdens. This aspect of the interaction is usually missed in standard assays that only study 2 time points (immediately after invasion incubation and 2/4 days). In this context, the killing and intracellular replication rates may also influence the final outcome of the interaction of MAP and MDMs. Statistical analysis of each process (e.g., killing and replication-stabilization phases) depicted in these curves was performed. Results indicated that strains 4H2 ($P < 0.05$) and 40A9 ($P < 0.05$) were killed much more rapidly than K-10, while 22F4 ($P < 0.001$) showed an unexpected increase in CFUs during the first 6 h. The intracellular replication rates (evaluated between 12 and 48 h) were similar for the wild type and all mutant strains, except for 3H4 ($P < 0.01$) and 40A9 ($P < 0.001$) that grew faster than K-10.

Figure 10 displays CFU burdens at Day 0 after invasion incubation (striped bars) and Day 2 (solid bars) for mutant and wild type strains. As the MAP inoculums for MDMs were approximately the same for all strains, the CFU burdens at Day 0 are proportional to strain invasiveness (**Figure 8**). Thus, direct comparisons of Day 0 CFU burdens yielded similar P values for pair-wise comparisons as those observed for differences in invasion, except that the decrease in invasiveness for 3H4 ($P < 0.001$) vs. K-10 had a greater significance level. Nonetheless, the analysis based on percent invasion presented in **Figure 8** is more accurate, as any differences in the inoculums are taken into account. Regarding strain intracellular survival, as indicated by the CFU burdens for each strain at Day 0 and Day 2, no significant differences were observed for strains 30H9, 40A9, and STM68 ($P > 0.1$). For K-10, the decrease observed in survival is moderate, but falls within statistical significance ($P < 0.05$). In contrast, marked decreases are observed for 2E11 ($P < 0.001$) and 4H2 ($P < 0.01$). Interestingly, 3H4 ($P < 0.001$) and 22F4 ($P < 0.001$) were able to survive and replicate significantly better than K-10 intracellularly. Comparisons of the overall macrophage CFU burdens at Day 2 among all strains allow us to determine the combined effects of invasion and intracellular survival/replication. The results indicate that strain 2E11 is definitively attenuated in comparison to K-10 ($P < 0.001$); while 4H2 is slightly attenuated, but this difference is not statistically significant. Strains 22F4, 40A9, and STM68 behaved similarly to K-10 ($P > 0.1$), while strains 3H4 ($P < 0.05$) and 30H9 ($P < 0.05$) seem to reach higher CFU burdens than K-10.

In summary for the interaction of MAP strains with MDMs, mutants 2E11, 3H4, and 22F4 were less invasive than K-10. In relation to survival, 2E11 and 4H2 displayed marked reductions. For the overall Day 2 CFU burdens, only 2E11 was attenuated. Overall, strains 22F4, 40A9, and STM68 behaved similarly to K-10, while 3H4 and 30H9 reached a higher number of intracellular bacilli. For the killing phase, 4H2 and 40A9 were killed faster than K-10 and all mutant strains were able to grow intracellularly at approximately the same rate, except for 3H4 and 40A9 that replicated faster.

Complementation analysis

We also attempted to develop a complementation system for the Tn*5367* transposon mutants using a derivative of the multi-copy plasmid pMV206_Hyg (George et al., 1995). To this end, vector pBUN277 was constructed carrying a *hyg* marker and the green fluorescent protein gene downstream from the mycobacterial heat shock promoter *hsp60*. Assessment of wild type K-10,

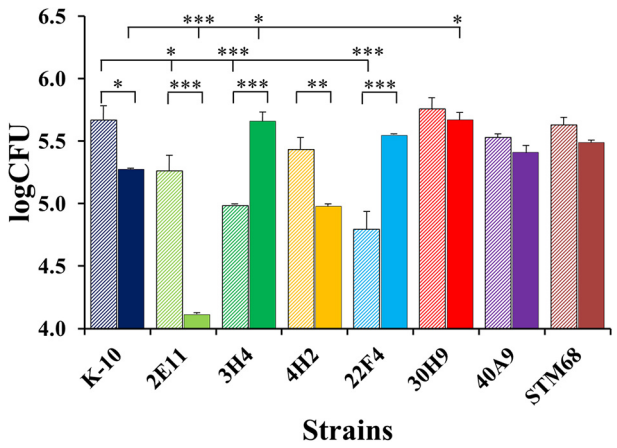

FIGURE 10 | MAP burdens of wild type K-10 and mutant strains in bovine macrophages. Procedures followed are described in Lamont and Sreevatsan (2010). Total CFU burdens at Day 0 (2 h after infection, striped bars) and Day 2 (solid bars) are displayed. Results represent means ($n = 3$) ± standard error of the mean. Statistical significance for pairwise determinations displayed by a line with tick marks is denoted with asterisks: **P*-value < 0.05, ***P*-value < 0.01 and ****P*-value < 0.001.

4H2 and the empty vector control 4H2 (pBUN277) in MDMs yielded anomalous results. The survival of 4H2 was significantly different ($P < 0.05$) from K-10 at 5 days post-infection, while the survival of 4H2 (pBUN277) was not significantly different ($P > 0.05$) from K-10 (unpublished results). In addition, the survival of 4H2 recombinant strains carrying either the wild type gene MAP1152 or MAP1156 yielded similar results to the empty vector control ($P > 0.05$). This data indicates that the complementation system developed was not appropriate and further attempts were no longer pursued for additional mutants.

DISCUSSION

The objective of our study was to generate a comprehensive MAP mutant bank and isolate strains with interesting phenotypic properties and identify genomic regions associated with virulence that could be targeted for further development of live-attenuated vaccine strains. Mutants identified for at least one phenotypic property potentially related to virulence are displayed in Table S1. This set of 123 strains represents ca. 1% of the mutant bank. The uniqueness of our approach was to perform the screen independently of homology searches for genes already identified in related mycobacterial species, so as to maximize hits in genes specific for MAP.

Statistical considerations, coupled with the demonstration that randomly picked mutants were independent, suggest that the library was comprehensive: e.g., mutants displayed unique hybridization bands to the IS*1096* probe (see Section Southern hybridization) and diverse phenotypes (Table S1). It is especially noteworthy that five of the mutants selected for the vaccine trail (3H4, 4H2, 22F4, 30H9, and 40A9) and three additional mutants identified as attenuated in BoMac cells or preliminary MDM assays (12G8, 23B5, and 37D1) were all associated with altered DCS susceptibility. As for the rapid screens for cell association, and biofilm and clump formation, five (1B11, 3D9, 4E1, 4E7, and 4F3) out of ca. 300 screened mutants (approximately 1.5%) of the pool, identified strains with properties that may relate to virulence, but did not overlap with the DCS altered susceptibility set. Thus, implementation of additional screens, or expansion of the screens reported herein may still reveal a significant number of potentially attenuated mutants. However, the inherent bias of IS*1096*-derived transposons limits somewhat the comprehensiveness of the mutant bank (McAdam et al., 2002; Shin et al., 2006). Fortunately, *Himar*-derived transposons with more random recognition sequences have been developed for mycobacteria (Sassetti and Rubin, 2003) and are already in use for MAP (Scandurra et al., 2009; Wang et al., 2014). These vectors may provide a more representative mutant repertoire, but at the cost of a significant increase (ca. 10-fold) in the number of mutants that should be screened for a comprehensive analyses. In addition, best recommended screening approaches for *Himar* libraries are focused on gene identification analyses under specified selection pressures (Sassetti and Rubin, 2003). Individual deletion mutants and complementation analysis must then be performed to further confirm the role of these genes in virulence. Thus, the library described herein is useful as source of individual mutants for identification of genes involved in MAP pathogenesis, but implementation of additional screens to formally determine its comprehensiveness may not be warranted. Nonetheless, as described, we performed three comprehensive screens (colony morphology, DCS hypersusceptibility and siderophore production), and three additional limited screens for reduced biofilm and clump formation, and decreased cell association with BoMac cells. Assuming that most of these insertions are in different genes, this collection may represent insertions in ca. 120 genes. In this context, previous studies with MTB demonstrated that 194 genes are required for infection in mice (Sassetti and Rubin, 2003).

Seven Tn*5367* mutants from the set depicted in Table S1 as well as STM68, a mutant from the Tn*5370* signature-tagged mutagenesis pool, were further characterized and their properties are summarized in **Table 2**. In our comprehensive screening of the mutant bank using a chromogenic assay for siderophore detection, only mutant 1F3 did not display a halo in the CAS plate assay. This mutant grew very slowly in broth cultures but was able to colonize goats (Livneh et al., 2005). Unfortunately, as indicated above, stocks in two laboratories failed to grow upon further attempts at replication and the transposon insertion site could not be determined. The CAS assay phenotype has been associated with impairment of siderophore synthesis or secretion in Msmeg (Fiss et al., 1994). Thus, the properties of 1F3 suggests that MAP has at least an additional siderophore-like molecule that may be involved in iron uptake and play important physiologic roles. Though MAP has a truncated *mbtA* gene that most likely underlies its inability to synthesize mycobactin (Li et al., 2005), mycobactin-dependence is observed mainly in MAP cultured directly from primary lesions or other clinical specimens. In passaged cultures, mycobactin dependence can be readily overcome in acidic iron-rich media (Lambrecht and Collins, 1992). Thus, we hypothesized that 1F3 may have had a lesion in a gene encoding for a siderophore-like molecule other than mycobactin.

Table 2 | Screening and characterization of MAP strains.

Strain[a]	ORF(s)—Mutated or Affected[b]	ORFs Function[c]	Original Screen and Further Comments[d]
1F3	Tn*5367* insertion was not identified	Not applicable	Chromogenic screen for siderophore synthesis or transport; mutant lost upon subsequent passages
2E11 Vaccine 316	Tn*5367* between MAP3695 (Rv0245) and FadE5 (Rv0244c)	MAP3695 (hypothetical protein) FadE5 (terpenoid and polyketide metabolism)	Attenuated in MDMs for invasion and intracellular survival
3H4 Vaccine 320	Tn*5367* between MAP2296c (Rv2478c) and MAP2297c (Rv0102)	MAP2296c and MAP2297c (hypothetical proteins)	DCS hypersusceptible mutant chosen as control for normal colony morphology. Attenuated for invasion in MDMs, but has faster intracellular replication
4H2 Vaccine 321	Tn*5367* between MAP1150c (Rv3640c) and MAP1151c (Rv2839c) Upstream from MAP1152 (Rv1808)-MAP1156 (Rv1425) cluster	MAP1150c (IS*1311* transposase) MAP1151c (translational initiation factor IF2) MAP1152 (PPE protein) MAP1156 (diacyglycerol O-acyltransferase)	Colony-morphology mutant, attenuated for invasion in BoMac cells, and invasion and survival in MDMs. Mutant also displayed DCS hypersusceptibility.
22F4 Vaccine 317	Tn*5367* within MAP0460 (Rv3597c, Lsr2)	Lsr2 (H-NS like iron-regulated DNA binding protein that also provides protection against oxidative stress)	DCS hypersusceptible; attenuated for survival in BoMac cells and invasion in MDMs
30H9 Vaccine 319	Tn*5367* within MAP1566 (Rv1645c) near 5′-end coding sequence	MAP1566 ORF downstream from ModA (MAP1565) in the mod operon	DCS hypersusceptible; attenuated for invasion in BoMac cells
40A9 Vaccine 318	Tn*5367* between MAP0282c (Rv3860) and MAP0283c (Rv2082)	MAP0282c and MAP0283c (hypothetical proteins, assigned with low confidence); or spontaneous rRNA mutations	Decreased susceptibility to DCS; transposon lost upon further passage; attenuated in MDMs by increased killing rate
STM68 Vaccine 315	Tn*5370* within MAP1566 (Rv1645c) near 3′-end coding sequence	MAP1566 ORF downstream from ModA (MAP1565) in the *mod* operon	Identified as MAP1566 insertion by direct sequencing of Tn*5370* signature-tagged mutagenesis pool

[a] *Laboratory designation followed by the vaccine trial designation (Bannantine et al., 2014; Hines et al., 2014).*

[b] *MAP ORF designation is followed by MTB definite or putative ortholog in parenthesis.*

[c] *See text for citations on ORFs functions as applicable.*

[d] *See text for further details.*

Mutant 2E11 was a false positive for reduced biofilm formation, but it was nonetheless selected for further studies, since preliminary assays indicated attenuation in MDMs. Assignment of the target gene for mutant 2E11 was not fully resolved in this study as the Tn*5367* insertion was mapped to the intergenic region (**Figure 5**) encoding an acyl-coA dehydrogenase (MAP3694c, aka FadE5) and a possible oxidoreductase (MAP3695). Interestingly, FadE5 is involved in lipid degradation (http://www.ncbi.nlm.nih.gov/biosystems/1743) including the metabolism of terpenoids and polyketides, such as geraniol, and these compound types have been associated with biofilm formation in bacteria (Zheng et al., 2013). MAP FadE5 is orthologous to MTB Rv0244c, which has been shown to be required for *in vitro* growth on cholesterol (http://tuberculist.epfl.ch). This mutant was the most attenuated in this study on account of both invasiveness and survival in MDMs.

Mutant 3H4 displayed a transposon insertion in the intergenic region between MAP2296c and MAP2297c. Both these ORFs encode for hypothetical proteins, with the MTB ortholog (Rv2478c) possibly encoding a non-essential DNA binding protein, and MAP2297c ortholog (Rv0102) identified as an integral essential membrane protein and ABC transporter that may underlie the DCS hypersusceptible phenotype (http://tuberculist.epfl.ch). Though, this mutant was originally selected as a normal colony morphotype control, it displayed hypersusceptibility to DCS. Nonetheless, this strain behaved similarly to the wild type K-10 strain in both BoMac cells and MDMs, except that it displayed an attenuated invasion phenotype in the interaction with MDMs that was compensated with a higher intracellular replication rate.

In 4H2, the transposon inserted within the intergenic region between MAP1150c and MAP1151c. MAP1150c is the transposase for IS*1311* (Murcia et al., 2007), an insertion sequence present at eight copies in the MAP genome (Li et al., 2005). Thus, any effect of this insertion on the MAP1150c is not likely to have a major impact on MAP physiology. In addition, the insertion may not have an effect on MAP1151c either as the transposon is located beyond the 3′-end of this coding sequence. However, there is a gene cluster (MAP1152-MAP1156) (Bannantine et al., 2011) that is transcribed from the complementary strand to MAP1150c,

whose expression could be effected by the transposon insertion that is located 634 bp upstream from the 5′-end of MAP1152. This gene cluster is very interesting since MAP1152, MAP1153 and MAP 1155 encode PPE proteins of the ancestral sublineage IV (Gey Van Pittius et al., 2006). PPE proteins have been suggested to play a role as host range determinants (Cole et al., 1998) and the immunopathogenesis of both humoral and cellular responses in MTB (Choudhary et al., 2003; Okkels et al., 2003) and MAP (Nagata et al., 2005). Other PPE proteins in MTB (Rv1807, Rv3872, and Rv3873) have been implicated in virulence since inactivation of the corresponding genes results in mutants attenuated in mice (Sassetti and Rubin, 2003). In addition, PPE and PE proteins function in pairwise combinations of interacting partners exposed to the cell surface (Riley et al., 2008) and both sets are markedly underrepresented in MAP (cf. 36 PPE proteins in MAP vs. 68 in MTB) (Li et al., 2005). The other members of the gene cluster, MAP1154 and MAP1156, encode proteins of an uncharacterized protein family. MAP1154 encodes a hypothetical protein, while MAP1156 has putative diacyglycerol O-acyltransferase activity (Bannantine et al., 2011). Mutant 4H2 was clearly attenuated in both BoMac and MDM cells, on account of reduced invasiveness and intracellular survival. Moreover, we have demonstrated that MAP1152 and MAP1156 engender humoral immunity responses that can be used to identify infected animals and thus, the corresponding mutants have potential for DIVA (differentiating infected from vaccinated animals) vaccine formulations (Bannantine et al., 2011).

Mutants 22F4 and 30H9 were identified as DCS hypersusceptible strains. Isolate 22F4 carries an insertion within the gene encoding the Lsr2 protein that has been implicated in various roles: dominant T cell responses in MTB (Stewart et al., 2002) and biofilm formation and colony morphology in Msmeg (Chen et al., 2006). Furthermore, a MAP *lsr2* deletion mutant has been constructed (Park et al., 2008) that showed similar properties and a marginal degree of attenuation in MDMs to 22F4 (Lamont et al., 2014), thus providing strong evidence that the transposon insertion, that is internal to *lsr2*, does disrupt the function of this gene.

Strain 30H9 has an insertion internal to MAP1566 and proximal to its 5′-end coding sequence. Likewise, STM68 carries an insertion in MAP1566 but closer to its 3′-end that could potentially have a greater effect on the downstream gene MAP1567. The cluster MAP1565-MAP1568 seems to comprise an operon encoding a high affinity molybdate transport system, as indicated by bioinformatic analysis (Braibant et al., 2000). Orthologs are present in *M. avium* strain 104 (MAV_2862, 99% identity), MTB (Rv1645c, 35% identity, 50% similarity) as well as other mycobacterial species. However, only the MAP and *M. avium* 104 strain orthologs are located within the Mod operon, making this arrangement unique to these species. We hypothesize that MAP1566 could be a chaperone that works in concert with this transport system, while MAP1565 (ModA) and MAP1567 (ModB) are integral membrane proteins that constitute and stabilize the transport channel. It seems that MAP1569 (ModD) has a function in fibronectin binding unrelated to this molybdenum transport system (Kumar et al., 2003) and thus it may correspond to a different transcriptional unit. Strong evidence for the transposon insertions affecting the functions of Mod operon (e.g., MAP1566 or MAP1567) is provided by the similar properties of both mutants in MDMs, mice (Bannantine et al., 2014) and goats (Hines et al., 2014). These mutants were attenuated in C57BL/6 mice but protective against wild type challenge, displayed low skin reactivity in goats and showed significant attenuation in MDM assays as analyzed elsewhere (Lamont et al., 2014). However, in this current analysis, 30H9 and STM68 were comparable to the wild type strain. Interestingly, another MAP1566 Tn*5367* mutant (WAg906), derived from the MAP wild type strain 989 (Cavaignac et al., 2000), was shown to be attenuated based on the average slope values obtained in long-term MDM assays as well as BALB/c mice at 12 weeks post-infection (Scandurra et al., 2010; Bannantine et al., 2014; Lamont et al., 2014). However, in protection challenge experiments, 30H9 and STM68 showed good protection in C57BL/6 mice against wild type challenge, while WAg906 failed to protect BALB/c mice. Use of different MAP and mouse strains may explain these results. These three mutants were attenuated for survival in goats, but only 30H9 and STM68 were tested for protection against challenge, displaying low efficacy (Scandurra et al., 2010; Hines et al., 2014).

As for 40A9, the loss of the transposon insertion does not allow us to make any definitive conclusions on the molecular basis underlying its attenuation. However, this mutant still retained the Kan-resistant phenotype suggesting the involvement of spontaneous mutations in ribosomal RNA genes (Du et al., 2013). Nonetheless, this mutant was the most protective from this collection in the goat trial (Hines et al., 2014). The most interesting property observed for this strain was a fast intracellular killing in MDMs followed by its ability to recover and grow (**Figure 9**), but otherwise this strain reached a similar CFU burden as K-10 at Day 2 post-infection (**Figure 10**).

Regarding the complementation studies, there are several reasons that may explain the anomalous results including: (i) the *hyg* marker may increase the survival of the host strains as it was observed for Msmeg recombinant strains (Chacon et al., 2009); (ii) the inherent instability of the Tn*5367* mutant strains with the potential for further transposition events by a cut and paste mechanism (McAdam et al., 1995); (iii) the possibility of spurious recombination events for strains carrying multiple copies of wild type DNA sequences in the complementing plasmids and the transposon interrupted copies in the genome. Due to these difficulties, conclusions regarding the roles of the genes identified in this study are still presumptive rather than definitive. Nonetheless, the bioinformatic analysis and the correlation with our previous results and those from other laboratories increase the confidence that most of these genes are relevant to MAP survival and pathogenesis. Moreover, MAP slow growth and low transformation efficiency place an onerous time demand on further attempts to revisit complementation studies (Foley-Thomas et al., 1995). These issues may underlie the lack of reported complementation analysis in previous MAP transposon mutant reports (Shin et al., 2006; Scandurra et al., 2009, 2010). To overcome these complications, we are currently implementing more solid strategies to construct and complement deletion mutants using different selection markers.

An important objective of this study was to compare the interaction of different MAP strains with BoMac cells and MDMs in this study and the parallel study in the vaccine trial (Lamont et al., 2014). In our studies, the order of attenuation in BoMac cells and MDM cultures (comparing invasion percentiles and slopes for each infection phase) was significantly different. Strain 30H9 displayed the greatest attenuation in BoMac cells, while it was the least attenuated in the MDM assays based on the analysis reported herein. Mutants 3H4 and 22F4 yielded less discrepancy, while 4H2 behaved similarly. However, when the strains were compared only by the average slope values in MDM assays (Lamont et al., 2014), results were closer to those obtained with BoMac cells, with 30H9 yielding the greatest attenuation among the four strains that were also tested in BoMac cells. Notably, 3H4, 22F4, and 30H9 had major differences in invasiveness for the two cell types: 3H4 and 22F4 were invasive for BoMac cells, but not for MDMs (**Figures 3**, **8**), while the opposite was observed for 30H9. The differences observed are likely due to the inherent nature of the BoMac cell line that has poor phagocytosis and decreased ability to sustain intracellular MAP replication, as shown previously for the wild type strain K-10 (Woo et al., 2006). A similar situation seems to occur in MDM aging cultures (Scandurra et al., 2010; Lamont et al., 2014). Thus, determination of the early kinetics at each phase (e.g., invasion, intracellular killing and replication), as done in this study, seems to provide the best assessment of strain attenuation for studies in ruminants. This analysis may be supplemented with assays to determine apoptosis and measure cytokines such as IL-10 (Scandurra et al., 2010; Kabara and Coussens, 2012; Lamont et al., 2014).

Comparing the results from this study with the recent vaccine trial, though not conclusive, sheds some light on the relation among the various models and vaccine protection for ruminants. Attenuation in BoMac cells and analysis of average slopes in MDM assays showed significant correlation with attenuation and protection in C57BL/6 mice vaccinated by intraperitoneal injection, but not with orally vaccinated goats (Bannantine et al., 2014; Hines et al., 2014; Lamont et al., 2014). In contrast, the analysis in this manuscript of MDM assays correlated well with protection results in goats. Indeed, the four strains tested in goats ranked similarly; except for the inversion between 2E11 (most attenuated in MDMs as reported here, but ranked 2nd in goats) and 40A9 (ranked 2nd in MDMs, but most protective in goats).

As to the MAP mutant properties necessary to elicit protective immunity in ruminants, based on the conditions tested in the vaccine trial, interplay between attenuation and virulence seems necessary. Moreover, a level of persistence (e.g., able to colonize well *in vivo* at early time points but lead to significant reduction in colonization at later times post-infection) has been hypothesized as one desirable property for the design of MTB live attenuated vaccines (Hingley-Wilson et al., 2003). For example, 40A9 would be considered rather wild type like, based on the CFU burdens at either Day 0 or Day 2 (**Figure 10**). However, this strain displays both faster killing and intracellular replication rates (**Figure 9**). Significant killing of 40A9 in their first encounter with macrophages may provide sufficient attenuation while preserving protective immunogenicity. The subsequent fast intracellular recovery may lead to a persistent behavior. Though, 40A9 was not tested in BALB/c mice for the persistent phenotype, this behavior was observed for Vaccine 329 that outperformed 40A9 in goats (Shin et al., 2006; Hines et al., 2014). In contrast, 30H9 and STM68 displayed a behavior similar to the wild type K-10 in each of the steps involved in the interaction of the mutant strains with MDMs (**Figures 8–10**), but performed worse in the goat vaccination trial. In addition, little correlation was observed between the mouse and goat trails, though in this case the more susceptible C57BL/6 mice were used (Bannantine et al., 2014). Thus, the level of protection of a candidate vaccine strain may depend on earlier interactions of the mutant strains with the oral, gastric and intestinal mucosa, and intracellular killing and replication rates in MDMs (Bermudez et al., 2010). In addition, there still remains significant issues regarding tissue culture (BoMac vs. MDM cells), analysis of tissue culture results, animal model (BALB/c and C57BL/6 mice or goats), dose (low vs. high) and routes of inoculation (intraperitoneal, oral and subcutaneous) that need further testing and standardization to make better predictions on protection for JD vaccines in cattle.

CONCLUSIONS

The major accomplishments and findings of this study are: (1) a comprehensive MAP Tn*5367* transposon mutant bank was constructed by indexing a large collection of independent mutants that was statistically representative of the full genome; (2) Tn*5367* mutants were inherently unstable due to the IS*1096* transposase presence within the transposed sequence; (3) phenotypic screens were effective in identifying attenuated mutants or processes of importance for pathogenesis or cell physiology: (a) the presence of additional siderophores other than mycobactin (e.g., 1F3), (b) the association of colony morphotypes with reduced virulence (e.g., 4H2 and 22F4), (c) the association of drug-susceptible (e.g., 22F4 and 30H9) or resistant (e.g., 4H2 and 40A9) phenotypes with reduced virulence and (d) the potential role of cell association, and biofilm and clump formation with virulence (see Section Miscellaneous screening); (4) mutant screening in BoMac cells and MDMs yields significantly different results; (5) strain invasiveness and slope values at each step in the interaction of MAP bacilli with MDMs, especially the slopes during the early killing phase, are the best predictors for protection against wild type challenge in the oral goat vaccination model; (6) the interaction of MAP with MDMs is complex and key aspects of this process involve: invasion, intracellular killing, intracellular replication and maintenance of CFU intracellular burdens; (7) mutant screening with BoMac cells may have significant biases and it should be abandoned as a routine methodology to assess attenuation; and (8) the most important stages of MAP interaction with MDMs in tissue culture occur at relatively short times (up to 48 h post-invasion incubation). Our results suggests that further studies with MAP mutants should focus on early step-wise analysis of their interactions with MDMs and the use of transposon delivery vectors that lack the transposase within the transposed element (e.g., Tn*5370* and the newly developed *Himar1* derivatives).

ACKNOWLEDGMENTS

The following Federal Agency sources are acknowledged for funding: USDA CSREES-NRI (99-35204-7789, 2004-35204-14231 and

JDIP 2004-35605-14243), USDA-BARD (IS-3673-05C), USDA-NIFA Animal Health ARD Station Project (NEB-14-141 and NEB-39-162). We also wish to acknowledge worthwhile discussions and advice from Drs. Luiz Bermudez (MDM assays), Ofelia Chacon (DCS screen), Jeffrey D. Cirillo (Tn*5370* phage materials and sequencing data), Amit Pandey (complementing plasmid constructions), Dilip Patel (MDM blind assays for complementation studies in Bermudez laboratory) and William R. Jacobs Jr. (various tools for mycobacterial genetic manipulations). We thank Shingo Ishihara and Harshdeep Dogra for technical assistance in preliminary PCR experiments and vector construction, respectively. Strains described in **Table 2** of this manuscript are available from the corresponding author's laboratory or the laboratories of the USDA-CAP Johne's Integrated Program (JDIP) sponsored vaccine trial participating institutions (Bannantine et al., 2014; Hines et al., 2014; Lamont et al., 2014) upon signing a modified Uniform Biological Material Transfer Agreement via Pennsylvania State University.

SUPPLEMENTARY MATERIAL

The Supplementary Material for this article can be found online at: http://www.frontiersin.org/journal/10.3389/fcimb.2014.00144/abstract

Figure S1 | (A–D) Screening of MAP mutants for susceptibility or resistance to DCS. All mutants were plated on MOADC-Plus media without **(A,C)** and with **(B,D)** DCS at 20 μg/ml and allowed to grow for 8 weeks. There are two different scale bars displayed since a Fisherbrand 08-757-14 round **(A,C)** or Corning 431110 square **(B,D)** plate was utilized. Mutants with altered DCS susceptibility are circled with black outlines: the rough colony morphotype 4H2 **(A,B)** displays a resistant phenotype while the smooth colony morphotype 22F4 **(C,D)** displays hypersusceptibility.

Figure S2 | Rapid screening for MAP mutants with decreased biofilm formation. The left image depicts a MAP mutant with reduced biofilm formation while the image on the right is a mutant with normal biofilm formation.

Figure S3 | (A,B) Rapid screening for MAP mutants with reduced cell association. A rapid *in vitro* assay was developed to screen the library for mutants with decreased cell association (e.g., less adherence and/or invasion) with BoMac cells. Cells were plated on a 16-well chamber slide and infected with MAP wild type and mutant strains. At 24 h post-incubation, slides were fixed and acid-fast bacteria were stained by the Auramine-Rhodamine method that yields green fluorescence for acid-fast bacilli. Representative microscopic images from an infection with the wild type strain K-10 **(A)** and a mutant with decreased cell association **(B)** are shown. Internal scale bar is 100 μm.

Figure S4 | (A,B) Rapid screening for MAP mutants with reduced clump formation. To test for mutants with reduced clump formation, a property that could be related to virulence, broth cultures were analyzed by microscopy. Microscopic images of the wild type strain K-10 **(A)** and a mutant with reduced clump formation **(B)** are shown. Internal scale bar is 10 μm.

REFERENCES

Bach, H., Sun, J., Hmama, Z., and Av-Gay, Y. (2006). *Mycobacterium avium* subsp. paratuberculosis PtpA is an endogenous tyrosine phosphatase secreted during infection. *Infect. Immun.* 74, 6540–6546. doi: 10.1128/IAI.01106-06

Bannantine, J. P., Everman, J., Rose, S. J., Babrak, L., Katani, R., Barletta, R. G., et al. (2014). Evaluation of eight live attenuated *Mycobacterium avium* subspecies paratuberculosis mutant strains for protection from colonization of tissues in mice. *Front. Cell. Infect. Microbiol.* 4:88. doi: 10.3389/fcimb.2014.00088

Bannantine, J. P., Paulson, A. L., Chacon, O., Fenton, R. J., Zinniel, D. K., Mcvey, D. S., et al. (2011). Immunogenicity and reactivity of novel *Mycobacterium avium* subsp. *paratuberculosis* PPE MAP1152 and conserved MAP1156 proteins with sera from experimentally and naturally infected animals. *Clin. Vaccine Immunol.* 18, 105–112. doi: 10.1128/CVI.00297-10

Bannantine, J. P., and Paustian, M. L. (2006). Identification of diagnostic proteins in *Mycobacterium avium* subspecies paratuberculosis by a whole genome analysis approach. *Methods Mol. Biol.* 345, 185–196. doi: 10.1385/1-59745-143-6:185

Bannantine, J. P., Wu, C. W., Hsu, C., Zhou, S., Schwartz, D. C., Bayles, D. O., et al. (2012). Genome sequencing of ovine isolates of *Mycobacterium avium* subspecies paratuberculosis offers insights into host association. *BMC Genomics* 13:89. doi: 10.1186/1471-2164-13-89

Bardarov, S., Bardarov, S. Jr., Pavelka, M. S. Jr., Sambandamurthy, V., Larsen, M., Tufariello, J., et al. (2002). Specialized transduction: an efficient method for generating marked and unmarked targeted gene disruptions in *Mycobacterium tuberculosis*, M. bovis BCG and M. smegmatis. *Microbiology* 148, 3007–3017.

Bardarov, S., Kriakov, J., Carriere, C., Yu, S., Vaamonde, C., McAdam, R. A., et al. (1997). Conditionally replicating mycobacteriophages: a system for transposon delivery to *Mycobacterium tuberculosis*. *Proc. Natl. Acad. Sci. U.S.A.* 94, 10961–10966. doi: 10.1073/pnas.94.20.10961

Bastida, F., and Juste, R. A. (2011). Paratuberculosis control: a review with a focus on vaccination. *J. Immune Based Ther. Vaccines* 9:8. doi: 10.1186/1476-8518-9-8

Bermudez, L. E., Petrofsky, M., Sommer, S., and Barletta, R. G. (2010). Peyer's patch-deficient mice demonstrate that *Mycobacterium avium* subsp. paratuberculosis translocates across the mucosal barrier via both M cells and enterocytes but has inefficient dissemination. *Infect. Immun.* 78, 3570–3577. doi: 10.1128/IAI.01411-09

Braibant, M., Gilot, P., and Content, J. (2000). The ATP binding cassette (ABC) transport systems of *Mycobacterium tuberculosis*. *FEMS Microbiol. Rev.* 24, 449–467. doi: 10.1111/j.1574-6976.2000.tb00550.x

Bull, T. J., Schock, A., Sharp, J. M., Greene, M., Mckendrick, I. J., Sales, J., et al. (2013). Genomic variations associated with attenuation in *Mycobacterium avium* subsp. *paratuberculosis vaccine strains*. *BMC Microbiol.* 13:11. doi: 10.1186/1471-2180-13-11

Cavaignac, S. M., White, S. J., De Lisle, G. W., and Collins, D. M. (2000). Construction and screening of *Mycobacterium paratuberculosis* insertional mutant libraries. *Arch. Microbiol.* 173, 229–231. doi: 10.1007/s002039900132

Chacon, O., Bermudez, L. E., Zinniel, D. K., Chahal, H. K., Fenton, R. J., Feng, Z., et al. (2009). Impairment of D-alanine biosynthesis in *Mycobacterium smegmatis* determines decreased intracellular survival in human macrophages. *Microbiology* 155, 1440–1450. doi: 10.1099/mic.0.024901-0

Chacon, O., Feng, Z., Harris, N. B., Caceres, N. E., Adams, L. G., and Barletta, R. G. (2002). *Mycobacterium smegmatis* D-Alanine Racemase Mutants Are Not Dependent on D-Alanine for Growth. *Antimicrob. Agents Chemother.* 46, 47–54. doi: 10.1128/AAC.46.2.47-54.2002

Chen, J. M., German, G. J., Alexander, D. C., Ren, H., Tan, T., and Liu, J. (2006). Roles of Lsr2 in colony morphology and biofilm formation of *Mycobacterium smegmatis*. *J. Bacteriol.* 188, 633–641. doi: 10.1128/JB.188.2.633-641.2006

Chen, J. W., Faisal, S. M., Chandra, S., Mcdonough, S. P., Moreira, M. A., Scaria, J., et al. (2012a). Immunogenicity and protective efficacy of the *Mycobacterium avium* subsp. paratuberculosis attenuated mutants against challenge in a mouse model. *Vaccine* 30, 3015–3025. doi: 10.1016/j.vaccine.2011.11.029

Chen, J. W., Scaria, J., and Chang, Y. F. (2012b). Phenotypic and transcriptomic response of auxotrophic *Mycobacterium avium* subsp. paratuberculosis leuD mutant under environmental stress. *PLoS ONE* 7:e37884. doi: 10.1371/journal.pone.0037884

Cho, D., Shin, S. J., Talaat, A. M., and Collins, M. T. (2007). Cloning, expression, purification and serodiagnostic evaluation of fourteen *Mycobacterium paratuberculosis* proteins. *Protein Expr. Purif.* 53, 411–420. doi: 10.1016/j.pep.2006.12.022

Choudhary, R. K., Mukhopadhyay, S., Chakhaiyar, P., Sharma, N., Murthy, K. J., Katoch, V. M., et al. (2003). PPE antigen Rv2430c of *Mycobacterium tuberculosis* induces a strong B-cell response. *Infect. Immun.* 71, 6338–6343. doi: 10.1128/IAI.71.11.6338-6343.2003

Cirillo, J. D., Barletta, R. G., Bloom, B. R., and Jacobs, W. R. Jr. (1991). A novel transposon trap for mycobacteria: isolation and characterization of IS1096. *J. Bacteriol.* 173, 7772–7780.

Cole, S. T., Brosch, R., Parkhill, J., Garnier, T., Churcher, C., Harris, D., et al. (1998). Deciphering the biology of *Mycobacterium tuberculosis* from the complete genome sequence. *Nature* 393, 537–544. doi: 10.1038/31159

Connell, N. D., Medina-Acosta, E., Mcmaster, W. R., Bloom, B. R., and Russell, D. G. (1993). Effective immunization against cutaneous leishmaniasis with recombinant bacille Calmette-Guerin expressing the Leishmania surface proteinase gp63. *Proc. Natl. Acad. Sci. U.S.A.* 90, 11473–11477. doi: 10.1073/pnas.90.24.11473

Cox, J. S., Chen, B., Mcneil, M., and Jacobs, W. R. Jr. (1999). Complex lipid determines tissue-specific replication of *Mycobacterium tuberculosis* in mice. *Nature* 402, 79–83.

Du, Q., Dai, G., Long, Q., Yu, X., Dong, L., Huang, H., et al. (2013). *Mycobacterium tuberculosis* rrs A1401G mutation correlates with high-level resistance to kanamycin, amikacin, and capreomycin in clinical isolates from mainland China. *Diagn. Microbiol. Infect. Dis.* 77, 138–142. doi: 10.1016/j.diagmicrobio.2013.06.031

Faisal, S. M., Chen, J. W., Yan, F., Chen, T. T., Useh, N. M., Yan, W., et al. (2013). Evaluation of a *Mycobacterium avium* subsp. paratuberculosis leuD mutant as a vaccine candidate against challenge in a caprine model. *Clin. Vaccine Immunol.* 20, 572–581. doi: 10.1128/CVI.00653-12

Feng, Z., and Barletta, R. G. (2003). Roles of *Mycobacterium smegmatis* D-alanine: D-alanine ligase and D-alanine racemase in the mechanisms of action of and resistance to the peptidoglycan inhibitor D-cycloserine. *Antimicrob. Agents Chemother.* 47, 283–291. doi: 10.1128/AAC.47.1.283-291.2003

Feng, Z., Caceres, N. E., Sarath, G., and Barletta, R. G. (2002). *Mycobacterium smegmatis* L-alanine dehydrogenase (Ald) is required for proficient utilization of alanine as a sole nitrogen source and sustained anaerobic growth. *J. Bacteriol.* 184, 5001–5010. doi: 10.1128/JB.184.18.5001-5010.2002

Fiss, E. H., Yu, S., and Jacobs, W. R. Jr. (1994). Identification of genes involved in the sequestration of iron in mycobacteria: the ferric exochelin biosynthetic and uptake pathways. *Mol. Microbiol.* 14, 557–569. doi: 10.1111/j.1365-2958.1994.tb02189.x

Foley-Thomas, E. M., Whipple, D. L., Bermudez, L. E., and Barletta, R. G. (1995). Phage infection, transfection and transformation of *Mycobacterium avium* complex and *Mycobacterium paratuberculosis*. *Microbiology* 141(Pt. 5), 1173–1181. doi: 10.1099/13500872-141-5-1173

George, K. M., Yuan, Y., Sherman, D. R., and Barry, C. E. 3rd. (1995). The biosynthesis of cyclopropanated mycolic acids in *Mycobacterium tuberculosis*. Identification and functional analysis of CMAS-2. *J. Biol. Chem.* 270, 27292–27298. doi: 10.1074/jbc.270.45.27292

Gey Van Pittius, N. C., Sampson, S. L., Lee, H., Kim, Y., Van Helden, P. D., and Warren, R. M. (2006). Evolution and expansion of the *Mycobacterium tuberculosis* PE and PPE multigene families and their association with the duplication of the ESAT-6 (esx) gene cluster regions. *BMC Evol. Biol.* 6:95. doi: 10.1186/1471-2148-6-95

Halouska, S., Fenton, R. J., Zinniel, D. K., Marshall, D. D., Barletta, R. G., and Powers, R. (2014). Metabolomics analysis identifies d-Alanine-d-Alanine ligase as the primary lethal target of d-Cycloserine in mycobacteria. *J. Proteome Res.* 13, 1065–1076. doi: 10.1021/pr4010579

Harris, N. B., Feng, Z., Liu, X., Cirillo, S. L., Cirillo, J. D., and Barletta, R. G. (1999). Development of a transposon mutagenesis system for *Mycobacterium avium* subsp. paratuberculosis. *FEMS Microbiol. Lett.* 175, 21–26. doi: 10.1111/j.1574-6968.1999.tb13597.x

Hines, M. E. 2nd., Turnquist, S. E., Ilha, M. R., Rajeev, S., Jones, A. L., Whittington, L., et al. (2014). Evaluation of novel oral vaccine candidates and validation of a caprine model of Johne's Disease. *Front. Cell. Infect. Microbiol.* 4:26. doi: 10.3389/fcimb.2014.00026

Hingley-Wilson, S. M., Sambandamurthy, V. K., and Jacobs, W. R. Jr. (2003). Survival perspectives from the world's most successful pathogen, *Mycobacterium tuberculosis*. *Nat. Immunol.* 4, 949–955. doi: 10.1038/ni981

Kabara, E., and Coussens, P. M. (2012). Infection of Primary Bovine Macrophages with *Mycobacterium avium* Subspecies paratuberculosis Suppresses Host Cell Apoptosis. *Front. Microbiol.* 3:215. doi: 10.3389/fmicb.2012.00215

Kumar, P., Amara, R. R., Challu, V. K., Chadda, V. K., and Satchidanandam, V. (2003). The Apa protein of *Mycobacterium tuberculosis* stimulates gamma interferon-secreting CD4+ and CD8+ T cells from purified protein derivative-positive individuals and affords protection in a guinea pig model. *Infect. Immun.* 71, 1929–1937. doi: 10.1128/IAI.71.4.1929-1937.2003

Lambrecht, R. S., Carriere, J. F., and Collins, M. T. (1988). A model for analyzing growth kinetics of a slowly growing Mycobacterium sp. *Appl. Environ. Microbiol.* 54, 910–916.

Lambrecht, R. S., and Collins, M. T. (1992). *Mycobacterium paratuberculosis*. Factors that influence mycobactin dependence. *Diagn. Microbiol. Infect. Dis.* 15, 239–246. doi: 10.1016/0732-8893(92)90119-E

Lamont, E. A., and Sreevatsan, S. (2010). Paradigm redux–*Mycobacterium avium* subspecies paratuberculosis-macrophage interactions show clear variations between bovine and human physiological body temperatures. *Microb. Pathog.* 48, 143–149. doi: 10.1016/j.micpath.2010.02.002

Lamont, E. A., Talaat, A. M., Coussens, P. M., Bannantine, J. P., Grohn, Y. T., Katani, R., et al. (2014). Screening of *Mycobacterium avium* subsp. paratuberculosis mutants for attenuation in a bovine monocyte derived macrophage model. *Front. Cell. Infect. Microbiol.* 4:87. doi: 10.3389/fcimb.2014.00087

Li, L., Bannantine, J. P., Zhang, Q., Amonsin, A., May, B. J., Alt, D., et al. (2005). The complete genome sequence of *Mycobacterium avium* subspecies paratuberculosis. *Proc. Natl. Acad. Sci. U.S.A.* 102, 12344–12349. doi: 10.1073/pnas.0505662102

Li, L., Munir, S., Bannantine, J. P., Sreevatsan, S., Kanjilal, S., and Kapur, V. (2007). Rapid expression of *Mycobacterium avium* subsp. paratuberculosis recombinant proteins for antigen discovery. *Clin. Vaccine Immunol.* 14, 102–105. doi: 10.1128/CVI.00138-06

Livneh, A., Golan, L., Rosenshine, I., Zinniel, D. K., Chahal, H. K., Chacon, O., et al. (2005). "*In vivo* and *in vitro* characterization of *Mycobacterium avium* subsp. *paratuberculosis* (MAP) mutants," in *Proceeding of the 8th International Colloquium on Paratuberculosis* (Copenhagen: International Association for Paratuberculosis Inc.).

Lu, Z., Schukken, Y. H., Smith, R. L., and Grohn, Y. T. (2013). Using vaccination to prevent the invasion of *Mycobacterium avium* subsp. paratuberculosis in dairy herds: a stochastic simulation study. *Prev. Vet. Med.* 110, 335–345. doi: 10.1016/j.prevetmed.2013.01.006

McAdam, R. A., Quan, S., Smith, D. A., Bardarov, S., Betts, J. C., Cook, F. C., et al. (2002). Characterization of a *Mycobacterium tuberculosis* H37Rv transposon library reveals insertions in 351 ORFs and mutants with altered virulence. *Microbiology* 148, 2975–2986.

McAdam, R. A., Weisbrod, T. R., Martin, J., Scuderi, J. D., Brown, A. M., Cirillo, J. D., et al. (1995). *In vivo* growth characteristics of leucine and methionine auxotrophic mutants of Mycobacterium bovis BCG generated by transposon mutagenesis. *Infect. Immun.* 63, 1004–1012.

Murcia, M. I., Garcia, M. J., Otal, I., Gomez, A. B., and Menendez, M. C. (2007). Molecular features of *Mycobacterium avium* human isolates carrying a single copy of IS1245 and IS1311 per genome. *FEMS Microbiol. Lett.* 272, 229–237. doi: 10.1111/j.1574-6968.2007.00769.x

Nagata, R., Muneta, Y., Yoshihara, K., Yokomizo, Y., and Mori, Y. (2005). Expression cloning of gamma interferon-inducing antigens of *Mycobacterium avium* subsp. paratuberculosis. *Infect. Immun.* 73, 3778–3782. doi: 10.1128/IAI.73.6.3778-3782.2005

Okkels, L. M., Brock, I., Follmann, F., Agger, E. M., Arend, S. M., Ottenhoff, T. H., et al. (2003). PPE protein (Rv3873) from DNA segment RD1 of *Mycobacterium tuberculosis*: strong recognition of both specific T-cell epitopes and epitopes conserved within the PPE family. *Infect. Immun.* 71, 6116–6123. doi: 10.1128/IAI.71.11.6116-6123.2003

Ott, S. L., Wells, S. J., and Wagner, B. A. (1999). Herd-level economic losses associated with Johne's Disease on US dairy operations. *Prev. Vet. Med.* 40, 179–192. doi: 10.1016/S0167-5877(99)00037-9

Park, K. T., Dahl, J. L., Bannantine, J. P., Barletta, R. G., Ahn, J., Allen, A. J., et al. (2008). Demonstration of allelic exchange in the slow-growing bacterium *Mycobacterium avium* subsp. paratuberculosis, and generation of mutants with deletions at the pknG, relA, and lsr2 loci. *Appl. Environ. Microbiol.* 74, 1687–1695. doi: 10.1128/AEM.01208-07

Reddy, V. M., Luna-Herrera, J., and Gangadharam, P. R. (1996). Pathobiological significance of colony morphology in *Mycobacterium avium* complex. *Microb. Pathog.* 21, 97–109. doi: 10.1006/mpat.1996.0046

Riley, R., Pellegrini, M., and Eisenberg, D. (2008). Identifying cognate binding pairs among a large set of paralogs: the case of PE/PPE proteins of *Mycobacterium tuberculosis*. *PLoS Comput. Biol.* 4:e1000174. doi: 10.1371/journal.pcbi.1000174

Sampson, S. L., Dascher, C. C., Sambandamurthy, V. K., Russell, R. G., Jacobs, W. R. Jr., Bloom, B. R., et al. (2004). Protection elicited by a double leucine and

pantothenate auxotroph of *Mycobacterium tuberculosis* in guinea pigs. *Infect. Immun.* 72, 3031–3037. doi: 10.1128/IAI.72.5.3031-3037.2004

Sassetti, C. M., and Rubin, E. J. (2003). Genetic requirements for mycobacterial survival during infection. *Proc. Natl. Acad. Sci. U.S.A.* 100, 12989–12994. doi: 10.1073/pnas.2134250100

Scandurra, G. M., De Lisle, G. W., Cavaignac, S. M., Young, M., Kawakami, R. P., and Collins, D. M. (2010). Assessment of live candidate vaccines for paratuberculosis in animal models and macrophages. *Infect. Immun.* 78, 1383–1389. doi: 10.1128/IAI.01020-09

Scandurra, G. M., Young, M., De Lisle, G. W., and Collins, D. M. (2009). A bovine macrophage screening system for identifying attenuated transposon mutants of *Mycobacterium avium* subsp. paratuberculosis with vaccine potential. *J. Microbiol. Methods* 77, 58–62. doi: 10.1016/j.mimet.2009.01.005

Schwyn, B., and Neilands, J. B. (1987). Universal chemical assay for the detection and determination of siderophores. *Anal. Biochem.* 160, 47–56. doi: 10.1016/0003-2697(87)90612-9

Shin, S. J., Wu, C. W., Steinberg, H., and Talaat, A. M. (2006). Identification of novel virulence determinants in *Mycobacterium paratuberculosis* by screening a library of insertional mutants. *Infect. Immun.* 74, 3825–3833. doi: 10.1128/IAI.01742-05

Stabel, J. R. (1998). Johne's Disease: a hidden threat. *J. Dairy Sci.* 81, 283–288. doi: 10.3168/jds.S0022-0302(98)75577-8

Stabel, J. R., and Stabel, T. J. (1995). Immortalization and characterization of bovine peritoneal macrophages transfected with SV40 plasmid DNA. *Vet. Immunol. Immunopathol.* 45, 211–220. doi: 10.1016/0165-2427(94)05348-V

Stewart, G. R., Wernisch, L., Stabler, R., Mangan, J. A., Hinds, J., Laing, K. G., et al. (2002). Dissection of the heat-shock response in *Mycobacterium tuberculosis* using mutants and microarrays. *Microbiology* 148, 3129–3138.

Sweeney, R. W. (1996). Transmission of paratuberculosis. *Vet. Clin. North Am. Food Anim. Pract.* 12, 305–312.

Wang, J., Pritchard, J. R., Kreitmann, L., Montpetit, A., and Behr, M. A. (2014). Disruption of *Mycobacterium avium* subsp. paratuberculosis-specific genes impairs in vivo fitness. *BMC Genomics* 15:415. doi: 10.1186/1471-2164-15-415

Woo, S. R., Sotos, J., Hart, A. P., Barletta, R. G., and Czuprynski, C. J. (2006). Bovine monocytes and a macrophage cell line differ in their ability to phagocytose and support the intracellular survival of *Mycobacterium avium* subsp. paratuberculosis. *Vet. Immunol. Immunopathol.* 110, 109–120. doi: 10.1016/j.vetimm.2005.09.010

Wu, C. W., Glasner, J., Collins, M., Naser, S., and Talaat, A. M. (2006). Whole-genome plasticity among *Mycobacterium avium* subspecies: insights from comparative genomic hybridizations. *J. Bacteriol.* 188, 711–723. doi: 10.1128/JB.188.2.711-723.2006

Wu, C. W., Schramm, T. M., Zhou, S., Schwartz, D. C., and Talaat, A. M. (2009). Optical mapping of the *Mycobacterium avium* subspecies paratuberculosis genome. *BMC Genomics* 10:25. doi: 10.1186/1471-2164-10-25

Zhao, B., Collins, M. T., and Czuprynski, C. J. (1997). Effects of gamma interferon and nitric oxide on the interaction of *Mycobacterium avium* subsp. paratuberculosis with bovine monocytes. *Infect. Immun.* 65, 1761–1766.

Zhao, B. Y., Czuprynski, C. J., and Collins, M. T. (1999). Intracellular fate of *Mycobacterium avium* subspecies paratuberculosis in monocytes from normal and infected, interferon-responsive cows as determined by a radiometric method. *Can. J. Vet. Res.* 63, 56–61.

Zheng, Y. T., Toyofuku, M., Nomura, N., and Shigeto, S. (2013). Correlation of carotenoid accumulation with aggregation and biofilm development in Rhodococcus sp. SD-74. *Anal. Chem.* 85, 7295–7301. doi: 10.1021/ac401188f

Conflict of Interest Statement: Patent: Methods for the identification of Virulence Determinants. Raúl G. Barletta, N. Beth Harris. U.S. Patent No. 7,740,867, Granted June 22, 2010. The Review Editor, Jeffrey Cirillo, declares that, despite having collaborated with authors Raul Barletta and Denise Kinniel, the review process was handled objectively. The authors declare that the research was conducted in the absence of any commercial or financial relationships that could be construed as a potential conflict of interest.

Received: 30 May 2014; accepted: 25 September 2014; published online: 15 October 2014.

Citation: Rathnaiah G, Lamont EA, Harris NB, Fenton RJ, Zinniel DK, Liu X, Sotos J, Feng Z, Livneh-Kol A, Shpigel NY, Czuprynski CJ, Sreevatsan S and Barletta RG (2014) Generation and screening of a comprehensive Mycobacterium avium subsp. paratuberculosis transposon mutant bank. Front. Cell. Infect. Microbiol. ***4****:144. doi: 10.3389/fcimb.2014.00144*

This article was submitted to the journal Frontiers in Cellular and Infection Microbiology.

frontiers in
CELLULAR AND INFECTION MICROBIOLOGY

ORIGINAL RESEARCH ARTICLE
published: 30 June 2014
doi: 10.3389/fcimb.2014.00087

Screening of *Mycobacterium avium* subsp. *paratuberculosis* mutants for attenuation in a bovine monocyte-derived macrophage model

Elise A. Lamont[1], Adel M. Talaat[2], Paul M. Coussens[3], John P. Bannantine[4], Yrjo T. Grohn[5], Robab Katani[6], Ling-ling Li[6], Vivek Kapur[6] and Srinand Sreevatsan[1,7]*

[1] Department of Veterinary Population Medicine, University of Minnesota, St. Paul, MN, USA
[2] Department of Pathobiological Sciences, University of Wisconsin, Madison, WI, USA
[3] Department of Animal Sciences, Michigan State University, East Lansing, MI, USA
[4] Agricultural Research Service, National Animal Disease Center, United States Department of Agriculture, Ames, IA, USA
[5] College of Veterinary Medicine, Population Medicine and Diagnostic Sciences, Cornell University, Ithaca, NY, USA
[6] Department Veterinary and Biomedical Sciences, Penn State University, State College, PA, USA
[7] Department of Veterinary Biomedical Sciences, University of Minnesota, St. Paul, MN, USA

Edited by:
Thomas A. Ficht, Texas A&M University, USA

Reviewed by:
Jordi Torrelles, Ohio State University, USA
Roger W. Stich, University of Missouri, USA

****Correspondence:***
Srinand Sreevatsan, Veterinary Population Medicine, College of Veterinary Medicine, University of Minnesota, 1971 Commonwealth Avenue, Veterinary Science Building, St. Paul, MN 55108, USA
e-mail: sreev001@umn.edu

Vaccination remains a major tool for prevention and progression of Johne's disease, a chronic enteritis of ruminants worldwide. Currently there is only one licensed vaccine within the United States and two vaccines licensed internationally against Johne's disease. All licensed vaccines reduce fecal shedding of *Mycobacterium avium* subsp. *paratuberculosis* (MAP) and delay disease progression. However, there are no available vaccines that prevent disease onset. A joint effort by the Johne's Disease Integrated Program (JDIP), a USDA-funded consortium, and USDA—APHIS/VS sought to identify transposon insertion mutant strains as vaccine candidates in part of a three phase study. The focus of the Phase I study was to evaluate MAP mutant attenuation in a well-defined *in vitro* bovine monocyte-derived macrophage (MDM) model. Attenuation was determined by colony forming unit (CFUs) counts and slope estimates. Based on CFU counts alone, the MDM model did not identify any mutant that significantly differed from the wild-type control, MAP K-10. Slope estimates using mixed models approach identified six mutants as being attenuated. These were enrolled in protection studies involving murine and baby goat vaccination-challenge models. MDM based approach identified trends in attenuation but this did not correlate with protection in a natural host model. These results suggest the need for alternative strategies for Johne's disease vaccine candidate screening and evaluation.

Keywords: *Mycobacterium avium* subsp. *paratuberculosis*, Johne's disease, vaccine, macrophage, mutant, transposon mutagenesis, survival

INTRODUCTION

Vaccination is arguably the most successful story in medical research that has improved the longevity and quality of life for both humans and animals (Koff et al., 2013). Currently there is one licensed vaccine for Johne's disease, a chronic enteritis of ruminants worldwide caused by *Mycobacterium avium* subsp. *paratuberculosis* (MAP), within the United States (Patton, 2011). Mycopar (Boehringer, Ingelheim, Ridgefield, CT, USA) is a heat-killed bacterin of *Mycobacterium avium* mixed with an oil adjuvant. Other vaccine formulations available internationally, Gudair (Zoetis, Inc.) and Silirum (Pfizer), are composed of heat inactivated MAP strain 316F (for use in ovine paratuberculosis) and a heat killed strain of MAP (for use in bovine paratuberculosis), respectively (Reddacliff et al., 2006; Stringer et al., 2013). All licensed vaccines reduce fecal shedding of MAP but fail to produce protection from initial infection and sterilizing immunity in ruminants (Chiodini, 1993; Reddacliff et al., 2006; Rosseels and Huygen, 2008; Huttner et al., 2012) Furthermore, these vaccine formulations frequently result in granulomas and/or lesions at the site of injection as well as antibody responses that cross-react with other pathogenic mycobacteria, and does not reliably differentiate vaccinated from infected animals, creating difficulties in disease detection (Mackintosh et al., 2005; Eppleston and Windsor, 2007; Stabel et al., 2011; Thomsen et al., 2012; Hines et al., 2014). Due to undesirable consequences of vaccination, which includes injection site reactions and inference with TB diagnostics, the United States limits Mycopar to herds that have a high MAP prevalence or those that have limited resources (financial, facility, etc.) to achieve Johne's disease control program standards (Usda-Aphis, 2010).

Despite the risk of potential immunization sequelae, several studies indicate that vaccination is a necessary component for Johne's disease prevention (Kormendy, 1994; Lu et al., 2013). In a stochastic simulation model of MAP infection and vaccination,

Lu et al. showed that effective vaccination of animals reduced MAP prevalence to 0.44 and 0.19 at a 5 and 10 year follow-up period, respectively (Lu et al., 2013). It is important to note that the authors also concluded that a small chance (<0.15) of MAP persistence due to vertical transmission exists (Lu et al., 2013). Therefore, it is likely that Johne's disease eradication must encompass vaccination under the umbrella of a well-defined control program that includes standard management practices for rapid detection, hygiene, separation of newborns from adults, and culling of infected animals (Ferrouillet et al., 2009; Espejo et al., 2012).

The need for an improved Johne's disease vaccine within management programs prompted the implementation of a three-phase vaccine candidate evaluation that was administered by the Johne's Disease Integrated Program (JDIP). This vaccine project consisted of three blinded studies: Phase I involved the screening of 22 submitted strains of MAP, carrying deletions at critical housekeeping or putative virulence genes (herein collectively referred to as MAP mutants), for attenuation in a well-defined bovine monocyte-derived macrophage (MDM) model, Phase II involved identified attenuated mutants from Phase I evaluation in a mouse vaccination-challenge model, and Phase III involved the evaluation of selected mutants from Phase II in a goat challenge model to evaluate protection in a ruminant host, which is the target species. We herein report results from the Phase I study. Mutant MAP strains classified as candidates for further testing were defined as those displaying significant attenuation, particularly based on slope trends indicative of total bacterial decay over the first 48-h post infection.

MATERIALS AND METHODS

ETHICS STATEMENT

All animal work was conducted in accordance with the recommendations in the institutional guidelines and approved animal care and use committee (IACUC) protocols at the University of Minnesota (approval number 1106A01161). All other experiments were carried out in accordance with the University of Minnesota's Institutional Biosafety Committee (IBC) approved protocol number 0806H36901.

STUDY DESIGN

All experiments were conducted in a double-blind design. The attenuated mutant strains were cultured, coded, and shipped to the testing labs by the coordinating team at Penn State University. At the end of the study, the MDM survival data of strains was decoded and analyzed by the JDIP Statistical Core at Cornell University.

PURIFICATION OF BOVINE MONOCYTE-DERIVED MACROPHAGES (MDMs)

Purification of bovine MDMs was conducted using a published protocol (Janagama et al., 2006). Briefly, whole blood was collected from the jugular vein into gas sterilized vacuum buckets containing ACD or CPDA anticoagulant. The blood was centrifuged at 2000 × g for 20 min at room temperature (RT) and buffy coats were harvested and diluted 1:10 in PBS before separation over a 58% percol gradient. After centrifugation of the percol gradient at 400 × g for 30 min at RT, the mononuclear cells were collected using a sterile transfer pipette into a 20-ml new tube. Three PBS washes were performed on cells to remove remaining percol. After the last PBS wash, the cell pellet was resuspended in RPMI 1640 medium (Gibco, Invitrogen, Carlsbad, CA) with 20% autologous serum in Teflon wells. Cell suspensions were incubated inside a humidified chamber containing 5% CO_2 at 37°C and allowed to differentiate for 4 days before they were seeded only cell culture flasks (day 5). Cell culture medium was changed every 2–3 days.

BACTERIAL CELL CULTURE

MAP mutant strains submitted by multiple investigators were received at Pennsylvania State University and cultured in Middlebrook (MB) 7H9 supplemented with 10% glycerol, 1% oleic acid-dextrose-catalase (OADC) or ADC, 0.05% Tween-80, cycloheximide (1.0 g/L), mycobactin J (2 mg/mL) (Allied Monitor, and appropriate antibiotics at 37°C at 120 rpm. Growth was determined on a weekly basis by recording culture absorbance ($O.D._{600\,nm}$) after several passages through G25 and G27 needles. Upon reaching an $O.D._{600\,nm}$ of 0.5, cultures were tested for contamination by the absence of both growth on Brain-Heart Infusion (BHI) and blood agar for 48 h and *M. avium* specific PCR not present in MAP (primer sequences: F 5′-aaacccaagcagagaaacga; R 5′-gcgtcaatcaaagcctgttc). MAP mutant strains were blinded and shipped to testing laboratories, then used to infect MDMs immediately upon receipt. Colony counts were determined after shipment by plating serial dilutions (10^{-4} through 10^{-7}) of each culture (in triplicate) on MB7H9 agar plates and incubating for 4–6 weeks. Baseline CFUs were calculated based on averages obtained from triplicate plates of 10^{-5} and 10^{-6} dilutions.

MAP INVASION ASSAY

Unless stated otherwise, all incubations were conducted in a 37°C humidified chamber containing 5% CO_2. Bovine MDMs were counted via trypan blue exclusion, seeded at 2.0×10^6 cells in T-25 culture flasks, and allowed to adhere for 2 h in the humidified chamber (5% CO_2 at 37°C). Non-adherent cells were removed by washing flasks three times in 1× PBS. RPMI 1640 supplemented with 2% autologous serum (infection medium) was added to each flask prior to MAP invasion. MAP cultures were pelleted at 8000 × g for 10 min, washed thrice using 1× PBS, resuspended in infection medium (MOI 10:1), and vortex mixed for 5 min. MAP cells were repeatedly drawn through a 21-gauge needle to dissociate bacterial clumps. Cells were incubated at 37°C for 5 min to sediment any remaining clumps and only the upper 2/3 volume was used for the invasion assay. MDMs were infected with MAP for 2 h, washed thrice with 1× D-PBS to remove non-adherent bacteria, and recovered in fresh infection medium for the following time points: 3, 24, 48, 96, and 168 h. Time points were selected upon well-established steps in MAP invasion, gene and protein expression, and adaptation to the intracellular environment (Murphy et al., 2006; Scandurra et al., 2009, 2010; Lamont and Sreevatsan, 2010; Ghosh et al., 2013). Upon completion of time points, MDMs were washed thrice in 1× D-PBS and incubated with warmed 0.01% Triton X-100 in PBS for 5 min at RT.

The lysate was subjected to differential centrifugation at 388 × g and 8000 × g for 5 min each to remove MDMs and pellet MAP, respectively. MAP pellets were washed thrice in 1× PBS at 8000 × g for 5 min to remove any remaining detergent, and resuspended in 1.0 mL of 1× PBS. All time points were conducted in triplicate. During the infection time course, medium was replaced every 2 days. Recovered MAP cells were serially diluted in 1× PBS and plated on MB7H9 agar supplemented with 10% OADC, mycobactin J (2 mg/mL), and appropriate antibiotics (kanamycin or hygromycin). All plates were incubated at 37°C for 6–8 weeks. *IS900* colony PCR was performed on randomly selected colonies from each dilution to confirm purity as described (Bull et al., 2000). All dilutions were plated in duplicate.

STATISTICAL ANALYSIS PERFORMED BY THE UNIVERSITY OF MINNESOTA

CFU numbers from MAP mutant strains were normalized against the MAP K-10 starting inoculum in order to achieve direct comparisons at each post infection time point. Results were plotted and analyzed using One-Way analysis of variance (ANOVA) with Bonferroni correction in GraphPad Prism software (GraphPad Software, La Jolla, CA). *P* values of less than 0.05 were considered as statistically significant. Analysis is reflective of CFU counts from the University of Minnesota.

STATISTICAL ANALYSIS PERFORMED BY JDIP CORE

CFU numbers were submitted to the JDIP core. CFUs in bovine MDMs measured from different time points and the change (i.e., slope) between 3 and 48 h was calculated to compare mutants, as follows. CFU measurements were not normalized to the standard type inoculum. The natural logarithm was applied to mean CFUs/mL (calculated for each time point, cow and strain). Slope estimates were calculated by subtracting the (natural logarithm of the mean CFU/ml count at 3 h) from the (natural logarithm of the mean CFU/ml count at 48 h) and dividing by 45 (=48–3). Sixty-nine observations (one for each combination of university, strain and cow) were recorded and analyzed using PROC GLIMMIX ver. 9.2 in SAS (SAS Institute Inc., Cary, NC) using a linear regression model. The outcome variable was the slope estimate described above. These slope estimates were assumed to follow a normal distribution. The independent variable strain was a fixed effect, with 17 levels. University was a random effect with 2 levels. Final analysis included observations recorded from both the University of Minnesota and the University of Wisconsin-Madison.

RESULTS

MAP MUTANT COMPETENCE IN AN *IN VITRO* PRIMARY MONOCYTE-DERIVED MACROPHAGE MODEL

Survival of MAP mutants was performed in two stages. First, a direct comparison of all mutants against K-10 was performed. Second, a slope trend was determined using a mixed linear model approach. **Table 1** lists mutant identification, transposon insertion location and method. Survival of MAP mutants was determined at 3, 24, 48, 96, and 168 h p.i. in a well-defined bovine MDM model (**Figure 1**). Due to varying CFUs in bacterial inoculums, all strains were normalized to MAP K-10 inoculum. All MAP strains, including MAP K-10, showed similar CFU counts throughout the course of the study (**Figure 1**). Statistical analysis of mutant CFU results compared to MAP K-10 showed no significant ($P > 0.05$) differences at any time point.

In as much as, direct comparisons over the entire infection cycle did not capture differences, a mixed model approach was applied to identify slope trends between strains. Attenuation was determined by slope-value for each MAP strain (**Table 1**). Mutants that showed a negative slope were identified as attenuated in the MDM model. MAP mutant strains selected to proceed to Phase II studies were required to either show a decaying trend (i.e., negative slope-estimate) or induced apoptosis in PBMCs as described (Kabara and Coussens, 2012). Mutant strains 312–314 and 322–326 showed positive slopes; therefore, these mutants were excluded from the Phase II study (**Table 1**). Mutant strains 315, 316, 318, 319, and 321 showed negative slopes ranging from −0.0265 to −0.018 (**Table 1**). The inclusion of strains 320 and 329 (referred to as Mutant 219 in Kabara and Coussens, 2012) were based on apoptosis collected from another JDIP core laboratory (Kabara and Coussens, 2012). Based on these analyses, JDIP 315–321 and 329 were selected for further evaluation in Phase II studies.

DISCUSSION

Johne's disease vaccination was first described in 1926 using a live strain of MAP mixed with olive oil, paraffin, and pumice powder as an adjuvant (Valle and Rinjard, 1926). Johne's disease vaccine strategies have expanded and diversified due to the public availability of the MAP genome and gene regulation studies (Li et al., 2005; Bannantine and Talaat, 2010; Janagama et al., 2010; Chen et al., 2012). Currently, potential vaccine models for Johne's disease include heat-killed bacilli, live attenuated mutants, recombinant MAP proteins, and MAP genes integrated into viruses or unrelated bacterial plasmids (Cavaignac et al., 2000; Rosseels and Huygen, 2008; Faisal et al., 2013). However, the only licensed Johne's disease vaccine within the United States, Mycopar–comprised of heat-killed *M. avium* (erroneously labeled as MAP in the literature prior to 1993), and other heat-killed formulations do not provide protection against infection and is fraught with negative immunization sequelae (Chiodini, 1993; Ghadiali et al., 2004; Eppleston and Windsor, 2007; Paustian et al., 2008; Patton, 2011; Stringer et al., 2013). The use of Mycopar is restricted to herds with high MAP prevalence in order to reduce MAP shedding and/or delay disease onset (Usda-Aphis, 2010). In order to achieve Johne's disease eradication it is critical that a vaccine that elicits protection be included with strong, standardized management protocols. In a series of three studies (Phase I–III), MAP mutants submitted to JDIP were evaluated for vaccine candidacy. This study (Phase I) evaluated MAP mutant attenuation in an *in vitro* MDM model.

Screening of MAP mutants against strain K-10 was conducted in a well-defined *in vitro* bovine MDM model to define attenuation. Previous studies have shown that bovine MDMs serve as an efficient mechanism for rapid analysis of potential vaccine candidates (Langelaar et al., 2005; Scandurra et al., 2009, 2010). CFU data were first analyzed for the full 7-day period in an attempt to identify trends in attenuation. Since most drop in CFUs were

Table 1 | MAP mutant identification, strain information, and slope estimates.

JDIP core identification	Strain information				Slope estimate[a]
	Name	Background	Location	Method	
311	Δ482-3	43432-02 (Goat)	MAP0482 and MAP0483	Site directed deletion (McGarvey, unpublished)	−0.0421
312	K10-Δ*relA*	K-10 (Cattle)	*relA*/deletion of the region between 732th bp and 1604th bp of the gene	Phage/site directed (Park et al., 2008)	0.0270
313	K10-Δ*pknG*	K-10	*pknG*/deletion of the region between 406th bp and 2142th bp of the gene		0.0294
314	K10-Δ*lrs2*	K-10	*lsr2*/deletion of the region between 9th bp and 319th bp of the gene		0.0336
315	STM68 (GPM401)	K-10	Internal to MAP1566, insertion is located near the 3′ end	Transposon mutagenesis; phAE94 to introduce Tn5370 (Liveneh et al., 2005)	−0.0265
316	2E11 (GPM402)	K-10	Intergenic, 137 bp upstream from *fadE5*, between MAP3695 and FadE5	Transposon mutagenesis; phAE94 to introduce Tn5367 (Liveneh et al., 2005)	−0.0211
317	22F4 (GPM403)	K-10	Internal to *lsr2* (MAP0460)		0.0003
318	40A9 (GPM404)	K-10	Intergenic, between MAP0282c and MAP0283c		−0.018
319	30H9 (GPM405)	K-10	Internal to MAP1566		−0.0146
320	3H4 (GPM406)	K-10	Intergenic, between MAP2296c and MAP2297c		0.0186
321	4H2 (GPM407)	K-10	Intergenic between MAP1150c and MAP1151c		−0.0130
322	WAg906 (TM58)	989 (C strain; Type II)	MAP1566	Transposon mutagenesis (Tn5367) (Cavaignac et al., 2000)	0.0038
323	WAg915	K-10	*ppiA* (MAP0011) inactivated by allelic exchange	Site directed mutagenesis using a phage vector	0.0236
324	*kdpC*	ATCC 19698	MAP0997c *kdpC*	Transposon mutagenesis (Tn5367) (Shin et al., 2006)	−0.0025
325	*lipN*	K-10	Δ*lipN*	Homologous recombination (Wu et al., 2007)	0.0043
326	*umaA1*	ATCC 19698	MAP3963 *umaA1*	Transposon mutagenesis (Tn5367) (Shin et al., 2006)	−0.0284
329	*fabG2_2*	ATCC 19698	MAP2408c *fabG2_2*	Transposon mutagenesis (Tn 5367) (Wu et al., 2007)	0.0198

[a] *Slope-estimates based-off of data recorded from the University of Minnesota and the University of Wisconsin-Madison.*

restricted to an earlier infection time point a slope based approach was applied where each mutant was compared against others for 48-h post infection. Mutants with highest slopes (indicating higher rates of intracellular incompetence) were selected as likely attenuated strains for further screening in a mouse model for immunogenicity. While slope values and percent cell apoptosis predicted attenuation, it did not correlate with protection as determined by the results of Phase II and Phase III studies (Bannantine et al., 2014; Hines et al., 2014). For example, in Phase II trials MAP mutants 316–318 showed the highest bacterial burden in cultured tissues (spleen and liver) (Bannantine et al., 2014). Although MAP strain 315 outperformed all other mutants tested in the murine model, the undiluted Silirum vaccine offered the greatest protection as determined by decreased counts of bacterial burden in tissues (Bannantine et al., 2014). Poor protection against standard type infection using MAP mutant strains were also demonstrated in a goat challenge model (Hines et al., 2014). The MAP mutant strain 329 performed the best in the goat model as it reduced bacterial shedding, lowered bacterial burden, and decreased tissue lesion scores (Hines et al., 2014). However, like the murine study, strain 329 failed to outperform the Silirum vaccine. Together these data highlight the limitations of overextending the bovine MDM attenuation model as a proficient tool for initial screening of MAP mutants to predict vaccine candidacy i.e., immunogenicity or ability to prevent infection.

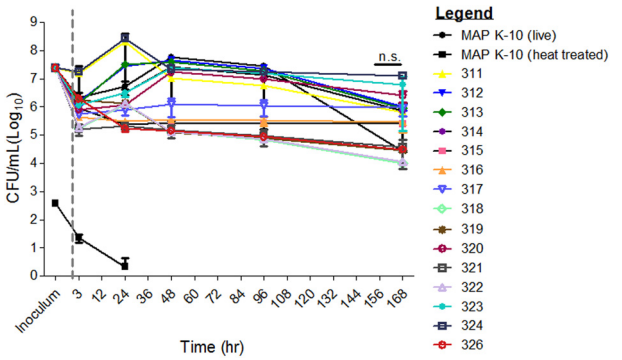

FIGURE 1 | Survival of MAP mutants in a primary cell *in vitro* bovine MDM model. All MAP mutant inoculums were normalized to that from MAP strain K-10. Bovine MDMs were incubated at 3, 24, 48, 96, and 168 h. and subsequently lysed for MAP CFU culture. MAP mutant CFU counts did not differ significantly from the control, MAP strain K-10. Error bars represents standard error from the mean (s.e.m). Experiment represents data from 2 cows from the University of Minnesota. All time points were conducted in triplicate. n.s. is abbreviated for not significant. Gray line separates inoculum from the infection time points.

Although traditional vaccine strategies largely rely on attenuation either by heat inactivation or mutation, this strategy appears to be unsuccessful for mycobacteria. For example, *Mycobacterium BCG*, the only licensed vaccine against human tuberculosis (TB), contains multiple deletions but has variable efficacy in adults and fails to protect against pulmonary TB (Behr, 2002; Lewis et al., 2003; Kaufmann, 2013). Current vaccine designs for TB include improvements upon BCG by the addition of foreign genes, such as listeriolysin, that forces the pathogen to be presented to the immune system via an unnatural mechanism (Grode et al., 2005). It is likely that Johne's disease vaccines will need to utilize similar strategies to elicit immunity. Promising Johne's disease vaccine candidates utilizing unconventional methods include those that present MAP antigens in a Salmonella backbone, recombinant MAP proteins and DNA constructs (Kadam et al., 2009; Santema et al., 2009, 2011; Chandra et al., 2012; Faisal et al., 2013).

Despite limitations in the MDM model to predict good vaccine candidates instead of simply measuring attenuation, screened MAP mutants may direct future design of vaccines. For instance, MAP mutants will provide critical clues as to how MAP is processed by the immune system. Host and MAP mutant transcriptomes will provide information pertaining to conserved pathways that should be considered during vaccine design (Lamont et al., 2013).

CONCLUSIONS

Phase I showed that attenuation of *in-vitro* growth rates in MDM do not correlate with ability to prevent infection in a relevant animal model of infection. These results highlight one of the limitations of the widely used bovine MDM model for vaccine candidate identification based on an attenuation phenotype alone. Future studies should consider alternate vaccine candidate screens and include multiple readouts including—antigen processing and presentation, efficiency of modulating subcellular processing events and ability of vaccine candidates to induce specific cytokines, in addition to the survival trait.

AUTHOR CONTRIBUTIONS

Elise A. Lamont was responsible for performing invasion assays in MDMs, primary analysis and interpretation, and writing of the manuscript. Srinand Sreevatsan, Adel Talaat, Paul M. Coussens, John P. Bannantine and Vivek Kapur were responsible for generating the ideas, obtaining funding, and project design. Yrjo T. Grohn was the JDIP Core statistician and responsible for calculating and interpreting slope data. Ling-ling Li and Robab Katani were responsible for culture, coding, and shipment of MAP mutant strains.

ACKNOWLEDGMENTS

We acknowledge the services by the Bovine Blood Collection Facility at the University of Minnesota. We appreciate the assistance of Derek Lieffring during blood collections. We thank the researchers, who supplied MAP mutant strains for inclusion in this study. We appreciate funding support from Dr. Michael Carter, Veterinary Services. This study was supported by the Johne's Disease Integrated Program and USDA/APHIS-VS.

REFERENCES

Bannantine, J. P., Everman, J. L., Rose, S., Babrak, L., Katani, R., Barletta, R. G., et al. (2014). Evaluation of eight live attenuated vaccine candidates for protection against challenge with virulent *Mycobacterium avium* subspecies paratuberculosis in mice. *Front. Cell. Infect. Microbiol.* 4:88. doi: 10.3389/fcimb.2014.00088

Bannantine, J. P., and Talaat, A. M. (2010). Genomic and transcriptomic studies in *Mycobacterium avium* subspecies paratuberculosis. *Vet. Immunol. Immunopathol.* 138, 303–311. doi: 10.1016/j.vetimm.2010.10.008

Behr, M. A. (2002). BCG–different strains, different vaccines? *Lancet Infect. Dis.* 2, 86–92. doi: 10.1016/S1473-3099(02)00182-2

Bull, T. J., Hermon-Taylor, J., Pavlik, I. I., El-Zaatari, F., and Tizard, M. (2000). Characterization of IS900 loci in *Mycobacterium avium* subsp. paratuberculosis and development of multiplex PCR typing. *Microbiology* 146 (Pt 12), 3285.

Cavaignac, S. M., White, S. J., De Lisle, G. W., and Collins, D. M. (2000). Construction and screening of Mycobacterium paratuberculosis insertional mutant libraries. *Arch. Microbiol.* 173, 229–231. doi: 10.1007/s002039900132

Chandra, S., Faisal, S. M., Chen, J. W., Chen, T. T., McDonough, S. P., Liu, S., et al. (2012). Immune response and protective efficacy of live attenuated Salmonella vaccine expressing antigens of *Mycobacterium avium* subsp. paratuberculosis against challenge in mice. *Vaccine* 31, 242–251. doi: 10.1016/j.vaccine.2012.09.024

Chen, J. W., Scaria, J., and Chang, Y. F. (2012). Phenotypic and transcriptomic response of auxotrophic *Mycobacterium avium* subsp. paratuberculosis leuD mutant under environmental stress. *PLoS ONE* 7:e37884. doi: 10.1371/journal.pone.0037884

Chiodini, R. J. (1993). Abolish Mycobacterium paratuberculosis strain 18. *J. Clin. Microbiol.* 31, 1956–1958.

Eppleston, J., and Windsor, P. (2007). Lesions attributed to vaccination of sheep with Gudair™ for the control of ovine paratuberculosis: post farm economic impacts at slaughter. *Aust. Vet. J.* 85, 129–133. doi: 10.1111/j.0005-0423.2007.00135.x

Espejo, L. A., Godden, S., Hartmann, W. L., and Wells, S. J. (2012). Reduction in incidence of Johne's disease associated with implementation of a disease control program in Minnesota demonstration herds. *J. Dairy Sci.* 95, 4141–4152. doi: 10.3168/jds.2011-4550

Faisal, S. M., Yan, F., Chen, T. T., Useh, N. M., Guo, S., Yan, W., et al. (2013). Evaluation of a Salmonella vectored vaccine expressing *Mycobacterium avium* Subsp. paratuberculosis antigens against challenge in a goat model. *PLoS ONE* 8:e70171. doi: 10.1371/journal.pone.0070171

Ferrouillet, C., Wells, S. J., Hartmann, W. L., Godden, S. M., and Carrier, J. (2009). Decrease of Johne's disease prevalence and incidence in six minnesota, USA, dairy cattle herds on a long-term management program. *Prev. Vet. Med.* 88, 128–137. doi: 10.1016/j.prevetmed.2008.08.001

Ghadiali, A. H., Strother, M., Naser, S. A., Manning, E. J., and Sreevatsan, S. (2004). *Mycobacterium avium* subsp. paratuberculosis strains isolated from Crohn's disease patients and animal species exhibit similar polymorphic locus patterns. *J. Clin. Microbiol.* 42, 5345–5348. doi: 10.1128/JCM.42.11.5345-5348.2004

Ghosh, P., Wu, C. W., and Talaat, A. M. (2013). Key role for the alternative sigma factor, SigH, in the intracellular life of *Mycobacterium avium* subsp. paratuberculosis during macrophage stress. *Infect. Immun.* 81, 2242–2257. doi: 10.1128/IAI.01273-12

Grode, L., Seiler, P., Baumann, S., Hess, J., Brinkmann, V., Nasser Eddine, A., et al. (2005). Increased vaccine efficacy against tuberculosis of recombinant Mycobacterium bovis bacille Calmette-Guerin mutants that secrete listeriolysin. *J. Clin. Invest.* 115, 2472–2479. doi: 10.1172/JCI24617

Hines, M. E. 2nd., Turnquist, S. E., Ilha, M. R., Rajeev, S., Jones, A. L., Whittington, L., et al. (2014). Evaluation of novel oral vaccine candidates and validation of a caprine model of Johne's disease. *Front. Cell. Infect. Microbiol.* 4:26. doi: 10.3389/fcimb.2014.00026

Huttner, K., Kramer, U., and Kleist, P. (2012). Effect of map-vaccination in ewes on body condition score, weight and map-shedding. *Berl. Munch. Tierarztl. Wochenschr.* 125, 449–451.

Janagama, H. K., Jeong, K., Kapur, V., Coussens, P., and Sreevatsan, S. (2006). Cytokine responses of bovine macrophages to diverse clinical *Mycobacterium avium* subspecies paratuberculosis strains. *BMC Microbiol.* 6:10. doi: 10.1186/1471-2180-6-10

Janagama, H. K., Lamont, E. A., George, S., Bannantine, J. P., Xu, W. W., Tu, Z. J., et al. (2010). Primary transcriptomes of *Mycobacterium avium* subsp. paratuberculosis reveal proprietary pathways in tissue and macrophages. *BMC Genomics* 11:561. doi: 10.1186/1471-2164-11-561

Kabara, E., and Coussens, P. M. (2012). Infection of primary bovine macrophages with *Mycobacterium avium* subspecies paratuberculosis suppresses host cell apoptosis. *Front. Microbiol.* 3:215. doi: 10.3389/fmicb.2012.00215

Kadam, M., Shardul, S., Bhagath, J. L., Tiwari, V., Prasad, N., and Goswami, P. P. (2009). Coexpression of 16.8 kDa antigen of *Mycobacterium avium* paratuberculosis and murine gamma interferon in a bicistronic vector and studies on its potential as DNA vaccine. *Vet. Res. Commun.* 33, 597–610. doi: 10.1007/s11259-009-9207-6

Kaufmann, S. H. (2013). Tuberculosis vaccines: time to think about the next generation. *Semin. Immunol.* 25, 172–181. doi: 10.1016/j.smim.2013.04.006

Koff, W. C., Burton, D. R., Johnson, P. R., Walker, B. D., King, C. R., Nabel, G. J., et al. (2013). Accelerating next-generation vaccine development for global disease prevention. *Science* 340:1232910. doi: 10.1126/science.1232910

Kormendy, B. (1994). The effect of vaccination on the prevalence of paratuberculosis in large dairy herds. *Vet. Microbiol.* 41, 117–125. doi: 10.1016/0378-1135(94)90141-4

Lamont, E. A., and Sreevatsan, S. (2010). Paradigm redux–*Mycobacterium avium* subspecies paratuberculosis-macrophage interactions show clear variations between bovine and human physiological body temperatures. *Microb. Pathog.* 48, 143–149. doi: 10.1016/j.micpath.2010.02.002

Lamont, E. A., Xu, W. W., and Sreevatsan, S. (2013). Host-*Mycobacterium avium* subsp. paratuberculosis interactome reveals a novel iron assimilation mechanism linked to nitric oxide stress during early infection. *BMC Genomics* 14:694. doi: 10.1186/1471-2164-14-694

Langelaar, M. F., Hope, J. C., Rutten, V. P., Noordhuizen, J. P., Van Eden, W., and Koets, A. P. (2005). *Mycobacterium avium* ssp. paratuberculosis recombinant heat shock protein 70 interaction with different bovine antigen-presenting cells. *Scand. J. Immunol.* 61, 242-250. doi: 10.1111/j.1365-3083.2005.01559.x

Lewis, K. N., Liao, R., Guinn, K. M., Hickey, M. J., Smith, S., Behr, M. A., et al. (2003). Deletion of RD1 from Mycobacterium tuberculosis mimics bacille Calmette-Guerin attenuation. *J. Infect. Dis.* 187, 117–123. doi: 10.1086/345862

Li, L., Bannantine, J. P., Zhang, Q., Amonsin, A., May, B. J., Alt, D., et al. (2005). The complete genome sequence of *Mycobacterium avium* subspecies paratuberculosis. *Proc. Natl. Acad. Sci. U.S.A.* 102, 12344–12349. doi: 10.1073/pnas.0505662102

Liveneh, A., Golan, L., Rosenshine, I., Zinniel, D. K., Chahal, H. K., Chacon, O., et al. (2005). "*In vivo* and *in vitro* characterization of *Mycobacterium avium* subsp. paratuberculosis (MAP) mutants," in *Proceedings of International Colloquium on Paratuberculosis.*

Lu, Z., Schukken, Y. H., Smith, R. L., and Grohn, Y. T. (2013). Using vaccination to prevent the invasion of *Mycobacterium avium* subsp. paratuberculosis in dairy herds: a stochastic simulation study. *Prev. Vet. Med.* 110, 335–345. doi: 10.1016/j.prevetmed.2013.01.006

Mackintosh, C. G., Labes, R. E., and Griffin, J. F. (2005). The effect of Johne's vaccination on tuberculin testing in farmed red deer (*Cervus elaphus*). *N. Z. Vet. J.* 53, 216–222. doi: 10.1080/00480169.2005.36549

Murphy, J. T., Sommer, S., Kabara, E. A., Verman, N., Kuelbs, M. A., Saama, P., et al. (2006). Gene expression profiling of monocyte-derived macrophages following infection with *Mycobacterium avium* subspecies avium and *Mycobacterium avium* subspecies paratuberculosis. *Physiol. Genomics* 28, 67–75. doi: 10.1152/physiolgenomics.00098.2006

Park, K. T., Dahl, J. L., Bannantine, J. P., Barletta, R. G., Ahn, J., Allen, A. J., et al. (2008). Demonstration of allelic exchange in the slow-growing bacterium *Mycobacterium avium* subsp. paratuberculosis, and generation of mutants with deletions at the pknG, relA, and lsr2 loci. *Appl. Environ. Microbiol.* 74, 1687–1695. doi: 10.1128/AEM.01208-07

Patton, E. A. (2011). Paratuberculosis vaccination. *Vet. Clin. North Am. Food Anim. Pract.* 27, 573–580, vi. doi: 10.1016/j.cvfa.2011.07.004

Paustian, M. L., Zhu, X., Sreevatsan, S., Robbe-Austerman, S., Kapur, V., and Bannantine, J. P. (2008). Comparative genomic analysis of *Mycobacterium avium* subspecies obtained from multiple host species. *BMC Genomics* 9:135. doi: 10.1186/1471-2164-9-135

Reddacliff, L., Eppleston, J., Windsor, P., Whittington, R., and Jones, S. (2006). Efficacy of a killed vaccine for the control of paratuberculosis in Australian sheep flocks. *Vet. Microbiol.* 115, 77–90. doi: 10.1016/j.vetmic.2005.12.021

Rosseels, V., and Huygen, K. (2008). Vaccination against paratuberculosis. *Expert Rev. Vaccines* 7, 817–832. doi: 10.1586/14760584.7.6.817

Santema, W., Hensen, S., Rutten, V., and Koets, A. (2009). Heat shock protein 70 subunit vaccination against bovine paratuberculosis does not interfere with current immunodiagnostic assays for bovine tuberculosis. *Vaccine* 27, 2312–2319. doi: 10.1016/j.vaccine.2009.02.032

Santema, W., Van Kooten, P., Hoek, A., Leeflang, M., Overdijk, M., Rutten, V. et al. (2011). Hsp70 vaccination-induced antibodies recognize B cell epitopes in the cell wall of *Mycobacterium avium* subspecies paratuberculosis. *Vaccine* 29, 1364–1373. doi: 10.1016/j.vaccine.2010.12.071

Scandurra, G. M., De Lisle, G. W., Cavaignac, S. M., Young, M., Kawakami, R. P., and Collins, D. M. (2010). Assessment of live candidate vaccines for paratuberculosis in animal models and macrophages. *Infect. Immun.* 78, 1383–1389. doi: 10.1128/IAI.01020-09

Scandurra, G. M., Young, M., De Lisle, G. W., and Collins, D. M. (2009). A bovine macrophage screening system for identifying attenuated transposon mutants of *Mycobacterium avium* subsp. paratuberculosis with vaccine potential. *J. Microbiol. Methods* 77, 58–62. doi: 10.1016/j.mimet.2009.01.005

Shin, S. J., Wu, C. W., Steinberg, H., and Talaat, A. M. (2006). Identification of novel virulence determinants in Mycobacterium paratuberculosis by screening a library of insertional mutants. *Infect. Immun.* 74, 3825–3833. doi: 10.1128/IAI.01742-05

Stabel, J. R., Waters, W. R., Bannantine, J. P., and Lyashchenko, K. (2011). Mediation of host immune responses after immunization of neonatal calves with a heat-killed *Mycobacterium avium* subsp. paratuberculosis vaccine. *Clin. Vaccine Immunol.* 18, 2079–2089. doi: 10.1128/CVI.05421-11

Stringer, L. A., Wilson, P. R., Heuer, C., and Mackintosh, C. G. (2013). A randomised controlled trial of silirum vaccine for control of paratuberculosis in farmed red deer. *Vet. Rec.* 173, 551. doi: 10.1136/vr.101799

Thomsen, V. T., Nielsen, S. S., Thakur, A., and Jungersen, G. (2012). Characterization of the long-term immune response to vaccination against *Mycobacterium avium* subsp. paratuberculosis in danish dairy cows. *Vet. Immunol. Immunopathol.* 145, 316–322. doi: 10.1016/j.vetimm.2011.11.021

Usda-Aphis (2010). *Uniform Program Standards for Johne's Disease Control Program*. Washington, DC: USDA.

Valle, H., and Rinjard, P. (1926). Etudes sur l'enterite paratuberculeuse des bovides. *Res. Gen. Med. Vet.* 35.

Wu, C. W., Schmoller, S. K., Shin, S. J., and Talaat, A. M. (2007). Defining the stressome of *Mycobacterium avium* subsp. paratuberculosis *in vitro* and in naturally infected cows. *J. Bacteriol.* 189, 7877–7886. doi: 10.1128/JB.00780-07

Conflict of Interest Statement: The authors declare that the research was conducted in the absence of any commercial or financial relationships that could be construed as a potential conflict of interest.

Received: 02 April 2014; accepted: 11 June 2014; published online: 30 June 2014.

Citation: Lamont EA, Talaat AM, Coussens PM, Bannantine JP, Grohn YT, Katani R, Li L-l, Kapur V and Sreevatsan S (2014) Screening of Mycobacterium avium subsp. paratuberculosis mutants for attenuation in a bovine monocyte-derived macrophage model. Front. Cell. Infect. Microbiol. ***4****:87. doi: 10.3389/fcimb.2014.00087*

This article was submitted to the journal Frontiers in Cellular and Infection Microbiology.

frontiers in
CELLULAR AND INFECTION MICROBIOLOGY

ORIGINAL RESEARCH ARTICLE
published: 01 July 2014
doi: 10.3389/fcimb.2014.00088

Evaluation of eight live attenuated vaccine candidates for protection against challenge with virulent *Mycobacterium avium* subspecies *paratuberculosis* in mice

John P. Bannantine[1]*, Jamie L. Everman[2,3], Sasha J. Rose[2,3], Lmar Babrak[2,3], Robab Katani[4], Raúl G. Barletta[5], Adel M. Talaat[6,7], Yrjö T. Gröhn[8], Yung-Fu Chang[8], Vivek Kapur[4] and Luiz E. Bermudez[2,3]

[1] *Infectious Bacterial Diseases, National Animal Disease Center, USDA-ARS, Ames, IA, USA*
[2] *Department of Biomedical Sciences, College of Veterinary Medicine, Oregon State University, Corvallis, OR, USA*
[3] *Department of Microbiology, College of Science, Oregon State University, Corvallis, OR, USA*
[4] *Department of Veterinary and Biomedical Sciences, Pennsylvania State University, University Park, PA, USA*
[5] *School of Veterinary Medicine and Biomedical Sciences, University of Nebraska, Lincoln, NE, USA*
[6] *Department of Pathobiological Sciences, University of Wisconsin-Madison, Madison, WI, USA*
[7] *Department of Food Hygiene, Cairo University, Cairo, Egypt*
[8] *Department of Population Medicine and Diagnostic Sciences, College of Veterinary Medicine, Cornell University, Ithaca, NY, USA*

Edited by:
Thomas A. Ficht, Texas A&M University, USA

Reviewed by:
John T. Belisle, Colorado State University, USA
Gregory T. Robertson, University of Texas Southwestern Medical Center at Dallas, USA

***Correspondence:**
John P. Bannantine, National Animal Disease Center, USDA-ARS, 1920 Dayton Avenue, Ames, IA 50010, USA
e-mail: john.bannantine@ars.usda.gov

Johne's disease is caused by *Mycobacterium avium* subsp. *paratuberculosis* (MAP), which results in serious economic losses worldwide in farmed livestock such as cattle, sheep, and goats. To control this disease, an effective vaccine with minimal adverse effects is needed. In order to identify a live vaccine for Johne's disease, we evaluated eight attenuated mutant strains of MAP using a C57BL/6 mouse model. The persistence of the vaccine candidates was measured at 6, 12, and 18 weeks post vaccination. Only strains 320, 321, and 329 colonized both the liver and spleens up until the 12-week time point. The remaining five mutants showed no survival in those tissues, indicating their complete attenuation in the mouse model. The candidate vaccine strains demonstrated different levels of protection based on colonization of the challenge strain in liver and spleen tissues at 12 and 18 weeks post vaccination. Based on total MAP burden in both tissues at both time points, strain 315 (MAP1566::Tn*5370*) was the most protective whereas strain 318 (intergenic Tn*5367* insertion between MAP0282c and MAP0283c) had the most colonization. Mice vaccinated with an undiluted commercial vaccine preparation displayed the highest bacterial burden as well as enlarged spleens indicative of a strong infection. Selected vaccine strains that showed promise in the mouse model were moved forward into a goat challenge model. The results suggest that the mouse trial, as conducted, may have a relatively poor predictive value for protection in a ruminant host such as goats.

Keywords: Johne's disease, *Mycobacterium*, vaccines, attenuated, mouse model, genomics

INTRODUCTION

The development of vaccines for Johne's disease, which affects cattle, sheep, and goats, is an attractive approach to control this disease. The ideal vaccine would stimulate a protective immune response to *Mycobacterium avium* subspecies *paratuberculosis* (MAP), the cause of this disease, and will not interfere with diagnostic tests. This would have a significant impact, given the wide distribution of the disease in Europe, Australia, New Zealand, Japan, India, and the United States. Furthermore, this condition is economically crippling in farmed livestock operations. Outdated figures from the National Animal Health Monitoring System suggested the prevalence of Johne's disease in U.S. dairy herds to be 68% and the cost to the industry to be approximately $250 million annually (Johnson-Ifearulundu et al., 1999). More recent data suggest this prevalence is on the rise with approximately 91% of dairy herds infected (Lombard et al., 2013).

Vaccination against MAP has been found to reduce the incidence of clinical disease, although animals are still susceptible to infection with MAP (Larsen et al., 1978). While there are significantly fewer bacteria in the intestinal tissues of vaccinated calves vs. non-vaccinated (Sweeney et al., 2009), perhaps the most tangible benefit to vaccination is that it lowers bacterial shedding levels in the feces. This helps decrease transmission to uninfected herd mates, which has been demonstrated more than once (Kormendy, 1994; Sweeney et al., 2009), but most recently by Knust et al. using a killed whole cell vaccine (Knust et al., 2013).

This study represents the second phase of a three-phase vaccine trial to identify the best available live attenuated vaccine candidates against Johne's disease. These strains were tested for attenuation in primary bovine macrophages in the first phase and prior to enrollment in the current study. All MAP mutants were attenuated to some degree in a primary bovine macrophage

model (Lamont et al., 2014); however, only the eight most attenuated in macrophages were evaluated in the current mouse study. The goal of this study was to determine the protective efficacy of eight MAP deletion mutants in C57BL/6 mice. Bacterial load in the spleen and liver were determined following vaccination and subsequent challenge with MAP. Five vaccine candidates showing the least amount of viable bacteria in these tissues were moved forward into phase three of the study, the goat trial (Hines et al., 2014).

Historically, live MAP vaccine formulations were attenuated by serial passage on solid media (Huygen et al., 2010). The vaccine currently used in the United States is based on a killed whole-cell bacterin derived from *M. avium* strain 18 in an oil adjuvant and sold under the name Mycopar. More recently, the introduction of random transposon insertions was achieved using mycobacteriophage and the first library of 5620 Tn*5367* insertional mutants was reported (Harris et al., 1999). Screening transposon library banks for virulence genes (Shin et al., 2006) and attenuation in animals (Scandurra et al., 2010) quickly followed. But it was only recently that a few laboratories have been able to construct defined knockouts by allelic exchange with this bacterium, which is slow growing and not easily amenable to genetic manipulation (Park et al., 2008; Scandurra et al., 2010; Chen et al., 2012). Although the macrophage trial mentioned above contains mutants constructed by allelic exchange, this communication only reports on transposon insertion mutants.

The ability to construct mutant strains has now made feasible the testing of live attenuated bacterial clones vs. heat killed preparations of MAP to determine which yields the most protective vaccine. This comparison was recently performed using the Mycopar vaccine and a live attenuated *leuD* mutant in mice. In that study, the live vaccine was more protective than the killed vaccine (Faisal et al., 2013). All commercially available MAP vaccine formulations include heat-inactivated mycobacteria and are sold under the Mycopar, Silirum, and Gudair trade names. Silirum and Mycopar are available, but not used in the United States while Gudair is used in Europe and Australia. In the current study, the heat-inactivated prep, Silirum, was used as a comparison to the live attenuated mutants. Silirum has recently been shown to lower clinical disease in New Zealand commercial deer farms; however no differences in weight gain or fecal shedding were observed between vaccinates and controls (Stringer et al., 2013).

MATERIALS AND METHODS

BACTERIAL CULTURES

MAP bovine strain K-10 was used as the challenge strain. It was cultured in Middlebrook 7H9 broth supplemented with 10% (v/v) oleic acid, albumin, dextrose, and catalase (OADC; Hardy, Santa Maria, CA) and 2 mg/L mycobactin J (Allied Monitor, Fayette, MO) at 37°C. Cultures were centrifuged and washed 3 times in phosphate-buffered saline (PBS; 150 mM NaCl, 10 mM NaPO4, pH 7.4) before bacterial pellets were resuspended to make a final 10^8 MAP/ml suspension to be used as the challenge inoculum. Strain 315 was derived by random transposon mutagenesis of wild type strain K-10 with Tn*5370*, whereas strains 316–321 were derived by random transposon mutagenesis of K-10 with Tn*5367* (**Table 1**). These strains grew at approximately the same rate in Middlebrook 7H9 broth cultures and displayed different levels of attenuation in bovine macrophages (Lamont et al., 2014; Rathnaiah et al., under review). Some of these mutants have been described elsewhere (Shin et al., 2006; Hines et al., 2014; Settles et al., 2014). The parental strains for these mutants are all K-10 except strain 329, which is the ATCC 19698 strain. Live-attenuated MAP vaccine strains were blinded at Penn State University and received by the laboratory conducting the mouse trial (Cornell University and Oregon State University). The commercial vaccine, Silirum, was purchased and used according to manufacturer recommendations (Pfizer; New York, NY).

MICE

Four week-old female C57BL/6 mice were obtained from Jackson Laboratory (Bar Harbor, ME) and were acclimated for 2 weeks prior to experimentation. All experiments were performed according to the guidelines of the institutional animal care and use committee at Oregon State University (ACUP #4122) and Cornell University (IACUC #2003-0007).

VACCINATION AND CHALLENGE OF MICE

The treatment groups for all mice are shown in **Table 1**. An inoculum for each of the 8 live-attenuated MAP vaccine strains and the wild-type MAP K-10 strain were quantified to an OD_{600} of 0.5 and diluted in the range of 1×10^5–2×10^6 MAP/ml in PBS. Silirum was used in the concentrated form as well as diluted in PBS, and PBS alone was used as a negative control. The manufacturer suggests that the standard bovine dose of Silirum is 1 ml/animal. A calculation based on the average weight of a Silirum vaccinated cow compared to a C57BL/6 mouse suggests the appropriate amount of diluted Silirum vaccine is a 100 µl dose from a 1:1000 dilution of the original Silirum vaccine (final dilution 1:10,000). Thirty mice per group were vaccinated via intraperitoneal injection with 100 µl of live-attenuated or wild-type MAP inoculum prepared as described above ($\sim 10^5$ MAP/animal; undiluted and 1:10,000 dilution of Silirum/animal). For quantification, vaccine strains were serially diluted and plated onto Middlebrook 7H11 agar plates alone or supplemented with kanamycin sulfate (100 µg/ml; kan), or hygromycin B (50 µg/ml; hyg) depending on strain requirements. Mice were vaccinated at time zero and then 6 weeks post-vaccination, mice were challenged with 100 µl of MAP K-10 containing $\sim 6.5 \times 10^6$ MAP by intraperitoneal injection. Two additional time points were taken post-challenge, each at 6-week intervals. They are the 6-week post challenge (12-week post vaccination) and the 12-week post challenge (18-week post vaccination) time points. The overall study design is summarized in **Figure 1**.

MOUSE ORGAN AND SERUM COLLECTION

At time 0, 6, 12, and 18-weeks post-vaccination blood was collected (5 mice/group/time point) by cardiac puncture. Blood was centrifuged for 15 min at 2500 × *g* and serum was collected and stored at −20°C until ready for antibody analysis. The protective efficacy of each attenuated MAP strain was evaluated by comparing splenomegaly as well as bacterial burden in mouse organs. For

Table 1 | Mouse treatment groups.

Group no.	Vaccine	Tn insertion	Background	Treatment
1	PBS (neg. control)	None	None	PBS-vaccinated, challenged
2	MAP K-10 (Pos. control)	None	K-10	K-10-vaccinated, challenged
3	Silirum (killed vaccine)	None	316F	Vaccinated, challenged
4	Strain 315	MAP1566 (3′ end)	K-10	Vaccinated, challenged
5	Strain 316	Intergenic between MAP3695 and MAP3694c (FadE5)	K-10	Vaccinated, challenged
6	Strain 317	MAP0460	K-10	Vaccinated, challenged
7	Strain 318	Intergenic between MAP0282c andMAP0283c	K-10	Vaccinated, challenged
8	Strain 319	MAP1566	K-10	Vaccinated, challenged
9	Strain 320	Intergenic between MAP2296c andMAP2297c	K-10	Vaccinated, challenged
10	Strain 321	Intergenic between MAP1150c andMAP1151c	K-10	Vaccinated, challenged
11	Strain 329	MAP2408c (FabG2_2)	ATCC 19698	Vaccinated, challenged

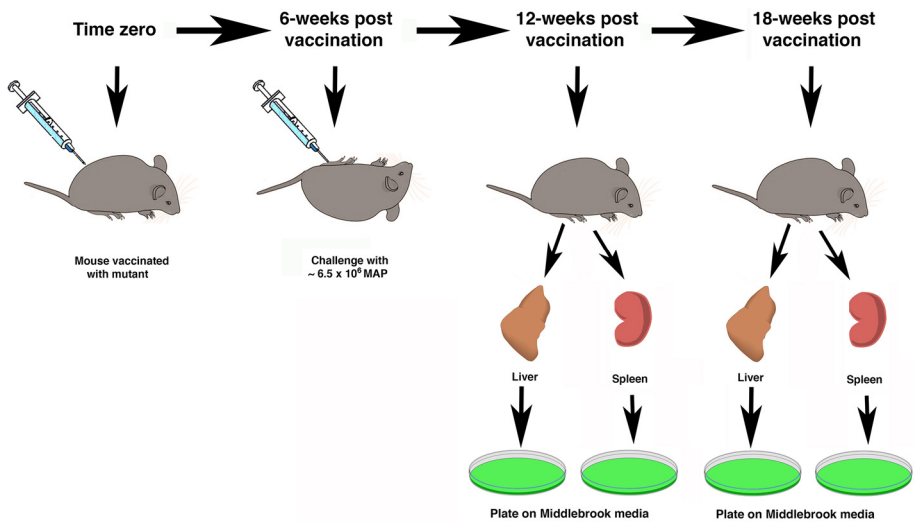

FIGURE 1 | Schematic overview of study design. The time scale at the top represents the weeks after vaccination. At time zero mice were immunized with attenuated mutant strains and controls. Mice were challenged by intraperitoneal injection with live MAP 6 weeks after vaccination. Five mice in each of 11 groups were sacrificed at the 12- and 18-week time points. Organs were collected for mycobacterial culture on Middlebrook media (green plates).

CFU enumeration, spleens and livers were collected from mice (5 mice/group/timepoint), weighed, and homogenized using 3-mm stainless steel beads in PBS for 5 min in a Bullet Blender (Next Advance; Averill Park, NY) as per manufacturer's instructions. Homogenates were serially diluted and plated onto 7H11 plates supplemented with polymyxin B (5 μg/ml), carbenicillin (22 μg/ml), and trimethoprim (2 μg/ml) and incubated for 25 days at 37°C. Total CFU on media without kan or hyg and CFU on media with kan or hyg was obtained for each timepoint to distinguish persistence of the vaccine strains (kan^r or hyg^r) vs. protection from the challenge strain (kan^s or hyg^s). The total CFU/organ on media with kan or hyg was subtracted from total CFU/organ on media without the selective antibiotic to obtain the total challenge strain CFU/organ. For groups vaccinated and/or challenged with wild-type MAP K-10 only (**Table 1** groups 1, 2, 3), total homogenates were cultured on 7H11 plates without kanamycin or hygromycin and total CFU/organ were used for analysis.

STATISTICAL ANALYSIS

Microsoft Excel software was used to perform Student's *t*-test analyses and analysis of variance. In addition, the Statistical Analysis System (SAS version 9.2; SAS Institute Inc., Cary, NC, 2009) procedure GLM (general linear models) was used to determine if there were differences in CFU counts between groups within each time point (12 and 18 weeks post-vaccination) and organ (liver and spleen). Both the original data (CFU counts) and log-transformed data [log(CFU) counts] were analyzed. In all analyses, differences between groups were considered significant when a probability value of less than 0.05 was obtained.

RESULTS

PERSISTENCE OF MAP MUTANTS AFTER VACCINATION OF MICE

Eight attenuated mutants were included in this study because initial data demonstrated their attenuation in cultured macrophages, which qualified them as candidate vaccines (Wu et al., 2007;

Lamont et al., 2014). To further test these live-attenuated strains of MAP, we measured the ability of each strain to initiate systemic infections in mice. Inoculation with Silirum vaccine, K-10 wild-type strain, PBS control, and candidate live-attenuated MAP vaccine strains 315 through 319 resulted in little or no detectable infection in livers and spleens of vaccinated animals at 6 weeks post-vaccination (**Table 2**). In contrast, candidate vaccine strains 320, 321, and 329 showed notably higher colony counts of MAP in liver and spleen homogenates 6 weeks after vaccination (**Table 2**). Persistence of these three strains continued out to 12-weeks post vaccination, but no antibiotic resistant colonies were detected by the 18-week time point in the spleen. These data suggest strains 320, 321, and 329 are persistent to at least 12 weeks in the spleen and at least 18 weeks in the liver using this model; however, the other vaccine candidates were clearly attenuated since they could not be cultured even at the earliest time point.

MAP COLONIZATION OF SPLEEN AND LIVER IN MICE

Six weeks after vaccination the mice were challenged by intraperitoneal injection with wild type MAP (**Figure 1**). The livers and spleens were collected from mice in each treatment group at the 12- and 18-week time points and cultured for MAP as described in the Materials and Methods section. As a general observation across all treatment groups, spleens had higher MAP burdens as compared to the liver and this difference was significant at the 18-week time point ($P < 0.05$).

Liver at 12 weeks post-vaccination

Culture results for the 12-week time point in liver are shown in the left panel of **Figure 2**. The K-10 vaccinated group (positive control) had significantly lower CFU counts in the liver than did mice in the diluted Silirum group and strain 318 group. Mice in the diluted Silirum group had significantly higher CFU counts in the liver than did mice in the undiluted Silirum group and all attenuated MAP strains except 318 and 320. These results suggest the diluted Silirum vaccine was too dilute to protect mice from MAP challenge. Mice in the strain 318 group had significantly higher CFU counts in the liver than did mice vaccinated with undiluted Silirum, strain 321 and strain 329. Thus at this time point, strain 315 was statistically the best attenuated vaccine in the liver.

Table 2 | Persistence of vaccine strains[a].

Vaccine strain	Initial culture conc.	Inoculum/mouse	Persistence as measured by kan- or hyg-resistant CFUs		
			CFUs at 6-weeks[b]	CFUs at 12-weeks[b]	CFUs at 18-weeks[b]
PBS (liver)	0	0	0	2760	1120
PBS (spleen)	0	0	0	3380	2570
MAP K-10 (liver)	1.47×10^6	1.47×10^5	0	ND[c]	ND
MAP K-10 (spleen)			3	ND	ND
Strain 315 (liver)	2.8×10^4	2.8×10^3	0	0	0
Strain 315 (spleen)			0	32	0
Strain 316 (liver)	1.8×10^5	1.8×10^4	0	0	0
Strain 316 (spleen)			0	8	0
Strain 317 (liver)	1.26×10^6	1.26×10^5	0	0	0
Strain 317 (spleen)			0	104	0
Strain 318 (liver)	4.2×10^5	4.2×10^4	0	0	0
Strain 318 (spleen)			0	0	0
Strain 319 (liver)	2.1×10^5	2.1×10^4	0	20	0
Strain 319 (spleen)			0	0	0
Strain 320 (liver)	4.2×10^6	4.2×10^5	554	420	34
Strain 320 (spleen)			2180	1410	0
Strain 321 (liver)	2.95×10^6	2.95×10^5	738	20	12
Strain 321 (spleen)			1550	2860	0
Strain 329 (liver)	2.14×10^6	2.14×10^5	476	580	2
Strain 329 (spleen)			206	712	0

[a] *All values are reported as average CFU/ml among five mice.*

[b] *All values represent kan- or hyg-resistant colonies except for the PBS control where the K-10 challenge was plated on non-selective media.*

[c] *ND, not determined. Because K-10 challenge dose could not be distinguished from K-10 vaccination dose, these values could not be obtained.*

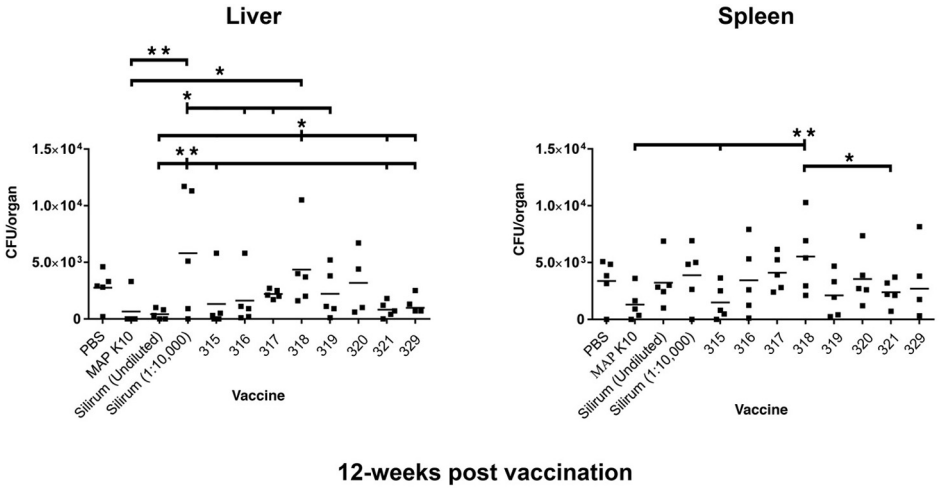

FIGURE 2 | MAP burden in liver and spleen at 12 weeks post vaccination. A single asterisk denotes statistical significance at $P < 0.05$ and two asterisks show statistical significance at $P < 0.01$. The bar in each treatment represents the average of five mice.

Spleen at 12 weeks post-vaccination

Mice in the strain 318 group had significantly higher CFU counts in the spleen than did mice in the K-10 vaccinated group, strain 315 group, and strain 321 group (**Figure 2**, right panel). In fact, vaccination with strain 318 resulted in the highest MAP burdens among mutant strains in both tissues at the 12-week time point. Strain 315 had the lowest average CFU count among the attenuated MAP mutants.

Liver at 18 weeks post-vaccination

There were no differences in CFU count in the liver between any experimental groups (**Figure 3**).

Spleen at 18 weeks post-vaccination

Mice in the undiluted Silirum group had higher CFU counts in the spleen than did mice in the K-10- vaccinated group, diluted Silirum group, and all the attenuated MAP vaccine treated groups (**Figure 3**). The undiluted Silirum treatment showed the highest levels of infection seen in the entire study.

Overall, vaccination with strain 319 resulted in low average CFUs in the spleen at both the 12- and 18-week time points but median CFU values in the liver. In contrast to vaccination with strain 315, which showed low CFUs in both tissues at both time points, strain 318 showed the least protection as measured by high bacterial loads in both organs. Both strains 315 and 321 showed equivalent protection against MAP at the 12-week post vaccination time point. However, strain 320 emerged as the best vaccine at the 18-week time point.

SPLEEN AND LIVER PATHOLOGY

The spleen and liver of each mouse were weighed prior to processing for culture. No significant differences were observed in the liver; however, vaccination with the undiluted Silirum had a significant effect on spleen size (**Figure 4**). At 18 weeks post vaccination, mice in all other experimental groups had significantly smaller spleens than the undiluted Silirum vaccinated group. The enlarged spleens of this one group demonstrate the strong toxicity or hyper-stimulation obtained with this high-dose whole-cell vaccine.

DISCUSSION

The development of new live MAP vaccine candidates is still in its early stages, yet through a three-phase vaccine trial using available attenuated mutants, several key insights can be obtained. The results will enable a unique look at how mouse vaccination and challenge data will predict protection in a ruminant model, since a selection of these vaccine strains were moved forward into a goat vaccine trial (Hines et al., 2014). In addition, a determination can be made of whether killed whole-cell vaccines, which are the current formulation in commercially available vaccines against Johne's disease, vs. live attenuated strains are better vaccines for Johne's disease. Here we showed that different live attenuated strains protect with varying degrees (ranked in order of lowest bacterial burden in both tissue combined to highest 315, 319, 321, 320, 329, 316, 317, and 318) against tissue infection in a mouse model, while the whole-cell vaccine Silirum, in the conditions tested, yielded poor protection either as diluted or undiluted formulations. This is similar to what was observed when comparing the live *leuD* mutant to the killed Mycopar vaccine. That study showed the *leuD* mutant was more protective against MAP challenge in goats (Faisal et al., 2013). The *leuD* mutant also induced a protection against MAP challenge in a mouse model (Chen et al., 2012). However, there are some differences between these two studies that make comparisons difficult. The latter study used a different bacterin (Mycopar derived from strain 18) and inoculation route (subcutaneous).

Nonetheless, these insights will be helpful when new MAP vaccine strains become available. For many years, it has been suggested that an effective anti-mycobacterial vaccine strain must replicate in the host tissue in order to induce protective immune responses. While this is the case for BCG vaccination against

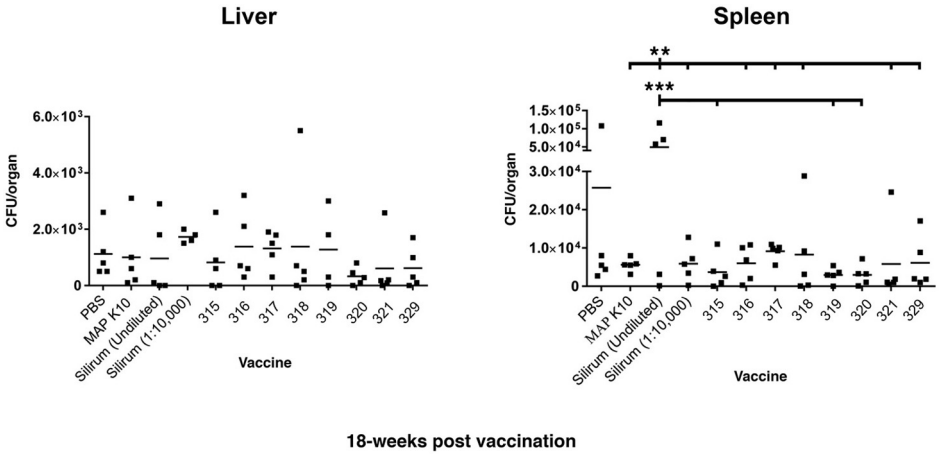

FIGURE 3 | MAP burden in liver and spleen at 18 weeks post vaccination. Two asterisks show statistical significance at $P < 0.01$ and three asterisks denote statistical significance at $P < 0.001$. The bar in each treatment represents the average of five mice.

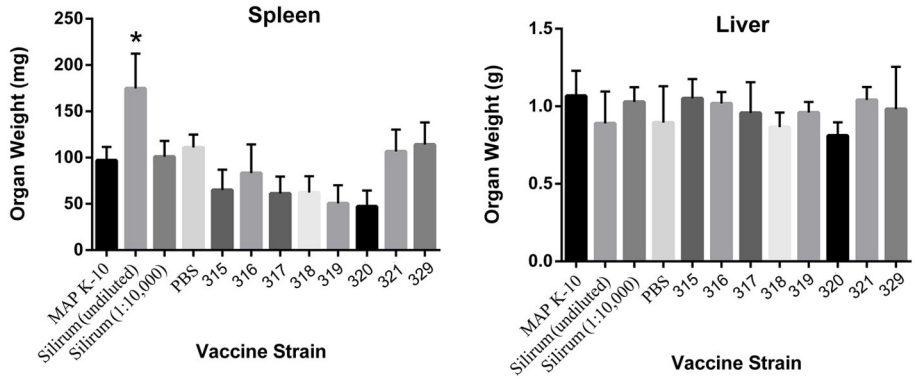

FIGURE 4 | Induction of splenomegaly in undiluted Silirum vaccinated mice at 18 weeks post vaccination. The graphs show the average spleen and liver weights of 5 mice per group. Statistically significant differences in spleen size of undiluted Silirum treated mice compared to other treatment groups are indicated by an asterisk ($P < 0.05$ for 329; $P < 0.01$ for 321 and PBS; $P < 0.005$ for K-10, diluted Silirum and 316; $P < 0.0005$ for 315, 317, 318, 319, and 320).

Mycobacterium tuberculosis infection, it remains an issue needing further experimentation for MAP vaccination. The trial in mice reported herein seems to indicate otherwise, but results in goats (Hines et al., 2014) are consistent with this hypothesis. Moreover, it is noted that while experimental vaccines were inoculated intraperitoneally in the current mouse trial, goats were vaccinated with a subset of these attenuated mutants and challenged by the oral route (Hines et al., 2014). Thus, factors other than animal species may contribute to the observed differences.

Our study measured both persistence of the vaccine strains as well as infection levels of the challenge strain in the spleen and liver. These two organs are primarily used to assess systemic implantation and organ compromise for MAP in the mouse at 6 and 12 weeks post challenge (Shin et al., 2006; Wu et al., 2007) although lymph nodes and intestinal tissues have also been cultured (Huntley et al., 2005; Shin et al., 2006; Cooney et al., 2014). Although not part of our study design, a recent paper suggests lymph nodes are a good tissue to track progression of MAP infection in the murine model (Cooney et al., 2014). Nonetheless, we observed slightly higher infection levels in the spleen as compared to the liver, which is commonly seen and may represent the result of greater vascularization in the spleen. We also observed three mutant strains that were able to persist for up to 12 weeks post vaccination, but were cleared by 18 weeks post vaccination. This is similar to that observed with the *fabG2_2* and *impA* mutants in a separate study (Shin et al., 2006). In fact, the *fabG2_2* mutant from that study is the same as strain 329 in the current study, thus confirming persistence for this mutant. Because these three mutants did not clearly outperform the more attenuated strains, it remains uncertain whether these more persistent mutants result in better protection from implantation and infection than fully attenuated mutants. It has been postulated previously that MAP mutants, which cannot survive in mouse peritoneal macrophages, might be a reason for the inability of attenuated strains to colonize mouse organs (Shin et al., 2006).

In our mouse model, the diluted Silirum vaccine demonstrated poor protection relative to the attenuated vaccine strains. The vaccine was designed for sheep and the manufacturer recommends 1 ml/ovine dose and thus 0.1 ml/mouse might be a reasonable empirical dosage, but there is no experimental data to verify this as an appropriate dose. Therefore, we chose to use Silirum undiluted and at a 1:10,000 dilution in this study. It was observed that any protective effect in the liver could be diluted out, since average numbers of colony forming units were lower in the undiluted Silirum relative to the 1:10,000 dilution. However, this trend did not hold true for either time point in the spleen. There were unusually high numbers of colony forming units in three of the five mice vaccinated with undiluted Silirum (**Figure 3**, right panel). In contrast, this same vaccine has been shown to be very effective at reducing mortality and delaying fecal shedding in Merino sheep (Reddacliff et al., 2006). The amount of Silirum vaccine given per mouse could have had a detrimental effect in a variety of ways. As the amount given to a mouse was more in proportion to what a farm animal would receive, it is possible that the components (oil, MAP antigens, etc.) of the vaccine inhibited its ability to fight off infection over the length of the trial. The undiluted vaccine could have had a toxic effect on the spleen, which may explain the enlarged spleens in the undiluted Silirum vaccinated group. This effect may have led to a higher level of colonization by the MAP challenge strain later during infection. It also might simply suggest that the mouse may not be a good predictive model for vaccines against Johne's disease.

This is not a comprehensive list of attenuated mutants in MAP. Unfortunately, the *leuD* mutant was not included in these studies. It has recently shown efficacy against MAP challenge in both a mouse and goat model (Chen et al., 2012; Faisal et al., 2013). However, this is the only published attenuated mutant of MAP that was not enrolled in the Johne's Disease Integrated Program's three-phase vaccine trial.

The wild-type challenge strain did not appear fully virulent in the mouse model. The K-10 strain used in this mouse study is the same strain that was used to construct most of the mutants. However, as has been clearly shown for *M. tuberculosis* (Ioerger et al., 2010), identical strains kept in different laboratories diverge over time. Therefore, the apparent slight attenuation of the wild type strain in the mouse may just reflect the natural passage history in two laboratories. Another possibility is that when inoculated at low dose it may just be that some mutants grew better at this time point, but if the time points were extended, their attenuation would be clearer.

The mouse model is used to understand invasion, virulence mechanisms, and evaluate vaccine strains, but it is limited in its ability to develop the full disease observed with MAP infection in ruminants. Due to this pitfall of the model, it is possible that wild-type MAP may provide similar, early protection as attenuated strains against subsequent infection. This is likely due to the common components in the whole cell bacterial vaccines of live-attenuated and non-attenuated strains. However, when translated to a caprine or bovine challenge model, this protection is abrogated as the wild-type virulent MAP strain is capable of progressing to the clinical stages of Johne's disease. The *in vitro* trials were for virulence and survival in macrophages, and so we hypothesized that the live-attenuated strains would be unable to progress to full infection in a ruminant model. The five selected mutants in our study were entered into a goat trial to examine which mutant is the best performer in a ruminant model. Analysis of these data are reported elsewhere (Hines et al., 2014) and results seem to suggest a low level of correlation, indicating that the mouse trial, as conducted, has a relatively poor predictive value for the results in a ruminant host such as goats. Alternatively, oral vaccination may not be the best route to evaluate attenuated strains in goats.

ACKNOWLEDGMENTS

Funding for conducting the three-phase vaccine trial was provided by the USDA-CAP grant JDIP and by USDA-APHIS. This work was also partially supported by NIFA Animal Health Projects (NEB-39-162 to Raúl G. Barletta) and the animal formula fund (NY-478-437 to Yung-Fu Chang).

REFERENCES

Chen, J. W., Faisal, S. M., Chandra, S., McDonough, S. P., Moreira, M. A., Scaria, J., et al. (2012). Immunogenicity and protective efficacy of the *Mycobacterium avium* subsp. *paratuberculosis* attenuated mutants against challenge in a mouse model. *Vaccine* 30, 3015–3025. doi: 10.1016/j.vaccine.2011.11.029

Cooney, M. A., Steele, J. L., Steinberg, H., and Talaat, A. M. (2014). A murine oral model for *Mycobacterium avium* subspecies *paratuberculosis* infection and immunomodulation with *Lactobacillus casei* ATCC 334. *Front. Cell. Infect. Microbiol.* 4:11. doi: 10.3389/fcimb.2014.00011

Faisal, S. M., Chen, J. W., Yan, F., Chen, T. T., Useh, N. M., Yan, W., et al. (2013). Evaluation of a *Mycobacterium avium* subsp. *paratuberculosis leuD* mutant as a vaccine candidate against challenge in a caprine model. *Clin. Vaccine Immunol.* 20, 572–581. doi: 10.1128/CVI.00653-12

Harris, N. B., Feng, Z., Liu, X., Cirillo, S. L., Cirillo, J. D., and Barletta, R. G. (1999). Development of a transposon mutagenesis system for *Mycobacterium avium* subsp. *paratuberculosis*. *FEMS Microbiol. Lett.* 175, 21–26. doi: 10.1111/j.1574-6968.1999.tb13597.x

Hines, M. E. 2nd., Turnquist, S. E., Ilha, M. R. S., Rajeev, S., Jones, A. L., Whittington, L., et al. (2014). Evaluation of novel oral vaccine candidates and validation of a caprine model of Johne's disease. *Front. Cell. Infect. Microbiol.* 4:26. doi: 10.3389/fcimb.2014.00026

Huntley, J. F., Stabel, J. R., Paustian, M. L., Reinhardt, T. A., and Bannantine, J. P. (2005). Expression library immunization confers protection against *Mycobacterium avium* subsp. *paratuberculosis* infection. *Infect. Immun.* 73, 6877–6884. doi: 10.1128/IAI.73.10.6877-6884.2005

Huygen, K., Bull, T., and Collins, D. M. (2010). "Development of new *paratuberculosis* vaccines," in *Paratuberculosis: Organism, Disease, Control,* eds M. A. Behr and D. M. Collins (Oxfordshire: CAB International), 353–368.

Ioerger, T. R., Feng, Y., Ganesula, K., Chen, X., Dobos, K. M., Fortune, S., et al. (2010). Variation among genome sequences of H37Rv strains of *Mycobacterium tuberculosis* from multiple laboratories. *J. Bacteriol.* 192, 3645–3653. doi: 10.1128/JB.00166-10

Johnson-Ifearulundu, Y., Kaneene, J. B., and Lloyd, J. W. (1999). Herd-level economic analysis of the impact of *paratuberculosis* on dairy herds. *J. Am. Vet. Med. Assoc.* 214, 822–825.

Knust, B., Patton, E., Ribeiro-Lima, J., Bohn, J. J., and Wells, S. J. (2013). Evaluation of the effects of a killed whole-cell vaccine against *Mycobacterium avium* subsp *paratuberculosis* in 3 herds of dairy cattle with natural exposure to the organism. *J. Am. Vet. Med. Assoc.* 242, 663–669. doi: 10.2460/javma.242.5.663

Kormendy, B. (1994). The effect of vaccination on the prevalence of *paratuberculosis* in large dairy herds. *Vet. Microbiol.* 41, 117–125.

Lamont, E. A., Talaat, A. M., Coussens, P. M., Bannantine, J. P., Grohn, Y. T., Katani, R., et al. (2014). Screening of Mycobacterium avium subspecies *paratuberculosis* mutants as vaccine candidates in a primary bovine monocyte-derived macrophage model. *Front. Cell. Infect. Microbiol.* 4:87. doi: 10.3389/fcimb.2014.00087

Larsen, A. B., Moyle, A. I., and Himes, E. M. (1978). Experimental vaccination of cattle against *paratuberculosis* (Johne's disease) with killed bacterial vaccines: a controlled field study. *Am. J. Vet. Res.* 39, 65–69.

Lombard, J. E., Gardner, I. A., Jafarzadeh, S. R., Fossler, C. P., Harris, B., Capsel, R. T., et al. (2013). Herd-level prevalence of *Mycobacterium avium* subsp. *paratuberculosis* infection in United States dairy herds in 2007. *Prev. Vet. Med.* 108, 234–238. doi: 10.1016/j.prevetmed.2012.08.006

Park, K. T., Dahl, J. L., Bannantine, J. P., Barletta, R. G., Ahn, J., Allen, A. J., et al. (2008). Demonstration of allelic exchange in the slow-growing bacterium *Mycobacterium avium* subsp. *paratuberculosis*, and generation of mutants with deletions at the *pknG*, *relA*, and *lsr2* loci. *Appl. Environ. Microbiol.* 74, 1687–1695. doi: 10.1128/AEM.01208-07

Reddacliff, L., Eppleston, J., Windsor, P., Whittington, R., and Jones, S. (2006). Efficacy of a killed vaccine for the control of *paratuberculosis* in Australian sheep flocks. *Vet. Microbiol.* 115, 77–90. doi: 10.1016/j.vetmic.2005.12.021

Scandurra, G. M., De Lisle, G. W., Cavaignac, S. M., Young, M., Kawakami, R. P., and Collins, D. M. (2010). Assessment of live candidate vaccines for *paratuberculosis* in animal models and macrophages. *Infect. Immun.* 78, 1383–1389. doi: 10.1128/IAI.01020-09

Settles, E. W., Kink, J. A., and Talaat, A. (2014). Attenuated strains of *Mycobacterium avium* subspecies *paratuberculosis* as vaccine candidates against Johne's disease. *Vaccine* 32, 2062–2069. doi: 10.1016/j.vaccine.2014.02.010

Shin, S. J., Wu, C. W., Steinberg, H., and Talaat, A. M. (2006). Identification of novel virulence determinants in *Mycobacterium paratuberculosis* by screening a library of insertional mutants. *Infect. Immun.* 74, 3825–3833. doi: 10.1128/IAI.01742-05

Stringer, L. A., Wilson, P. R., Heuer, C., and MacKintosh, C. G. (2013). A randomised controlled trial of Silirum vaccine for control of *paratuberculosis* in farmed red deer. *Vet. Rec.* 173, 551–556. doi: 10.1136/vr.101799

Sweeney, R. W., Whitlock, R. H., Bowersock, T. L., Cleary, D. L., Meinert, T. R., Habecker, P. L., et al. (2009). Effect of subcutaneous administration of a killed *Mycobacterium avium* subsp *paratuberculosis* vaccine on colonization of tissues following oral exposure to the organism in calves. *Am. J. Vet. Res.* 70, 493–497. doi: 10.2460/ajvr.70.4.493

Wu, C. W., Schmoller, S. K., Shin, S. J., and Talaat, A. M. (2007). Defining the stressome of *Mycobacterium avium* subsp. *paratuberculosis in vitro* and in naturally infected cows. *J. Bacteriol.* 189, 7877–7886. doi: 10.1128/JB.00780-07

Conflict of Interest Statement: The authors declare that the research was conducted in the absence of any commercial or financial relationships that could be construed as a potential conflict of interest.

Received: 21 February 2014; accepted: 11 June 2014; published online: 01 July 2014.
Citation: Bannantine JP, Everman JL, Rose SJ, Babrak L, Katani R, Barletta RG, Talaat AM, Gröhn YT, Chang Y-F, Kapur V and Bermudez LE (2014) Evaluation of eight live attenuated vaccine candidates for protection against challenge with virulent Mycobacterium avium subspecies paratuberculosis in mice. Front. Cell. Infect. Microbiol. ***4****:88. doi: 10.3389/fcimb.2014.00088*
This article was submitted to the journal Frontiers in Cellular and Infection Microbiology.

frontiers in
CELLULAR AND INFECTION MICROBIOLOGY

ORIGINAL RESEARCH ARTICLE
published: 04 March 2014
doi: 10.3389/fcimb.2014.00026

Evaluation of novel oral vaccine candidates and validation of a caprine model of Johne's disease

Murray E. Hines II[1]*, Sue E. Turnquist[1], Marcia R. S. Ilha[1], Sreekumari Rajeev[1], Arthur L. Jones[2], Lisa Whittington[1], John P. Bannantine[3], Raúl G. Barletta[4], Yrjö T. Gröhn[5], Robab Katani[6], Adel M. Talaat[7], Lingling Li[6] and Vivek Kapur[6]

[1] Tifton Veterinary Diagnostic and Investigational Laboratory, University of Georgia, Tifton, GA, USA
[2] College of Veterinary Medicine, Food Animal Health and Management Program, University of Georgia, Athens, GA, USA
[3] National Animal Disease Center, United States Department of Agriculture, Agricultural Research Service, Ames, IA, USA
[4] School of Veterinary Medicine and Biomedical Sciences, University of Nebraska, Lincoln, NE, USA
[5] Section of Epidemiology, Department of Population Medicine and Diagnostic Sciences, Cornell University, Ithaca, NY, USA
[6] Department of Veterinary Science, Penn State University, University Park, Pennsylvania, PA, USA
[7] Department of Pathobiological Sciences, University of Wisconsin-Madison, Madison, WI, USA

Edited by:
Thomas A. Ficht, Texas A&M University, USA

Reviewed by:
Philip R. Hardwidge, Kansas State University, USA
Subramanian Dhandayuthapani, Texas Tech Health Sciences Center, USA

***Correspondence:**
Murray E. Hines II, Tifton Veterinary Diagnostic and Investigational Laboratory, University of Georgia, PO Box 1389, 43 Brighton Road, Tifton, GA 31793, USA
e-mail: mhinesii@uga.edu

Johne's disease (JD) caused by *Mycobacterium avium* subspecies *paratuberculosis* (MAP) is a major threat to the dairy industry and possibly some cases of Crohn's disease in humans. A MAP vaccine that reduced of clinical disease and/or reduced fecal shedding would aid in the control of JD. The objectives of this study were (1) to evaluate the efficacy of 5 attenuated strains of MAP as vaccine candidates compared to a commercial control vaccine using the protocol proposed by the Johne's Disease Integrated Program (JDIP) Animal Model Standardization Committee (AMSC), and (2) to validate the AMSC Johne's disease goat challenge model. Eighty goat kids were vaccinated orally twice at 8 and 10 weeks of age with an experimental vaccine or once subcutaneously at 8 weeks with Silirum® (Zoetis), or a sham control oral vaccine at 8 and 10 weeks. Kids were challenged orally with a total of approximately 1.44×10^9 CFU divided in two consecutive daily doses using MAP ATCC-700535 (K10-like bovine isolate). All kids were necropsied at 13 months post-challenge. Results indicated that the AMSC goat challenge model is a highly efficient and valid model for JD challenge studies. None of the experimental or control vaccines evaluated prevented MAP infection or eliminated fecal shedding, although the 329 vaccine lowered the incidence of infection, fecal shedding, tissue colonization and reduced lesion scores, but less than the control vaccine. Based on our results the relative performance ranking of the experimental live-attenuated vaccines evaluated, the 329 vaccine was the best performer, followed by the 318 vaccine, then 316 vaccine, 315 vaccine and finally the 319 vaccine was the worst performer. The subcutaneously injected control vaccine outperformed the orally-delivered mutant vaccine candidates. Two vaccines (329 and 318) do reduce presence of JD gross and microscopic lesions, slow progression of disease, and one vaccine (329) reduced fecal shedding and tissue colonization.

Keywords: *Mycobacterium avium* subsp *paratuberculosis*, vaccine efficacy, mutant vaccines, diagnostic tests, goats

INTRODUCTION

There are conflicting data on the ability of current vaccines for Johne's disease (JD) to reduce shedding of *Mycobacterium avium* subspecies *paratuberculosis* (MAP), and killed "whole cell" MAP vaccines often generate serious local tissue reaction and cross-reactions to intradermal tests for *M. bovis*. This limits their usefulness for control programs (Rideout et al., 2003). To date, no vaccine has been developed that elicits an immune response that completely eliminates viable MAP from the host (sterile immunity). This is in part attributable to a lack of knowledge of the factors that regulate the immune response to MAP or to pathogenic mycobacteria in general (Flynn and Chan, 2001). Not all animals exposed to MAP progress to clinical disease, but it is unclear whether infection is never established in some animals or whether they develop an immune response that controls or eliminates the pathogen (Rideout et al., 2003). Experimental trials with vaccinated animals challenged with virulent MAP or by natural exposure have shown the beneficial effects of immunization (Saxegaard and Fodstad, 1985; Fridriksdottir et al., 2000; Reddacliff et al., 2006; Stringer et al., 2013). Vaccination has reduced the severity of lesions, reduced the frequency of clinical signs and delayed onset of disease (Harris and Barletta, 2001; Stringer et al., 2013). A vaccine that reduced the rate or eliminated infection and reduced or eliminated fecal shedding of the organism would be of tremendous value in JD control programs if it could reduce disease prevalence (Rideout et al., 2003). In addition to its use in a control program, an efficacious vaccine could significantly reduce production losses and

premature culling or death losses that are associated with JD in dairy cattle (Benedictus et al., 1987; NAHMS, 1997; Lombard et al., 2005). Similar studies of losses associated with Johne's disease in beef, sheep and goat herds have not been reported, but losses in these production systems are also likely to be substantial.

Virtually all researchers using a JD challenge model have been using different species of animals, challenge parameters, doses of MAP, dosage intervals and strains of MAP. This dramatically increases the number of variables between studies and makes direct comparison of challenge and vaccine efficacy trials very difficult and often impossible. A standardized challenge model for use in vaccine efficacy trials is absolutely essential to be able to directly compare the efficacy of various vaccine formulations. A similar conclusion of the necessity of a standardized challenge model for vaccine efficacy studies was made in August 2005 at the International Colloquium for *Paratuberculosis* held in Copenhagen during the "Role of Vaccination" workshop session. The Johne's Disease Integrated Program (JDIP) Animal Model Standardization committee (AMSC) was created to address this issue and has published suggested international guidelines for JD challenge studies in multiple species including cattle, sheep, goats, deer and mice (Hines et al., 2007b).

Recent longitudinal JD studies presented at the 2010 JDIP annual meeting in Denver, CO have suggested that JD management and environmental control practices have reduced the incidence of JD, but are not likely to be successful in eradicating JD or reducing the incidence of JD to acceptable levels within dairy herds. Subsequently, most JD researchers are of the opinion that an effective vaccine which eliminates fecal shedding and prevents clinical disease is the best option for long term control of JD. This led to the development of the JDIP and USDA APHIS/NIFA sponsored JD vaccine project which consisted of three blinded phases. Phase I consisted of evaluating vaccine candidates within *in vitro* macrophage studies at two independent laboratories. Twenty-two JD vaccine candidates were submitted by JD researchers worldwide for enrollment in the Phase I project. Phase II consisted of evaluating the best JD vaccine candidates as determined from the Phase I project (8 vaccine candidates) within an *in vivo* mouse challenge model performed at two different laboratories. Phase III consisted of evaluating the best five performing JD experimental vaccines as determined by the results of Phase I and II within an *in vivo* goat MAP challenge model using the AMSC recommended parameters.

The objectives of the Phase III goat vaccine trial were first to evaluate the efficacy of five MAP attenuated vaccine strains against a commercially available MAP vaccine (Silirum®, Pfizer) using the protocols and endpoints proposed by the AMSC, and second to validate the AMSC Johne's disease goat challenge model (see Hines et al., 2007b). The design of this study allows for a direct "head to head" comparison of the efficacy of the new experimental vaccines included within the study to identify vaccine candidates for further development.

MATERIALS AND METHODS

EXPERIMENTAL DESIGN

Eighty goat kids were vaccinated orally twice at 8 and 10 weeks of age with one of the attenuated vaccine strains or once subcutaneously at 8 weeks with Silirum®, or an oral sham control vaccine consisting of pasteurized goat milk. Kids were challenged orally with a total of 200 mg pelleted wet weight MAP (approximately 2.0×10^9 CFU) divided in 2 consecutive daily 100 mg doses (approximately 1.0×10^9 CFU each) using bovine MAP isolate ATCC-700535 (K10-like MAP strain). All experimental and control groups had 10 kids/group. **Table 1** lists the eight experimental and control groups with treatments. Blood and fecal samples were collected prior to vaccination (baseline samples) and similar samples were collected monthly throughout the study. Immunological tests evaluated include humoral response evaluation by AGID, ELISA, and cell mediated response by comparative purified protein derivative (PPD) skin testing (*M. avium*, Johnin, and *M. bovis* PPD's). Kids within each group were euthanized and necropsied at 13 months post-challenge. Gross and microscopic lesions and relative number of acid-fast bacilli were evaluated and scored at necropsy. Monthly fecal cultures and culture of selected necropsy tissues (tonsil, submandibular lymph nodes, liver, spleen, mesenteric lymph nodes, ileocecal lymph nodes, duodenum, jejunum, ileum, and spiral colon) were performed on Herrold's egg yolk medium (HEYM) and CFU/g determined for each specimen. Additional immunologic and diagnostic tests including AGID, ELISA, intradermal skin testing, fecal PCR and tissue PCR were performed throughout this study. Overall

Table 1 | Summary of experimental design and vaccines.

Experimental group	Vaccine (description/mutant insertion site)	Treatment
Group 1 (10 kids)	Negative control (Sham vaccine)	Sham-vaccinated, unchallenged
Group 2 (10 kids)	Control vaccine (Silirum0® vaccine)	Vaccinated, challenged
Group 3 (10 kids)	316 vaccine (between MAP3695 and FadE5)*	Vaccinated, challenged
Group 4 (10 kids)	315 vaccine (MAP1566)*	Vaccinated, challenged
Group 5 (10 kids)	319 vaccine (MAP1566)*	Vaccinated, challenged
Group 6 (10 kids)	318 vaccine (between MAP0282c and MAP0283c)*	Vaccinated, challenged
Group 7 (10 kids)	329 vaccine (fabG2_2)**	Vaccinated, challenged
Group 8 (10 kids)	Positive control (Sham vaccine)	Sham-vaccinated, challenged

Raúl G. Barletta mutant vaccine strains derived from K-10 by mutagenesis with IS1096 derived transposons.

***Adel M. Talaat mutant vaccine strain (Shin et al., 2006).*

necropsy lesion score for each animal was calculated by adding the individual gross, microscopic and acid-fast stain scores as defined in **Table 2**.

ANIMALS

The University of Georgia and Tifton Veterinary Diagnostic and Investigational Laboratory have AALAC accredited animal facilities. Animal care was performed in accordance with the procedures of the University of Georgia Institutional Animal Care and Use committee (UGA Animal Welfare Assurance # A3437-01). Two-month old kids were purchased from a farm with no previous history of Johne's disease where all the adult goats were test negative by MAP serum ELISA (Parachek®, Biocor Animal Health, Omaha, NE), AGID (New York State Animal Health Diagnostic Laboratory method—personal communication, Susan Stehman, Cornell University, NY) and fecal cultures were negative for MAP (this farm supplied the kids for the previous vaccine study—Hines et al., 2007a). The kids were moved to the animal facilities at the Tifton Veterinary Diagnostic and Investigational Lab, acclimated for 1 week and then randomly assigned to one of 8 groups of 10 kids. The "pen effect" was reduced by equalizing the distribution of kid sex and size between pens. Baseline fecal and blood specimens were collected and the initial PPD skin testing performed. The kids were vaccinated orally with the blinded attenuated JD vaccines from the Kapur[6] laboratory using two doses 2 weeks apart as per instructions provided. Each provided vaccine stock solution was blended using a 1:4 ratio with pasteurized goat milk and each individual dose was drawn into a 5 ml syringe. Kids were allowed to nurse the contents from the syringe or the contents were gently expressed on the back of the tongue during administration. All kids were housed in a restricted biosafety animal facility (BSL-2). Kids within challenged groups were housed separately from non-challenged groups in similar BSL-2 treatment rooms and managed identically. No contact was allowed between challenged and non-challenged groups at any time during the study. Free choice coastal Bermuda hay was available to the kids throughout the study. All kids were supplemented daily with a 10% protein commercial goat ration with no added antibiotics at a mean rate of 450 gm/kid/day. Goats were dewormed at monthly intervals using a combination of Moxidectin (Fort Dodge Laboratories, Fort Dodge, IA, USA) and Albendazole (Valbasen, Pfizer Animal Health, New York, NY, USA) given orally. All kids were vaccinated upon receipt (2 months old) with commercially-available tetanus toxoid (Professional Biological Company, Denver, CO, USA) and multivalent clostridial vaccine (Ultrabac 7, Pfizer Animal Health, New York, NY, USA). Male kids were castrated prior to start of the study (2 months old). Monthly blood and fecal samples were collected from each kid as described in the protocol for each test performed. All kids were necropsied at approximately 13 months post-challenge.

Table 2 | Scores for necropsy grading system categorized by lesion severity and presence of acid-fast bacilli (AFB).

Severity	Gross	Microscopic	No. AFB
None	0	0	0.00
Mild	4	1	0.25
Moderate	8	2	0.50
Severe	12	3	0.75

Individual severity scores for each of the three categories were summed to achieve the final lesion score for each kid at necropsy. Lowest and highest possible scores using this system are 0.0 and 15.75, respectively. The relative number of AFB is given the least weight in this system since both paucibacillary and pleuribacillary forms of JD are recognized in some affected animals without an apparent major difference in disease severity.

ORGANISM

The MAP strain used in this study was a bovine isolate of MAP ATCC—700535 (K10-like MAP strain) recovered from experimentally infected calves at University of Pennsylvania (Ray Sweeney) to help insure that virulent organisms are used for challenge.

VACCINE PREPARATION AND ADMINISTRATION

The Silirum® vaccine was obtained directly from Pfizer Animal Health and administered as a single dose according to manufacturer's recommendations by subcutaneous injection. The five experimental vaccines were cultured to equivalent optical densities (0.50 OD) and blinded (**Table 1**) off-site at Penn State University before being shipped to UGA. After the goats in the project had acclimated for 5 days, the experimental vaccines were administered orally in two 5 ml doses 2 weeks apart in commercially pasteurized goat milk at approximately 1.0×10^8 organisms per dose. The orally administered sham vaccines for the positive and negative control groups consisted of two 5 ml doses of commercially pasteurized goat milk.

CHALLENGE PROTOCOL

The challenge inoculum was grown in Middlebrook 7H9 liquid media containing OADC, supplemented with mycobactin J (Allied Monitor, Fayette, MO, USA) and 1% glycerol. All bacteria were freshly cultivated for approximately 12 weeks, and never refrigerated or frozen prior to use. Organisms were pelleted by centrifugation at 3000 $\times$ g for 10 min at RT in a pre-weighed large cone-bottomed centrifuge tube and the supernatant discarded. After draining the excess fluid, an accurate wet weight of the bacterial pellet was determined and the volume calculated to result in a final concentration of 20 mg organisms per ml (Hines et al., 2007a,b). The inoculum was vortexed at maximum output for 2–3 min with three glass beads to break up clumped bacilli. Whole commercially pasteurized goat's milk was added to 80% of final volume needed to make the inoculum palatable and mixed by inversion thoroughly immediately prior to use. All kids in all challenge groups were challenged at the same time period 3 weeks after the last dose of vaccine given. Each kid was allowed to nurse 5 ml of the inoculum (100 mg pelleted wet weight, approximately 1.0×10^9 CFU) from a syringe or the inoculum was gently expressed on the back of the tongue. Similar doses of inoculum were prepared and given on the next day for a total of 2 doses (total of approximately 2.0×10^9 CFU). The actual CFU of the inoculum was determined by dilution and

plating on Middlebrook 7H10 agar plus OADC and mycobactin J, and the total of both doses was found to be 1.44×10^9 CFU per challenged animal.

GROSS AND MICROSCOPIC LESIONS

A complete detailed necropsy was performed on each animal by board-certified veterinary pathologists. Tissue specimens obtained at necropsy were fixed in 10% buffered neutral formalin overnight, processed routinely and embedded in paraffin blocks. Serial sections were cut 4–6 μm thick and stained with H&E or Kinouyan's acid-fast stains. All specimens were described microscopically (blinded) by the same pathologist noting the presence, location and number of granulomatous lesions and presence and number of acid-fast bacilli. The combined gross and histologic descriptions for each animal were randomly scrambled, then blindly rated and given a lesion score by another veterinary pathologist unfamiliar with animal's group and the vaccines used within the study, but with extensive experience in the diagnosis of JD. The lesion rating system (**Table 2**; Hines et al., 2007a,b) was applied to the gross and histologic descriptions for each animal. Individual lesion severity scores for gross and microscopic lesions, and relative number of acid-fast bacilli, were summed to achieve the final lesion score for each kid at necropsy.

FECAL AND TISSUE CULTURE

Monthly fecal specimens were cultured using the sedimentation method currently recommended by National Veterinary Services Laboratory (Whitlock et al., 2000) using Herrold's egg yolk medium (HEYM with ANV, BBL; Becton Dickinson and Co, Sparks, MD, USA) with and without supplementation with mycobactin J (Allied Monitor, Fayette, MO, USA). CFU obtained from 3 HEYM tubes were averaged and adjusted to represent final CFU per gram of feces.

Specimens of tonsil, submandibular lymph nodes, mesenteric lymph nodes, ileocecal lymph nodes, liver, spleen, duodenum, jejunum, ileum and spiral colon were obtained at necropsy for mycobacterial culture. Each tissue specimen was trimmed and weighed to achieve a 2 g specimen, decontaminated, blended in a stomacher and cultured as previously described (Hines et al., 1998, 2007a). A 0.5 ml aliquot of this tissue suspension was saved for tissue PCR analysis. HEYM tubes with and without mycobactin J were incubated at 37°C and observed weekly for a minimum of 16 weeks at which time visible colonies were counted. All positive mycobacterial cultures were confirmed by PCR targeting IS900 (Rajeev et al., 2005). CFU obtained from 3 HEYM tubes were averaged and adjusted to represent final CFU per gram of tissue (CFU/g).

FECAL AND TISSUE PCR

The DNA from monthly fecal specimens and tissues obtained from necropsy (tonsil, submandibular lymph nodes, mesenteric lymph nodes, ileocecal lymph nodes, liver, spleen, duodenum, jejunum, ileum, and spiral colon) were extracted using a Qiagen tissue DNA extraction protocol per manufacturer's instructions. PCR to detect MAP in feces and necropsy tissues targeting IS MAP02 (Stabel and Bannantine, 2005) was performed using the 4405545 AgPath-ID™ MAP (Johne's) Reagent Kit (Life Technologies/Albion, Grand Island, NY) with an ABI 7900 Real-Time Thermocycler in duplicate according to manufacturer's recommendations. Both cycle threshold (CT) values and positive/negative results were obtained on monthly fecal specimens and tissues collected at necropsy. CT values ≤37 were considered a positive result and inconclusive samples were repeated.

PCR VERIFICATION OF MAP STRAINS RECOVERED FROM FECES TO EVALUATE PERSISTENCE

To determine the persistence of the vaccine strains, primers were designed to amplify target regions specific to the knockout mutant yet able to distinguish vaccine from challenge strains based on product size. Colonies obtained from fecal culture slants of HEYM were picked and placed in 30 ul of distilled water and boiled for 5 min. The lysate was briefly centrifuged (13,000 × g, 1 min) and 5 ul was removed and used as template for amplification. Forward and reverse primers (**Table 3**) were added at 25 pmol each along with EconoTaq PLUS GREEN 2X master mix (Lucigen Corp). IS900 amplification was used as a positive control for all templates. The amplification conditions varied depending on the vaccine strain tested and were 94°C for 1 min followed by 25 cycles at 94°C for 30 s, 62°C for 30 s and 72°C for 2 min followed by a hold at 72°C for 5 min.

SEROLOGIC TESTS FOR MAP

Serum collected from the goats pre- and post-vaccination and inoculation, and monthly thereafter, was evaluated by AGID and ELISA. Reagents and methods of the Johne's AGID protocol at the New York Animal Health Diagnostic Laboratory (NYAHDL) were used for AGID testing (personal communication, Susan Stehman, Cornell University, NY, USA). ELISA testing was done using a commercially-available USDA approved ELISA kit for goats (Parachek®, Biocor Animal Health, Omaha, NE, USA), according to manufacturer's recommendations.

INTRADERMAL SKIN TESTING

Standard *M. bovis* PPD (serial # 10033X), *M. avium* PPD (serial # 30-EXP-0303) and Johnin PPD (Johnin OT serial # 133–8705) were obtained from NVSL (Ames, IA, USA). One-tenth ml of each PPD was injected intradermally using standard tuberculin syringes on previously clipped skin of the cervical region. Injection sites were marked with a black marker pen for easier determination of injection site location. The kids were intradermal tested prior to vaccination, just prior to challenge, and again prior to necropsy. The cervical side was alternated between each series of PPD skin tests. The response to the PPD injections (skin thickness/induration) was measured using calipers at 72 h post-injection.

STATISTICAL ANALYSIS

Univariate analysis at each time point was conducted, to see if there were any differences between groups in the outcome measure. Because the data were sparse in some months, Fisher's Exact Test in PROC FREQ of SAS (SAS Institute, 2009) was used for categorical analyses (e.g., whether a goat tested Positive or Negative in a particular month). PROC UNIVARIATE of SAS (SAS Institute, 2009) was used to determine the mean and median

Table 3 | PCR primers used to detect survival of MAP mutant vaccine strains.

Mutant Strains	JDIP ID#	Name	Sequence (5′-3′)	Length	ORF	ORF size	POI	WT amplicon	Mutant amplicon
315/STM68	jdip005-F	MAP1566 Forward	GCTCTAGAGCTGGCATCAGGGCACTCAAGAAA	32	MAP1566	1074	1032	1179	3700 estimated
	jdip005-R	MAP1566 Reverse	CCCAAGCTTGGGTATTCGCTGCACAGCATGTCAGGT	36					
316/2E11	jdip006-F	2E11-IP-F	GCTGCAGCAACCAGCCGA	18	FadE5[1]	1836	137 bp upstream	1845	5241
	jdip006-R	2E11-IP-R	CCACCGTCACCGCAGGTAGA	20	MAP3695[1]	1074	30 bp upstream		
319/30H9	jdip009-F	MAP1566 Forward	GCTCTAGAGCTGGCATCAGGGCACTCAAGAAA	32	MAP1566	1074	272	1179	4575
	jdip009-R	MAP1566 Reverse	CCCAAGCTTGGGTATTCGCTGCACAGCATGTCAGGT	36					
318/40A940A9		AMT152	TTGCTCTTCCGCTTCTTCT (sequencing primer)	19	MAP0282c MAP0283c[2]	792 513	N/A	N/A	N/A
329/fabG2_2*	jdip019_R1	AMT 38	GTA ATA CGA CTC ACT ATA GGG CNN NNC ATG						
	jdip019_R1	AMT 858	TGC AGC AAC GCC AGG TCC ACA CT						
	jdip019_R2	AMT 39	TAA TAC GAC TCA CTA TAG GG						
	jdip019_R2	AMT 859	CTC TTG CTC TTC CGC TTC TTC TCC						

[1] *These genes are encoded in opposite directions, away from the POI.*

[2] *Transposon lost upon further replication.*

**Shin et al. (2006).*

values of numerical variables (e.g., culture CFU) in a particular month.

However, because the time points are not independent from each other, a mixed model, accounting for the correlation between months, was used [PROC MIXED in SAS (SAS Institute, 2009)] for numerical outcomes. Two sets of models were fitted, the first including all months, and the second excluding months for which the values were all 0. Month was the repeated factor, Goat ID was the subject factor, and an autoregressive covariance structure (this assumes that measurements taken closer together in time are more highly correlated than those taken further apart in time) was used. For weight and BCS (only one outcome), general linear models (PROC GLM of SAS, SAS Institute, 2009) were used. PROC GLM was also used to look at, e.g., CFU within each month. Pairwise differences between groups were studied.

PROC LIFETEST of SAS (SAS Institute, 2009) was used to generate Kaplan-Meier plots, with group as the stratification variable. Time (months) to the first Positive result was of interest. If the goat had all negative results (i.e., still tested negative at Month 15), it was censored (i.e., did not experience the event of interest). However, some groups (1 and 2) did not have any events, so "the likelihood ratio test for strata homogeneity is questionable." Therefore, this was run again, omitting Groups 1 and 2. Tests of Equality over Strata [Log-Rank, Wilcoxon, −2 Log (Likelihood Ratio)] indicated whether there were differences among the groups, with respect to time to first positive result.

Because many of the raw data values (e.g., CFU) have great variation, the natural logarithm of these values was taken, to normalize the data, and the above analyses were re-run. To overcome the large variation in absolute values, which can cause problems in parametric analysis, a non-parametric approach was used, based on ranks of the groups. Within each outcome measure and time point, the groups were ranked, from 1 = best-performing (e.g., low CFU, or low proportion of positive responses) to 8 = worst-performing (e.g., high CFU, or high proportion of positive responses). Overall ranks were then obtained for each outcome measure, over time. The analysis was done in SAS's PROC NPAR1WAY (SAS Institute, 2009). In all analyses, statistical significance was assumed at $P < 0.05$.

RESULTS

MORBIDITY AND MORTALITY NOT ATTRIBUTABLE TO JOHNE'S DISEASE

All 80 kids completed the study. Only occasional mild injuries occurred during the 13 months in our BSL-2 facility. Infestation with anthelmintic resistant *Haemonchus spp.* nematodes initially necessitated a monthly deworming schedule using a combination of Moxidectin and Albendazole orally, but after 6 months intestinal nematodes were eliminated. Sporadic mild clinical cases of intestinal coccidiosis required periodic 10 day treatments of the entire flock (all groups, challenged or non-challenged) with Amprolium (Corid®, Merial Limited, Iselin, NJ, USA) administered in drinking water tanks. A few kids within all groups had low numbers of *Monezia spp.* tapeworms in the small intestine.

CLINICAL SIGNS ATTRIBUTABLE TO JOHNE'S DISEASE

No appreciable differences were detected between any of the treatment groups throughout the study in average daily weight gain evaluated just before necropsy (data not shown). Body condition score of goats in group 1 (negative control) was higher than that in groups 3 (316 vaccinated; $P < 0.05$) and 4 (315 vaccinated; $P < 0.05$). Body condition score was higher in goats in group 7 (329 vaccinated) than in goats in groups 3 (316 vaccinated), 4 (315 vaccinated), 5 (319 vaccinated), 6 (318 vaccinated), and 8 (positive control) (*P*-values all less than 0.05) (data not shown). Distinct clinical signs attributable to JD were not observed in any challenged kids during the first 11 months post-challenge. However, in the last few weeks of the study, one kid in group 4 given the 315 vaccine and 2 kids in group 6 given the 318 vaccine began to manifest mild clinical signs including weight loss, decreased body condition scores, rough hair coat and minimal diarrhea (pasty non-pelleted feces) and had body condition scores $\leq$2 consistent with JD. None of the challenged animals in the positive control group (8) or Silirum® vaccinated group (2) manifested obvious clinical signs of JD.

EFFECTS OF VACCINE ON ANTEMORTEM VACCINATION SITE REACTION

Tissue reaction at the Silirum® vaccination site in group 2 kids was measured pre-vaccination, at 2 months, at 6 months and again at 13 months post-vaccination (data not shown). Reactions consisted of localized swelling of the subcutis and overlying skin with formation of a variable-sized firm subcutaneous nodule approximately 1–2 weeks post-vaccination that decreased in size over time, but persisted in most cases to the end of the study. Hair loss or ulceration at the injection sites were not detected. The one dimensional thickness of any subcutaneous nodule (vaccine granuloma) and overlying skin at the vaccination sites in the brisket region was measured using calipers. If a reaction was not detectable at a vaccination site by palpation, the average skin thickness of the injection site was used. Only a single Silirum® vaccinated kid (#30) developed abscessation with drainage at the injection site. The maximum size of the tissue reaction ranged between 25–30 mm and generally occurred at 1–2 weeks post-vaccination and regressed slowly over time. Vaccine tissue reactions of 7–10 mm were still present in 40% of Silirum® vaccinated kids at necropsy. Histopathology of these remaining vaccination reactions revealed a nodular granuloma comprised of granulomatous inflammation admixed with lymphocytes and plasma cells with occasional foci of necrosis surrounded by granulation tissue and fibrosis. None of the experimental vaccines were given by injection.

EFFECTS OF VACCINE ON GROSS LESIONS

Kids in challenged groups 3–8 had moderate to severe gross lesions consisting primarily of moderate to marked mesenteric and ileocecal lymph node enlargement with numerous variable-sized (1–10 mm) cortical tan foci of granulomatous inflammation. Occasional kids in these groups had mild to moderate thickening of the ileal and jejunal mucosa, but obvious corrugation was not detected. Some kids in groups 3–8 had prominent gross enlargement of lymphatics with associated lymphangitis.

Challenged kids in group 2 (Silirum® vaccinated) showed minimal to mild gross lesions consisting primarily of mild mesenteric and ileocecal lymph node enlargement with occasional small cortical 1–3 mm tan foci of granulomatous inflammation. Obvious thickening of the small intestinal mucosa in these groups was generally not evident.

EFFECTS OF VACCINE ON TISSUE MICROSCOPIC LESIONS

Tonsil and submandibular lymph nodes

Microscopic lesions consisting of variable but usually low numbers of microgranulomas (granulomas with less than approximately 30 macrophages) were detected in submandibular lymph nodes, as well as tonsil in occasional kids of the challenged groups. Only rarely were microgranulomas detected in submandibular lymph nodes or tonsil in kids given the Silirum® vaccine (group 2). No granulomatous lesions were detected in these tissues from kids within the non-challenged negative control group (group 1).

Mesenteric and ileocecal lymph nodes

The mesenteric and ileocecal lymph nodes of non-challenged control kids (group 1) often had mild to moderate lymphoid hyperplasia with mild medullary histiocytosis and scattered medullary clusters of eosinophils. Lesions in mesenteric and ileocecal lymph nodes of challenged kids varied in degree of severity but were generally similar. These lesions consisted of variable numbers of microgranulomas, scattered patchy foci of granulomatous inflammation containing occasional multinucleate Langhan's giant cells and variable numbers of acid-fast bacilli primarily within the cortex of the nodes. In more severe cases, the microgranulomas and patchy foci of granulomatous inflammation tended to coalesce to form large granulomas or sheets of granulomatous inflammation containing variable numbers of Langhan's multinucleate giant cells and more numerous acid-fast bacilli. The number of acid-fast bacilli was generally lower in lymph nodes from group 2 (Silirum® vaccinated) than in group 4 (315 vaccinated) ($P < 0.05$); and lower in groups 2 (Silirum®; $P = 0.05$), 3 (316 vaccinated; $P < 0.05$), and 7 (329 vaccinated; $P < 0.05$) than in group 8 (positive control).

Intestines

All kids in all groups (challenged and non-challenged) had varying degrees (mild to moderate) of lymphoplasmacytic, eosinophilic and globule leukocyte infiltrate within all sections of small intestine consistent with parasitic enteritis (**Figure 1A**). No non-challenged kids in any group had granulomatous lesions or acid-fast bacilli compatible with JD. The small intestinal lesions attributable to JD consisted of microgranulomas, granulomas and patchy foci of granulomatous inflammation with epithelioid macrophages, variable numbers of multinucleate Langhan's giant cells and acid-fast bacilli within the mucosa, submucosa and Peyer's patches. The intestinal lesions were most severe in the terminal jejunum, less severe in the proximal jejunum and ileum and only evident in the duodenum within occasional more severely affected kids in groups 4 (315 vaccine), 5 (319 vaccine), and 8 (positive control). Lesion scores (**Figure 2**) were lower in group 2 (Silirum® vaccine) than in group 5 (319 vaccine; $P < 0.05$). Lesion scores were lower in groups 2 (Silirum®; $P < 0.05$), 6 (318 vaccine; $P \leq 0.05$), and 7 (329 vaccine; $P \leq 0.05$) than in group 8 (positive control). Variable degrees of lymphatic dilation and associated granulomatous lymphangitis were present in these groups. Most kids in group 2 given the Silirum® vaccine had lower numbers of microgranulomas, foci of granulomatous inflammation, Langhan's giant cells and acid-fast bacilli (**Figure 1B**). In groups 4 (315 vaccine), 5 (319 vaccine), and 8 (positive control) these lesions were of greater severity and granulomatous foci often coalesced to form large sheets of epithelioid macrophages containing numerous acid-fast bacilli and less Langhan's giant cells within the mucosa, submucosa and Peyer's patches of the small intestine (**Figure 1C**) and occasional small foci of granulomatous inflammation (microgranulomas) were present in the large intestine. The 329 vaccine showed the least lesion score among all the attenuated vaccines, although it was not statistically significantly different from the other attenuated vaccines.

Other organs

The liver was the only other organ where lesions and/or acid-fast bacilli compatible with JD were detected. The liver lesions in challenged kids consisted of variable numbers of microgranulomas, rare Langhan's giant cells and rare acid-fast bacilli that were present in most kids from all challenged groups. Liver microgranulomas were more common in groups 3–8 and only rarely present in group 2 (Silirum® vaccine) kids.

EFFECTS OF VACCINE ON LESION SCORE

All kids in all challenged groups had at least subtle lesions compatible with JD suggesting none of the vaccines completely abrogated infection. Only the control vaccine appeared to show a reduction in mean lesion score at 13 months post-challenge (**Figure 2**), compared with the positive control ($P < 0.05$). The 319 vaccine showed a slightly higher (+11.9%; $P = 0.17$) lesion score than the sham-vaccinated challenged positive control group (group 8), and the 318 and 329 vaccine groups (groups 6 and 7) showed a slightly lower lesion score [−15.7% ($P < 0.05$) and −18.4% ($P < 0.05$) respectively] than group 8. Mean lesion scores from groups 3–8 did not appear statistically different from each other.

EFFECTS OF VACCINE ON FECAL SHEDDING OF MAP

The effect of vaccination on fecal shedding was determined by both fecal culture and fecal PCR. There was an initial spike of fecal shedding (**Figure 3**) at 7 months post-challenge that subsided by 8 months post-challenge, but returned by 9 months and persisted to the end of the study in most groups with the exception of group 2 (Silirum® vaccine). The Silirum® vaccine (group 2—**Figure 3**) showed a reduction in fecal CFU/g at all time points post-challenge as compared to the positive control group (8) although this reduction was not statistically significant ($P = 0.06$). The 315, 316, 318, and 329 vaccines (groups 3–6) had similar levels of fecal shedding as compared to the positive control group and the 329 vaccine (group 7) had slightly less shedding (but comparable; $P = 0.10$) than the positive control group.

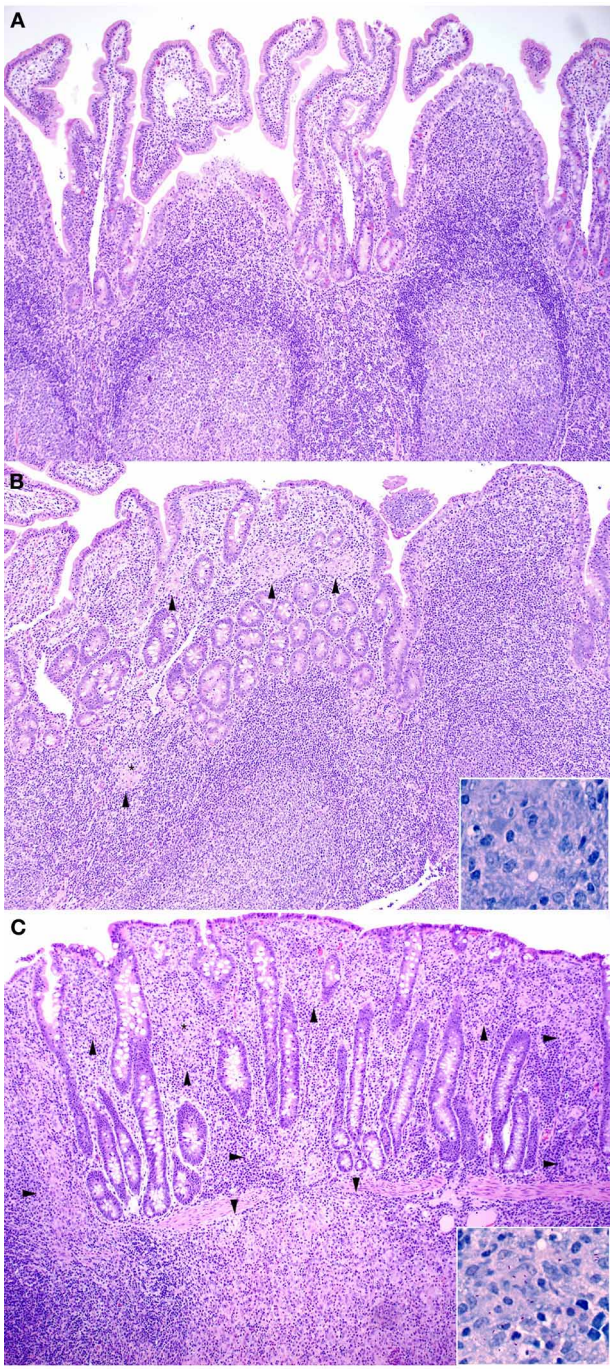

FIGURE 1 | (A–C) Note how the severity of microscopic lesions increases along with the lesion score. Arrowheads indicate foci of granulomatous inflammatory infiltrate. **(A)** Representative Hematoxylin and Eosin stained section of non-challenged Sham vaccinated control ileum sample (100X). Lesion score = 0. **(B)** Hematoxylin and Eosin stained section of Silirum® vaccinated and challenged ileum sample (100X). Inset shows Kinouyan's acid-fast stain with a single acid-fast bacillus in center from area labeled with a small star (600X). Lesion score = 3.54. **(C)** Hematoxylin and Eosin stained section of higher lesion score in a 319 vaccine (group 5) ileum sample (100X). Inset shows Kinouyan's acid-fast stain with multiple acid-fast bacilli from area labeled by a small star (600X). Lesion score = 10.42.

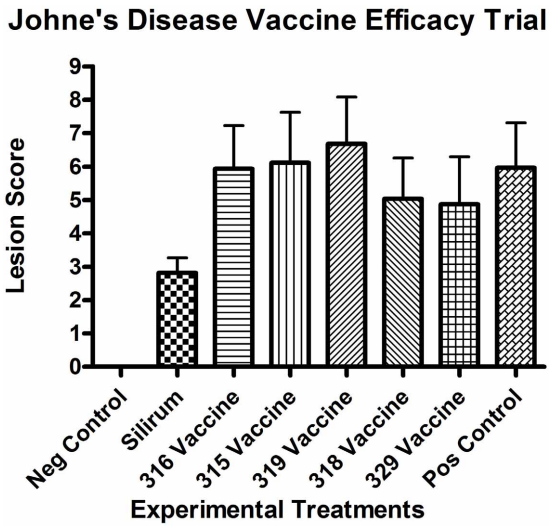

FIGURE 2 | Necropsy lesion scores for the challenged control and experimental groups at 13 months post-challenge. All negative controls (group 1, non-challenged kids) had lesion scores of 0. (Error bars represent standard error of the mean).

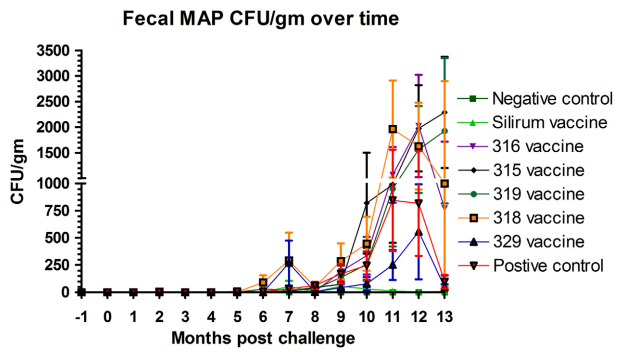

FIGURE 3 | Monthly fecal culture results on Herrold's Egg Yolk medium with and without mycobactin J throughout the study. No positive samples were detected in the non-challenged control group. (Error bars represent standard error of the mean, −1 is baseline bleeding, 0 is challenge date and 1–13 represents months post-challenge).

AgPath-ID™ MAP PCR was performed on the monthly fecal specimens obtained from all kids in the study. Both fecal PCR CT values and Positive/Negative results were obtained. **Figure 4** shows the results of fecal PCR over time represented as percent positive samples. No PCR positive samples were detected in the negative control group (group 1) throughout the study. Sporadic PCR positive samples were detected from 0 to 5 months post-challenge in several treatment groups. Beginning at 5–6 months post-challenge all challenged groups progressively increased in PCR positivity. At 9 months post-challenge the Silirum® vaccinated group percent positivity leveled off at 40–50% and remained near this level till the end of the study, while all other challenged groups continued to increase to near 100% positivity by the end of the study.

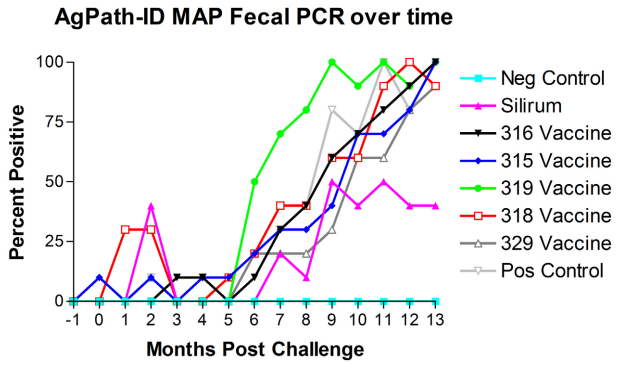

FIGURE 4 | Monthly fecal AgPath-ID™ PCR results throughout the study. No positive samples were detected in the non-challenged control group. (−1 is baseline bleeding, 0 is challenge date and 1–13 represents months post-challenge).

To determine the persistence of the vaccine strains on fecal shedding, primers were designed to amplify target regions specific to each knockout mutant vaccine yet able to distinguish vaccine from challenge strains based on product size. PCR amplifications were performed on selected colonies obtained from fecal culture of multiple goats from each group given one of the live mutant vaccines. Only the challenge strain was identified from the amplified products. The vaccine strains were not among any of the colonies suggesting that they were not persistent in the goats. For *in vitro* cultures, amplification was not successful using primers from vaccines 318 and 329 due to the instability of the corresponding mutations (Raul G. Barletta and Adel M. Talaat, unpublished results). Amplicons specific for insertions in other vaccine candidates were identified correctly.

EFFECTS ON TISSUE COLONIZATION OF MAP

In intestinal tissues, kids vaccinated with Silirum® (group 2) had dramatically lower mean numbers of MAP CFU/g than the positive control group (8) (*P*-value range 0.0013–0.1044). As shown in **Table 4**, mean MAP CFU/g cultured from each tissue individually were reduced by 10+ fold in most tissues from Silirum® vaccinated kids. Kids vaccinated with the 315 and 319 vaccines (groups 4 and 5) had in general higher (although not statistically significant) CFU/g in most tissues than those of the positive control group (group 8). In general, either no or very low MAP CFU/g were cultured from non-intestinal tissues (liver, spleen, tonsil, and submandibular lymph nodes) in all challenged groups. The highest numbers of CFU/g were cultured from intestinal tissues including mesenteric and ileocecal lymph nodes, ileum, jejunum and duodenum, but much lower numbers were cultured from spiral colon.

AgPath-ID™ MAP PCR was performed on the tissue specimens obtained from all goats at necropsy. Both tissue PCR CT values and Positive/Negative results were obtained. **Table 5** shows the tissue PCR results represented as percent positive samples. No PCR positive samples were detected in the negative control group (group 1) throughout the study. Only the Silirum® vaccinated group (group 2; $P < 0.05$) and 329 vaccinated group (group 7; $P < 0.05$) showed reductions in percent positivity as compared to the positive control group (group 8).

AGID

The results of AGID testing are shown in **Figure 5**. No non-challenged kids (group 1) became AGID positive during the study. All kids in challenged groups remained negative on the AGID test until 8 months post-challenge. The percentage of AGID positive animals in remaining challenged groups increased from 8 months to 13 months. However, no animals in group 2 (Silirum® vaccine) had become positive by the end of the study, and only 1 kid in group 7 (329 vaccine) became positive on the AGID test at 13 months post-challenge.

ELISA

Optical density measurements of the Parachek® ELISA over time are shown in **Figure 6**. Sensitivity values of the ELISA test, from 1 to 7 months, 1 to 9 months, and 1 to 15 months, for each of the six vaccines, are shown in **Table 6**; the cutoff value was set at ELISA_OD = 0.25. If the ELISA test was positive at any time point in the interval, the animal was considered to be positive. Sensitivity improved as the study progressed. Vaccination with the Silirum® vaccine (group 2) resulted in an almost immediate rise in ELISA OD values that leveled off at 3–4 months post-challenge, tended to fluctuate slightly and trend slightly lower, but persisted throughout the study. None of the sham-vaccinated non-challenged kids (group 1) developed significant OD values. ELISA OD values in the remaining groups (groups 3–8) began to rise between 4 and 6 months and continued to rise through the remainder of the study as the disease progressed. Sensitivity and specificity are usually used to assess test performance. In this study, the same test (ELISA) was used in different vaccine groups to see how it performed with different vaccines (**Table 6**). That is, the test *per se* is constant, but the vaccines (experimental treatments) are variable.

PPD SKIN TESTS

Three comparative cervical PPD skin tests including *M. avium* PPD, *M. bovis* PPD, and Johnin PPD were performed at the beginning of the study, after vaccination but prior to challenge and before necropsy (13 months post-challenge). Results of PPD skin testing over time are shown in **Figures 7A–C**. When a 2.0 mm cutoff above normal skin thickness was used for positive skin test reactions, spontaneous false-positive PPD skin test reactions were common in all groups for *M. avium*. Vaccination resulted in false-positive PPD skin test reactions for *M. avium* PPD in the Silirum®, 315, 316, and 319 vaccinated groups, and Johnin PPD in the Silirum® and 316 vaccinated groups. When a 2.0 mm cutoff above normal skin thickness was used for positive skin test reactions, false-positive reactions for *M. bovis* were detected particularly in the Silirum® vaccinated group and to a lesser extent in the 316 and 329 groups, and remained consistently negative in the three time points evaluated for vaccines 315 and 318.

Overall, there was a significant difference in ranking of treatment groups in the skin tests (combined). Goats in the 318 and 315 groups had lower skin thickness (across all tests) than did goats in the positive control group ($P = 0.0011$ and $P = 0.0037$, respectively).

Table 4 | HEYM tissue culture (CFU/gm) means and ranges, by vaccine group (rounded to nearest whole number).

Tissues	(−) control	Silirum®	316 vaccine	315 vaccine	319 vaccine	318 vaccine	329 vaccine	(+) control
Group	1	2	3	4	5	6	7	8
Liver	0	0	0	37	13	1	76	1
	(0–0)	(0–0)	(0–2)	(0–197)	(0–101)	(0–3)	(0–749)	(0–8)
Spleen	0	0	1	5	1	0	0	1
	(0–0)	(0–0)	(0–6)	(0–43)	(0–5)	(0–2)	(0–0)	(0–13)
Tonsil	0	0	1	1	0	0	0	0
	(0–0)	(0–0)	(0–3)	(0–6)	(0–2)	(0–0)	(0–2)	(0–0)
Submandibular LN	0	0	0	14	0	0	0	0
	(0–0)	(0–0)	(0–0)	(0–102)	(0–2)	(0–2)	(0–0)	(0–0)
Mesenteric LN-1	0	55	511	1095	964	651	480	772
	(0–0)	(0–477)	(0–1440)	(2–1440)	(59–1440)	(0–1440)	(0–1440)	(2–1440)
Mesenteric LN-2	0	86	616	797	926	620	653	828
	(0–0)	(0–757)	(0–1440)	(0–1440)	(30–1440)	(0–1440)	(0–1440)	(11–1440)
Ileocecal LN	0	63	412	770	980	727	536	589
	(0–0)	(0–259)	(0–1440)	(0–1440)	(13–1440)	(0–1440)	(0–1440)	(16–1440)
Ileum	0	5	240	585	564	397	175	362
	(0–0)	(0–22)	(0–1440)	(0–1440)	(0–1440)	(0–1440)	(0–1440)	(0–1440)
Jejunum-1	0	33	448	893	958	569	323	870
	(0–0)	(0–98)	(0–1440)	(2–1440)	(130–1440)	(0–1440)	(0–1440)	(19–1440)
Jejunum-2	0	87	614	1053	858	583	351	720
	(0–0)	(0–786)	(0–1440)	(0–1440)	(5–1440)	(0–1440)	(0–1440)	(53–1440)
Jejunum-3	0	7	474	883	598	804	454	619
	(0–0)	(0–19)	(0–1440)	(0–1440)	(18–1440)	(0–1440)	(0–1440)	(10–1440)
Duodenum	0	1	107	722	422	192	91	353
	(0–0)	(0–5)	(0–885)	(0–1440)	(0–1440)	(0–1440)	(0–878)	(0–1440)
Spiral colon	0	0	44	227	204	27	4	9
	(0–0)	(0–0)	(0–235)	(0–1440)	(0–1440)	(0–168)	(0–22)	(0–78)

LN, Lymph node.

Table 5 | Tissue AgPath-ID MAP PCR percent positive.

Tissues	(−) control	Silirum®	316 vaccine	315 vaccine	319 vaccine	318 vaccine	329 vaccine	(+) control
Group	1	2	3	4	5	6	7	8
Liver	0	0	90	100	60	60	30	70
Spleen	0	0	70	90	40	50	40	60
Tonsil	0	0	70	70	80	50	40	90
Submandibular LN	0	10	90	60	60	50	30	60
Mesenteric LN-1	0	70	100	70	100	100	90	100
Mesenteric LN-2	0	70	100	70	100	90	90	90
Ileocecal LN	0	60	90	80	100	90	50	100
Ileum	0	50	90	100	90	90	80	100
Jejunum-1	0	60	100	100	90	80	80	100
Jejunum-2	0	70	100	100	100	100	90	100
Jejunum-3	0	70	100	90	100	100	90	100
Duodenum	0	0	100	100	80	50	50	70
Spiral Colon	0	0	80	100	60	60	50	90

LN, Lymph node.

DISCUSSION

Development of an effective control strategy against Johne's disease in dairy herds remains an elusive goal despite the presence of commercial vaccines for cattle (Mycopar®) and small ruminants (Silirum®). With the development of molecular and genomic tools to study MAP, the causative agent of JD, we sought to take a rational approach for developing live attenuated vaccine by focusing on MAP mutants that were shown to be attenuated

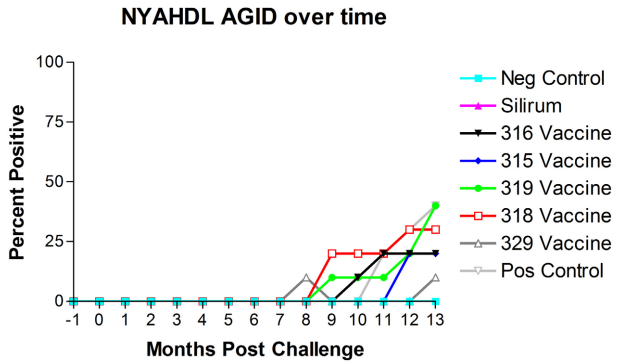

FIGURE 5 | New York Animal Health Diagnostic Laboratory (NYAHDL) AGID test results over time. The NYAHDL AGID is an agar gel immunodiffusion test for measuring serum antibody to *Mycobacterium avium* subsp. *paratuberculosis*. Note that no animals in the Silirum® vaccine group and only 1 animal in the 329 vaccine group (group 7) became AGID positive. (−1 is baseline bleeding, 0 is challenge date and 1–13 represents months post-challenge).

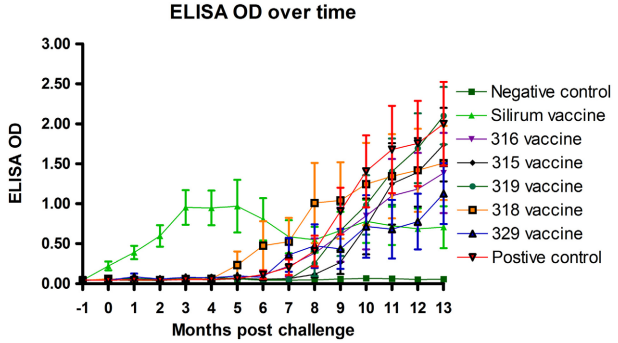

FIGURE 6 | Parachek® ELISA optical density (OD) readings over time. Note the almost immediate increase in ELISA OD for the Silirum® vaccinated group, the progressive increase in ELISA OD in most vaccine groups beginning around 5 months post-challenge and the leveling off of the Silirum® vaccinated group OD values at 9–13 months post-challenge. (Error bars represent standard error of the mean, −1 is baseline bleeding, 0 is challenge date and 1–13 represents months post-challenge).

during infection (Shin et al., 2006). Drs. Barletta and Talaat have now generated stable deletion mutants that could be tested in a second trial with the methods reported in this manuscript. However, at the time this phase of the efficacy project was started genetically stable versions of these mutants were not yet available. The primary goals of this study were to (1) to evaluate the efficacy of 5 attenuated strains of MAP as vaccine candidates compared to a commercial control, and (2) to validate the AMSC Johne's disease goat challenge model (see Hines et al., 2007b). However, another goal of our study was to develop an easy-to-administer oral vaccine against JD in comparison to the commercially available vaccines administered via subcutaneous injection.

All challenged baby goats (kids) in the study had lesions compatible with JD suggesting none of the vaccines prevented

Table 6 | Sensitivity (%) of the Parachek® ELISA, by vaccine. The cutoff value was set at ELISA_OD = 0.25.

Vaccine (group)	Months 1–7	Months 1–9	Months 1–15
Silirum® (2)	100	100	100
316 (3)	0	20	60
315 (4)	0	0	60
319 (5)	10	10	100
318 (6)	10	30	50
329 (7)	10	30	50

infection and that the goat model used in this study is highly efficient (100%) in producing active JD in challenged goats. As expected, none of the unchallenged kids had gross or microscopic lesions compatible with JD. The gross and microscopic lesions observed in this study were generally similar to those described previously (Clarke, 1997; Storset et al., 2001; Munjal et al., 2005; Hines et al., 2007a).

A key disadvantage of currently licensed vaccines is the development of skin lesions at the site of inoculation. In this study, ante-mortem vaccine site reaction was not an issue with the experimental vaccines as they were given by the oral route. However, the control vaccine used in our study produced significant tissue reaction at the injection site that persisted to the end of the study in approximately 40% of the kids in group 2. The control vaccine group (group 2, Silirum®) showed a marked reduction in fecal CFU/g at all time points post-challenge and a lesser reduction in fecal CFU/g was found with one of the experimental vaccines (vaccine 329). However, wide variation in fecal and tissue MAP CFU/g occurred both among and within groups, which reduced statistical power and probably indicates the need for evaluation of larger numbers of animals in future studies. A similar pattern was observed for the lesions scores and tissue colonization data obtained following histological and bacteriological analyses. It is noteworthy to mention here that the mean MAP CFU/g cultured from individual tissues were reduced by 10+ fold in most tissues from control vaccinated kids (group 2, Silirum®). These data also suggest that spread of MAP infection is limited beyond the intestine in the Silirum® vaccinated goats. Our findings are consistent with prior studies (Saxegaard and Fodstad, 1985; Fridriksdottir et al., 2000; Reddacliff et al., 2006; Hines et al., 2007a) that show that "whole cell" bacterins can reduce fecal shedding of MAP. However, this relationship was not evident in other studies (Wentink et al., 1994; Koets et al., 2000, 2006). It is possible that subcutaneous inoculation of the experimental mutant vaccines could provide a similar shedding pattern to that observed in the control vaccine group.

Real time PCR using the AgPath-ID™ PCR test (**Figure 4**) was able to detect the presence of MAP within feces significantly earlier than HEYM fecal culture and likely detected the 315 vaccine strain at 0 months post-challenge (prior to administration of the challenge). MAP was detected by PCR in some animals from the Silirum®, 315 and 318 vaccinated groups at 2–3 months post-challenge that is likely due to the challenge MAP strain, but in

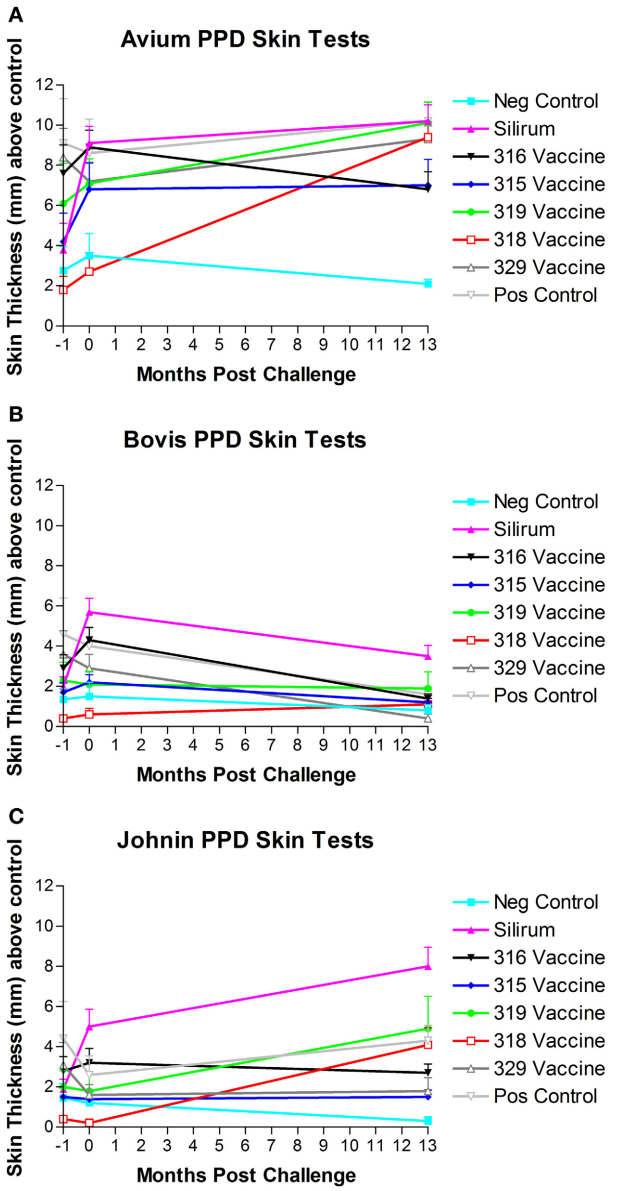

FIGURE 7 | (A–C) PPD skin test results over time. Note the strong skin responses to *M. avium* **(A)** and Johnin **(C)** PPD in multiple groups, and the generally lower responses to *M. bovis* **(B)** PPD with the exception of the Silirum® and 316 vaccines. (Error bars represent standard error of the mean, −1 is baseline bleeding, 0 is challenge date and 1–13 represents months post-challenge).

the 315 and 318 vaccinated groups the vaccine strains MAP could have still been present and contributed.

The dependence of JD control programs on diagnostic tests based on the immune responses generated after exposure/infection with MAP complicates the widespread use of JD vaccines in the field. All kids in challenged groups remained negative on the AGID test until 8 months post-challenge, none of the control vaccinated kids ever became positive on AGID and only one animal in the 329 vaccine group became positive on AGID. These findings demonstrate the limited usefulness of the AGID test as it tends to only detect the more advanced cases of JD in goats. Subcutaneous vaccination with the Silirum® vaccine (group 2, positive control vaccine) resulted in an almost immediate rise in ELISA OD values after vaccination that leveled off at 3–4 months post-challenge, tended to fluctuate slightly and trend slightly lower over time, but persisted throughout the study. None of the sham-vaccinated non-challenged kids (group 1) developed significant OD values. ELISA OD values in the remaining groups (groups 3–8, experimental vaccines and positive control group) began to rise between 5 and 8 months post-challenge and continued to rise through the remainder of the study as the disease progressed. Since all experimental mutant vaccines were administered by the oral route, this may explain why ELISA OD values in these vaccines were initially subdued and humoral immunity was delayed until 5–8 months post-challenge.

Another complication of using whole bacterin or live attenuated vaccine is the cross reactivity to skin testing for *M. bovis* infection or for even natural infection with field isolates of MAP. Our analysis indicated that spontaneous false-positive PPD skin test reactions were common in all groups for *M. avium* even prior to vaccination. This is not uncommon due to the high exposure to environmental mycobacteria within the southeastern US which complicates the interpretation of skin test and γ-interferon results. Vaccination resulted in false-positive PPD skin test reactions for *M. avium* PPD in control, Silirum®, 315, 316 and 319 vaccinated groups, and Johnin PPD in the Silirum® and 316 vaccinated groups. When a 2.0 mm cutoff above normal skin thickness was used for positive skin test reactions, false-positive reactions for *M. bovis* were detected particularly in the Silirum® vaccinated group and to a lesser extent in the 316 and 329 groups. These findings indicate that several of the vaccines and particularly the Silirum® vaccine significantly impact the results of PPD skin testing and produce false positive results with the tuberculosis (*M. bovis*) skin test that may impact tuberculosis control testing programs.

Other reports evaluating the performance of attenuated mutant MAP strains that include evaluation of live attenuated vaccines in a ruminant model are sparse within the literature. A recent report evaluated a MAP *leuD* mutant as a vaccine candidate in a goat challenge model (Faisal et al., 2013). However, the study by Faisal and coauthors did not utilize the suggested standardized challenge parameters proposed for goat challenge models by the AMSC. Their study did not include a negative non-challenged control group to prove that none of the animals were infected before or during the study, Mycopar® was used instead of Silirum® as a positive control vaccine, a non-K10-like MAP strain was used as the challenge MAP strain, and persistence of the attenuated vaccine strain was not evaluated. In our hands, not all of our vaccine constructs were stable during culturing, most likely because of their nature as transposon mutants. In future experiments, using a stable mutant constructed by allelic exchange, for example, could provide a better alternative. Therefore, direct comparison of results between these two studies is not possible due to the number of extraneous variables involved.

CONCLUSIONS

We found that (1) The AMSC proposed standard goat MAP challenge model is highly efficient in producing infection in goats and is a valid model for JD challenge and/or vaccine efficacy studies; (2) none of the control or experimental oral vaccines in this study prevented MAP infection, although administration of the 329 vaccine lowered the incidence of infection and reduced lesion scores; (3) only the control vaccine (Silirum®) showed a clear reduction in lesion score, MAP fecal shedding and tissue colonization, but it induced tissue damage in the site of inoculation that persisted in 40% of the animals; (4) based on evaluation of lesion scores, fecal shedding and tissue colonization the relative performance ranking of the vaccines evaluated in this study Silirum® was the best performer, then the 329 vaccine, 318 vaccine, 316 vaccine, 315 vaccine and the 319 vaccine was the worst performer; and (5) oral delivery may not be a viable alternative to deliver live attenuated vaccines against JD. Our results suggest that although vaccination with Silirum® does not prevent infection or eliminate MAP fecal shedding, it reduces presence of JD gross and microscopic lesions, slows progression of disease, reduces fecal shedding and reduces tissue colonization.

AUTHOR CONTRIBUTIONS

Murray E. Hines II was the principle investigator in this study who was mostly responsible for the conception, design and execution of this study. He was involved in all aspects of the project and performed most of the writing of grants and manuscripts. Sue E. Turnquist was involved in the overall project design, execution of the project, acquisition of samples/data and interpretation of necropsy data. Marcia R. S. Ilha was involved in the overall project design, execution of the project, acquisition of samples/data and evaluation of necropsy data. Sreekumari Rajeev was involved in the overall project design, execution of the project and acquisition of samples/data. Arthur L. Jones was involved with the overall project design, sample/data acquisition and assisted the project with veterinary support. Lisa Whittington was the primary person in the project responsible for sample and data acquisition. Raúl G. Barletta contributed several vaccine strains (315, 316, 318, and 319), developed the PCR detection method for the strains provided and contributed to the overall trial design and participated in manuscript writing. John P. Bannantine was involved with the overall project design and performed the PCR analysis to determine the survival of the mutant vaccine strains in this project. Yrjö T. Gröhn was the statistician for the project and was involved with the overall project design, data analysis/interpretation and manuscript writing for the project. Robab Katani and Lingling Li were involved with production and blinding of the mutant vaccine strains. Adel M. Talaat was involved in the overall project design, provided vaccine strain 329 and contributed to the manuscript writing. Vivek Kapur is the principle investigator of JDIP and was involved with the overall design of the project, blinding of the mutant vaccine strains and interpretation of the data.

ACKNOWLEDGMENTS

The authors gratefully thank the numerous employees at the Tifton Veterinary Diagnostic and Investigational Laboratory for their assistance on this research project including Kim Bridges, Alan Bryant, Randall Gay, Kristie Goins, Jill Johnson, Jason Porter, Tammie Vann, Cindy Watson, and others. The authors wish to thank Dr. Ray Sweeney for providing original aliquots of the challenge strain (ATTC-700535) in this study. This study was supported in part by US Department of Agriculture (Veterinary Services/APHIS) grant #07-9100-1136-CA, by Agriculture and Food Research Initiative competitive grant # 4453-UG-USDA-8710 from the USDA National Institute of Food and Agriculture, by a donation from Pfizer Animal Health, Inc. (Zoetis) and additional support from the Veterinary Diagnostic and Investigational Laboratory, University of Georgia, Tifton, Georgia, USA. Raúl G. Barletta also acknowledges funding from NIFA Animal Health Project NEB-39-162.

REFERENCES

Benedictus, G., Dujkhuizen, A. A., and Stelwagen, J. (1987). Economic losses due to *paratuberculosis* in dairy cattle. *Vet. Rec.* 121, 142–145. doi: 10.1136/vr.121.7.142

Clarke, C. J. (1997). The pathology and pathogenesis of *paratuberculosis* in ruminantsand other species. *J. Comp. Pathol.* 116, 217–61. doi: 10.1016/S0021-9975(97)80001-1

Faisal, S. M., Chen, J. W., Yan, F., Chen, T. T., Useh, N. M., Yan, W., et al. (2013). Evaluation of a *Mycobacterium avium* subsp. *paratuberculosis* leuD mutant as a vaccine candidate against challenge in a caprine model. *Clin. Vaccine Immunol.* 20, 572–581. doi: 10.1128/CVI.00653-12

Flynn, J. L., and Chan, J. (2001). Immunology of tuberculosis. *Annual Rev. Immunol.* 19, 93–129. doi: 10.1146/annurev.immunol.19.1.93

Fridriksdottir, V., Gunnarsson, E., Sigurdarson, S., and Gudmundsdottir, K. B. (2000). *Paratuberculosis* in Iceland: epidemiology and control measures, past and present. *Vet. Microbiol.* 77, 263–267. doi: 10.1016/S0378-1135(00)00311-4

Harris, N. B., and Barletta, R. G. (2001). *Mycobacterium avium* subsp. *Paratuberculosis* in Veterinary Medicine. *Clin. Microbiol. Rev.* 14, 489–512. doi: 10.1128/CMR.14.3.489-512.2001

Hines, M. E. 2nd., Frazier, K. S., Baldwin, C. A., Cole, J. R. Jr., and Sangster, L. T. (1998). Efficacy of vaccination for *Mycobacterium avium* with whole cell and subunit vaccines in experimentally infected swine. *Vet. Microbiol.* 63, 49–59. doi: 10.1016/S0378-1135(98)00224-7

Hines, M. E. 2nd., Stabel, J., Sweeney, R., Griffin, F., Talaat, A., Bakker, D., et al. (2007b). Experimental challenge models for Johne's disease: a review and proposed international guidelines. *Vet. Microbiol.* 122, 197–222. doi: 10.1016/j.vetmic.2007.03.009

Hines, M. E. 2nd., Stiver, S., Giri, D., Whittington, L., Watson, C., Johnson, J., et al. (2007a). Efficacy of spheroplastic and cell wall competent vaccines for *Mycobacterium avium* subsp. *paratuberculosis* in experimentally-challenged baby goats. *Vet. Microbiol.* 120, 261–283. doi: 10.1016/j.vetmic.2006.10.030

Koets, A. Hoek, A. Langelaar, M., Overdijk, M., Santema, W., Franken, P., et al. (2006). Mycobacterial 70kD heat-shock protein is an effective subunit vaccine against bovine paratuberculosis. *Vaccine* 24, 2550–2559. doi: 10.1016/j.vaccine.2005.12.019

Koets, A. P., Adugna, G., Janss, L. L., van Weering, H. J., Kalis, C. H., Wentink, G. H., et al. (2000). Genetic variation of susceptibility to *Mycobacterium avium* subsp. *paratuberculosis* infection in dairy cattle. *J. Dairy. Sci.* 83, 2702–2708. doi: 10.3168/jds.S0022-0302(00)75164-2

Lombard, J. E., Garry, F. B., McClusky, B. J., and Wagner, B. A. (2005). Risk of removal and effects on milk production associated with *paratuberculosis* status in dairy cows. *J. Am. Vet. Med. Assoc.* 12, 1975–1980. doi: 10.2460/javma.2005.227.1975

Munjal, S. K., Tripath, B. N., and Paliwal, O. P. (2005). Progressive immunopathological changes during early stages of experimental infection of goats with *Mycobacterium avium* subspecies *paratuberculosis*. *Vet. Path.* 42, 427–436. doi: 10.1354/vp.42-4-427

National Animal Health Monitoring System (NAHMS). (1997). *Johne's Disease on U.S. Dairy Operations*. USDA: APHIS: VS, CEAH, NAHMS: Fort Collins, CO.

Rajeev, S., Zhang, Y., Sreevatsan, S., Motiwala, A. S., and Byrum, B. (2005). Evaluation of multiple genomic targets for identification and confirmation of

Mycobacterium avium subsp. *paratuberculosis* isolates using real-time PCR. *Vet. Microbiol.* 105, 215–221. doi: 10.1016/j.vetmic.2004.10.018

Reddacliff, L., Eppleston, J., Windsor, P., Whittington, R., and Jones, S. (2006). Efficacy of a killed vaccine for the control of *paratuberculosis* in Australian sheep flocks. *Vet. Microbiol.* 115, 77–90. doi: 10.1016/j.vetmic.2005.12.021

Rideout, B. A., Brown, S. T., Davis, W. C., Gay, J. M., Giannella, R. A., Hines II, M. E., et al. (2003). *The Diagnosis and Control of Johne's Disease: Committee on the Diagnosis and Control of Johne's Disease. National Academy of Sciences.* Washington, DC: National Academy Press.

SAS Institute. (2009). *SAS Help and Documentation (SAS version 9.2)*. Cary, NC: SAS Institute Inc.

Saxegaard, F., and Fodstad, F. H. (1985). Control of *paratuberculosis* (Johne's disease) in goats by vaccination. *Vet. Rec.* 116, 439–441. doi: 10.1136/vr.116.16.439

Shin, S. J., Wu, C.-W., Steinberg, H., and Talaat, A. M. (2006). Identification of novel virulence determinants in *Mycobacterium paratuberculosis* by screening a library of insertional mutants. *Infect. Immun.* 7, 3825–3833. doi: 10.1128/IAI.01742-05

Stabel, J. R., and Bannantine, J. P. (2005). Development of a nested PCR method targeting a unique multicopy element, ISMap02, for detection of *Mycobacterium avium* subsp. *paratuberculosis* in fecal samples. *J. Clin. Microbiol.* 43, 4744–4750. doi: 10.1128/JCM.43.9.4744-4750.2005

Storset, A. K., Hasvold, H. J., Valheim, M., Brun-Hansen, H., Berntsen, G., Whist, S. K., et al. (2001). Subclinical *paratuberculosis* in goats following experimental infection. An immunological and microbiological study. *Vet. Immunol. Immunopathol.* 80, 271–287. doi: 10.1016/S0165-2427(01)00294-X

Stringer, L. A., Wilson, P. R., Heuer, C., and Mackintosh, C. G. (2013). A randomized controlled trial of Silirum vaccine for control of paratuberculosis in farmed red deer. *Vet. Rec.* 173:551. doi: 10.1136/vr.101799

Wentink, G. H., Bongers, J. H., Zeeuwen, A. A., and Jaartsveld, F. H. (1994). Incidence of *paratuberculosis* after vaccination against *M. paratuberculosis* in two infected dairy herds. *Zentralbl. Vet. B* 41, 517–522.

Whitlock, R. H., Wells, S. J., Sweeney, R. W., and Van Tiem, J. (2000). ELISA and fecal culture for *paratuberculosis* (Johne's disease): sensitivity and specificity of each method. *Vet. Microbiol.* 77, 387–98. doi: 10.1016/S0378-1135(00)00324-2

Conflict of Interest Statement: Pfizer Animal Health (now Zoetis) provided the Silirum® vaccine used on the vaccine control group in this study free of charge and made a donation of $10,000 to support this study. Adel M. Talaat declares his affiliation with Pan Genome Systems, Inc. Neither company was allowed to contribute to or influence the design, conduction, interpretation or evaluation of this study and the data/results from this study have not been provided to them. No patents or copyrights are involved.

Received: 04 December 2013; paper pending published: 09 January 2014; accepted: 12 February 2014; published online: 04 March 2014.

Citation: Hines ME II, Turnquist SE, Ilha MRS, Rajeev S, Jones AL, Whittington L, Bannantine JP, Barletta RG, Gröhn YT, Katani R, Talaat AM, Li L and Kapur V (2014) Evaluation of novel oral vaccine candidates and validation of a caprine model of Johne's disease. Front. Cell. Infect. Microbiol. ***4****:26. doi: 10.3389/fcimb.2014.00026*

This article was submitted to the journal Frontiers in Cellular and Infection Microbiology.

frontiers in
CELLULAR AND INFECTION MICROBIOLOGY

ORIGINAL RESEARCH ARTICLE
published: 16 July 2014
doi: 10.3389/fcimb.2014.00093

Cellular and humoral immune responses in sheep vaccinated with candidate antigens MAP2698c and MAP3567 from *Mycobacterium avium* subspecies *paratuberculosis*

Ratna B. Gurung†, Auriol C. Purdie, Richard J. Whittington* and Douglas J. Begg

Faculty of Veterinary Science, The University of Sydney, Camden, NSW, Australia

Edited by:
John Bannantine, National Animal Disease Center, USA

Reviewed by:
Paul M. Coussens, Michigan State University, USA
John Bannantine, National Animal Disease Center, USA

****Correspondence:***
Richard J. Whittington, Faculty of Veterinary Science, The University of Sydney, 425 Werombi Rd., Camden, NSW 2570, Australia
e-mail: richard.whittington@sydney.edu.au

†Present address:
Ratna B. Gurung, National Centre for Animal Health, Serbithang, Ministry of Agriculture and Forests, Serbithang, Bhutan

Control of Johne's disease, caused by *Mycobacterium avium* subspecies *paratuberculosis* (MAP) in ruminants using commercially available vaccine reduces production losses, mortality, fecal shedding and histopathological lesions but does not provide complete protection from infection and interferes with serological diagnosis of Johne's disease and bovine tuberculosis. At this time no recombinant antigens have been found to provide superior protection compared to whole killed or live-attenuated MAP vaccines. Therefore, there is a need to evaluate more candidate MAP antigens. In this study recombinant MAP antigens MAP2698c and MAP3567 were formulated with four different MONTANIDE™ (ISA 50V2, 61VG, 71VG, and 201VG) adjuvants and evaluated for their ability to produce specific immune responses in vaccinated sheep. The cellular immune response was measured with an interferon-gamma (IFN-γ) release assay and the humoral immune response was measured by antibody detection enzyme linked immunosorbent assay. Recombinant vaccine formulation with the antigen MAP2698c and MONTANIDE™ ISA 201VG adjuvant produced strong whole-MAP as well as MAP2698c-specific IFN-γ responses in a high proportion of the vaccinated sheep. The formulation caused less severe injection site lesions in comparison to other formulations. The findings from this study suggest that the MAP2698c + 201VG should be evaluated in a challenge trial to determine the efficacy of this vaccine candidate.

Keywords: adjuvant, antibody, antigen, ELISA, paratuberculosis, sheep

INTRODUCTION

Johne's disease caused by *Mycobacterium avium* subspecies *paratuberculosis* (MAP), is an economically significant disease of ruminant species particularly cattle and sheep (Ott et al., 1999; Morris et al., 2006). MAP vaccines used in livestock contain heat-killed (Gudair® 316F strain, Mycopar strain 18, ID-Lelystad and 5889 Bergey) or live modified (Neoparasec-strain 316F and OSLO-strain 316F/2E) MAP cells Rosseels and Huygen (2008). Vaccination using a currently available commercial vaccine reduces production loss, mortality, histopathological lesions (Wentink et al., 1994; Griffin et al., 2009), bacterial shedding in feces (Kormendy, 1994; Juste et al., 2009; Alonso-Hearn et al., 2012) and extends the average life of vaccinated animals but does not provide complete protection from infection (Reddacliff et al., 2006; Windsor, 2006). Furthermore, the use of killed or live-attenuated vaccine is limited mainly to sheep due to the cross reaction it produces with the immunological diagnosis of bovine tuberculosis in cattle (Stringer et al., 2011). Potential inadvertent self-injection by the handler with the commercial vaccines is also a concern due to severe injection site reactions (Windsor et al., 2005; Windsor, 2006). Recombinant MAP vaccines should have various merits over killed or attenuated vaccines in terms of antigen production and human safety. The most commonly evaluated recombinant proteins have been Hsp 70 (Koets et al., 2006), antigen 85, 74F, SOD, 35 kDa (Chen et al., 2008; Kathaperumal et al., 2008; Park et al., 2008), mpt (Heinzmann et al., 2008), 95 kDa (Bull et al., 2007), P22 (Rigden et al., 2006), 65 kDa (Velaz-Faircloth et al., 1999), and 16.8 kDa (Kadam et al., 2009). Many of the recombinant vaccines were reported to induce strong cellular as well as antibody mediated immune responses (Rigden et al., 2006; Kathaperumal et al., 2008; Roupie et al., 2008). Some of the recombinant vaccines also induced partial protection from infection (Kathaperumal et al., 2009). At this time no recombinant MAP antigens are used in commercial vaccines. Therefore, there is a need to evaluate more MAP antigens to identify potential vaccine candidates.

MAP2698c, a fatty acid dehydrogenase encoded by the *desA2* gene, is an ortholog of Rv1094 of *Mycobacterium tuberculosis* involved in mycobacterial fatty acid metabolism, which is important for maintaining a robust cell wall, intracellular survival, growth and pathogenicity (Dyer et al., 2005). MAP3567 is a surface-exposed hypothetical protein overlapped with cell wall protein (He and De Buck, 2010). Both antigens were reported to be upregulated under *in vitro* stress conditions

(Gumber and Whittington, 2009). *In silico* analysis suggested that MAP2698c and MAP3567 proteins contained relatively more T and B cell epitopes than other stress regulated MAP proteins (Gurung et al., 2012a). These proteins were found to be detected by antibodies and induced recall of cell mediated immune responses from MAP infected sheep suggesting that they are also expressed under *in vivo* conditions as they are recognized by the host immune system. Therefore, we are investigating their potential immunogenicity as vaccine antigens.

The aim of this study was to evaluate cellular immune response using interferon-gamma (IFN-γ) release assay as well as humoral immune response using antibody enzyme linked immunosorbent assay (ELISA) in sheep against the recombinant antigens MAP2698c and MAP3567, when they were administered in formulation with four mineral oil based adjuvants from the MONTANIDE ISA range.

MATERIALS AND METHODS

ANIMALS

A total of 34 Merino wethers, between 24 and 36 months of age were sourced from a flock in Armidale, New South Wales, Australia and moved to the University of Sydney farms. The source flock was monitored and tested negative for more than 3 consecutive years (MN3) under the Market Assurance Program for sheep (Animal Health Australia). Among the 34 wethers, 32 were randomly divided into eight groups of four animals for vaccination and the remaining two sheep were used as unvaccinated controls. All animal experiments in this study were carried out with approval from the University of Sydney Animal Ethics Committee. During the study the animals were managed under conventional Australian sheep farming conditions by grazing in open paddocks.

ANTIGEN AND ADJUVANT

Recombinant MAP antigens, MAP2698c and MAP3567 were cloned, expressed and purified as previously described (Gurung et al., 2012b). Four mineral oil based MONTANIDE ISA adjuvants were used for the formulation of the recombinant vaccines. The adjuvants were 50V2, 71VG, and 61VG (water in oil formulations) and 201VG (a water in oil in water formulation). Each recombinant vaccine was formulated by mixing the required antigen with the selected adjuvants to obtain a 50 μg/ml final concentration of antigen. The required volume of recombinant vaccine was prepared by mixing antigen and adjuvant at 1:1 ratio (antigen + 50V2, antigen + 201VG); 2:3 ratio (antigen + 61VG) and 3:7 ratio (antigen + 71VG) and vortexed until emulsified.

IMMUNIZATION OF ANIMALS

The sheep within the groups were vaccinated with: MAP2698c + 50V2 (group I), MAP2698c + 61VG (group II), MAP2698c + 71VG (group III), MAP2698c + 201VG (group IV), MAP3567+50V2 (group V), MAP3567+61VG (group VI), MAP3567+71VG (group VII), MAP3567+201VG (group VIII) (**Table 1**). The animals were given 1 ml of the required vaccine formulation by subcutaneous injection behind the left ear on the upper neck region. Four weeks after primary immunization, a booster was given on the right side of the neck with the same vaccine.

Table 1 | Number of animals with cellular (IFN-γ SP% > 38%) and humoral immune (antibody SP% > 70%) responses to recombinant antigen vaccine.

Group*	Vaccine formulation	Number of animals responding to vaccine			
		IFN-γ response		Antibody response	
	Antigen + adjuvant	*a*	*b*	*a*	*b*
I	MAP2698c + 50V2	1	1	0	3
II	MAP2698c + 61VG	0	2	0	2
III	MAP2698c + 71VG	0	0	0	4
IV	MAP2698c + 201VG	0	3	0	2
V	MAP3567 + 50V2	1	1	4	4
VI	MAP3567 + 61VG	2	3	4	4
VII	MAP3567 + 71VG	0	0	3	4
VIII	MAP3567 + 201VG	1	0	3	4

*a, MAP 316v specific response; b, vaccine antigen specific response; *Four animals in each group.*

BLOOD SAMPLING AND INJECTION SITE LESION MONITORING

Blood was collected by venipuncture into lithium-heparin tubes (9 ml) and a tube without anti-coagulant (8 ml) (Vacuette®) on the day of primary vaccination (pre-vaccination) and at 2 week intervals thereafter (post-vaccination) except the final bleed which had only a 1 week interval. The injection site was inspected for lesions at the time of blood sample collection. The injection site areas were palpated and if a lesion was present, its size was recorded. A Vernier caliper was used to measure one directional lesion diameter in cm.

IFN-GAMMA ASSAY

Whole blood stimulation

Heparinized blood (500 μl per well) was placed in a 48-well plate (Falcon®) and stimulated with 500 μl of antigen at a required final concentration: 10 μg/ml of French pressed whole cell MAP strain 316v (MAP 316v) antigen, 5 μg/ml of pokeweed mitogen (PWM); and 10 μg/ml of MAP2698c or MAP3567 recombinant antigen. The 316v antigen was used for MAP-specific stimulation, PWM was used as a non-specific stimulant and recombinant MAP antigens were used for antigen-specific stimulation. All antigens were diluted in culture media containing RPMI 1640, 10% v/v fetal calf serum (FCS), penicillin, streptomycin, β-mercaptoethanol, and L-glutamine (GIBCO®, Life Technologies). The negative control consisted of 500 μl of culture medium with 500 μl of blood. The plate was incubated at 37°C with 5% CO_2 for 48 h. The plasma supernatant was then harvested and stored at −20°C. All blood stimulation experiments were set up immediately after each bleed.

IFN-γ ELISA

The IFN-γ ELISA was performed as previously described (Wood et al., 1990; Begg et al., 2009). Optical density values

were normalized across plates using the following calculation: Sample-to-positive (SP) % = [(Mean sample OD) − (Mean negative control OD)]/[(Mean positive control OD) − (Mean negative control OD)] × 100.

SERUM ANTIBODY ASSAY

Serum adsorption

The serum was diluted (1:100) in a diluent (0.1% v/v FCS in PBS 0.05% v/v Tween 20) (FCS in PBST) containing 1.3 mg/ml of heat-killed *Mycobacterium phlei (M. phlei)* (Elizabeth Macarthur Agricultural Institute, New South Wales, Australia) and adsorbed overnight at 4°C with constant end-to-end shaking. The adsorbed serum was centrifuged at 2500 × *g* for 10 min at room temperature (RT) to separate the supernatant from the particulate *M. phlei*.

Serum antibody ELISA

The antibody ELISA was performed using a modified version of a previously described method (Yokomizo et al., 1983, 1985). Antigens (MAP 316v, recombinants MAP2698c and MAP3567) diluted in coating buffer (0.1 M carbonate buffer, pH 9.6) were immobilized onto flat-bottom 96-well microplates (Nunc MaxiSorp, South Australia, Australia) and incubated overnight at 4°C. The plate was machine-washed (Tecan, Aim Lab, Victoria, Australia) 5 times with wash buffer (reverse osmosis water with tween 0.05% v/v) and then blocked with 100 µl/well of a mixture of 1% v/v FCS (Gibco®, Victoria, Australia) at RT for 30 min.

The plate was machine washed 5 times as above. The adsorbed serum supernatant (50 µl) was added to the required wells and incubated for 1 h at RT. The plate was machine as above prior to the addition of horse radish peroxidase (HRP)-labeled mouse anti-sheep monoclonal conjugate (Clone GT-34, Sigma, New South Wales, Australia) (50 µl) (1:40,000) in diluent (0.1% v/v FCS in PBST), and then incubated for 1 h at RT. The plate was machine washed as above and 100 µl of 3′, 3′, 5′, 5′ tetra-methylbenzidine (TMB) substrate was added. The plate was incubated at RT for 20 min in the dark after which the chromogenic reaction was stopped by the addition of stop solution (50 µl of 2 M sulphuric acid). The optical density (OD) was measured at 450 nm using a plate reader (Multiskan Ascent, Thermo Scientific, Victoria, Australia).

All serum samples were tested after each bleed. The ELISA result is presented as sample-to-positive (SP) % = [(Mean sample OD) − (Mean negative control OD)]/[(Mean positive control OD) − (Mean negative control OD)] × 100.

STATISTICAL ANALYSIS

Significant differences in IFN-γ and antibody responses between samples collected pre-vaccination and post vaccination were analyzed by one-way ANOVA with Bonferroni corrections for multiple comparisons in each vaccine group as previously described (Burton et al., 2009) using GraphPad Prism 4.0 (GraphPad Software Inc., La Jolla, USA) ($P < 0.05$, 95% CI). Responses were also compared between vaccinated and unvaccinated controls.

RESULTS

IFN-γ RESPONSE

The cell mediated immune response to the recombinant vaccine was evaluated by measuring MAP 316v antigen as well as vaccine antigen specific IFN-γ responses. MAP 316v specific IFN-γ responses of the sheep in response to vaccination with the formulation of MAP2698c were similar between the adjuvants (**Figure 1A**). The sheep vaccinated with MAP3567 + 61VG formulation showed the highest MAP 316v specific IFN-γ responses among the different formulations (**Figure 1B**). However, great variation was observed between the groups of sheep vaccinated with MAP3567 vaccines depending on the adjuvant.

The vaccine antigen (MAP2698c) specific IFN-γ response was highest for formulations prepared from MAP2698c + 61VG and MAP2698c + 201VG (**Figure 2A**) with the response to MAP2698c + 201VG formulation at 9 weeks post-vaccination significantly higher than those pre-vaccination ($P < 0.05$). Similarly, formulations prepared from MAP3567 + 61VG induced the highest vaccine antigen specific IFN-γ responses followed by the MAP3567 + 50V2 formulation (**Figure 2B**). The IFN-γ responses from MAP3567 + 61VG formulation at 4 and

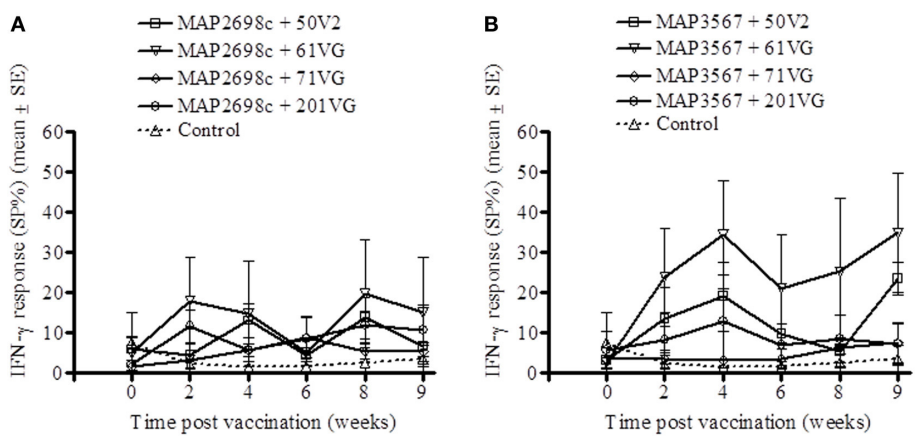

FIGURE 1 | MAP 316v specific IFN-γ responses from recombinant antigen vaccinated sheep. (A) Responses in sheep vaccinated with MAP2698c vaccine; **(B)** Responses in sheep vaccinated with MAP3567 vaccine. Data are mean ± *SE*.

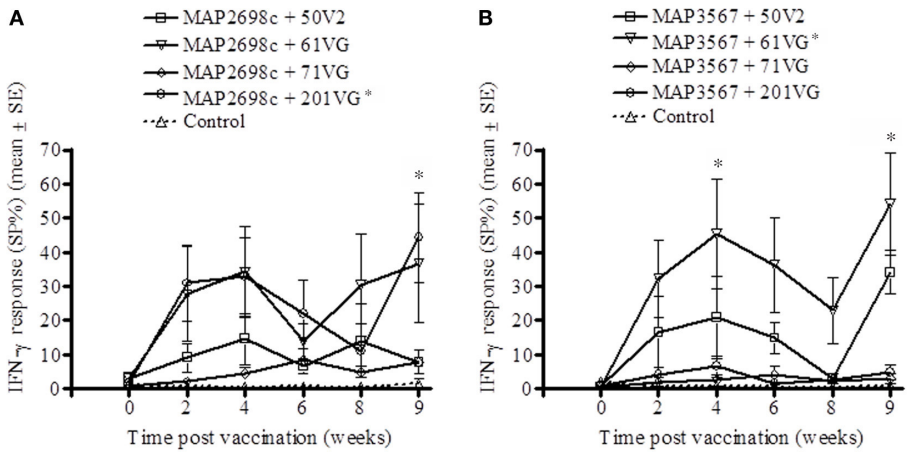

FIGURE 2 | Vaccine antigen specific IFN-γ responses of sheep vaccinated with the different formulations of recombinant antigen vaccines. (A) MAP2698c-specific IFN-γ responses from sheep vaccinated with MAP2698c + adjuvants; **(B)** MAP3567-specific IFN-γ responses from sheep vaccinated with MAP3567 + adjuvants. Data are mean ± *SE*. *Significantly higher SP% compared to pre-vaccination ($P < 0.05$).

9 weeks post-vaccination were significantly higher than those pre-vaccination ($P < 0.05$).

SERUM ANTIBODY RESPONSE

The humoral immune response to recombinant vaccine was evaluated by measuring MAP 316v and vaccine antigen specific serum antibody levels. MAP 316v antibody responses from sheep vaccinated with MAP2698c and all four adjuvant combinations were not distinguishable from those pre-vaccination or from unvaccinated controls (**Figure 3A**). The MAP 316v antibody responses from the vaccines formulated with MAP3567 and all four adjuvants showed significant responses ($P < 0.05$) which remained high until 8 weeks post primary vaccination (**Figure 3B**).

The vaccine antigen specific antibody responses were strong for MAP2698c (**Figure 4A**) as well as MAP3567 (**Figure 4B**) vaccines. The formulations of MAP2698c with the four adjuvants showed similar patterns of vaccine antigen specific antibody responses, and the response to MAP2698c + 71VG at 6 weeks post primary vaccination was significantly higher than those pre-vaccination ($P < 0.05$). In contrast, antibody responses to MAP3567 formulations were similar to those of MAP 316v specific antibody responses. The antibody responses to the formulations of MAP3567 and all four adjuvants were significantly higher than those pre-vaccination ($P < 0.05$) at all sampling time-points ($P < 0.05$).

PROPORTION OF ANIMALS RESPONDING TO VACCINATION

A recent study conducted to examine the protective level of IFN-γ response using a validated animal infection model (Begg et al., 2010) found that an 38% or greater SP of IFN-γ response was suggestive of a protective response in animals challenged with live MAP inoculum (de Silva., personal communication). A cut-point of 70% SP antibody as an indicator of humoral immune response to exposure was considered. These two thresholds (38% SP IFN-γ response and 70% SP antibody response) were used to examine the proportion of animals responding to recombinant vaccine. The number of animals with MAP 316v and vaccine antigen specific responses above these thresholds is shown in **Table 1**. Statistical analysis was not undertaken due to the small group sizes. A higher proportion of animals showed > 38% SP IFN-γ response to formulations prepared from MAP2698c + 61VG, MAP2698c + 201VG, and MAP3567 + 61VG (range: 39–90 SP%). The proportion of animals showing vaccine antigen specific IFN-γ responses was higher than that of MAP 316v specific responses. None of the animals that received MAP2698c vaccine formulations showed MAP 316v specific antibody responses > 70% SP.

INJECTION SITE LESIONS AND LESION PREVALENCE

Lesion prevalence was analyzed for each antigen/adjuvant combination. The majority of the animals (75%) developed injection site lesions i.e., lesion diameter > 0.5 cm. The animals that developed the most lesions were those vaccinated with MAP3567 + 61VG (87.5%) and MAP3567 + 201VG (54.2%) as shown in **Figure 5A**. Average lesion prevalence in animals vaccinated with MAP2698c (33%) was lower than in those vaccinated with the MAP3567 vaccines (45%).

Except for the animals vaccinated with MAP2698c + 61VG, the mean lesion size for all other adjuvant groups were smaller than 2.2 cm and decreased over the study period (**Figure 5B**). The mean lesion size for MAP2698c + 61VG was 2.35 cm and rapidly decreased over the study period. In animals that received MAP2698c + 201VG formulation, the injection site lesions had completely resolved by the end of the study period. The injection site lesion recovery in animals that received MAP3567 vaccine was similar between different formulations (**Figure 5C**). However, the lesions that developed in response to the MAP3567 vaccine were more severe in comparison to those in response to MAP2698c vaccine. The mean lesion size was greatest for the MAP3567 + 61VG group and persisted at 1.73 cm until the end of the study period. Some of these lesions resulted in wool loss and a discharging sinus at the injection sites in animals vaccinated with

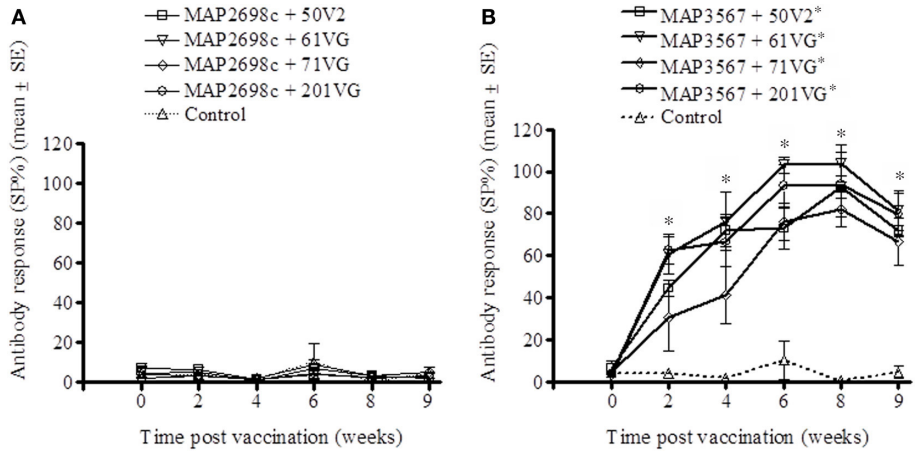

FIGURE 3 | MAP 316v antibody responses of serum from sheep vaccinated with the different formulations of recombinant antigen vaccines. (A) MAP 316v antibody responses in sheep vaccinated with MAP2698c + adjuvants; **(B)** MAP 316v antibody responses in sheep vaccinated with MAP3567 + adjuvants. Data are mean ± *SE*. *Significantly higher SP% compared to pre-vaccination ($P < 0.05$).

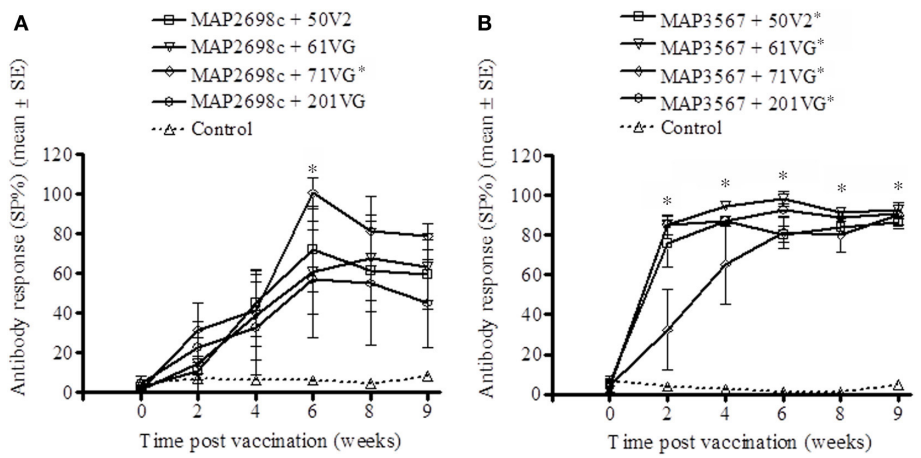

FIGURE 4 | Vaccine antigen specific antibody responses of serum from sheep vaccinated with the different formulations of recombinant antigen vaccines. (A) MAP2698c-specific antibody responses in sheep vaccinated with MAP2698c + adjuvants; **(B)** MAP3567-specific antibody responses in sheep vaccinated with MAP3567 + adjuvants. Data are mean ± *SE*. *Significantly higher SP% compared to pre-vaccination ($P < 0.05$).

MAP3567 + 61VG. A higher proportion of animals vaccinated with vaccine MAP3567 had large lesions compared to those vaccinated with MAP2698c.

DISCUSSION

The evaluation of recombinant MAP antigens as vaccine candidates in this study was focused on cell mediated and humoral immune responses in sheep following vaccination with different formulations prepared from combinations of recombinant antigens and four different adjuvants. Expression of cytokines such as IFN-γ is believed to contribute to protection against intracellular pathogens including MAP but it is not known what level of response is adequately protective (Appelberg, 1994; Appelberg et al., 1994; Stabel, 1996; Chandra et al., 2012). A recent study using a validated animal infection model has suggested that animals with an early IFN-γ response of 38% SP or greater are more likely to be protected against oral challenge with live MAP (de Silva et al., personal communication). This cut-off was used in this study to assess the proportion of sheep with an IFN-γ response. At worst it can be regarded as an arbitrary cut-off. In this study the recombinant vaccine formulations were found to induce strong IFN-γ responses, as high as 90% SP, in some vaccinated animals. The assessment of the best vaccine formulation recommneded to carry forward from this study was based on five criteria: (a) antigen specific IFN-γ response, (b) MAP 316v specific IFN-γ response, (c) adjuvant effect on IFN-γ response, (d) injection site lesions and (e) antibody response. Recombinant vaccine formulated with MAP2698c antigen and 201VG adjuvant induced stronger MAP 316v as well as recombinant antigen specific IFN-γ responses in vaccinated animals compared to the unvaccinated controls and pre-vaccination. The vaccine also produced lower lesion prevalence and severity compared to other

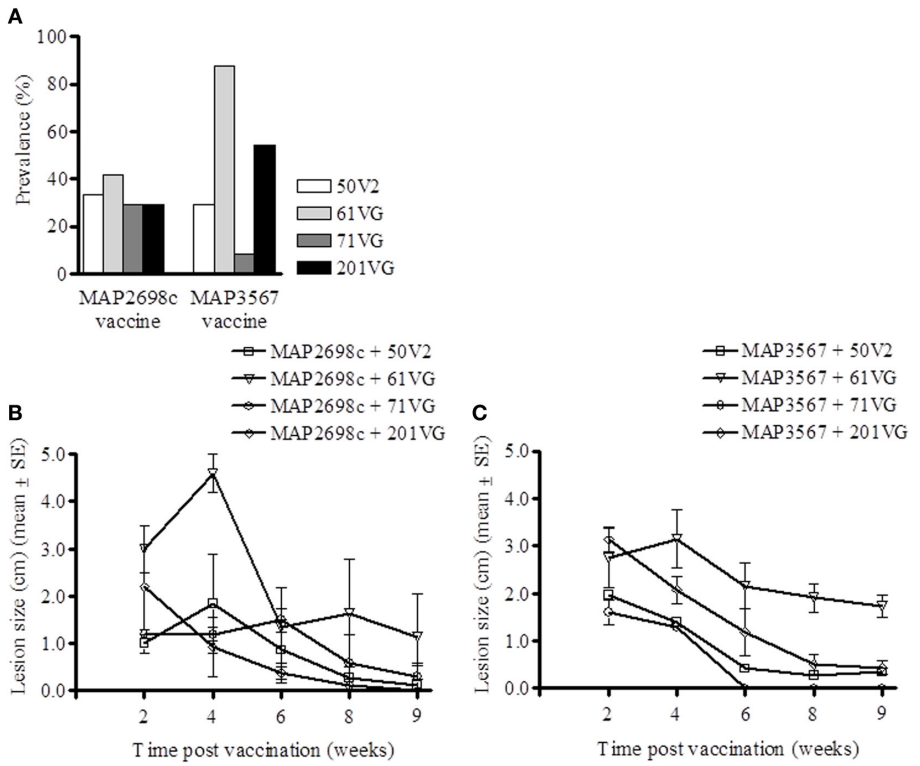

FIGURE 5 | Vaccine injection site lesion prevalence and lesion size. (A) Lesion prevalence during the study period; **(B)** Vaccine formulation (MAP2698c + adjuvants) lesion size and trend; and **(C)** Vaccine formulation (MAP3567 + adjuvants) lesion size and trend. Data are mean ± *SE*.

formulations. The antibody response was slightly lower from this formulation, and antibody is thought to play a lesser role in protection against MAP infections (Rosseels and Huygen, 2008).

Lesions at the vaccine injection site have been observed in a high proportion of animals following vaccination against paratuberculosis (Sigurdsson and Tryggvadottir, 1950; Chiodini et al., 1984; Windsor and Eppleston, 2006). Lesions are thought to be caused by the oil-based adjuvants which are non-absorbable, act as irritants and increase antigen persistence to induce sustained immune responses (Hope, 1995). In lambs that received Gudair™ vaccine, 65% of them developed injection site lesions and these lesions persisted for up to 4 years in 20% of the vaccinated animals (Eppleston and Windsor, 2007). The lesion prevalence and sizes in this study were monitored for a 9 week period following primary vaccination and were observed to be decreasing post-vaccination. The formulation MAP3567 and the adjuvant MONTANIDE™ ISA 61VG resulted in a high proportion of sheep with severe lesions. This formulation may not qualify as a vaccine candidate on animal welfare grounds due to the initial high number of large lesions and the possibility of downgrading carcass value at slaughter. These data also indicate that it is not just the adjuvants that are responsible for the injection site lesions but the combination between adjuvant and antigen. Sheep vaccinated with the MAP2698c formulation showed substantial levels of IFN-γ responses in a high proportion of vaccinated animals and low prevalence of injection site lesions. The vaccine formulated with MAP3567 showed a strong antibody response for all adjuvant groups and caused more severe lesions.

The findings from this study suggest that MAP2698c and MAP3567 antigens may have potential as candidate antigens for cell mediated and antibody mediated immune response studies, respectively. These findings are also supported by a previous study in which we reported the presence of a greater number of T cell epitopes for the MAP2698c protein and a greater number of B cell epitopes for the MAP3567 protein compared to other proteins (Gurung et al., 2012a). Antigenicity of these antigen was confirmed in clinically infected sheep Gurung et al. (2012b). Furthermore, MAP3567 is reported to be a surface-exposed protein overlapped with the cell wall proteins that may be more accessible to circulating antibodies and effect antigen-antibody binding to clear pathogens in natural infection conditions (He and De Buck, 2010). Sheep vaccinated with MAP2698c antigen were not able to produce MAP 316v specific antibodies. However, we previously reported that MAP2698c antigen is able to be used to detect specific antibodies from MAP infected sheep (Gurung et al., 2012b). These findings suggest that the MAP 316v antigen may either not contain MAP2698c protein or it is not in a form that can be recognized by the serum antibodies from MAP2698c vaccinated sheep.

Due to the likely protective immune function of IFN-γ and the relatively lower degree of lesion development at the site of vaccine injection from MAP2698c + 201VG vaccine compared to that of

other formulations, this vaccine should be evaluated further in sheep. A longitudinal study in a larger cohort of animal is required to evaluate whether it induces protective immunity against MAP infection.

ACKNOWLEDGMENTS

This work was supported by Meat and Livestock Australia and by Cattle Council of Australia, Sheepmeat Council of Australia and WoolProducers Australia through Animal Health Australia. Mrs. Anna Waldron and Ms Nicole Carter of the Farm Animal Health group provided laboratory assistance in arranging ELISA reagents. Dr Graeme Eamens, Department of Primary Industry, Elizabeth Macarthur Agricultural Institute kindly allowed access to MAP 316v antigen. Mr Craig Kristo, Mr Nobel Toribio, and James Dalton provided help in animal handling and sample collection. The authors also thank the Tall Bennett Group, NSW Australia for the gift of adjuvants and Dr Om Dhungyel for his support in preparing vaccine used in this study.

REFERENCES

Alonso-Hearn, M., Molina, E., Geijo, M., Vazquez, P., Sevilla, I. A., Garrido, J. M., et al. (2012). Immunization of adult dairy cattle with a new heat-killed vaccine is associated with longer productive life prior to cows being sent to slaughter with suspected paratuberculosis. *J. Dairy Sci.* 95, 618–629. doi: 10.3168/jds.2009-2860

Appelberg, R. (1994). Protective role of interferon gamma, tumor necrosis factor alpha and interleukin-6 in *Mycobacterium tuberculosis* and *M. avium* infections. *Immunobiology* 191, 520–525. doi: 10.1016/S0171-2985(11)80458-4

Appelberg, R., Castro, A. G., Pedrosa, J., Silva, R. A., Orme, I. M., and Minoprio, P. (1994). Role of gamma interferon and tumor necrosis factor alpha during T-cell- independent and -dependent phases of *Mycobacterium avium* infection. *Infect. Immun.* 62, 3962–3971.

Begg, D. J., de Silva, K., Bosward, K., Di Fiore, L., Taylor, D. L., Jungersen, G., et al. (2009). Enzyme-linked immunospot: an alternative method for the detection of interferon gamma in Johne's disease. *J. Vet. Diagn. Invest.* 21, 187–196. doi: 10.1177/104063870902100202

Begg, D. J., de Silva, K., Di Fiore, L., Taylor, D. L., Bower, K., Zhong, L., et al. (2010). Experimental infection model for Johne's disease using a lyophilised, pure culture, seedstock of *Mycobacterium avium* subspecies *paratuberculosis*. *Vet. Microbiol.* 141, 301–311. doi: 10.1016/j.vetmic.2009.09.007

Bull, T. J., Gilbert, S. C., Sridhar, S., Linedale, R., Dierkes, N., Sidi-Boumedine, K., et al. (2007). A novel multi-antigen virally vectored vaccine against *Mycobacterium avium* subspecies *paratuberculosis*. *PLoS ONE* 2:e1229. doi: 10.1371/journal.pone.0001229

Burton, A. B., Wagner, B., Erb, H. N., and Ainsworth, D. M. (2009). Serum interleukin-6 (IL-6) and IL-10 concentrations in normal and septic neonatal foals. *Vet. Immunol. Immunopathol.* 132, 122–128. doi: 10.1016/j.vetimm.2009.05.006

Chandra, S., Faisal, S. M., Chen, J. W., Chen, T. T., McDonough, S. P., Liu, S., et al. (2012). Immune response and protective efficacy of live attenuated Salmonella vaccine expressing antigens of *Mycobacterium avium* subsp. *paratuberculosis* against challenge in mice. *Vaccine* 31, 242–251. doi: 10.1016/j.vaccine.2012.09.024

Chen, L. H., Kathaperumal, K., Huang, C. J., McDonough, S. P., Stehman, S., Akey, B., et al. (2008). Immune responses in mice to *Mycobacterium avium* subsp. *paratuberculosis* following vaccination with a novel 74F recombinant polyprotein. *Vaccine* 26, 1253–1262. doi: 10.1016/j.vaccine.2007.12.014

Chiodini, R. J., Van Kruiningen, H. J., and Merkal, R. S. (1984). Ruminant paratuberculosis (Johne's disease): the current status and future prospects. *Cornell Vet.* 74, 218–262.

Dyer, D. H., Lyle, K. S., Rayment, I., and Fox, B. G. (2005). X-ray structure of putative acyl-ACP desaturase DesA2 from *Mycobacterium tuberculosis* H37Rv. *Protein Sci.* 14, 1508–1517. doi: 10.1110/ps.041288005

Eppleston, J., and Windsor, P. A. (2007). Lesions attributed to vaccination of sheep with Gudair for the control of ovine paratuberculosis: post farm economic impacts at slaughter. *Aust. Vet. J.* 85, 129–133. doi: 10.1111/j.0005-0423.2007.00135.x

Griffin, J. F. T., Hughes, A. D., Liggett, S., Farquhar, P. A., Mackintosh, C. G., and Bakker, D. (2009). Efficacy of novel lipid-formulated whole bacterial cell vaccines against *Mycobacterium avium* subsp. *paratuberculosis* in sheep. *Vaccine* 27, 911–918. doi: 10.1016/j.vaccine.2008.11.053

Gumber, S., and Whittington, R. J. (2009). Analysis of the growth pattern, survival and proteome of *Mycobacterium avium* subsp. *paratuberculosis* following exposure to heat. *Vet. Microbiol.* 136, 82–90. doi: 10.1016/j.vetmic.2008.10.003

Gurung, R. B., Purdie, A. C., Begg, D. J., and Whittington, R. J. (2012a). *In silico* identification of epitopes in *Mycobacterium avium* subsp. *paratuberculosis* proteins that were upregulated under stress conditions. *Clin. Vaccine Immunol.* 19, 855–864. doi: 10.1128/CVI.00114-12

Gurung, R. B., Purdie, A. C., Begg, D. J., and Whittington, R. J. (2012b). *In silico* screened *Mycobacterium avium* subsp. *paratuberculosis* (MAP) recombinant proteins upregulated under stress conditions are immunogenic in sheep. *Vet. Immunol. Immunopathol.* 149, 186–196. doi: 10.1016/j.vetimm.2012.06.026

He, Z., and De Buck, J. (2010). Localization of proteins in the cell wall of *Mycobacterium avium* subsp. *paratuberculosis* K10 by proteomic analysis. *Proteome Sci.* 8:21. doi: 10.1186/1477-5956-8-21

Heinzmann, J., Wilkens, M., Dohmann, K., and Gerlach, G. F. (2008). *Mycobacterium avium* subsp. *paratuberculosis*-specific mpt operon expressed in M. bovis BCG as vaccine candidate. *Vet. Microbiol.* 130, 330–337. doi: 10.1016/j.vetmic.2008.01.014

Hope, A. F. (1995). "Vaccination of cattle against Johne's disease in Australia," in *Final Report to Dairy Research and Development Corporation* (West Meadows, VIC).

Juste, R. A., Alonso-Hearn, M., Molina, E., Geijo, M., Vazquez, P., Sevilla, I. A., et al. (2009). Significant reduction in bacterial shedding and improvement in milk production in dairy farms after the use of a new inactivated paratuberculosis vaccine in a field trial. *BMC Res. Notes* 2:233. doi: 10.1186/1756-0500-2-233

Kadam, M., Shardul, S., Bhagath, J. L., Tiwari, V., Prasad, N., and Goswami, P. P. (2009). Coexpression of 16.8 kDa antigen of *Mycobacterium avium paratuberculosis* and murine gamma interferon in a bicistronic vector and studies on its potential as DNA vaccine. *Vet. Res. Commun.* 33, 597–610. doi: 10.1007/s11259-009-9207-6

Kathaperumal, K., Kumanan, V., McDonough, S., Chen, L. H., Park, S. U., Moreira, M. A. S., et al. (2009). Evaluation of immune responses and protective efficacy in a goat model following immunization with a coctail of recombinant antigens and a polyprotein of *Mycobacterium avium* subsp. *paratuberculosis*. *Vaccine* 27, 123–135. doi: 10.1016/j.vaccine.2008.10.019

Kathaperumal, K., Park, S. U., McDonough, S., Stehman, S., Akey, B., Huntley, J., et al. (2008). Vaccination with recombinant *Mycobacterium avium* subsp. *paratuberculosis* proteins induces differential immune responses and protects calves against infection by oral challenge. *Vaccine* 26, 1652–1663. doi: 10.1016/j.vaccine.2008.01.015

Koets, A., Hoek, A., Langelaar, M., Overdijk, M., Santema, W., Franken, P., et al. (2006). Mycobacterial 70 kD heat-shock protein is an effective subunit vaccine against bovine paratuberculosis. *Vaccine* 24, 2550–2559. doi: 10.1016/j.vaccine.2005.12.019

Kormendy, B. (1994). The effect of vaccination on the prevalence of paratuberculosis in large dairy herds. *Vet. Microbiol.* 41, 117–125. doi: 10.1016/0378-1135(94)90141-4

Morris, C. A., Hickey, S. M., and Henderson, H. V. (2006). The effect of Johne's disease on production traits in Romney, Merino and Merino x Romney-cross ewes. *N. Z. Vet. J.* 54, 204–209. doi: 10.1080/00480169.2006.36698

Ott, S. L., Wells, S. J., and Wagner, B. A. (1999). Herd-level economic losses associated with Johne's disease on US dairy operations. *Prev. Vet. Med.* 40, 179–192. doi: 10.1016/S0167-5877(99)00037-9

Park, S. U., Kathaperumal, K., McDonough, S., Akey, B., Huntley, J., Bannantine, J. P., et al. (2008). Immunization with a DNA vaccine cocktail induces a Th1 response and protects mice against *Mycobacterium avium* subsp. *paratuberculosis* challenge. *Vaccine* 26, 4329–4337. doi: 10.1016/j.vaccine.2008.06.016

Reddacliff, L., Eppleston, J., Windsor, P., Whittington, R., and Jones, S. (2006). Efficacy of a killed vaccine for the control of paratuberculosis in Australian sheep flocks. *Vet. Microbiol.* 115, 77–90. doi: 10.1016/j.vetmic.2005.12.021

Rigden, R. C., Jandhyala, D. M., Dupont, C., Crosbie-Caird, D., Lopez-Villalobos, N., Maeda, N., et al. (2006). Humoral and cellular immune responses in sheep immunized with a 22 kilodalton exported protein of *Mycobacterium avium* subspecies *paratuberculosis*. *J. Med. Microbiol.* 55, 1735–1740. doi: 10.1099/jmm.0.46785-0

Rosseels, V., and Huygen, K. (2008). Vaccination against paratuberculosis. *Expert Rev. Vaccines* 7, 817–832. doi: 10.1586/14760584.7.6.817

Roupie, V., Leroy, B., Rosseels, V., Piersoel, V., Noel-Georis, I., Romano, M., et al. (2008). Immunogenicity and protective efficacy of DNA vaccines encoding MAP0586c and MAP4308c of *Mycobacterium avium* subsp. *paratuberculosis* secretome. *Vaccine* 26, 4783–4794. doi: 10.1016/j.vaccine.2008.07.009

Sigurdsson, B., and Tryggvadottir, A. G. (1950). Immunization with heat-killed *Mycobacterium paratuberculosis* in mineral oil. *J. Bacteriol.* 59, 541–543.

Stabel, J. R. (1996). Production of γ-interferon by peripheral blood mononuclear cells: an important diagnostic tool for detection of subclinical paratuberculosis. *J. Vet. Diagn. Invest.* 8, 345–350. doi: 10.1177/104063879600800311

Stringer, L. A., Wilson, P. R., Heuer, C., Hunnam, J. C., and Mackintosh, C. G. (2011). Effect of vaccination and natural infection with *Mycobacterium avium* subsp. *paratuberculosis* on specificity of diagnostic tests for bovine tuberculosis in farmed red deer (*Cervus elaphus*). *N. Z. Vet. J.* 59, 218–224. doi: 10.1080/00480169.2011.596182

Velaz-Faircloth, M., Cobb, A. J., Horstman, A. L., Henry, S. C., and Frothingham, R. (1999). Protection against *Mycobacterium avium* by DNA vaccines expressing mycobacterial antigens as fusion proteins with green fluorescent protein. *Infect. Immun.* 67, 4243–4250.

Wentink, G. H., Bongers, J. H., Zeeuwen, A. A., and Jaartsveld, F. H. (1994). Incidence of paratuberculosis after vaccination against M. paratuberculosis in two infected dairy herds. *Zentralbl. Veterinarmed. B* 41, 517–522.

Windsor, P. (2006). Research into vaccination against ovine Johne's disease in Australia. *Small Rumin. Res.* 62, 139–142. doi: 10.1016/j.smallrumres.2005.07.044

Windsor, P. A., Bush, R., Links, I., and Eppleston, J. (2005). Injury caused by self-inoculation with a vaccine of a Freund's complete adjuvant nature (Gudair) used for control of ovine paratuberculosis. *Aust. Vet. J.* 83, 216–220. doi: 10.1111/j.1751-0813.2005.tb11654.x

Windsor, P. A., and Eppleston, J. (2006). Lesions in sheep following administration of a vaccine of a Freund's complete adjuvant nature used in the control of ovine paratuberculosis. *N. Z. Vet. J.* 54, 237–241. doi: 10.1080/00480169.2006.36704

Wood, P. R., Corner, L. A., and Plackett, P. (1990). Development of a simple, rapid *in vitro* cellular assay for bovine tuberculosis based on the production of gamma interferon. *Res. Vet. Sci.* 49, 46–49.

Yokomizo, Y., Merkal, R. S., and Lyle, P. A. (1983). Enzyme-linked immunosorbent assay for detection of bovine immunoglobulin G1 antibody to a protoplasmic antigen of *Mycobacterium paratuberculosis*. *Am. J. Vet. Res.* 44, 2205–2207.

Yokomizo, Y., Yugi, H., and Merkal, R. S. (1985). A method for avoiding false-positive reactions in an enzyme-linked immunosorbent assay (ELISA) for the diagnosis of bovine paratuberculosis. *Nihon Juigaku Zasshi* 47, 111–119. doi: 10.1292/jvms1939.47.111

Conflict of Interest Statement: This work was supported by Meat and Livestock Australia and by Cattle Council of Australia, Sheepmeat Council of Australia and WoolProducers Australia through Animal Health Australia.

Received: 15 May 2014; accepted: 24 June 2014; published online: 16 July 2014.
Citation: Gurung RB, Purdie AC, Whittington RJ and Begg DJ (2014) Cellular and humoral immune responses in sheep vaccinated with candidate antigens MAP2698c and MAP3567 from Mycobacterium avium subspecies paratuberculosis. Front. Cell. Infect. Microbiol. ***4****:93. doi: 10.3389/fcimb.2014.00093*
This article was submitted to the journal Frontiers in Cellular and Infection Microbiology.

frontiers in
CELLULAR AND INFECTION MICROBIOLOGY

ORIGINAL RESEARCH ARTICLE
published: 04 September 2014
doi: 10.3389/fcimb.2014.00120

Enhanced expression of codon optimized *Mycobacterium avium* subsp. *paratuberculosis* antigens in *Lactobacillus salivarius*

Christopher D. Johnston[1], John P. Bannantine[2], Rodney Govender[1], Lorraine Endersen[1], Daniel Pletzer[3], Helge Weingart[3], Aidan Coffey[1], Jim O'Mahony[1]* and Roy D. Sleator[1]

[1] Biological Sciences Department, Cork Institute of Technology, Cork, Ireland
[2] United States Department of Agriculture - Agricultural Research Service, National Animal Disease Center, Ames, IA, USA
[3] School of Engineering and Science, Jacobs University Bremen, Bremen, Germany

Edited by:
Adel M. Talaat, University of Wisconsin–Madison, USA

Reviewed by:
Martin S. Pavelka, University of Rochester, USA
Jan Peter Van Pijkeren, University of Wisconsin–Madison, USA

***Correspondence:**
Jim O'Mahony, Department of Biological Sciences, Cork Institute of Technology, Rossa Avenue, Bishopstown, Cork, Ireland
e-mail: jim.omahony@cit.ie

It is well documented that open reading frames containing high GC content show poor expression in A+T rich hosts. Specifically, G+C-rich codon usage is a limiting factor in heterologous expression of *Mycobacterium avium* subsp. *paratuberculosis* (MAP) proteins using *Lactobacillus salivarius*. However, re-engineering opening reading frames through synonymous substitutions can offset codon bias and greatly enhance MAP protein production in this host. In this report, we demonstrate that codon-usage manipulation of MAP2121c can enhance the heterologous expression of the major membrane protein (MMP), analogous to the form in which it is produced natively by MAP bacilli. When heterologously over-expressed, antigenic determinants were preserved in synthetic MMP proteins as shown by monoclonal antibody mediated ELISA. Moreover, MMP is a membrane protein in MAP, which is also targeted to the cellular surface of recombinant *L. salivarius* at levels comparable to MAP. Additionally, we previously engineered MAP3733c (encoding MptD) and show herein that MptD displays the tendency to associate with the cytoplasmic membrane boundary under confocal microscopy and the intracellularly accumulated protein selectively adheres to the MptD-specific bacteriophage fMptD. This work demonstrates there is potential for *L. salivarius* as a viable antigen delivery vehicle for MAP, which may provide an effective mucosal vaccine against Johne's disease.

Keywords: MAP antigens, MptD, MMP, codon optimization, expression host, *paratuberculosis*, MAP vaccine, Johne's disease

INTRODUCTION

Mycobacterium avium subsp. *paratuberculosis* (MAP) is an intracellular pathogen and the etiological agent of Johne's disease, a chronic inflammatory disorder of the gastrointestinal tract which affects multiple ruminant species including cattle (Chacon et al., 2004). Live attenuated vaccine formulations against Johne's disease do not appear to offer adequate protection against MAP infection in goats (Hines et al., 2014) and while heat-killed whole cell vaccines that are commercially available do show some efficacy, these also fail to provide full protection against MAP in models of infection (Rosseels and Huygen, 2008). Moreover, issues relating to interference with diagnostic assays for bovine tuberculosis have further hindered their widespread development and application (Buddle et al., 2010; Bastida and Juste, 2011; Coad et al., 2013). These limitations combined with the availability of complete genome sequences for MAP (Li et al., 2005; Bannantine et al., 2014) have focused recent attention on experimental subunit based vaccine strategies against MAP (Bull et al., 2007; Rosseels and Huygen, 2008). One particularly promising subunit vaccine for MAP is the 70 kDa heat shock protein termed Hsp70 (Koets et al., 2006), which activates B cells (Vrieling et al., 2013).

Lactobacillus are interesting candidates for the development of novel oral vaccine vectors due to certain strains widespread use in the food industry and GRAS (generally regarded as safe) status (Yu et al., 2013). Specific members of this genus are also an attractive alternative to using attenuated pathogens for mucosal delivery strategies because they can survive the upper gastrointestinal tract (GI) and colonize the lower GI tract (Bermudez-Humaran et al., 2011). Numerous studies have substantiated the potential of specific *Lactobacilli* strains to serve as live vaccine delivery vehicles against a broad spectrum of mucosal pathogens including *Bacillus anthracis*, *Streptococcus pneumonia, Clostridium difficile* and the Avian Influenza Virus H5N1 (Campos et al., 2008; Sleator and Hill, 2008; Mohamadzadeh et al., 2010; Wang et al., 2012). MAP is particularly well-suited to *Lactobacillus* vector delivery because it is a pathogen transmitted by ingestion of contaminated feces or milk and passes through the GI tract where it infects the intestinal mucosa (Bannantine and Bermudez, 2013).

However, despite the obvious advantages of *Lactobacillus* based mucosal immunization; encompassing the inherent ability of specific strains to survive gastric transit, adhere to the intestinal epithelium (Messaoudi et al., 2012), and stimulate both mucosal and systemic immune responses (Mohamadzadeh et al., 2009), there are known difficulties in expression of G+C rich coding sequences in the A+T rich *Lactobacillus* host (Johnston et al., 2013). Indeed, we recently determined that the significantly divergent genomic G+C content of MAP and *Lactobacillus salivarius* (69 and 33% respectively) leads to a disparity in codon usage, which significantly impedes recombinant MAP protein synthesis. To alleviate this translation inefficiency likely due to ribosomal pausing at rare codons (Buchan and Stansfield, 2007), codon optimization of a MAP gene (MAP3733c) was performed by introducing a series of synonymous mutations; modifying the coding region to better suit the codon bias of *L. salivarius*. It was shown that synthesis of a MAP specific membrane protein within *L. salivarius* could be markedly enhanced (>37-fold) owing to codon optimization, resulting in the abundance of MAP-GFP protein fusion fluorescence in recombinant cells (Johnston et al., 2013). However, that protein was never confirmed to truly represent the native protein as no monoclonal antibodies or other specific detection reagents were developed against it.

Because MAP surface proteins likely play the dominant role in the initial interactions with bovine intestinal cells (Bannantine et al., 2003; He and De Buck, 2010; Gurung et al., 2012), we here focused on two important MAP membrane proteins, MMP (MAP2121c) and the previously studied MptD (MAP3733c). MMP, encoded by MAP2121c, is a ∼33.5 kDa surface protein which shares homology to a *Mycobacterium leprae* 35-kDa major membrane protein-1 (MMP-1) (Winter et al., 1995), previously identified as a potent immunodominant antigen capable of inducing T-lymphocyte responses in paucibacillary leprosy patients (Triccas et al., 1996). MptD is a MAP specific, virulence associated membrane protein which is surface expressed during natural infection, warranting its further investigation as a prophylactic antigen (Stratmann et al., 2004; Shin et al., 2006; Cossu et al., 2011).

A significant limitation of current whole cell MAP vaccine strategies is interference with cellular immune assays and tuberculin skin tests for bovine tuberculosis (*M. bovis*), which restricts their widespread application in many countries (Kohler et al., 2001; Scandurra et al., 2010). It is notable that although MMP is not specific to MAP, with homologs existing in other mycobacterial species including *M. avium* (MAC) and *M. leprae,* previous genetic and serological evidence suggests that the protein is absent from *M. tuberculosis* and *M. bovis* (Triccas et al., 1998; Banasure et al., 2001). In addition, a DNA vaccine incorporating the *M. leprae* MMP-1 protein in isolation demonstrated significant levels of protective efficacy against *M. leprae* footpad infection in outbred Swiss Albino mice (Martin et al., 2001). As such, if an MMP-based vaccine against Johne's disease were to display strong prophylactic efficacy, as it has done against Leprosy, it leads to the exciting prospect of a vaccine formulation that could overcome issues with interference of bovine tuberculosis screening assays.

Herein, we analyzed MAP proteins recoded using synonymous substitutions and expressed in *L. salivarius*. Faithful expression and antigenicity was examined using a combination of fluorescence microscopy, monoclonal antibody- and bacteriophage-based ELISA.

MATERIALS AND METHODS

STRAINS, PLASMIDS, BACTERIOPHAGE, AND GROWTH CONDITIONS

The strains and plasmids used in this study are listed in **Table 1**. *Mycobacterium avium* subsp. *paratuberculosis* strain K-10 (ATCC BAA968) were propagated in Middlebrook 7H9 broth supplemented with OADC (BD Biosciences), 2 μg/ml of Mycobactin J and 0.2% glycerol and incubated at 37°C for 6–10 weeks. *Escherichia coli* DH5α electrocompetent cells (Invitrogen) were used as intermediate cloning hosts for all vector constructs within this study and grown at 37°C in Luria-Bertani (LB) media. *Lactobacillus salivarius* NRRL B-30514 (kindly donated by Dr. Norman Stern, USDA), was used throughout this study as the host for individual vector constructs and was grown aerobically at 37°C in MRS media (Fluka).

Plasmids pNZ9530 and pNZ8048 were originally obtained from the University College Cork culture collection, while pUC57 vectors containing codon-optimized synthetic GFP and MptDsynth genes were obtained from the Cork Institute of Technology culture collection (Johnston et al., 2013). Cultures of *E. coli* harboring individual vectors were supplemented with Erythromycin (Ery, 200 μg/ml), Chloramphenicol (Cm, 12.5 μg/ml), or Ampicillin (Amp, 200 μg/ml) for pNZ9530, pNZ8048, and pUC57 containing cells respectively. Recombinant *L. salivarius* cells were subcultured from 40% v/v glycerol stocks at −20°C and grown using antibiotic selection. *L. salivarius* (pNZ9530) cultures were supplemented with 5 μg/ml Ery, while *L. salivarius* harboring both pNZ9530 and pNZ8048 constructs were grown in the presence of 5 μg/ml Ery and 10 μg/ml Cm.

The M13 phage fMptD, originally isolated from the Ph.D.−12 phage display library (New England Biolabs), was obtained from the laboratory of Gerald F. Gerlach (University of Veterinary Medicine, Hanover, Germany). Bacteriophage fMptD was propagated using standard methods previously described (Chappel et al., 1998). Phage titers were assessed by a standard plaque assay test (Sambrook et al., 1990). Purified high titer phage solutions (10^{10} pfu/ml) were stored at 4°C until required.

NUCLEIC ACID ISOLATION

Mycobacterial DNA was prepared as described previously by Douarre et al. (2010). Plasmid DNA was isolated from *E. coli* DH5α using a plasmid extraction kit as per the manufacturer's instructions (Sigma Aldrich). Plasmid isolation from *Lactobacillus* strains was also carried out using this kit, after initial incubation (30 min at 37°C) in protoplast buffer (20 mM Tris-HCl, 5 mM EDTA, 0.75 M Sucrose, 10 mg/ml lyzozyme and 50 U/ml mutanolysin pH 7.5). Quantitative analysis was carried out using microspectrophotometry (Nanodrop, De, USA) and plasmid DNA concentration was normalized to 250 ng/μl.

Table 1 | Strains, Phage, and Plasmids used in this study.

Plasmid, phage, and strains	Relevant genotype or characteristics	Source or References
PLASMIDS		
pNZ9530	N.I.C.E system helper plasmid. Ery^r, *nisRK* cloned in pIL252, expression of *nisRK* driven by *rep* read through, low copy number	Pavan et al., 2000
pNZ8048	N.I.C.E system expression plasmid. Cm^r, carries the nisin-inducible promoter P*nisA*	Pavan et al., 2000
pNZ:MAP3733c	pNZ8048 with MptD fused to GFP gene under control of P*nisA* promoter	This work
pNZ:MAP3733synth	pNZ8048 with codon optimized MptDsynth gene under control of P*nisA* promoter	This work
pNZ:MAP3733c-GFP	pNZ8048 with MptD fused to GFP gene under control of P*nisA* promoter	Johnston et al., 2013
pNZ:MAP3733synth-GFP	pNZ8048 with codon optimized MptDsynth fused to GFP gene under control of P*nisA* promoter	Johnston et al., 2013
pNZ:MAP2121c	pNZ8048 with MMP fused to GFP gene under control of P*nisA* promoter	This work
pNZ:MAP2121synth	pNZ8048 with codon optimized MMPsynth gene under control of P*nisA* promoter	This work
pNZ:MAP2121c-GFP	pNZ8048 with MMP fused to GFP gene under control of P*nisA* promoter	This work
pNZ:MAP2121synth-GFP	pNZ8048 with codon optimized MMPsynth fused to GFP gene under control of P*nisA* promoter	This work
pNZ:GFP	pNZ8048 with *L. salivarius* codon optimized GFP gene under control of P*nisA* promoter	Johnston et al., 2013
PHAGE		
Phage fMptD	Phage isolated from the Ph.D.-12 phage display library, with a dodecapeptide sequence (GKNHHHQHHRPQ) fused to the N-terminus of its minor coat protein (pIII)	Stratmann et al., 2004
STRAINS		
Mycobacterium avium* subsp. *paratuberculosis		
MAP K-10	American bovine virulent isolate and sequencing project reference strain	Li et al., 2005
Escherichia coli		
DH5α	Intermediate cloning host	Invitrogen
Lactobacillus salivarius		
NRRL B-30514	Host strain, originally isolated from cecal contents of broiler chicken. Aerobic	Stern et al., 2006
L. salivarius pNZ9530	Host strain harboring pNZ9530 helper plasmid, Ery^r	Johnston et al., 2013
L. salivarius pNZ8048	Harbors pNZ9530 plasmid and pNZ8048 expression plasmid lacking insert. Ery^r and Cm^r	Johnston et al., 2013
L. salivarius MAP3733c	Harbors pNZ9530 and pNZ:MAP3733c plasmids. Ery^r and Cm^r	This work
L. salivarius MAP3733synth	Harbors pNZ9530 and pNZ:MAP3733synth plasmids. Ery^r and Cm^r	This work
L. salivarius MAP3733c-GFP	Harbors pNZ9530 and pNZ:MAP3733c-GFP plasmids. Ery^r and Cm^r	Johnston et al., 2013
L. salivarius MAP3733synth-GFP	Harbors pNZ9530 and pNZ:MAP3733synth-GFP plasmids. Ery^r and Cm^r	Johnston et al., 2013
L. salivarius MAP2121c	Harbors pNZ9530 and pNZ:MAP2121c plasmids. Ery^r and Cm^r	This work
L. salivarius MAP2121synth	Harbors pNZ9530 and pNZ:MAP2121synth plasmids. Ery^r and Cm^r	This work
L. salivarius MAP2121c-GFP	Harbors pNZ9530 and pNZ:MAP2121c-GFP plasmids. Ery^r and Cm^r	This work
L. salivarius MAP2121synth-GFP	Harbors pNZ9530 and pNZ:MAP2121synth-GFP plasmids. Ery^r and Cm^r	This work
L. salivarius GFP	Harbors pNZ9530 and pNZ:GFP plasmids. Ery^r and Cm^r	Johnston et al., 2013

CODON OPTIMIZATION OF MAP2121c

MAP2121c encodes a major membrane protein (MMP) in MAP. Because this protein has been implicated in the early events of infection in the bovine intestinal musoca, it is an ideal candidate for testing expression in *L. salivarius* as a potential mucosal vaccine. We have previously described a strategy for the codon optimization of the MAP3733c gene for expression in *L. salivarius* (Johnston et al., 2013). Here we used the same strategy for MAP2121c; briefly, a bioinformatics analysis was performed to identify codons from MAP2121c that could be modified at the third base position without a change in the resulting amino acid (termed a synonymous substitution). Coding sequences were synthesized by GenScript USA Inc. (Piscataway, NJ). Constructs were cloned as described below and confirmed by DNA sequencing. Final sequences for each gene are available from GenBank (Accession numbers: KC854397 and KC517484). All modifications to MAP2121c are summarized in **Table 2**.

Table 2 | Modification and codon optimization of MAP genes.

Gene	Length (bp)	G+C content	Unfavorable codons*	Modified codons	Source
MAP2121c	924	66.5%	276/307	0/307	This work
MAP2121synth	924	32.8%	7/307	279/307	This work

**Codons were deemed unfavorable due to the presence of a guanine or cytosine within the 3rd base of the triplet.*

PCR AMPLIFICATIONS AND MODIFICATIONS

PCR primers are listed in Supplementary Table S1. Primers were designed for the native and codon optimized MAP genes (MAP2121c, MAP3733c, MAP2121synth, and MAP3733synth) based on either MAP strain K-10 sequence data available from the NCBI database (NC_002944) or using the sequence from GenScript synthesized genes. All conventional PCR reactions were carried out using high fidelity Velocity DNA polymerase Kit (Bioline) in accordance with the manufacturer's instructions. Restriction enzymes and T4 DNA ligase were purchased from Roche Diagnostics (Mannheim, Germany) and New England Biolabs (Beverly, MA, USA) and used as per manufacturer's recommendations. Ligation reaction mixtures were purified using the High Pure PCR product purification kit (Roche).

MAP GENE AND FUSION CONSTRUCTS

Individual MAP gene constructs (native and synthetic) were cloned into the *E. coli-L. lactis* shuttle vector pNZ8048, a derivative of pNZ124 that allows expression of proteins under the control of the nisin-inducible promoter *PnisA*, part of the NIsin Controlled Expression (NICE) system (Pavan et al., 2000). Nisin induced expression was achieved in *L. salivarius* via co-transformation of a dual plasmid system; pNZ8048 with insert to be expressed downstream of *PnisA* and pNZ9530 providing the necessary *nisRK* regulatory genes in *trans* (de Ruyter et al., 1996).

Two native MAP genes, MAP2121c and MAP3733c (designated "c" to indicate that each is originally transcribed on the complimentary strand of the MAP K-10 genome) and two synthetic codon optimized counterparts of these, designated MAP2121synth and MAP3733synth, were initially cloned forming pNZ:2121c, pNZ:3733c, pNZ:2121synth, and pNZ:3733synth. To facilitate fluorometric analysis of each of these genes during expression and monitor subcellular localization of proteins within the host cell, a C-terminus GFP gene was translationally fused to each gene construct forming pNZ:2121c-GFP, pNZ:3733c-GFP, pNZ:2121synth-GFP, and pNZ:3733synth-GFP. The fusion of GFP and individual MAP genes was performed using Splicing by Overlap Extension (SOEing) as previously described (Johnston et al., 2013).

The GFP coding region used for fusions throughout this study was codon optimized for use within *L. salivarius*. The GFP gene sequence cloned into pNZ8048 (Johnston et al., 2013) was used to provide a comparative control for subsequent assays and designated pNZ:GFP.

TRANSFORMATION AND INDUCTION OF *L. SALIVARIUS* CONSTRUCTS

Competent *L. salivarius* (pNZ9530) were transformed individually with each of the MAP gene constructs (**Table 1**) as described previously (Johnston et al., 2013). Overnight cultures of recombinant *L. salivarius* strains were subcultured (1:100 dilution) into fresh MRS broth (Cm 8 μg/ml, Ery 3.5 μg/ml) and incubated with agitation (100 rpm) at 37°C. At an optical density (OD_{600nm}) of 0.35, nisin was added at a final concentration of 10 ng/ml and cultures were incubated statically at 37°C for 2 h. 10 ml aliquots of each culture were then harvested by centrifugation (6000 rpm for 5 min) for subsequent analysis.

FLUORESCENCE MICROSCOPY

To facilitate visualization of cells using fluorescence microscopy, induced *L. salivarius* strains (*L.sal* GFP, *L.sal* MAP2121c-GFP, *L.sal* MAP2121synth-GFP, *L.sal* MAP3733c-GFP, *L.sal* MAP3733synth-GFP) were fixed using 3.7% formaldehyde, washed with PBS (pH 7.2), subsequently resuspended in 1 ml PBS and stored at 4°C until visualized. For detection of GFP fusion peptides, *L. salivarius* cell images were taken using a Zeiss LSM 510 META laser-scanning microscope equipped with Argon and Helium-Neon lasers (Carl Zeiss, Oberkochen, Germany) at a resolution of 2048 × 2048 pixels, using LSM 5 software (version 3.2; Carl Zeiss). Equal settings were used for detection of green fluorescence among different strains (Amplifier Offset: 0.05, Amplifier Gain: 1, Gain: 820).

PREPARATION OF WHOLE CELL *L. SALIVARIUS* FOR ELISA

To determine if recombinant MMP and MMPsynth peptides were displayed on the surface of whole cell *L. salivarius*, nisin-induced strains were harvested, washed and resuspended in PBS and coated directly to the wells of a Nunc Maxisorp plate (1×10^9 cells/ml). To determine if these peptides were accumulating within the cytoplasm of *L. salivarius*, 500 μl of the harvested cells were transferred to 2 ml screw cap tubes with 0.3 g glass beads (Sigma, 150–212 μm, acid washed) and lysed (4000 rpm for 45 s) using a MagNA Lyser Instrument (Roche). Subsequently, 100 μl aliquots of crude cell lysate were added to individual wells of the same Maxisorp plate.

In the analysis of MptD proteins, similar techniques were applied for whole-cell and cell-lysate preparations, however, use of the alternative bacteriophage (fMptD) detection method necessitated the substitution of PBS for TBS in all washing and subsequent steps. MAP strain K-10, processed in the same manner, was included in all assays to provide a comparative control.

MONOCLONAL ANTIBODY BASED ELISA OF MMP

Maxisorp plates containing recombinant *L. salivarius* (pNZ, MMP, MMPsynth, MMP-GFP, and MMPsynth-GFP), as well as MAP K-10, whole cells and cell lysate were incubated at 37°C for 1 h and then blocked with a 5% (w/v) solution of dry skimmed milk powder in PBS. A 100-μl aliquot of purified monoclonal antibody 13E1 or 8G2, appropriately diluted in PBS plus 0.1% tween 20 (PBS/T) was added to each test well. Samples were incubated at 37°C for 1 h on a rocking platform. The wells were washed and 100 μl of secondary antibody (Peroxidase-labeled, Anti-Mouse IgG detection antibody) diluted in PBS/T containing 1% (w/v) milk powder was added. After a 1 h incubation at 37°C the wells were washed and 100 μl of 3,3′,5,5′-Tetramethylbenzidine Liquid Substrate System for ELISA (Sigma)

was added per well. The substrate was left to develop in the dark at room temperature for 30 min after which the reaction was stopped by addition of 50 µl of a 10% HCl solution. Absorbance readings were read at 450 nm using a microplate reader. The binding response values against each respective recombinant cell type were normalized by dividing the absorbance level obtained in test wells by that obtained in parallel control wells treated with diluent buffer without the addition of the primary monoclonal antibody.

BACTERIOPHAGE-fMptD BASED ELISA OF MptD

Due to a lack of monoclonal antibodies available for the MptD protein, the fMptD bacteriophage (Stratmann et al., 2006) was used in lieu of the primary binding antibody within MptD ELISA. Maxisorp plates containing recombinant *L. salivarius* (pNZ, MptD, MptDsynth, MptD –GFP, and MptDsynth-GFP), as well as MAP K-10, whole cells and cell lysate were incubated at 37°C for 1 h and then blocked with a 5% (w/v) solution of dry skimmed milk powder in TBS. Plates were washed with TBS/T (TBS + 0.1% [v/v] Tween-20) and 100 µl of fMptD (10^9 pfu/ml) diluted in TBS/T was added to each test well after which samples were incubated at 37°C for 1 h on a rocking platform. Individual wells were subsequently washed and 100 µl of the detection antibody, HRP Conjugated anti-M13 monoclonal antibody (GE Healthcare), diluted in TBS/T containing 1% (w/v) milk powder was added. After 1 h incubation at 37°C the wells were washed, 100 µl of TMB Liquid Substrate (Sigma) was added per well and color developed as already described.

STATISTICAL ANALYSIS

Statistical analysis was carried out using GraphPad Prism (version 4.03; GraphPad Software, San Diego, CA). Means with standard error (s.e.m.) are presented in each graph. Differences between two groups were calculated using unpaired Student's *t*-test. Differences were considered significant at $P < 0.05$.

RESULTS

DISTINCT LOCALIZATION OF MAP-GFP FUSION PEPTIDES

In our previous work we confirmed poor fluorescence for the native MptD-GFP fusion protein expressed in *L. salivarius*, and showed markedly improved expression through codon optimization of the synthetic gene (MptDsynth-GFP; **Figures 1E,F**) (Johnston et al., 2013). Here, consistent with our previous findings for MptD, induction and confocal microscopy of the native MMP-GFP fusion resulted in no fluorescence (**Figure 1C**) similar to the *L. salivarius* wild type control (**Figure 1A**). In contrast, improved levels of fluorescence were noted for codon optimized MMPsynth-GFP after induction under identical conditions as the native variant (**Figure 1D**).

While an even distribution of strong fluorescence was observed within pNZ:GFP-containing bacilli (**Figure 1B**), both engineered MAP fusion displayed different fluorescence patterns when expressed within *L. salivarius* (**Figures 1D,F**). MMPsynth-GFP was aggregated (**Figure 1D**) whereas MptD was more uniformly distributed around the periphery of the cells (**Figure 1F**).

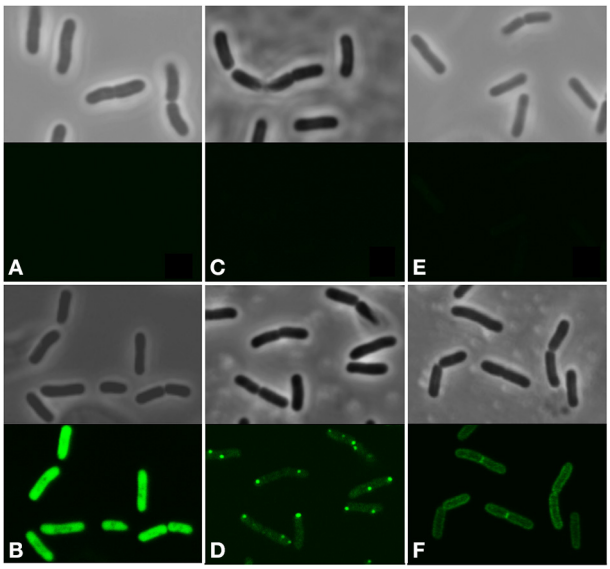

FIGURE 1 | Representative phase contrast (upper panel) and fluorescent microscopy (lower panel) images of recombinant *L. salivarius* cells. (A) Control cells pNZ:8048. **(B)** *L. salivarius* GFP cells displayed fluorescence observed throughout individual bacilli. **(C)** Negligible levels of fusion fluorescence were observed from MMP-GFP cells, **(D)** while fluorescent foci, suggestive of aggregation, were observed toward the polar regions of individual cells for the codon optimized variant MMPsynth-GFP. **(E)** Low levels of fluorescence prevented determination of the subcellular localization of native MptD-GFP fusions within *L. salivarius* cells, while **(F)** codon optimized MptDsynth-GFP fusion proteins demonstrated the tendency to localize toward the cellular membrane periphery. All culture assays were performed in triplicate, multiple images were taken from each sample and representative pictures were chosen. Bars represent 5 µm.

MptD-GFP (MAP3733c/synth)

In silico TMHMM analysis of MptD suggests the presence of six transmembrane segments (TMSs) within the 208 amino acids and a large external loop at positions 147–175, with both N and C termini being cytoplasmic associated. In cases where transmembrane proteins have their native C-terminus located in the cytoplasm, fusion of a GFP tag is particularly useful for analysis of protein localization. If the fusion is expressed at the cytoplasmic membrane the GFP peptide may fold correctly and fluoresce allowing visualization of protein localized at this membrane, however if it aggregates and forms inclusion bodies the downstream GFP might not fold correctly and therefore not fluoresce (Drew et al., 2005), although this will be largely protein dependant.

The MptDsynth-GFP fusion peptides demonstrated a tendency to localize at the periphery of individual cells (**Figure 1F**), suggestive of membrane domain insertion and conformation. This result extends our initial findings with MptD (Johnston et al., 2013).

MMP-GFP (MAP2121c/synth)

Confocal microscopy of *L. salivarius* MMP-GFP resulted in undetectable fluorescence from individual bacilli (**Figure 1C**), further supporting our previous hypothesis that native MAP

genes are poorly translated within *L. salivarius*. However, fluorescent foci were observed within the re-engineered sequence (MMPsynth-GFP) suggesting the presence of aggregated GFP fusion proteins within the cytoplasm of *L. salivarius* (**Figure 1D**). This result was not expected since MMP was predicted to be more soluble than MptD using SOLpro1.0 software (Magnan et al., 2009).

RECOMBINANT MptD ACCUMULATES WITHIN THE CYTOPLASM OF *L. SALIVARIUS*

To investigate whether the *L. salivarius* expressed MptD protein was analogous to the native MAP protein, we utilized a modified version of the fMptD bacteriophage mediated ELISA protocol outlined by Rosu et al. (2009), to probe both whole-cell and cell-lysates of recombinant *L. salivarius* transformed with both MptD-GFP gene constructs. Two constructs lacking the GFP fusion were also included to control for potential interference from the tag (**Figures 2A,B**).

Investigation of the crude cell lysates (**Figure 2A**) from recombinant *L. salivarius* revealed MptD phage binding to both native and codon optimized MptD constructs lacking a GFP fusion tag with a 2.2-fold increase in signal observed for the codon optimized variant over native ($P = 0.0008$), and 2-fold when compared to MAP K-10 ($P = 0.0007$). Interestingly, in a manner similar to MMP analysis, the addition of a GFP fusion to each of these constructs appears to have effectively inhibited phage binding, possibly by masking the MptD epitope with GFP or prevention of a conformational structure from forming.

Based on the results from confocal microscopy (**Figure 1F**), we also examined intact cells (**Figure 2B**) to determine if the tendency of MptD to localize toward the periphery of *L. salivarius* represented true surface exposure. However, despite abundant concentrations of MptD detected within the cytoplasm, no signal ($P =< 0.05$ vs. control) could be detected from unbroken cells expressing either native or re-engineered MptD in the presence or absence of a GFP tag. MptD was detected at similar levels in MAP regardless of the cell preparation (**Figures 2A,B**).

RE-ENGINEERED MMP DISPLAYS TWO DISTINCT EPITOPES

The aggregation observed during confocal microscopy of MMPsynth-GFP prompted further investigation of MMP folding within the *L. salivarius* host. To examine the possibility that the C-terminus GFP tag was itself associating with the MMP peptide, potentially leading to the fluorescent aggregates observed (**Figure 1D**): two additional constructs, *L. salivarius* with native and codon optimized MMP genes lacking a GFP fusion (pNZ:MAP2121c and pNZ:MAP2121synth), were included in the assays.

Antigenic determinants or epitopes which are recognized on a target protein by an antibody can exist in multiple forms ranging from linear, present on both native or misfolded peptides, to discontinuous or conformationally complex epitopes which are displayed through the native folding of a protein (Brown et al., 2011). In this study, ELISA analysis was performed using two monoclonal antibodies specific to the MMP protein (8G2 and 13E1), which detected two distinct epitopes (Bannantine et al., 2007).

ELISA analysis with mAb 8G2 (linear epitope)

The 8G2 antibody is reported to associate with a linear epitope present within a 77-amino acid sequence near the N-terminus

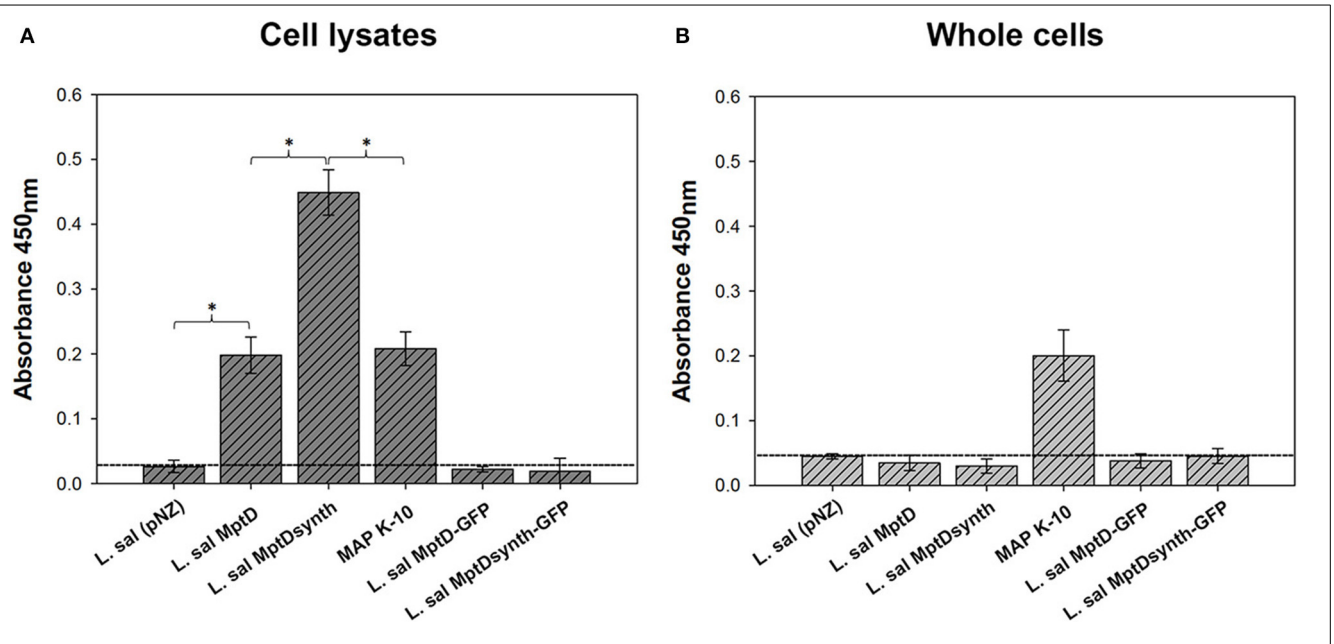

FIGURE 2 | Comparative fMptD-mediated ELISA analysis of recombinant *L. salivarius* cell lysate and whole-cell against MAP K-10 (A,B). Standard deviation of triplicate results is indicated by error bars. Statistically significant difference was observed at $*P < 0.05$. Horizontal dashed lines indicate the negative control threshold for each assay.

of MMP (Bannantine et al., 2007). ELISA analysis with 8G2 on crude cell lysates of recombinant *L. salivarius*-MMP constructs revealed that the linear epitope could be detected in all MMP constructs (**Figure 3A**), with a significant 6.4-fold signal increase noted for the engineered MMPsynth compared to native MMP.

While microscopy data indicate that heterologously expressed MMP largely accumulates in the cytosol (**Figure 1D**), intriguingly, the engineered MMP was also detected during whole-cell ELISA using the 8G2 antibody (**Figure 3B**). Although these levels were low, the signal detected was approximate to that of the MAP K-10 control strain (**Figure 3B**). Notably, as MMP expression is enhanced in *L. salivarius*, more protein is localized on the surface (**Figure 3B**).

ELISA analysis with mAb 13E1

Analysis of *L. salivarius* cellular lysates with 13E1 indicated that the epitope recognized by this mAb is blocked when MMP is fused to GFP fusions (**Figure 3C**). However, this epitope appears to be restored by removal of the GFP tag, with 4-fold higher levels of MMP detected from codon optimized MMPsynth when compared to the native gene ($P = 0.0009$), and 1.5-fold when compared to the MAP K-10 control strain ($P = 0.003$).

However, most intriguingly is that MMP protein could also be detected from whole cell *L. salivarius* MMPsynth using the 13E1 antibody, which was comparable to that in MAP K-10, albeit both were present at low levels (**Figure 3D**). While it has previously been indicated that MMP contains a 30 amino acid hydrophobic

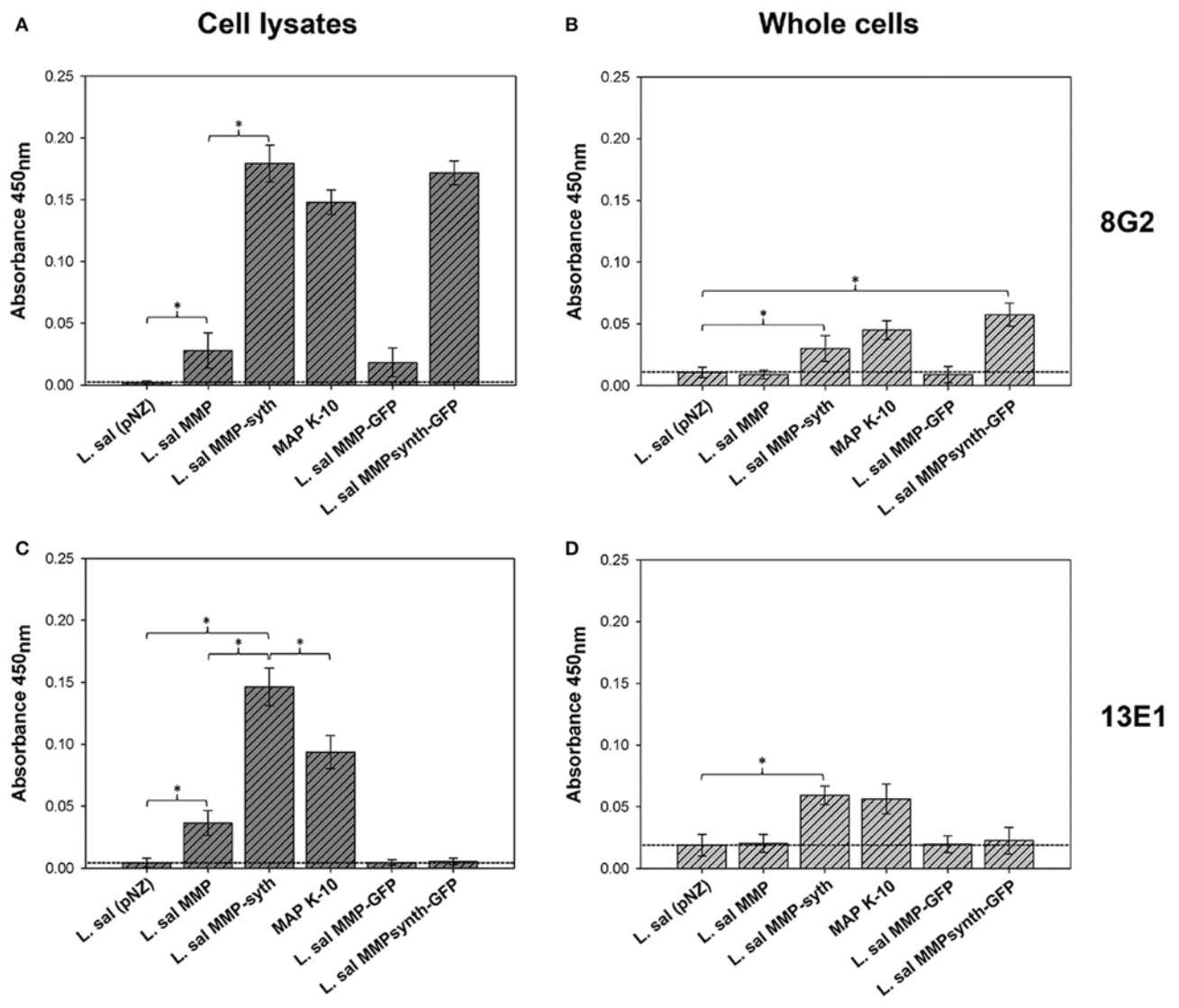

FIGURE 3 | Comparative ELISA analysis of recombinant *L. salivarius* cell-lysate and whole-cell against MAP K-10, using two monoclonal antibodies directed against MMP. The 8G2 antibody detects MMP **(A,B)**. The mAb13E1 antibody detects a discontinuous epitope on MMP (**C,D**). The average value of *L. sal* MMP-GFP and *L. sal* MMP are below the negative control threshold. Standard deviation of triplicate results is indicated by error bars. Statistically significant difference was observed at $^*P < 0.05$. Horizontal dashed lines indicate the negative control threshold for each assay.

domain near the C-terminal end suggestive of a membrane protein, the protein lacks a discernible N-terminal signal sequence (Bannantine et al., 2003). Moreover, it has already been experimentally demonstrated that MMP is both surface exposed and actively shed from live MAP bacilli (Yakes et al., 2008), suggesting that MMP is translocated in a non-classical manner similar to other mycobacterial proteins (Pallen, 2002; Bendtsen et al., 2005).

DISCUSSION

There have been several efforts at heterologous expression of MAP proteins. *E. coli* expression of an impressive collection of over 650 MAP proteins has been constructed (Bannantine et al., 2010) and these proteins have been incorporated into a protein array to monitor antibody response in different disease stages (Bannantine et al., 2008). Efforts have also been devoted to *in vitro* transcription-translation (Li et al., 2007), but those efforts did not yield much protein to work with. Interestingly MMP was a test protein in that study as well. More recently, MAP proteins have been expressed in a *Salmonella* vaccine delivery strategy (Faisal et al., 2013). Our group is the first to use the probiotic genus *Lactobacillus* as a vaccine vector for MAP. We have overcome the limitations of low expression yields through re-engineering GC-rich coding sequences. No efforts have been made to express MAP proteins in a faster growing species of *Mycobacterium* such as *M. smegmatis.*

We show that MptD, which contains six transmembrane domains, was targeted to the cell periphery, likely the cytoplasmic membrane, while MMP formed aggregates in the cytoplasm of *L. salivarius*. In general, proteins which are located within the cytoplasmic membrane must be targeted to a translocation site prior to their insertion and/or translocation (Fekkes and Driessen, 1999). However, in the case of MptD, such integral membrane proteins generally do not contain a signal sequence. Instead, their hydrophobic TMSs function as an internal signal for targeting and insertion which needs to be recognized early in the translocation pathway to prevent their aggregation in the cytoplasm (Fekkes and Driessen, 1999).

It is known that addition of any fusion tag to the N- or C-termini of a peptide can modify specific structural characteristics either by sterically interfering with protein interactions or disrupting conformational folding (Snapp, 2009). The lack of 13E1 antibody recognition formed by MMP-GFP fusion led us to propose that the fluorescent foci within *L. salivarius* MMPsynth-GFP were related to a masking effect of the MMP epitope with GFP and not representative of translational errors brought about through codon optimization. The GFP tag does not appear to impede localization of MMP at the cell surface, suggesting that this effect is steric at the C-terminus only and does not provide clues on secondary folding that might be required for localization. In originally isolating the 13E1 antibody, Bannantine and coworkers immunized mice with an N-terminal maltose-binding protein fusion with MMP (Bannantine et al., 2007). This suggests that the addition of a large (∼40 kDa) protein tag at the N- terminus does not structurally impede the epitope of MMP. However, in our study GFP was at the C-terminus and while it is possible that the GFP tag might mask the 13E1 epitope irrespective of its fused location, it is also possible that the C-terminus is more heavily involved than the N-terminal region in producing the epitope. In support of this, Li et al. (2007) expressed the MMP protein with a six-histidine tag at the C-terminus, noting that the recombinant antigen could not be detected by MAP antibodies in pooled positive serum samples from cattle shedding MAP bacilli (Li et al., 2007).

Detailed studies have demonstrated that MMP is a surface-located virulence factor involved in mediating the invasion of bovine epithelial cells and is transcriptionally upregulated in oxygen limiting and solute stress conditions similar to those encountered within the intestine (Bannantine et al., 2003; Wu et al., 2007). Based upon *in silico* analysis MMP is structurally dissimilar to MptD and analysis lacks polytopic transmembrane domains or highly hydrophobic stretches. The aggregates observed were initially considered to be indicative of translational disorder through synonymous codon modification, since MMP expression in native MAP appears throughout the bacilli by electron microscopy (Bannantine et al., 2003). Alternatively, aggregation could be a consequence of *L. salivarius* reacting to over expression by inducing vesicle formation to compensate for inefficient processing or secretion of a non-host protein. Unfortunately, the negligible fluorescence for native MMP-GFP prevented direct comparison to determine if these foci also occurred in the absence of synonymous mutations necessitating use of the monoclonal antibody based ELISA.

The detection of a non-classically exported protein, such as MMP, from the extracellular surface of *L. salivarius* could indeed be attributed to cell lysis during experimental handling. However, this would presumably have also occurred for those *L. salivarius* cells expressing recombinant MptD, yet this was not observed (**Figure 2**). Nevertheless, we acknowledge the behavior of the MMP recombinant strains may be different than the MptD recombinants and despite the lack of fMptD phage binding in whole cells, we cannot rule out cell lysis in the whole cell experiments with the MMP strains. As such, we have yet to determine the mechanism by which MMP was effectively presented in such a manner from our heterologous host strain.

Generally, there are three strategies available for the subcellular distribution of recombinant antigens from *Lactobacillus* based vaccine hosts and while cell surface display and secretion are favored, these can result in degradation of recombinant peptides due to exposure to proteolytic enzymes associated with gastric and pancreatic fluids (Kajikawa et al., 2011). Cytoplasmic expression on the other hand, subverts this and protects heterologously expressed peptides from degradation by encapsulation within the cytosol, as well as facilitating the accumulation of high concentrations of the antigenic component intracellularly (de Ruyter et al., 1996). As such, our *L. salivarius* MMPsynth host may provide an interesting combination of both high concentrations of cytoplasmically accumulated MMP, with the added advantage of superficial surface exposure.

Additionally, these results further demonstrate that heterologously expressed codon optimized MptD retains fMptD epitope presentation in *L. salivarius*. However, ELISA data also suggests that MptD, or at least the epitope recognized by the

fMptD phage, is not exposed on the surface of *L. salivarius*. It has already been shown that MptD expression on the cell surface of a recombinant host can be achieved using fMptD for both *M. smegmatis* and *M. bovis* BCG (Stratmann et al., 2004; Heinzmann et al., 2008); which could be due to the presence of mycobacterium specific chaperones facilitating appropriate presentation of the MptD protein (Goldstone et al., 2008). However, *mptD* is naturally present on a six gene operon (*mptA-F*) transcribed as a single polycistronic mRNA molecule [60] and in both the aforementioned studies, the recombinant hosts were not transformed with the *mptD* gene in isolation. The *M. smegmatis* harbored a vector including *mptC-F* genes of the mpt operon (Stratmann et al., 2004) while the *M. bovis* BCG host contained the entire operon integrated into the chromosome (Heinzmann et al., 2008). Consequently, it is possible that for effective MptD cell surface display, some ancillary Mpt proteins may also be required. The MptE protein (with five predicted TMSs) encoded by MAP3732c, located immediately downstream and overlapping the MAP3733c gene on the *mpt* operon, is a credible candidate in this respect owing to its association with the C-terminus of the MptD protein.

In future studies it may be interesting to ascertain if the sequential addition of this and other auxiliary *mpt* genes to *L. salivarius* enables native surface display of the MptD protein. Nevertheless, the lack of cell surface display may not be entirely disadvantageous in the context of a MAP antigen delivery host. The association of the MptD protein with the *L. salivarius* membrane, while incomplete, likely sequestered hydrophobic domains thus preventing undesirable aggregation and allowing higher levels of intracellular MptD to accumulate. Moreover it is clear from the analysis of cellular lysate that abundant MptD epitope could be detected within the cytoplasm, indicating that the synthetic gene and the *L. salivarius* host can effectively express and present MptD antigens.

CONCLUSION

In conclusion, we have demonstrated that the synonymous mutation of 279 rare or unfavorable codons within the MMP coding region facilitates improved protein synthesis within *L. salivarius*. Furthermore, both synthetic MMP and MptD proteins retain their epitopes or structural characteristics allowing them to effectively mimic the MAP expressed protein. Importantly, we also noted that while codon optimization enhances heterologous overexpression, the addition of a C-terminus GFP tag to both proteins may obstruct some conformational structure from forming.

Nevertheless, in the absence of a GFP tag and any extrinsic signaling peptide, both proteins displayed slight, yet noteworthy, tendencies to associate in the intended location within *L. salivarius*; MMP being detected on the cell surface, while the multi-TMSs containing protein MptD associated with the cytoplasmic membrane boundary. This work underscores the potential of *Lactobacillus salivarius* to be used within a subunit vaccine development against MAP, as additional antigens are optimized for *L. salivarius* expression, the next step will require *in-vivo* testing to demonstrate true efficacy.

FUNDING INFORMATION

The author's acknowledge the financial assistance of the Irish Government through funding under the Food Institutional Research Measure (FIRM) grant 08RDCIT617 as well as the USDA-Agricultural Research Service.

ACKNOWLEDGMENTS

The authors thank Norman Stern for providing the *Lactobacillus salivarius* NRRL B-30514 strain, Gerald F. Gerlach for providing the fMptD bacteriophage, and Alan Lucid for his assistance with bioinformatic analysis. The technical assistance of Janis K. Hansen at the USDA's National Animal Disease Center is gratefully acknowledged.

SUPPLEMENTARY MATERIAL

The Supplementary Material for this article can be found online at: http://www.frontiersin.org/journal/10.3389/fcimb.2014.00120/abstract

REFERENCES

Banasure, K. D., Basagoudanavar, S. H., Chaudhury, P., Tiwari, V., Parihar, N. S., and Goswami, P. P. (2001). Identification and characterization of a gene encoding a 35-kDa protein from *Mycobacterium avium* subspecies *paratuberculosis*. *FEMS Microbiol. Lett.* 196, 195–199. doi: 10.1111/j.1574-6968.2001.tb10564.x

Bannantine, J. P., and Bermudez, L. E. (2013). No holes barred: invasion of the intestinal mucosa by *Mycobacterium avium* subsp. *paratuberculosis*. *Infect Immun.* 81, 3960–3965. doi: 10.1128/IAI.00575-13

Bannantine, J. P., Huntley, J. F., Miltner, E., Stabel, J. R., and Bermudez, L. E. (2003). The *Mycobacterium avium* subsp. *paratuberculosis* 35 kDa protein plays a role in invasion of bovine epithelial cells. *Microbiology* 149, 2061–2069. doi: 10.1099/mic.0.26323-0

Bannantine, J. P., Li, L., Mwangi, M., Cote, R., Raygoza Garay, J. A., and Kapur, V. (2014). Complete genome sequence of *Mycobacterium avium* subsp. paratuberculosis, isolated from human breast milk. *Genome Announc.* 2:e01252-13. doi: 10.1128/genomeA.01252-13

Bannantine, J. P., Paustian, M. L., Waters, W. R., Stabel, J. R., Palmer, M. V., Li, L., et al. (2008). Profiling bovine antibody responses to *Mycobacterium avium* subsp. paratuberculosis infection by using protein arrays. *Infect Immun.* 76, 739–749. doi: 10.1128/IAI.00915-07

Bannantine, J. P., Radosevich, T. J., Stabel, J. R., Berger, S., Griffin, J. F., and Paustian, M. L. (2007). Production and characterization of monoclonal antibodies against a major membrane protein of *Mycobacterium avium* subsp. *paratuberculosis*. *Clin. Vaccine Immunol.* 14, 312–317. doi: 10.1128/CVI.00353-06

Bannantine, J. P., Stabel, J. R., Bayles, D. O., and Geisbrecht, B. V. (2010). Characteristics of an extensive *Mycobacterium avium* subspecies *paratuberculosis* recombinant protein set. *Protein Expr. Purif.* 72, 223–233. doi: 10.1016/j.pep.2010.03.019

Bastida, F., and Juste, R. A. (2011). *Paratuberculosis* control: a review with a focus on vaccination. *J. Immune Based Ther. Vaccines* 9:8. doi: 10.1186/1476-8518-9-8

Bendtsen, J. D., Kiemer, L., Fausboll, A., and Brunak, S. (2005). Non-classical protein secretion in bacteria. *BMC Microbiol.* 5:58. doi: 10.1186/1471-2180-5-58

Bermudez-Humaran, L. G., Kharrat, P., Chatel, J. M., and Langella, P. (2011). Lactococci and lactobacilli as mucosal delivery vectors for therapeutic proteins and DNA vaccines. *Microb. Cell Fact.* 10(Suppl. 1), S4. doi: 10.1186/1475-2859-10-S1-S4

Brown, M. C., Joaquim, T. R., Chambers, R., Onisk, D. V., Yin, F., Moriango, J. M., et al. (2011). Impact of immunization technology and assay application on antibody performance–a systematic comparative evaluation. *PLoS ONE* 6:e28718. doi: 10.1371/journal.pone.0028718

Buchan, J. R., and Stansfield, I. (2007). Halting a cellular production line: responses to ribosomal pausing during translation. *Biol. Cell* 99, 475–487. doi: 10.1042/BC20070037

Buddle, B. M., Wilson, T., Denis, M., Greenwald, R., Esfandiari, J., Lyashchenko, K. P., et al. (2010). Sensitivity, specificity, and confounding factors of novel serological tests used for the rapid diagnosis of bovine tuberculosis in farmed red deer (Cervus elaphus). *Clin. Vaccine Immunol.* 17, 626–630. doi: 10.1128/CVI.00010-10

Bull, T. J., Gilbert, S. C., Sridhar, S., Linedale, R., Dierkes, N., Sidi-Boumedine, K., et al. (2007). A novel multi-antigen virally vectored vaccine against *Mycobacterium avium* subspecies *paratuberculosis*. *PLoS ONE* 2:e1229. doi: 10.1371/journal.pone.0001229

Campos, I. B., Darrieux, M., Ferreira, D. M., Miyaji, E. N., Silva, D. A., Areas, A. P., et al. (2008). Nasal immunization of mice with *Lactobacillus casei* expressing the Pneumococcal Surface Protein A: induction of antibodies, complement deposition and partial protection against *Streptococcus pneumoniae* challenge. *Microbes Infect.* 10, 481–488. doi: 10.1016/j.micinf.2008.01.007

Chacon, O., Bermudez, L. E., and Barletta, R. G. (2004). Johne's disease, inflammatory bowel disease, and *Mycobacterium paratuberculosis*. *Annu. Rev. Microbiol.* 58, 329–363. doi: 10.1146/annurev.micro.58.030603.123726

Chappel, J. A., He, M., and Kang, A. S. (1998). Modulation of antibody display on M13 filamentous phage. *J. Immunol. Methods* 221, 25–34. doi: 10.1016/S0022-1759(98)00094-5

Coad, M., Clifford, D. J., Vordermeier, H. M., and Whelan, A. O. (2013). The consequences of vaccination with the Johne's disease vaccine, Gudair, on diagnosis of bovine tuberculosis. *Vet. Rec.* 172, 266. doi: 10.1136/vr.101201

Cossu, A., Rosu, V., Paccagnini, D., Cossu, D., Pacifico, A., and Sechi, L. A. (2011). MAP3738c and MptD are specific tags of *Mycobacterium avium* subsp. paratuberculosis infection in type I diabetes mellitus. *Clin. Immunol.* 141, 49–57. doi: 10.1016/j.clim.2011.05.002

de Ruyter, P. G., Kuipers, O. P., and De Vos, W. M. (1996). Controlled gene expression systems for *Lactococcus lactis* with the food-grade inducer nisin. *Appl. Environ. Microbiol.* 62, 3662–3667.

Douarre, P. E., Cashman, W., Buckley, J., Coffey, A., and O'mahony, J. M. (2010). Isolation and detection of *Mycobacterium avium* subsp. *paratuberculosis* (MAP) from cattle in Ireland using both traditional culture and molecular based methods. *Gut Pathog.* 2:11. doi: 10.1186/1757-4749-2-11

Drew, D., Slotboom, D. J., Friso, G., Reda, T., Genevaux, P., Rapp, M., et al. (2005). A scalable, GFP-based pipeline for membrane protein overexpression screening and purification. *Protein Sci.* 14, 2011–2017. doi: 10.1110/ps.051466205

Faisal, S. M., Yan, F., Chen, T. T., Useh, N. M., Guo, S., Yan, W., et al. (2013). Evaluation of a *Salmonella* vectored vaccine expressing *Mycobacterium avium* subsp. *paratuberculosis* antigens against challenge in a goat model. *PLoS ONE* 8:e70171. doi: 10.1371/journal.pone.0070171

Fekkes, P., and Driessen, A. J. (1999). Protein targeting to the bacterial cytoplasmic membrane. *Microbiol. Mol. Biol. Rev.* 63, 161–173.

Goldstone, R. M., Moreland, N. J., Bashiri, G., Baker, E. N., and Shaun Lott, J. (2008). A new Gateway vector and expression protocol for fast and efficient recombinant protein expression in *Mycobacterium smegmatis*. *Protein Expr. Purif.* 57, 81–87. doi: 10.1016/j.pep.2007.08.015

Gurung, R. B., Purdie, A. C., Begg, D. J., and Whittington, R. J. (2012). *In silico* screened *Mycobacterium avium* subsp. paratuberculosis (MAP) recombinant proteins upregulated under stress conditions are immunogenic in sheep. *Vet. Immunol. Immunopathol.* 149, 186–196. doi: 10.1016/j.vetimm.2012.06.026

He, Z., and De Buck, J. (2010). Localization of proteins in the cell wall of *Mycobacterium avium* subsp. *paratuberculosis* K10 by proteomic analysis. *Proteome Sci.* 8:21. doi: 10.1186/1477-5956-8-21

Heinzmann, J., Wilkens, M., Dohmann, K., and Gerlach, G. F. (2008). *Mycobacterium avium* subsp. paratuberculosis-specific mpt operon expressed in M. bovis BCG as vaccine candidate. *Vet. Microbiol.* 130, 330–337. doi: 10.1016/j.vetmic.2008.01.014

Hines, M. E., Turnquist, S. E., Ilha, M. R., Rajeev, S., Jones, A. L., Whittington, L., et al. (2014). Evaluation of novel oral vaccine candidates and validation of a caprine model of Johne's disease. *Front. Microbiol.* 4:26. doi: 10.3389/fcimb.2014.00026

Johnston, C., Douarre, P. E., Soulimane, T., Pletzer, D., Weingart, H., Macsharry, J., et al. (2013). Codon optimisation to improve expression of a *Mycobacterium avium* ssp. paratuberculosis-specific membrane-associated antigen by Lactobacillus salivarius. *Pathog. Dis.* 68, 27–38. doi: 10.1111/2049-632X.12040

Kajikawa, A., Nordone, S. K., Zhang, L., Stoeker, L. L., Lavoy, A. S., Klaenhammer, T. R., et al. (2011). Dissimilar properties of two recombinant *Lactobacillus acidophilus* strains displaying *Salmonella* FliC with different anchoring motifs. *Appl. Environ. Microbiol.* 77, 6587–6596. doi: 10.1128/AEM.05153-11

Koets, A., Hoek, A., Langelaar, M., Overdijk, M., Santema, W., Franken, P., et al. (2006). Mycobacterial 70 kD heat-shock protein is an effective subunit vaccine against bovine *paratuberculosis*. *Vaccine* 24, 2550–2559. doi: 10.1016/j.vaccine.2005.12.019

Kohler, H., Gyra, H., Zimmer, K., Drager, K. G., Burkert, B., Lemser, B., et al. (2001). Immune reactions in cattle after immunization with a *Mycobacterium paratuberculosis* vaccine and implications for the diagnosis of *M. paratuberculosis* and *M. bovis* infections. *J. Vet. Med. B Infect. Dis. Vet. Public Health* 48, 185–195. doi: 10.1046/j.1439-0450.2001.00443.x

Li, L., Bannantine, J. P., Zhang, Q., Amonsin, A., May, B. J., Alt, D., et al. (2005). The complete genome sequence of *Mycobacterium avium* subspecies *paratuberculosis*. *Proc. Natl. Acad. Sci. U.S.A.* 102, 12344–12349. doi: 10.1073/pnas.0505662102

Li, L., Munir, S., Bannantine, J. P., Sreevatsan, S., Kanjilal, S., and Kapur, V. (2007). Rapid expression of *Mycobacterium avium* subsp. paratuberculosis recombinant proteins for antigen discovery. *Clin. Vaccine Immunol.* 14, 102–105. doi: 10.1128/CVI.00138-06

Magnan, C. N., Randall, A., and Baldi, P. (2009). SOLpro: accurate sequence-based prediction of protein solubility. *Bioinformatics* 25, 2200–2207. doi: 10.1093/bioinformatics/btp386

Martin, E., Roche, P. W., Triccas, J. A., and Britton, W. J. (2001). DNA encoding a single mycobacterial antigen protects against leprosy infection. *Vaccine* 19, 1391–1396. doi: 10.1016/S0264-410X(00)00374-1

Messaoudi, S., Madi, A., Prevost, H., Feuilloley, M., Manai, M., Dousset, X., et al. (2012). *In vitro* evaluation of the probiotic potential of *Lactobacillus salivarius* SMXD51. *Anaerobe* 18, 584–589. doi: 10.1016/j.anaerobe.2012.10.004

Mohamadzadeh, M., Duong, T., Sandwick, S. J., Hoover, T., and Klaenhammer, T. R. (2009). Dendritic cell targeting of *Bacillus anthracis* protective antigen expressed by *Lactobacillus acidophilus* protects mice from lethal challenge. *Proc. Natl. Acad. Sci. U.S.A.* 106, 4331–4336. doi: 10.1073/pnas.0900029106

Mohamadzadeh, M., Durmaz, E., Zadeh, M., Pakanati, K. C., Gramarossa, M., Cohran, V., et al. (2010). Targeted expression of anthrax protective antigen by *Lactobacillus gasseri* as an anthrax vaccine. *Future Microbiol.* 5, 1289–1296. doi: 10.2217/fmb.10.78

Pallen, M. J. (2002). The ESAT-6/WXG100 superfamily—and a new Gram-positive secretion system? *Trends Microbiol.* 10, 209–212. doi: 10.1016/S0966-842X(02)02345-4

Pavan, S., Hols, P., Delcour, J., Geoffroy, M. C., Grangette, C., Kleerebezem, M., et al. (2000). Adaptation of the nisin-controlled expression system in *Lactobacillus plantarum*: a tool to study *in vivo* biological effects. *Appl. Environ. Microbiol.* 66, 4427–4432. doi: 10.1128/AEM.66.10.4427-4432.2000

Rosseels, V., and Huygen, K. (2008). Vaccination against *paratuberculosis*. *Expert Rev. Vaccines* 7, 817–832. doi: 10.1586/14760584.7.6.817

Rosu, V., Ahmed, N., Paccagnini, D., Gerlach, G., Fadda, G., Hasnain, S. E., et al. (2009). Specific immunoassays confirm association of *Mycobacterium avium* Subsp. *paratuberculosis* with type-1 but not type-2 diabetes mellitus. *PLoS ONE* 4:e4386. doi: 10.1371/journal.pone.0004386

Sambrook, J., Fritsch, E. F., and Maniatis, T. (1990). Molecular-cloning–a laboratory manual, 2nd Edition. *Nature* 343, 604–660.

Scandurra, G. M., De Lisle, G. W., Cavaignac, S. M., Young, M., Kawakami, R. P., and Collins, D. M. (2010). Assessment of live candidate vaccines for *paratuberculosis* in animal models and macrophages. *Infect. Immun.* 78, 1383–1389. doi: 10.1128/IAI.01020-09

Shin, S. J., Wu, C. W., Steinberg, H., and Talaat, A. M. (2006). Identification of novel virulence determinants in *Mycobacterium paratuberculosis* by screening a library of insertional mutants. *Infect. Immun.* 74, 3825–3833. doi: 10.1128/IAI.01742-05

Sleator, R. D., and Hill, C. (2008). Designer probiotics: a potential therapeutic for *Clostridium difficile*? *J. Med. Microbiol.* 57, 793–794. doi: 10.1099/jmm.0.47697-0

Snapp, E. L. (2009). Fluorescent proteins: a cell biologist's user guide. *Trends Cell Biol.* 19, 649–655. doi: 10.1016/j.tcb.2009.08.002

Stern, N. J., Svetoch, E. A., Eruslanov, B. V., Perelygin, V. V., Mitsevich, E. V., Mitsevich, I. P., et al. (2006). Isolation of a *Lactobacillus salivarius* strain and purification of its bacteriocin, which is inhibitory to *Campylobacter jejuni* in the chicken gastrointestinal system. *Antimicrob. Agents Chemother.* 50, 3111–3116. doi: 10.1128/AAC.00259-06

Stratmann, J., Dohmann, K., Heinzmann, J., and Gerlach, G. F. (2006). Peptide aMptD-mediated capture PCR for detection of *Mycobacterium avium* subsp. *paratuberculosis* in bulk milk samples. *Appl. Environ. Microbiol.* 72, 5150–5158. doi: 10.1128/AEM.00590-06

Stratmann, J., Strommenger, B., Goethe, R., Dohmann, K., Gerlach, G. F., Stevenson, K., et al. (2004). A 38-kilobase pathogenicity island specific for *Mycobacterium avium* subsp. *paratuberculosis* encodes cell surface proteins expressed in the host. *Infect Immun.* 72, 1265–1274. doi: 10.1128/IAI.72.3.1265-1274.2004

Triccas, J. A., Roche, P. W., Winter, N., Feng, C. G., Butlin, C. R., and Britton, W. J. (1996). A 35-kilodalton protein is a major target of the human immune response to *Mycobacterium leprae*. *Infect. Immun.* 64, 5171–5177.

Triccas, J. A., Winter, N., Roche, P. W., Gilpin, A., Kendrick, K. E., and Britton, W. J. (1998). Molecular and immunological analyses of the *Mycobacterium avium* homolog of the immunodominant *Mycobacterium leprae* 35-kilodalton protein. *Infect. Immun.* 66, 2684–2690.

Vrieling, M., Santema, W., Vordermeier, M., Rutten, V., and Koets, A. (2013). Hsp70 vaccination-induced primary immune responses in efferent lymph of the draining lymph node. *Vaccine* 31, 4720–4727. doi: 10.1016/j.vaccine.2013.08.021

Wang, Z., Yu, Q., Gao, J., and Yang, Q. (2012). Mucosal and systemic immune responses induced by recombinant *Lactobacillus* spp. expressing the hemagglutinin of the avian influenza virus H5N1. *Clin. Vaccine Immunol.* 19, 174–179. doi: 10.1128/CVI.05618-11

Winter, N., Triccas, J. A., Rivoire, B., Pessolani, M. C., Eiglmeier, K., Lim, E. M., et al. (1995). Characterization of the gene encoding the immunodominant 35 kDa protein of *Mycobacterium leprae*. *Mol. Microbiol.* 16, 865–876. doi: 10.1111/j.1365-2958.1995.tb02314.x

Wu, C. W., Schmoller, S. K., Shin, S. J., and Talaat, A. M. (2007). Defining the stressome of *Mycobacterium avium* subsp. *paratuberculosis in vitro* and in naturally infected cows. *J. Bacteriol.* 189, 7877–7886. doi: 10.1128/JB.00780-07

Yakes, B. J., Lipert, R. J., Bannantine, J. P., and Porter, M. D. (2008). Impact of protein shedding on detection of *Mycobacterium avium* subsp. *paratuberculosis* by a whole-cell immunoassay incorporating surface-enhanced Raman scattering. *Clin. Vaccine Immunol.* 15, 235–242. doi: 10.1128/CVI.00335-07

Yu, Q., Zhu, L., Kang, H., and Yang, Q. (2013). Mucosal *Lactobacillus* vectored vaccines. *Hum. Vaccin. Immunother.* 9, 805–807. doi: 10.4161/hv.23302

Conflict of Interest Statement: The Associate Editor Dr. Adel Talaat declares that despite having collaborated with the author Dr. John Bananntine, the review process was handled objectively and no conflict of interest exists. The authors declare that the research was conducted in the absence of any commercial or financial relationships that could be construed as a potential conflict of interest.

Received: 24 April 2014; accepted: 15 August 2014; published online: 04 September 2014.

*Citation: Johnston CD, Bannantine JP, Govender R, Endersen L, Pletzer D, Weingart H, Coffey A, O'Mahony J and Sleator RD (2014) Enhanced expression of codon optimized Mycobacterium avium subsp. paratuberculosis antigens in Lactobacillus salivarius. Front. Cell. Infect. Microbiol. **4**:120. doi: 10.3389/fcimb.2014.00120*

This article was submitted to the journal Frontiers in Cellular and Infection Microbiology.

frontiers in
CELLULAR AND INFECTION MICROBIOLOGY

OPINION ARTICLE
published: 17 September 2014
doi: 10.3389/fcimb.2014.00133

Mycobacterial glycoproteins: a novel subset of vaccine candidates

Antonio Facciuolo and Lucy M. Mutharia*

Department of Molecular and Cellular Biology, University of Guelph, Guelph, ON, Canada
**Correspondence: lmuthari@uoguelph.ca*

Edited by:
John Bannantine, National Animal Disease Center, USA

Reviewed by:
Torsten Eckstein, Colorado State University, USA
Franck Emmanuel Biet, Institut National de la Recherche Agronomique, France

Keywords: *Mycobacterium*, glycoproteins, paratuberculosis, bovine tuberculosis, vaccination

Over the last two decades significant research efforts and resources have been devoted to identifying mycobacterial proteins of value to diagnostic assays and vaccine formulations. These scientific endeavors were often preceded by first identifying a target population of proteins, for example cytoplasmic, cell envelope, or extracellular. However, many of these endeavors have overlooked the posttranslational modifications (PTM) to which these protein subsets may be targets of. Consequently, we may be missing essential molecular information relevant to the function and antigenicity of these effector molecules, and in turn the pathobiology of these bugs. Moreover, heterologous expression of mycobacterial proteins in hosts lacking homologous PTM systems negates any functional and/or antigenic role the PTM may impart. Functional and pathogenic roles of PTMs, such as protein glycosylation, have been reported for other Gram-positive bacteria, especially in reference to mucosal pathogens (reviewed by Szymanski and Wren, 2005). Our objective in this piece is to shed light on the lack of PTM studies so that current and future researchers hunting for diagnostic and vaccine candidates shall: (i) be made aware of PTMs of mycobacterial proteins, and (ii) come to understand their growing importance to both pathobiology and immunogenicity. Interestingly, the last 5 years has only yielded 2 reports on the global analyses of mycobacterial glycoproteins, both for *M. tuberculosis* (Mtb), and over the last decade only a few studies demonstrated the importance of PTMs to the pathobiology and antigenicity of select proteins in Mtb, *M. bovis*, and *Mycobacterium avium* subsp. *paratuberculosis* (MAP). In this communication we present the opinion that in a world of cross-reactive epitopes, and high amino acid sequence similarity between *M. bovis*, MAP, and their saprophytic counterparts, PTM diversity amongst these species may confer a new level of epitope-specificity for select antigens. We will also highlight that in the case of protein glycosylation, the type and extent of glycosyl moieties should not been seen as having the same outcome. Furthermore, the presence or absence of the PTM of proteins included in subunit vaccine formulations or attenuated strains, may enhance or mask the processing, presentation, and immunogenicity of relevant epitopes. Collectively, these data call to action critical analyses of the components we use to formulate mycobacterial vaccines. As the vast majority of PTM studies have focused on glycosylation, this PTM will be the focal point of discussion.

Abbreviations: LC, liquid chromatography; MS, mass spectrometry; MHC, major histocompatibility complex; TCR, T-cell receptor; BCR, B-cell receptor; BCG, Bacillus Calmette-Guérin; PPD, purified protein derivative; PBMC, peripheral blood mononuclear cell; MR, mannose receptor; DC-SIGN, dendritic cell-specific intercellular adhesion molecule-3-grabbing non-integrin.

HISTORY OF MYCOBACTERIAL GLYCOPROTEINS

Espitia and Mancilla (1989) first identified 3 glycoproteins in Mtb H37Rv culture filtrate (CF) using mannose-binding lectin Concanavalin A. Immunoblotting revealed 2 of the glycoproteins (Rv1860-Apa, Rv0934) were reactive with 38% of serum samples from active TB patients tested; no reactivity was detected with healthy control samples. Subsequent studies mapped the glycosylated peptides of the Mtb Apa adhesin protein using endopeptidase digestion and MS analysis (Dobos et al., 1995). Horn et al. (1999) examined the antigenicity of the Apa protein in *M. bovis* BCG-immunized guinea pigs. Using MS, they demonstrated mannosylation of native Apa purified from Mtb and *M.bovis*, mannosylation of recombinantly expressed Apa in *M.smegmatis*, however with 2–3 additional mannose residues per branch, and the lack of mannosylation of recombinant *E.coli* Apa. In T-cell assays, native Mtb and *M. bovis* Apa protein elicited similar levels of lymphoproliferation, whereas recombinant *E.coli* Apa showed negligible activity. Interestingly, recombinant *M. smegmatis* Apa lymphoproliferation was 10-fold less despite similar, albeit increased, glycosylation patterns as the native proteins. This report was the first to demonstrate that mycobacterial proteins stimulate more robust immunological responses as glycoconjugates, and that species-specific differences in glycosylation alter this response. Interestingly, glycosylation differences for Apa of Mtb and *M.marinum* have also been demonstrated, however, the functional implication of this is yet to be elucidated (Coddeville et al., 2012). To date, no follow up studies have addressed, (i) differential mannosylation in *M. smegmatis*, *M. bovis*, and Mtb, and (ii) why variation in glycosylation results in an altered immunological response.

Recently two complimentary approaches, Con A lectin affinity chromatography, and MS analysis for O-linked hexosylation, were taken to address

global protein glycosylation in Mtb CF. Interestingly, the MS analyses identified 13 glycoproteins in Mtb CF in contrast to the 41 captured by affinity chromatography (González-Zamorano et al., 2009; Smith et al., 2014). Liu et al. (2013) first linked a functional and virulent role to the Mtb mannosyl transferase membrane protein (Rv1002c) by establishing a Δ*Rv1002c* mutant. Murine alveolar macrophages co-cultured with the ΔRv1002c mutants showed a 50% reduction in uptake over H37Rv. Moreover, median survival of SCID mice challenged with the Δ*Rv1002c* mutants increased by 41 days over H37Rv. Collectively, these data highlight the significant contribution of glycoproteins to infectivity and virulence of Mtb. In another study, MS mapping of the *M.bovis* glycoprotein MPB83 identified a unique mannose linkage not previously reported in Mtb glycoproteins (Michell et al., 2003). These data raise interesting questions such as: (i) how this linkage may affect interactions with immunological receptors such as the TCR, MHC, and/or BCR by enhancing/masking/modulating its binding, and (ii) whether these linkages are part of the antigenic determinant, and if so, do they impart species-specificity even in highly homologous proteins.

GLYCOSYLATION AND ANTIGENICITY

Glycosylation-dependent peptide epitopes were demonstrated by ELISA using mannosidase-treated recombinant Mtb Apa expressed in *Streptomyces* (Lara et al., 2004). Reactivity of serum from TB patients was significantly reduced after Apa was treated with mannosidase. In our lab, similar observations were found with 17 MAP CF glycoproteins purified by Con A lectin-affinity chromatography. Both bovine and ovine paratuberculosis serum contained antibodies against these antigens. However, only bovine serum activity was abrogated after mannosidase treatment of these antigens (Mutharia et al., 1997). Currently, our lab is identifying these, and other MAP glycoproteins, among the complement of secreted proteins we recently identified (Facciuolo et al., 2013). Using Con A lectin blotting on MAP CF proteins concentrated and resolved by RPLC we can reproducibly detect 14 reactive bands by SDS-PAGE in the range of 10–75 kDa (Facciuolo and Mutharia, unpublished). Applying Con A lectin-affinity chromatography 9 unique bands were eluted, and resolved by SDS-PAGE. By 2D PAGE, 6 of these 9 unique bands have horizontal spot series (on average 3 spots) indicative of PTMs. To our knowledge, this is the most extensive reporting on MAP glycoproteins.

Recently, protein glycosylation on T-cell antigenicity and vaccination was elucidated using native and recombinant Apa-protein isoforms of Mtb (Nandakumar et al., 2013). In BCG+ PPD+ individuals, CD4+ cytokine-secreting cells were significantly higher in PBMCs stimulated with the native protein than the recombinant isoform. Moreover, the native glycosylated Apa uptake was higher than that of the unglycosylated recombinant isoform in dendritic cells from PBMCs of both BCG+ and BCG− individuals. *In vitro* analyses showed only the glycosylated isoform bound recombinant human innate immune receptors such MR, DC-SIGN, and DC-SIGNR. Despite these significant differences, both protein isoforms were equally protective in BALB/c mice as subunit vaccines stimulating similar CD4+ cytokine and serum antibodies responses. These data suggest that glycosylation is necessary for antigenicity, but not induction of protective immunity. The outcomes of these data are quite interesting when also considering the earlier studies by Ishioka et al. (1992). Using synthetic peptides, three GlcNAc-position-dependent outcomes were observed in BALB/c immunized mice. Positioning of the GlcNAc conjugated amino acid could either limit lymphoproliferative responses to the glycosylated peptide only, abolish antigenicity of the peptide, or result in antigenicity of both the glycosylated and unglycosylated peptide isoforms. The authors speculated that the consequences were the result of MHC-TCR interactions where the glycoconjugate: is the antigenic determinant, interfered with the MHC binding site, or was distal of the critical MHC binding pocket, respectively. In light of these data, careful analyses and consideration of both glycosylation status and their site of attachment on proteins are needed to ensure the efficacy of these molecules in stimulating the desired immunological response. These considerations should also be applied in the development of attenuated strains as the presence or absence of glycosylated proteins may either enhance/mask protective stimulators/inducers of innate/adaptive immunity.

The complexity of glycosylation in addition to the consequences it carries calls to action a bottom-up approach in screening for novel vaccine candidates. The potential of these effector molecules to contain species-specific glycosylation markers may benefit vaccine formulations, in addition to diagnostic assays. The technical hurdles in obtaining the necessary quantity and fidelity of glycoproteins from slower growing *Mycobacterium* currently presents the greatest challenge in this field, but has had some measure of success via heterologous expression, or native purification by lectin-affinity purification coupled with LC. These technical challenges might best be served by efforts to glycoengineer PTM systems in faster growing species. The sum of these data may aid in identifying those effector molecules, (i) that exclusively require their PTM for antigenicity, (ii) where the PTM is dispensable for protective immunity, and (iii) containing new subsets of protective or relevant antigens that had been masked by the presence of a PTM.

REFERENCES

Coddeville, B., Wu, S. W., Fabre, E., Brassart, C., Rombouts, Y., Burguière, A., et al. (2012). Identification of the *Mycobacterium marinum* Apa antigen O-mannosylation sites reveals important glycosylation variability with the *M. tuberculosis* Apa homologue. *J. Proteomics*. 75, 5695–5705. doi: 10.1016/j.jprot.2012.07.017

Dobos, K. M., Swiderek, K., Khoo, K. H., Brennan, P. J., and Belisle, J. T. (1995). Evidence for glycosylation sites on the 45-kilodalton glycoprotein of *Mycobacterium tuberculosis*. *Infect Immun*. 63, 2846–2853.

Espitia, C., and Mancilla, R. (1989). Identification, isolation and partial characterization of *Mycobacterium tuberculosis* glycoprotein antigens. *Clin. Exp. Immunol*. 77, 378–383.

Facciuolo, A., Kelton, D. F., and Mutharia, L. M. (2013). Novel secreted antigens of *Mycobacterium paratuberculosis* as serodiagnostic biomarkers for Johne's disease in cattle. *Clin. Vaccine Immunol*. 20, 1783–1791. doi: 10.1128/CVI.00380-13

González-Zamorano, M., Mendoza-Hernández, G., Xolalpa, W., Parada, C., Vallecillo, A. J., Bigi, F., et al. (2009). *Mycobacterium tuberculosis* glycoproteomics based on ConA-lectin affinity capture of mannosylated proteins. *J. Proteome Res*. 8, 721–733. doi: 10.1021/pr800756a

Horn, C., Namane, A., Pescher, P., Riviere, M., Romain, F., Puzo, G., et al. (1999). Decreased capacity of recombinant 45/47-kDa molecules (Apa) of *Mycobacterium tuberculosis* to stimulate T lymphocyte responses related to changes in their mannosylation pattern. *J. Biol. Chem*. 274, 32023–32030. doi: 10.1074/jbc.274.45.32023

Ishioka, G. Y., Lamont, A. G., Thomson, D., Bulbow, N., Gaeta, F. C., Sette, A., et al. (1992). MHC interaction and T cell recognition of carbohydrates and glycopeptides. *J. Immunol*.148, 2446–2451.

Lara, M., Servin-Gonzalez, L., Singh, M., Moreno, C., Cohen, I., Nimtz, M., et al. (2004). Expression, secretion, and glycosylation of the 45- and 47-kDa glycoprotein of *Mycobacterium tuberculosis* in *Streptomyces lividans*. *Appl. Environ. Microbiol*. 70, 679–685. doi: 10.1128/AEM.70.2.679-685.2004

Liu, C. F., Tonini, L., Malaga, W., Beau, M., Stella, A., Bouyssie, D., et al. (2013). Bacterial protein-O-mannosylating enzyme is crucial for virulence of *Mycobacterium tuberculosis*. *Proc. Natl. Acad. Sci. U.S.A*. 110, 6560–6565. doi: 10.1073/pnas.1219704110

Michell, S. L., Whelan, A. O., Wheeler, P. R., Panico, M., Easton, R. L., Etienne, A. T., et al. (2003). The MPB83 antigen from *Mycobacterium bovis* contains O-linked mannose and (1–>3)-mannobiose moieties. *J. Biol. Chem*. 278, 16423–16432. doi: 10.1074/jbc.M207959200

Mutharia, L. M., Moreno, W., and Raymond, M. (1997). Analysis of culture filtrate and cell wall-associated antigens of *Mycobacterium paratuberculosis* with monoclonal antibodies. *Infect. Immun*. 65, 387–394.

Nandakumar, S., Kannanganat, S., Dobos, K. M., Lucas, M., Spencer, J. S., Fang, S., et al. (2013). O-mannosylation of the *Mycobacterium tuberculosis* adhesin apa is crucial for T Cell antigenicity during infection but is expendable for protection. *PLoS Pathog*. 9:e1003705. doi: 10.1371/journal.ppat.1003705

Smith, G. T., Sweredoski, M. J., and Hess, S. (2014). O-linked glycosylation sites profiling in *Mycobacterium tuberculosis* culture filtrate proteins. *J. Proteomics*. 97, 296–306. doi: 10.1371/journal.ppat.1003705

Szymanski, C. M., and Wren, B. W. (2005). Protein glycosylation in bacterial mucosal pathogens. *Nat. Rev. Microbiol*. 3, 225–237. doi: 10.1038/nrmicro1100

Conflict of Interest Statement: The authors declare that the research was conducted in the absence of any commercial or financial relationships that could be construed as a potential conflict of interest.

Received: 10 July 2014; accepted: 03 September 2014; published online: 17 September 2014.
Citation: Facciuolo A and Mutharia LM (2014) Mycobacterial glycoproteins: a novel subset of vaccine candidates. Front. Cell. Infect. Microbiol. ***4****:133. doi: 10.3389/fcimb.2014.00133*
This article was submitted to the journal Frontiers in Cellular and Infection Microbiology.